Opioid Research

Methods and Protocols

Edited by

Zhizhong Z. Pan

HUMANA PRESS

1
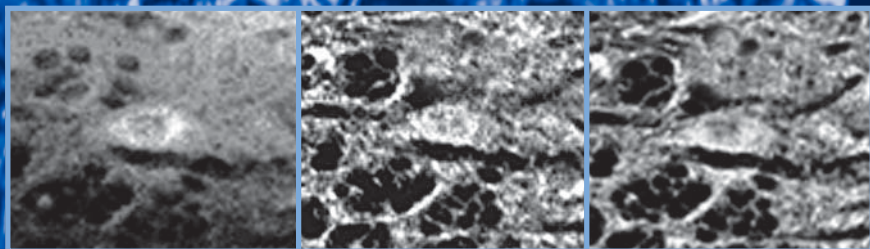
Molecular Cloning of Opioid Receptors by cDNA Library Screening

Ying-Xian Pan

1. Introduction

In order to obtain cDNA clones encoding opioid receptors, one conventional strategy is to screen a cDNA library by using either a nucleic acid probe or an antibody probe. Many opioid receptor cDNA clones have been identified by the cDNA library screening *(1–16)*. Different types of cDNA libraries made from a variety of tissues or cells are available from various companies such as Strategene, ClonTech, and Invitrogen. cDNA libraries are commonly constructed in bacteriophage λ vectors, which are advantageous in their highly efficient and reproducible packaging systems in vitro. However, cDNA expression libraries are usually made in mammalian expression plasmid vectors, which can be screened by expression cloning with a specific radiolabeled ligand or an antibody probe in a mammalian cell line. Choice of the screening procedures depends upon the available probe and cDNA library. A nucleic acid probe is ideal for screening its homologs, or associated splicing variants or full-length cDNAs. If only a partial protein sequence is on hand, degenerate primers can be designed to screen cDNA libraries with a direct polymerase chain reaction (PCR) or with a hybridization procedure. Alternatively, a specific antibody could be generated against the protein sequence and used in the cDNA library screening. A successful cDNA library screening relies on several factors: a high-quality cDNA library, a well-made probe, and the performer's experience. This chapter mainly focuses on the procedures used for screening λZAPII bacteriophage libraries. It describes the screening procedures of using nucleic acid probes and antibody probes. Also discussed is a PCR screening procedure, which provides an efficient assay for identifying a cDNA clone and serves

as an initial screening for the hybridization screening to determine whether the cDNA library contains the gene interested.

2. Materials

1. λZAPII cDNA library with XL-1Blue MRF' and SORL strains, and ExAssist helper phage (Stratagene).
2. Luria-Bertani (LB) broth: Dissolve 10 g of Bacto tryptone, 5 g of Bacto yeast extract, and 5 g of NaCl in 800 mL H$_2$O, adjust the pH to 7.2 with 1 M NaOH, and bring the volume to 1 L. Sterilize the medium by autoclaving.
3. LB plates: Add 4 g agar in 330 mL of LB broth (1.2% agar). Autoclaved, cool and pour the medium into 15 × 100 mm sterile polystyrene plates (approx 30 mL per plate). Cool the plates at room temperature and store at 4°C.
4. 50 mg/mL ampicillin stock: Dissolve 2 g ampicillin in 40 mL of H$_2$O. Filtrate the solution through a 0.22-μm filter and store at –20°C.
5. 10 mg/mL kanamycin stock: Dissolve 0.5 g kanamycin in 50 mL of H$_2$O. Filtrate the solution through a 0.22-μm filter and store at –20°C.
6. 5 mg/mL tetracyclin stock: Dissolve 0.25 g tetracycline in 50 mL 100% ethanol. Store the solution at –20°C.
7. LB/ampicillin plates, LB/tetracycline plates, and LB/kanamycin plates: Prepare the LB plates as described above except for adding appropriate antibiotics (100 μg/mL ampicillin, 12.5 μg/mL tetracycline, and 50 μg/mL kanamycin) into the autoclaved medium when the medium is cooled to < 50°C. Alternatively, appropriate amount of antibiotics can be directly plated onto LB plates.
8. 20% maltose stock: Dissolve 10 g maltose in 50 mL of H$_2$O. Filtrate the solution through a 0.22-μm filter and store at 4°C.
9. 1 M MgSO$_4$.
10. NZY broth: Dissolve 22 g NZCYM powder in final 1 L of H$_2$O. Sterilize the dissolved medium by autoclaving.
11. NZY plates: Add 5 g agar into 330 mL NZY broth (1.5% agar). Autoclave, cool and pour the medium into sterile polystyrene plates (approx 30 mL per 15 × 100 mm plate or approx 80 mL per 15 × 150 mm plate). Cool the plates at room temperature and store at 4°C.
12. 0.7% top agarose: Add 2.1 g agarose into 300 mL NZY broth. Sterilize the medium by autoclaving.
13. SM buffer: Dissolve 5.8 g of NaCl and 2 g of MgSO$_4$.7H$_2$O in 800 mL of H$_2$O. Add 50 mL of 1 M Tris-HCl, pH 7.5, and 5 mL of 2% gelatin. Bring to 1 L with H$_2$O and autoclave the solution.
14. 100 mM IPTG stock: Dissolve 1.19 g isopropyl-β-D-thio-galactopyranoside (IPTG) in 50 mL of H$_2$O. Filtrate the solution through a 0.22-μm filter and store at –20°C.
15. 2% X-gal stock: Dissolve 1 g 5-bromo-4-chloro-3-indoyl-β-D-galacpyranoside (X-gal) in 50 mL of dimethylform amide. Store in a foil-wrapped tube at –20°C.

16. LB/IPTG/X-gal/ampicillin plates: Prepare the LB plates as described earlier except for adding 0.2 m*M*/mL IPTG, 0.008% X-gal, and 100 μg/mL ampicillin into the autoclaved medium when the medium is cooled to <50°C. Harden the plates at room temperature and store in dark at 4°C.
17. Falcon 2059 polypropylene tubes (17 × 100 mm).
18. Spectrophotometer.
19. Nylon Transfer Membrane, 137 mm (Micron Separations Inc.).
20. Nitrocellulose Transfer and Immobilization Membranes, 82 mm and 132 mm (Schleicher & Schell).
21. Round glass dishes, 150 × 75 mm and 100 × 75 mm.
22. Water bath.
23. Vacuum oven.
24. Transfer buffer A: 0.5 *M* NaOH, and 1.5 *M* NaCl in H_2O.
25. Transfer buffer B: 0.5 *M* Tris-HCl, pH 8.0, and 1.5 *M* NaCl in H_2O.
26. Transfer buffer C: 0.2 *M* Tris-HCl, pH 7.5, and 2 × SSC in H_2O.
27. 20 × SSC (3 *M* NaCl and 0.3 *M* Na citrate): Dissolve 175.3 g of NaCl and 88.2 g of Na citrate in 800 mL of H_2O. Adjust the pH to 7.0 with 10 *M* NaOH and bring to 1 L with H_2O.
28. 50 × Denhardt's solution: Dissolve 1 g of bovine serum albumin (BSA), 1 g of Ficoll 400, and 1 g of polyvinylpyrrolidone (PVP, Mt: 360,000) in 100 mL of H_2O. Store the solution at –20°C.
29. 10 mg/mL salmon sperm DNA (ssDNA): Dissolve 1 g of ssDNA in 100 mL distilled water at 4°C overnight. Sonicate the solution to break DNA down to small pieces and store at –20°C.
30. Hybridization buffer: 6 × SSC, 5 × Denhardt's solution, and 0.1% SDS in H_2O.
31. Wash buffer A: 2 × SSC and 0.1% SDS in H_2O.
32. Wash buffer B: 0.2 × SSC and 0.1% SDS in H_2O.
33. Quick spin sephadex G25 column (Boehringer Mannheim).
34. Plasmid Mini prep kit (Qiagen).
35. Platinum Taq DNA polymerase (Invitrogen).
36. PCR Thermal cycler.
37. α-^{32}P-dCTP, 3000 Ci/mmol, 10 mCi/mL (NEN).
38. ^{125}I-Protein A (NEN).
39. Radiation Monitors (Geiger counters) for both ^{32}P and ^{125}I.
40. TTBS buffer: 10 m*M* Tris-HCl, pH 7.4, 150 m*M* NaCl, and 0.05% Tween-20 in H_2O.
41. pCRII-TOPO vector (Invitrogen).
42. TOP10F' competent cells (Invitrogen).
43. Transfer trays (~35 × 45 cm).
44. Hybridization oven with shaker.
45. Zymoclene Gel DNA Recovery Kit (Zymo Research).

3. Methods

3.1. Screening a λZAPII cDNA Library with a Nucleic Acid Probe (17)

3.1.1. Titering the cDNA Library

3.1.1.1. PREPARATION OF THE HOST BACTERIAL STRAIN

1. Inoculate a single colony of freshly streaked XL-1Blue MRF' strain in 20 mL of LB broth containing 0.2% (v/v) maltose and 10 mM MgSO$_4$ in a sterile 50-mL flask, and shake the flask overnight at 30°C (*see* **Note 1**).
2. Transfer the LB broth containing the cells into a sterile 500-mL conical tube, and spin the tube for 10 min at 1000x g.
3. Discard the supernatant and resuspend the pellet in 5 mL of 10 mM MgSO$_4$ by gently vortexing.
4. Dilute the cell suspension with 10 mM MgSO$_4$ until the cell density reaches approximately OD$_{600}$ = 0.5.

3.1.1.2. DILUTION OF THE cDNA LIBRARY

Scrape a chunk of the library from the frozen stock tube (approx 20–30 μL after melting) with a sterile metal scraper into a sterile 1.5-mL tube (*see* **Note 2**). Make serial dilution of the melted library. If the original titer is 10^{10} plaque forming unit (PFU)/mL, label five 1.5-mL sterile tubes as 10^7, 10^6, 10^5, 10^4, and 10^3, respectively. Add 999 μL of SM buffer into the 10^7 tube and 900 μL into the rest tubes. Pipet 1 μL of the stock library into the 10^7 tube and gently mix by flipping the tube several times. Then transfer 100 μL solution from the 10^7 tube into the 10^6 tube and gently mix the tube. Do the same transferring and mixing for the rest tubes by following the order of the tubes.

3.1.1.3. INFECTION OF THE HOST CELLS WITH THE λ PHAGES

1. Prepare top agarose and NZY plates for plating. Completely melt the top agarose in a microwave oven, and then keep it in a 48°C water bath (not over 50°C) for at least 30 min. Warm five 15 × 100 mm NZY plates at 37°C.
2. Label five Falcon 2059 tubes as above phage dilution tubes. Mix 1 μL of the diluted phages with 200 μL host cells (from **3.1.1.1.**, **step 4**) in the individual 2059 tubes.
3. Incubate the tubes for 15 min at 37°C with gently shaking.
4. Add 3 mL 0.7% warmed top agarose into the tubes, quickly mix by handswirling, and pour on the NZY plate. Gently rotate the plate to make the top agarose evenly distributed on the plate. Remove bubbles with swirling or with a pipet tip if necessary. Cool the plates at room temperature for approx 30 min.
5. Incubate the plates for 6–8 h at 37°C, count the plaques, and determine the titer of the library as PFU/mL.

3.1.2. Plating the cDNA Library

1. Prepare the host cells as described in **Subheading 3.1.1.**
2. Prepare approx 180 mL top agarose and 20 150-mm NZY plates as described in **Subheading 3.1.1.** for screening approx 10^6 PFU (*see* **Note 3**)
3. Plating procedure: Prepare 20 Falcon 2059 tubes. For each 150 mm NZY plate, mix 1–3 µL of the diluted phages (approx 50,000 PFU) with 600 µL of the diluted cells ($OD_{600} = 0.5$) in a Falcon 2059 tube. Incubate the tube for 15 min at 37°C. Add 7 mL of warmed 0.7% top agarose, quickly mix, and plate the mixture on a warmed 15 × 150 mm NZY plate. Incubate the plates for approx 8 h at 37°C and then store the plates at 4°C overnight or at least 2 h (*see* **Note 4**).

3.1.3. Transferring Plaques to Nylon Membranes (see **Note 5**)

1. Preparation of transfer buffers, 3MM papers and three transfer trays. Make fresh Transfer buffers A, B, and C. Place three trays on bench and label them as A, B, and C in sequential order. Cut 3MM papers to fit them inside each trays. Then soak the 3MM papers with appropriate transfer buffers, and remove any bubbles between the 3MM paper and the tray by rolling a pipet on the 3MM paper.
2. Label the nylon membranes with a pencil. Hold the nylon membrane (the labeled face toward the plate) with both hands, lay the middle portion of the membrane onto the middle of the cold plate and then slowly put the rest membrane down to avoid bubbles between the membrane and the surface of the plate. Remove air bubbles by gently rolling the bubbles toward the edge of the plate with fingers if necessary.
3. Let the membrane stay on the plate for 5 min. Pinch three asymmetric holes through the membrane into the agar around the edge of the membrane by using a 19-gage needle.
4. Lift the membrane with a forceps and directly place the membrane onto the 3MM soaked with Transfer buffer A and denature the membrane for 2 min. Put the labeled face or the face containing the phages up so that the phages on the membrane do not directly contact with the 3MM paper. Avoid air bubbles between the membrane and the 3MM.
5. Transfer the membrane to the second tray containing Transfer buffer B and neutralize the membrane for 5 min.
6. Transfer the membrane to the third tray containing Transfer buffer C and neutralize for 1 min.
7. Place the membrane on a dry 3MM paper to dry the membrane.
8. Sandwich the membranes with 3MM paper and cover them with a sheet of aluminum foil. Bake the membranes at 80°C in a vacuum oven for 2 h to crosslink the phage DNA to the membrane.
9. Make the duplicate membrane on the same plate as described above except for incubating the membrane on the plate for 8–10 min. Make the same marks on the membranes as the holes on the previous membranes with the 19-gage needle.

3.1.4. Preparing a ^{32}P-Labeled Double-Stranded DNA Probe by an Asymmetric PCR (see **Note 6**)

1. Amplify a DNA fragment from a plasmas or BAC or genomic DNA by PCR with a sense primer and an antisense primer.
2. Load the PCR sample on an agarose gel and purify the amplified DNA fragment from the gel by using a Zymoclean Gel DNA Recovery kit. Sequence the PCR fragment if necessary.
3. In a PCR tube, add 5 μL of 10× reaction buffer without $MgCl_2$, 1.5 μL of 50 m*M* $MgCl_2$, 3 μL of dNTP containing 1 m*M* of each dGTP, dTTP, and dATP, 3 μL of 0.1 m*M* dCTP, 1 μL of 0.2 μ*M* sense primer, 1 μL of 20 μ*M* antisense primer, 1–5 ng of the PCR fragment, 10 μL of α-^{32}P-dCTP, 2.5 U of Platinum *Taq* DNA polymerase, and bring water to 50 μL (*see* **Note 7**).
4. Perform PCR with an initial 1 min denaturing at 94°C , then 30 thermal cycles, each cycle consisting of a 20-s melting step at 94°C , a 20-s annealing step at various temperatures depending upon the primer, a 1–2 min extension step at 72°C , and a final 5 min extension at 72°C.
5. Perform an exactly same PCR just without α-^{32}P-dCTP in a separate PCR tube, which is used for monitoring the PCR performance and estimating the concentration of the amplified DNA by analyzing its cold product on a agarose gel.
6. Purify the ^{32}P-labeled DNA fragment by using a Quick spin sephadex G25 column (following the manufactory protocols). Count 1 μL of eluted probe in a scintillation counter and determine the specific activity of the probe by dividing the total counts by the estimated DNA concentration.

3.1.5. Prehybridizing, Hybridizing, and Washing

1. Prepare enough the hybridization solution for both prehybridization and hybridization. Preheat the hybridization solution to 65°C. Boil the ssDNA for 10 min and then add the boiled ssDNA into the hybridization solution at 100 μg/mL.
2. Add the preheated hybridization solution into a round 75 × 150-mm glass dish (approx 5 mL/membrane). Lay the baked membranes into the solution one by one with the labeled face (or face containing the phages) up. Do not place next membrane until the previous one is completely wet and soaked.
3. Cover the glass dish with a plastic wrap and seal with a rubberband. Incubate the glass dish at 65°C with shaking for 2–4 hr.
4. Boil appropriate amount of the probe for 10 min and cool on ice for 5 min. Then add the probe into the fresh hybridization solution containing 100 μg/mL ssDNA in a round 75 × 150-mm glass dish (10^6 cpm/mL).
5. Transfer the prehybridized membranes into the hybridization solution containing the probe one at a time.
6. Seal the dish with the plastic wrap and rubber band. Incubate the dish at 65°C for 14–20 h with shaking.
7. Wash the membranes with Wash buffer A twice at 55°C , each for 15 min with shaking.

8. Wash the membranes with Wash buffer B once at 55°C for 15 min. After washing, count several membranes with a Geiger counter to monitor the radioactive signal. If the signal is very strong, continue washing the membranes in Wash buffer B at 55°C or a high temperature. If the signal is very weak, stop the washing.

9. Wrap a 35 × 43 cm in 3MM paper with plastic wrap, which can hold six membranes. Transfer the wet membranes onto the wrap and cover the membranes with another plastic wrap to avoid membrane dry (*see* **Note 8**). Expose the membranes to BioMax MS film with MS screen in –80°C overnight.

10. Develop the films and make the markers on the films following the three holes pinched during the lifting procedure. Find the potential positive clones by matching the same positive spots on the duplicate membranes (*see* **Note 9**).

3.1.6. Secondary and Tertiary Screening (*see* **Note 10**)

1. Align the plate with the film by matching their markers under a white-light box. Pick up a pipe of agar containing the positive phages by using the thick end of a sterile 53/4" glass Pasteur pipet and blow it into a 2-mL tube containing 1 mL SM buffer with 50 μL of Chloroform. Vortex and keep the tubes at 4°C overnight.

2. Titer the phages in 100 mm NZY plates as described in **Subheading 3.1.1.**

3. Plate two 100 mm NZY plates for each positive clone with the diluted phages, one containing 100–200 PFU and another 1000–2000 PFU, as described in **Subheading 3.1.2.** (*see* **Note 10**).

4. Lift the phages onto 82 mm Nitrocellulose membranes as described in **Subheading 3.1.3.**.

5. Hybridize the membranes with the probe as described in **Subheading 3.1.5.**

6. Pick up a single positive plaque with the thin end of the Pasteur pipet from the plate and blow it into a tube containing 1 mL SM buffer with 50 μL chloroform. Vortex and store the tube at 4°C for next in vivo excision. Perform tertiary screening if the single positive plaque cannot be obtained.

3.1.7. In Vivo Excision (*see* **Note 11**)

1. Prepare XL1-Blue MRF' and SOLR cells as described in **Subheading 3.1.1.1.** except for streaking the SOLR cells on LB/kanamycin (50 μg/mL) plate.

2. Transfer the XL1-Blue MRF' and SOLR cells into 50-mL conical tubes, centrifuge the tubes for 10 min at $1000g$, resuspend the cell pellets with 10 mM MgSO$_4$, and adjust the cell densities of both cells to OD$_{600}$ = 1.0.

3. Add 200 μL of XL-1Blue MRF' cells (OD$_{600}$ = 1.0) to a Falcon 2059 tube. Mix the cells with 250 μL of the phage stock tube containing the single positive plaque picked up from the plates and 1 μL of the ExAssist helper phage. Incubate the tube for 15 min at 37°C.

4. Add 3 mL of LB media to the tube. Continue incubating the tube for 3 h with shaking.

5. Transfer the tube into a 70°C water bath and incubate for 20 min. Then centrifuge the tube for 15 min at 1000 g. Store the supernatant containing the excised pBluescript phagemid at 4°C , which is stable for approx 1 mo.

6. Mix 10 μL of the supernatant with 200 μL of SOLR cells (OD_{600} = 1.0) prepared above in a 1.5-mL tube, and incubate the tube for 15 min at 37°C.
7. Plate 50 μL of the mixture on a LB/ampicillin plate. Incubate the plates overnight at 37°C.

3.1.8. Isolating pBluescript Plasmids Containing the cDNA Inserts From Positive Colonies

1. Inoculate five colonies from each positive clone into five separate 17 × 100 poly-styrene tubes containing 5 mL LB broth with 100 μg/mL ampicillin. Incubate the tubes overnight at 37°C with shaking.
2. Isolate pBluescript plasmids from the cells by using a pladmid miniprep kit.
3. Analyze the cDNA inserts by restriction enzyme digestions and sequencing (*see* **Note 12**).

3.2. Screening a λZAPII cDNA Library with an Antibody

1. Determine the optimal working conditions of the antibodies including antibody titers, blocking reagents, and washing stringency on nitrocellulose membranes spotted different amount of the antigen or tissue or cell extract expressing the antigen (*see* **Note 13**).
2. Perform the same procedures as described in **Subheadings 3.1.1.** and **3.1.2.** Use 20 150- mm NZY plates to plate approx 50,000 PFU per plate. But incubate the NZY plates at 37°C for only approx 4 h until small plaques appear.
3. During the 4-h incubation, prepare the nitrocellulose membranes. Label the nitrocellulose membranes with a pencil. Treat the membranes with 10 m_M IPTG water solution for 1–2 min and dry the membranes on 3MM paper (*see* **Note 14**).
4. When the small plaques are visible after 4-h incubation, place the labeled IPTG-treated membranes to the NZY plates as described in **Subheading 3.1.3.**, **step 2**. Incubate the plates with the membranes for 4 h at 37°C.
5. Cool the plates at 4°C for 30 min. Make three asymmetric markers on the mem-branes and plates as described in **Subheading 3.1.3.** Lift the membrane with forceps and place it into a round 75 × 150-mm glass dish containing TTBS buffer.
6. Make duplicate membrane on the same plate as described earlier except for incu-bating the plate at 37°C for 12 h. Lift the membranes as described earlier.
7. Wash the membranes in the glass dish containing TTBS buffer at room tempera-ture three times, each for 10 min, with shaking.
8. Transfer the membranes one by one into the blocking solution (2% BSA in TTBS Buffer) and incubate at room temperature with shaking for 1 h.
9. Transfer the membranes one by one into the blocking solution containing the primary antibody with appropriate dilution. Incubate with shaking for 1 hour at room temperature or overnight at 4°C depending upon the optimal condition for the antibody obtained from **Subheading 3.2.1.**
10. Wash the membranes in TTBS buffer at room temperature four times, each for 5 min (*see* **Note 15**).

11. Block the membranes in the blocking solution at room temperature for 1 h.
12. Incubate the membranes in the blocking solution containing appropriate ^{125}I-labeled protein A (approx 10^6 cpm/mL) at room temperature for 1 h.
13. Wash the membranes in TTBS buffer at room temperature four times, each for 5 min.
14. Place the membranes on the 3MM paper wrapped with a plastic wrap as described in **Subheading 3.1.5.**, **step 9**. Expose the membranes to BioMax MS film with MS screen at –80°C overnight. Develop the films and find the potential positive clones on duplicated membranes. Pick up the positive plaques as described in **Subheading 3.1.6.**
15. Perform the secondary or tertiary screening same as the initial screening described above except for plating lower density of the phages on the plates in order to isolate a single phage clone.
16. Perform in vivo excision and plasmid minipreps as described in **Subheadings 3.1.7** and **3.1.8.**

3.3. Screening cDNA Libraries by PCR

3.3.1. Design Primers from a DNA Sequence (see **Note 16**)

Use the Oligo Analysis Tool in a DNA analysis program to select both sense and antisense primers from the specific gene sequence by the following general criteria: 1) length of 18–30 base; 2) high melting temperature (Tm) (over 70°C) with a high G/C content (between 50–70%); 3) less secondary structures such as stem-loop, hairpins, and less primer-primer dimers estimated by their free energy, ΔG; and 4) selecting a G or C at both the 3'-end and the 5'-end *(18)*.

3.3.2. Design Degenerate Primers from Partial Protein Sequences (see **Note 17**)

List all the potential DNA coding sequences for a particular protein sequence. Select the sense or antisense primers by following the general criteria aforementioned if possible. If the number of the oligonucleotides in the degenerate primer is too high, reduce the number by selecting only the codons that are preferentially used in a certain species *(19,20)*. Synthesize the degenerate primer that contains a pool of mixing oligonucleotides by incorporating two or three or four bases in the wobble positions.

3.3.3. PCR (see **Note 16**)

1. Perform PCR with the sense and antisense primers designed from above by using the cDNA library stock as the template. In a PCR tube, add 10 µL of 10× reaction buffer without MgCl$_2$, 3 µL of 50 mM MgCl$_2$, 20 µL of dNTP containing 1 mM of each dGTP, dTTP, dATP, and dCTP, 1 µL of 20 µM sense primer, 1 µL of 20 µM antisense primer, 1 µL of the cDNA library stock, 5 U of Platinum *Taq* DNA polymerase, and bring water to 100 µL.

2. Perform PCR with an initial 2 min denaturing at 94°C , then 35 thermal cycles, each cycle consisting of a 30-s melting step at 94°C , a 2–5 min annealing/extension step at 68°C , and final 5-min extension at 72°C.

3. Analyze 10 µL of the PCR products on 1% agarose gel with 0.2 µg/mL ethidium bromide.

3.3.4. Cloning and Sequencing PCR Fragments (see **Note 18**)

1. Ligate the PCR fragment into pCRII-TOPO vector by following the manufactory protocol.

2. Transform the ligation products into one shot TOP10F' competent cells by following the manufactory protocol.

3. Isolate the plasmid DNA from TOP10F' cells as described in **Subheading 3.1.8.**

4. Sequence the DNA insert in the plasmid by using appropriate primers from the vector.

3.3.5. PCR to Obtain Full Length of cDNAs (see **Note 19**)

If the sequence of the PCR fragment is correct, perform further PCR or screen the library by using the PCR fragment as the probe (*see* **Subheading 3.1.**) to obtain the full length of the cDNA sequence.

4. Notes

1. XL1-Blue MFR' strain is used for tittering and plating λZAPII library and should be streaked on LB plate containing 12.5 µg/mL of tetracycline. The streaked plates can be stored at 4°C for 1 wk.

2. The library is usually supplied in frozen SM buffer containing 7% DMSO and repeated freeze-thaw cycles should be avoided. The melted library stock can be stored for 1–2 wk at 4°C without significant decrease of the titer.

3. In general, approx 50,000 PFU can be plated on a 150 mm plate for the λZAP library. Therefore, 20 150-mm plates can screen approx 10^6 PFU, which is enough for one person to handle.

4. To avoid overgrowing of the plaques, it is better to monitor the plates after 7-h incubation. After incubation, the plates should be kept cold at 4°C , which will help prevent top agarose from sticking onto the nylon membrane during lifting. But the longer storage of the plates at 4°C is not recommended.

5. The major advantage of nylon membranes over nitrocellulose membranes is their durability, which allows to bear baking in an 80°C oven after lifting and multiple rounds of hybridizations with different probes on the same membranes. I successfully hybridized the same lifted nylon membranes with five consecutive probes, which led to identify several cDNA clones from a single library lifting. However, it is not necessary to use nylon membranes in the secondary or the tertiary screening, but nitrocellulose membranes trend brittle after baking and should be carefully handled. Wear gloves and use forceps to handle the membranes in all the procedures.

6. Different types of probes can be used: RNA probe, single-strand, or double-strand DNA probe and oligonucleotide probe. We prefer using double-strand probes mainly because its template can be easily obtained from the plasmid clones or PCR. A double-strand probe with very high specific activity (10^8–10^9 cpm/μg) can be easily generated by using an asymmetric PCR. In the asymmetric PCR, the 100-fold excess antisense primer as to the sense primer will generate much more antisense strand DNA than sense strand DNA, which facilitates the hybridization. Optimal length of the probe is about 500 bp –1000 bp although a shorter or longer fragment can be used.

7. There are many *Taq* DNA polymeraes available from different companies. No matter what type of *Taq* DNA polymerase used, Mg concentration should be carefully adjusted because it is critical for the enzyme activity. The annealing temperature is usually set at 5°C below the primer *Tm*. The extension time depends upon the length of the template, which is generally 1 min for 1 kb.

8. The membranes should be always kept wet because dried membranes tend to crosslink the probe with the membrane. It is difficult to further wash away the nonspecific binding of the probe or strip the probe once the membrane has dried.

9. Ideal positive clones should be shown in duplicate membranes. However, do not ignore the potential positive dots that show only in one of the duplicate membranes if the dot seems real. The secondary screening will determine if they are true positive clones.

10. A single plaque contains approx 10^6 phages. The pipe of agar holds approx 20 plaques equivalent to approx 2×10^7 phages. The purpose of plating two plates with two different densities in the secondary screening is to obtain the single positive plaque in the plate with low-density phages and not to miss the clone with the plate with high-density phages. However, lifting duplicate membranes in the secondary screening is unnecessary.

11. The phage particles in plaques contain whole λZAPII vector including the pBluescript with the cDNA insert. In vivo excision allows efficiently excising the pBluscript phagemid (approx 3 kb) from the λZAPII vector with the help of the ExAssist helper phage and SOLR cells.

12. The cDNA insert in the pBluscript plasmid can be directly sequenced with six unique primers located at the flanking regions of the cDNA insert. Multiple restriction sites in the polylinker allow easily subcloning the cDNA insert into other vectors.

13. It is highly recommended to optimize the binding conditions for both primary and secondary antibodies on the nitrocellulose membranes unless previous Western blot analysis has already provided such information. There is no specific formula for antibody screening because each primary antibody appears to have its own optimized binding conditions.

14. Because there is an inducible *lac* promoter upstream from the *LacZ* gene where the cDNA fragments are inserted, the purpose of the IPTG treatment is to induce expression of the *LacZ*-insert fusion proteins from the promoter. It should be noticed that in theory, only one-third of the cDNA inserts can generate in-frame

fusion proteins with the *LacZ* as a result of random ends of the cDNA fragments cloned in the vector. If the library is made nonunidirectionally, the possibility of producing the fusion proteins from the cDNA inserts will be further reduced by 50%. Therefore, it is better to use a unidirectional λZAP library.

15. Many other ^{125}I-labeled secondary antibodies can be used, such as Protein G, Goat antimouse or antirabbit or antihuman IgG. Other nonradioisotope screening approaches with the secondary antibody conjugated to alkaline phosphatase (AP) or biotin can also be used.

16. Almost all computer DNA analysis softwares contain an oligo design program, such as GeneRunner, Vector NTI, and DNA Star. Although there are general rules for designing an oligonucleotide used in either PCR or sequencing or antisense studies, PCR primers with a higher Tm (over 70°C) are preferred to be used in a two-step PCR. In the two-step PCR, after denaturing at 94°C in the first step, the second step that combines both annealing and extension steps into one single step, is performed at 68°C , which can improve specificity and reduce background of the PCR.

17. A degenerate primer contains all possible oligonucleotides that encode for a given protein sequence by using its variable genetic codes. If the given protein sequence has many amino acids which have four or more codons, the number of the possible oligonucleotides within the primer will be very high, which can greatly dilute the concentration of the actual primer sequence since only one of the oligonucleotides represents the protein sequence. Therefore, it is recommended to select the protein sequence containing amino acids with less codons if possible. Another way to decrease the olgonucleotide numbers is to use only partial codons based upon codon usages for a given amino acid. An example is given in **Table 1**. The sequence contains $2 \times 2 \times 2 \times 6 \times 2 \times 4 = 334$ oligonucleotides, each 21 bases in length. However, the number of the oligonucleotides can be greatly reduced to $2 \times 2 \times 2 \times 2 \times 2 = 32$ by ignoring the codons with lower codon frequency for *Leu* and *Thr*. The codon usage in various species was described by Sharp and Lathe et al. *(19,20)*.

18. Any kind of cDNA library stock can serve as the PCR template. Usually, 1 μL of the cDNA library stock contains 10^7–10^9 PFU or clones, which can be easily screened in a single PCR tube. Performing the same PCR in several PCR tubes can also increase the clone numbers to be screened. It is highly recommended to perform a PCR with appropriate primers in the cDNA library that will be considered to be screened through hybridization screening. Such PCR will provide useful information whether the cDNA library contains the gene interested. If the PCR cannot detect any signals, it is unlikely that the cDNA clones will be obtained by hybridization screening. Although many vectors are available for cloning PCR products, I prefer using pCRII-TOPO vector because of its high efficiency, quickness, and less DNA input.

19. In all the cDNA libraries, the cDNA fragments are cloned in the certain vectors. Such cloning provides the anchor sequences for designing primers that can be used in 5'RACE and 3'RACE PCRs. In the 5'RACE and 3'RACE PCRs, the further 5'-end or 3'-end sequences can be easily amplified by vector primers from

Table 1
A Degenerate Primer for a Seven Amino Acid Sequence

Amino acid sequence	Lys	Tyr	Leu	Met	Glu	Thr	Trp
All possible DNA sequences (total 334 oligonucleotides)			A			A	
	A	T	G		A	G	
	AA	TA	CT	ATG	GA	AC	TGG
	G	C	C		G	C	
			T			T	
			T				
			TT				
			G				
Designed degenerated primer (total 32 oligonucleotides)	A	T	G		A	A	
	AA	TA	CT	ATG	GA	AC	TGG
	G	C	C		G	C	

flanking regions of the cDNA inserts and primers from the partial PCR fragment sequence. Once the potential translation start and stop codons are identified in the 5'-end and 3'-end PCR fragments, the primers from the 5'- and 3'-noncoding regions can be used in PCR to generate a full-length cDNA fragment.

Acknowledgment

References

1. Chen, Y., Mestek, A., Liu, J., Hurley, J. A., and Yu, L. (1993) Molecular cloning and functional expression of a μ-opioid receptor from rat brain. *Mol. Pharmacol.* **44,** 8–12.
2. Wang, J. B., Imai, Y., Eppler, C. M., Gregor, P., Spivak, C. E., and Uhl, G. R. (1993) μ opiate receptor: cDNA cloning and expression. *Proc Nat Acad Sci USA* **90,** 10,230–10,234.
3. Thompson, R. C., Mansour, A., Akil, H., and Watson, S. J. (1993) Cloning and pharmacological characterization of a rat μ opioid receptor. *Neuron* **11,** 903–913.
4. Minami, M., Toya, T., Katao, Y., Maekawa, K., Nakamura, S., Onogi, T., et al. (1993) Cloning and expression of a cDNA for the rat kappa-opioid receptor. *FEBS Lett.* **329,** 291–295.

5. Raynor, K., Kong, H., Chen, Y., Yasuda, K., Yu, L., Bell, G. I., et al. (1994) Pharmacological characterization of the cloned kappa-, δ- , and μ-opioid receptors. *Mol. Pharmacol.* **45,** 330–334.

6. Chen, Y., Mestek, A., Liu, J., and Yu, L. (1993) Molecular cloning of a rat kappa opioid receptor reveals sequence similarities to the μ and δ opioid receptors. *Biochem. J.* **295,** 625–628.

7. Pan, Y.-X., Cheng, J., Xu, J., Rossi, G. C., Jacobson, E., Ryan-Moro, J., et al. (1995) Cloning and functional characterization through antisense mapping of a kappa₃-related opioid receptor. *Mol. Pharmacol.* **47,** 1180–1188.

8. Chen, Y., Fan, Y., Liu, J., Mestek, A., Tian, M., Kozak, C. A., et al. (1994) Molecular cloning, tissue distribution and chromosomal localization of a novel member of the opioid receptor gene family. *FEBS Lett.* **347,** 279–283.

9. Keith, D., Jr., Maung, T., Anton, B., and Evans, C. (1994) Isolation of cDNA clones homologous to opioid receptors. *Regulat. Peptides* **54,** 143–144.

10. Lachowicz, J. E., Shen, Y., Monsma, F. J., Jr., and Sibley, D. R. (1995) Molecular cloning of a novel G protein-coupled receptor related to the opiate receptor family. *J. Neurochem.* **64,** 34–40.

11. Wick, M. J., Minnerath, S. R., Lin, X., Elde, R., Law, P.-Y., and Loh, H. H. (1994) Isolation of a novel cDNA encoding a putative membrane receptor with high homology to the cloned μ, δ, and kappa opioid receptors. *Mol. Brain Res.* **27,** 37–44.

12. Mollereau, C., Parmentier, M., Mailleux, P., Butour, J. L., Moisand, C., Chalon, P., et al. (1994) ORL-1, a novel member of the opioid family: cloning, functional expression and localization. *FEBS Lett.* **341,** 33–38.

13. Fukuda, K., Kato, S., Mori, K., Nishi, M., Takeshima, H., Iwabe, N., et al. (1994) cDNA cloning and regional distribution of a novel member of the opioid receptor family. *FEBS Lett.* **343,** 42–46.

14. Bouvier, C., Unteutsch, A., Hagen, S., Zhu, W. Z., Bunzow, J. R., and Grandy, D. K. (1994) Agonist properties of methadone at the cloned rat μ opioid receptor. *Regulat. Peptides* **54,** 31–32.

15. Wang, J. B., Johnson, P. S., Imai, Y., Persico, A. M., Ozenberger, B. A., Eppler, C. M., et al. (1994) cDNA cloning of an orphan opiate receptor gene family member and its splice variant. *FEBS Lett.* **348,** 75–79.

16. Halford, W. P., Gebhardt, B. M., and Carr, D. J. J. (1995) Functional role and sequence analysis of a lymphocyte orphan opioid receptor. *J. Neuroimmunol.* **59,** 91–101.

17. Short, J. M., Fernandez, J. M., Sorge, J. A., and Huse, W. D. (1988) Lambda ZAP: a bacteriophage lambda expression vector with in vivo excision properties. *Nuc. Acids Res.* **16,** 7583–7600.

18. Pasternak, G. W. and Pan, Y. X. (2000) Antisense mapping: assessing functional significance of genes and splice variants. *Meth. Enzymol.* **314,** 51–60.

19. Sharp, P. M., Cowe, E., Higgins, D. G., Shields, D. C., Wolfe, K. H., and Wright, F. (1988) Codon usage patterns in Escherichia coli, Bacillus subtilis, Saccharomyces cerevisiae, Schizosaccharomyces pombe, Drosophila melanogaster and Homo sapiens; a review of the considerable within- species diversity. *Nuc. Acids Res.* **16,** 8207–8211.

20. Lathe, R. (1985) Synthetic oligonucleotide probes deduced from amino acid sequence data. Theoretical and practical considerations. *J. Mol.Biol.* **183,** 1–12.

2

Expression of Opioid Receptors in Mammalian Cell Lines

Ying-Xian Pan

1. Introduction

Three major opioid receptors, δ (DOR-1) *(1,2)*, μ (MOR-1) *(3–5)*, and κ (KOR-1) *(6–9)*, and an opioid-like receptor (ORL-1/KOR-3) *(10–16)* have been identified by molecular cloning. Although each of the cloned opioid receptors is derived from a single gene, a number of alternatively spliced variants from their own genes have been isolated *(16–20)*. One extraordinary example is the mouse μ opioid receptor (*Oprm*) gene in which alternative splicing of the fourteen exons generates at least 15 variants *(21–25)*. It is difficult to study these cloned receptors in vivo. But expressing individual receptors in a particular cell line through transfection of the cloned receptor cDNAs offers a valuable system for exploring their pharmacological and biological properties, as well as their structure and function relationships. To successfully express the cloned receptors, several factors must be considered.

1.1. Choice of Cell Lines

Criteria for choosing a cell line for expression of opioid receptors include no expression of endogenous opioid receptors, easy handling, fast growing, and accessibility for transfections. Several nonneuronal cell lines, such as the Chinese hamster ovary (CHO), the human embryonic kidney (HEK) 293, and the African green monkey kidney (COS-7) cell lines, are commonly used for expressing the cloned opioid receptors. However, differential expression of endogenous G-proteins and other factors involved in the signal transduction pathways among the cell lines may contribute to different pharmacological or biochemical profiles for the same receptors. Therefore, functional comparison

between two or more receptors should be made in the same cell line with cautious interpretation of the results in terms of the restricted cell environment.

1.2. Choice of Mammalian Expression Vectors

For expression in a mammalian cell line, an opioid receptor cDNA containing its own or a Kozak consensus translation initiation site *(26)* has to be subcloned into mammalian expression vectors. Many mammalian expression vectors are available from a variety of sources. All mammalian expression vectors contain components necessary for both their propagation in bacteria and the transcription of the inserted DNA in mammalian cells. A cytomegalovirus (CMV) promoter or a SV40 promoter is commonly used for permitting high-level constitutive transcription of the inserted DNA in various mammalian cell lines, whereas a polyadenylation signal site is always built at the downstream of the inserted DNA for efficient transcription termination and polyadenylation of mRNA. However, choosing a vector mainly relies on the selectivity of its polylinker for efficient cloning and the availability of its antibiotic resistant genes for selection of stable cell clones. Additionally, many inducible vector systems are available for permitting control of transcription level of the inserted DNA. Common inducible systems include the Tet-Off or Tet-On system (ClonTech and Invitrogen) regulated through tetracycline, the Ecdysone-inducible system (Invitrogen) responsive to Muristerone A and the LacSwitch inducible system (Stratagene) induced by isopropylthiogalactose (IPTG). Recently, a Flp-In vector system (Invitrogen) has been developed to generate stable cell lines through Flp recombinase-mediated integration, in which a cDNA is integrated into a specific and transcriptionally active genomic site in the host cells.

1.3. Choice of Transfection Methods

Methods such as diethylaminoethyl (DEAE)-dextran transfection, calcium phosphate transfection, electroporation, and liposome-mediated transfection have been developed to introduce DNA into mammalian cells by using different mechanisms *(27)*. Choice of a transfection method depends upon the type of cell lines used, the detailed procedures, and overall costs. For a given cell line, different methods with the same DNA may have different transfection efficiencies by severalfold. For instance, the rank order of transfection efficiency in CHO cells from our laboratory is: LipofectAmine (Invitrogen, one type of liposome-mediated transfections) > DEAE-dextran transfection > Calcium phosphate transfection. The procedures in most liposome-mediated transfections are more convenient than those of DEAE-dextran or Calcium phosphate transfection, but the cost of the liposome-mediated transfection is

much higher than those of DEAE-dextran or Calcium phosphate transfection if a large number of cells are used.

1.4. Transient Transfection and Stable Transfection

DNA can be transiently or stably transfected into cell lines, depending upon the type of applications used in the transfected cell lines. A transient transfection allows the transfected genes to be expressed within a short period of time and the cells are usually harvested or analyzed after a 24–72 h transfection. The transient transfection provides a convenient way to obtain results quickly. A stable transfection allows obtaining individual cells in which the transfected DNA is integrated into the active transcription sites of the host genome through an antibiotic selection that is often based upon expression of the antibiotic resistant gene in the same transfected DNA. It takes a relatively long time, usually 2 wk–2 mo, depending on the cell types and the antibiotics, to obtain the stable cells. However, the cells stably expressing the transfected receptors at a relatively constant level are valuable for applications that require a large number of cells, such as receptor binding and G-protein coupling studies.

This chapter describes procedures for cloning the cDNA into the mammalian expression vector. Also presented are both a transient transfection with DEAE-dextran and a stable transfection with LipofectAmine reagent in CHO cells. Finally, methods to verify expression of the transfected cDNAs are briefly discussed.

2. Materials

1. pcDNA3.1 vector series (Invitrogen) (*see* **Note 1**).
2. Restriction enzymes with 10× reaction buffers (New England BioLab) (*see* **Note 2**).
3. DNA Clean and Concentrator (ZYMO Research) (*see* **Note 3**).
4. T4 DNA ligase with 10× ligation buffer (NEB).
5. JM109 competent cells (> 10^8 colony-forming unit (cfu)/µg) (Promega) (*see* **Note 5**).
6. Plasmid Mini and Maxi kits (Qiagen).
7. 1% agarose gel with 0.2 µg/mL ethidium bromide.
8. TBE buffer: 89 mM Tris base, 89 mM boric acid, and 2 mM ethylenediamine tetraacetic acid (EDTA) in H_2O.
9. F12 medium (Invitrogen).
10. Fetal bovine serum (FBS).
11. pCH110 vector (Amersham).
12. Phosphate-buffered saline (PBS): 8 mM Na_2HPO_4, 1.5 mM KH_2PO_4, 137 mM NaCl, and 27 mM KCl in H_2O. Adjust pH to 7.4.
13. DEAE-dextran stock: Dissolve 5 g DEAE-dextran (Amersham) in 100 ml of PBS. Sterilize the solution by filtrating through a 0.22-µm filter and store at –20°C.

14. 0.25 *M* chloroquine. Dissolve 6.45 g chloroquine in 50 mL of H_2O. Sterilize by filtrating a 0.22 μm filter and store in a foil-wrapped tube at –20°C.
15. CHO cells (ATCC).
16. OPTI-MEM I reduced serum medium (Invitrogen).
17. LipofectAmine (Invitrogen).
18. 10% dimethyl sulfoxide (DMSO) solution in PBS. Filtrate the solution through a 0.22-μm filter.
19. Treated-Tris-HCl buffer: 50 m*M* Tris-HCl, pH 7.4 at 25°C, 1 m*M* EDTA, and 100 m*M* NaCl.
20. Water bath.
21. Tissue culture hood.
22. CO_2 cell culture incubator.

3. Methods

3.1. Cloning the cDNA Fragment into pcDNA3.1 (see *Note 1*)

3.1.1. Digesting the cDNA and pcDNA3.1 with Restriction Enzymes (see *Note 2*)

1. For digesting with single restriction enzyme, pipet 5–10 μg of DNA, 3 μL of 10× restriction buffer, and appropriate volume of ddH_2O into a sterile microcentrifuge tube. Then add <3 μL of 10–20 U restriction enzyme to bring the final volume to 30 μL. Incubate the tube at the proper temperature (most at 37°C) for >1 h.
2. For digesting with two restriction enzymes, simultaneously cut DNA with the two enzymes in the same reaction if both enzymes are active in the same buffer. However, if one buffer cannot fit two enzymes, digest DNA with one enzyme at a time. Purify the digested DNA with a DNA Clean & Concentrator kit by following the manufactory protocol to remove the buffer and enzyme. Then digest the purified DNA with the second enzyme.

3.1.2. Purifying the Digested DNA and pcDNA3.1 (see *Note 3*)

1. Run the digested DNA on 1% agarose gel in TBE buffer.
2. Cut off the gel containing the desired DNA band and extract the DNA from the gel by using a Zymoclean Gel DNA Recovery kit by following the manufactory protocol.
3. Purify the digested pcDNA3.1 with the DNA Clean & Concentrator.
4. Analyze a small portion of the purified DNA fragment and pcDNA3.1 on 1% agarose gel to estimate the purity and quantity of the DNA and pcDNA3.1 for next ligation reaction.

3.1.3. Ligating the Digested DNA Fragment into the Digested pcDNA3.1 (see *Note 4*)

1. Add the digested DNA fragment and the digested pcDNA3.1 at 5:1–10:1 ratio in a sterile 1.5-mL microcentrifuge tube and bring the volume to 17 μL with H_2O.
2. Incubate the tube at 37°C for 5 min and place the tube on ice for 3 min.
3. Add 2 μL of 10× T4 DNA ligase buffer and 1 μL of T4 DNA ligase (400 U), and gently vortex the tube.
4. Incubate the tube at room temperature overnight.

3.1.4. Transformation and Isolation

1. Transform the ligated DNA into JM109 competent cells by following the manufactory protocol (*see* **Note 5**).
2. Isolate individual plasmids from 5–10 colonies by using a Pladmid Miniprep kit (*see* **Note 6**).
3. Digest approx 0.5 µg of the isolated DNA with appropriate restriction enzymes to identify the constructs with right inserts.
4. Further confirm the orientation and sequence of the inserts by sequencing with proper primers.

3.2. Transient Transfection with DEAE-dextran Method in CHO Cells (see *Note 7*)

3.2.1. Preparation of DNA and CHO Cells

1. Purify DNA with a Plasmid Maxi prep kit. Estimate the DNA concentration and purity by measuring its OD_{260} and ratio of OD_{260}/OD_{280} in a ultraviolet (UV) spectrophotometer, respectively.
2. Thaw a vial of frozen CHO cells (approx 10^7 cells) quickly in a 37°C water bath and transfer the cells into a 100-mm tissue culture dish containing 15 ml of F12 medium with 10% FBS (complete medium).
3. Grow the cells in a humidified culture incubator with 5% CO_2 at 37°C to approx 90% confluence.
4. To expend the cells, aspirate the medium, add 5 mL of PBS containing 1 m*M* EDTA, incubate at 37°C for 5 min, lift the cells by pipetting with a 10-mL pipet, and transfer the lifted cells equally into five 150-mm tissue culture dishes, each containing 25 mL of complete medium.
5. Grow the cells to 85–90% confluence at the time of transfection (*see* **Note 8**).

3.2.2. Preparation of DNA-DEAE-Dextran Complex and Transfection Medium

1. For transfection with five 150 mm dishes, mix 200 µg of DNA with appropriate volume of PBS in a sterile 50-mL conical tube.
2. Add 0.75 mL of DEAE-dextran stock (50 mg/mL) into the tube with a final volume of 3.75 mL and gently swirl the tube.
3. Incubate the tube at room temperature for 5 min.
4. For transfection with five 150-mm dishes, mix 60 mL of serum-free F12 medium with 24 µL of 0.25 *M* Chloroquine stock in a 100-mL sterile glass bottle.
5. Add 3.75 mL of the DNA-DEAE-dextran mixture into the bottle and gently mix.

3.2.3. Incubation and Shocking

1. Aspirate the complete media from the dishes, wash the dishes with 15 mL of serum-free F12 media, and completely remove the F12 medium.
2. Add 12.7 mL of the transfection medium into each dish.
3. Incubate the dishes in the incubator at 37°C for 3 h.

4. Aspirate the transfection medium and add 10 mL of 10% DMSO solution (*see* **Note 9**).
5. Incubate the dishes at room temperature for 90–120 s.
6. Aspirate 10% DMSO solution and wash the cells with 15 ml of serum-free F12 medium once.
7. Add 20 mL of complete medium and incubate the dishes in the incubator with 5% CO_2 at 37°C.
8. Harvest or analyze the cells after 24–72 h.

3.3. Stable Transfection with LipofectAmine in CHO Cells (see *Note 7 and 10*)

3.3.1. Determining the Optimum Concentration of Antibiotics for Selection (see *Note 11*)

1. Pass CHO cells as described in **Subheading 3.2.1.** into one 12-well plates with 1:15 dilution.
2. Add 12 different concentrations of antibiotics into individual 12 wells.
3. Replace the medium with fresh medium containing the antibiotic every 3 d.
4. Choose the concentration in which the antibiotic kills 99% cells after 10–14 d selection.

3.3.2. Preparation of DNA, CHO Cells and DNA-LipofectAmine Complex

1. Perform DNA purification as described in **Subheading 3.2.1.** (*see* **Note 12**).
2. Grow and expend the cells as described in **Subheading 3.2.1.**, **steps 2–5** except for using a 6-well tissue culture plate and growing the cells to 80% confluence at the time of transfection.
3. Label two sterile 1.5-mL tubes as A and B. In A tube, mix 1 μg of DNA with 100 μL of OPTI-MEM medium. In B tube, dilute 6 μL of LipofectAmine into 100 μL of OPTI-MEM medium.
4. Transfer 106 μL of the LipofectAmine-containing medium from B tube to A tube containing the DNA and gently vortex.
5. Incubate A tube at room temperature for 30 min.

3.3.3. Incubating DNA-LipofectAmine Complex with CHO Cells

1. Aspirate the medium from the 6-well plate.
2. Wash the cells with serum-free F12 medium once and remove the medium.
3. Add 0.8 mL of serum-free F12 medium into A tube containing the complex, and gently mix.
4. Transfer the diluted solution (approx 1 mL) into the washed six well.
5. Incubate the plate in the incubator at 37°C for 5–8 h (not overnight).
6. After 5–8 h incubation, aspirate the medium containing the complex and add 2 mL of complete medium.
7. Continue incubating the plate for 24–48 h.

3.3.4. Selecting Stably Transfected Cells with an Appropriate Antibiotics

1. After 24–48 h of incubation, aspirate the complete medium and wash the cells with 2 mL of serum-free F12 medium once.
2. Add 0.5 mL of PBS containing 1 m*M* EDTA.
3. Incubate the plate at 37°C for 5 min.
4. Lift the cells with a pipet and transfer the lifted cells into one 150-mm culture dish containing 25 ml of complete medium with the appropriate antibiotics (approx 1:15 pass).
5. Incubate the dish for 10–14 d until individual colonies grow. During the incubation, replace the medium with the fresh selective medium every 3 d.

3.3.5. Isolating Individual Colonies (see **Note 13**)

1. Aspirate the medium and rinse the cells with PBS once.
2. Add 20 mL of PBS.
3. Pick up 10–20 foci one at a time by using a 200 μL pipet under a microscope with 10× objective.
4. Find the colony under microscope, loosen the colony by gently scraping with the pipet tip.
5. Suck out 30 μL of PBS containing the loosened colony into the tip, transfer into a well of the 96-well plate containing 30 μL PBS with 2 m*M* EDTA, and gently mix with the pipet.
6. Incubate the 96 well at room temperature for 5–20 min.
7. Transfer the cell suspension from the 96 well into a six-well plate containing 2 mL of the selective medium.
8. Continue passing the cells from the six well to large plates until appropriate amount of the cells are obtained for further analysis.

3.4. Verification of Opioid Receptor Expression in Transfected Cells

3.4.1. Verification of the Expression by Receptor Binding

1. Prepare cell membranes as in our previous studies *(23–25,28)*. Rinse the cells with PBS twice and add approx 5–10 mL PBS just to cover the plate.
2. Scrap the cells off the plates with a rubber policeman (*see* **Note 14**).
3. After collecting the cells in a centrifuge tube, spin the tube at 1000 *g*, resuspend the cells in cold Treated-Tris-HCl buffer containing 0.1 m*M* phenylmethanesulfonyl fluoride and homogenize with a polytron homogenizer at 4°C for 30 s.
4. Centrifuge the homogenate at 20,000*g* for 30 min at 4°C, resuspend the membrane pellet in 0.32 *M* sucrose, and store at –80°C.
5. Choose an appropriate radiolabeled ligand for a receptor binding assay: for all types of opioid receptors, [³H]-Diprenorphine and [³H]-Naloxone; for μ opioid

receptors, [³H]-DAMGO; for δ opioid receptors, [³H]-DPDPE; for κ opioid receptors, [³H]-U69593; and for ORL-1/KOR-3, [³H]-OFQ or [¹²⁵I]-OFQ.

6. Perform binding assays *(23,28–31)*.

3.4.2. Verification of mRNA Expression by RT-PCR or Northern Blot Analysis

1. To determine transcription level of the transfected receptor DNA, extract total RNA from 10^6 cell (one 6 well) by using a RNeasy mini kit (Qiagen).
2. Perform RT reaction with Superscript II reverse transcriptase (Invitrogen) and random hexamers.
3. Perform PCR by using the first-strand cDNA from the RT reaction as template with appropriate primers derived from the transfected opioid receptor sequences *(10,19,25)*.
4. Analyze the PCR products on 1% agarose gel.
5. Perform Northern blot analysis with an appropriate probe *(10,23,25,32)* .

3.4.3. Verification of Protein Expression by Western Blot or Immunostaining

Perform Western blot analysis or immunostaining with appropriate polyclonal or monoclonal antibodies on the whole cells or the isolated membrane *(10,33)*.

4. Notes

1. I prefer using the pcDNA3.1 vector series since its (+) and (–) versions offer a polylinker with 16 unique cloning sites in both orientations, providing more choices for cloning. It also offers three sets of different selection markers, neomycin, hygromycin, and zeocin, which allow for selection of double- or triple-stable cells with cotransfection of different cDNA clones. The first step of the cloning is to find unique restriction enzyme sites in both the polylinker of the vector and the cDNA-containing plasmid, so that they can lift out the entire cDNA fragment from the plasmid without cutting its own coding regions. Using the fragments with different cohesive ends can facilitate unidirectional ligation. If no appropriate restriction enzyme sites are available to lift the fragment from its plasmid, the fragment containing proper restriction sites at its both 5'- and 3'-ends can be generated by PCR with the gene-specific sense and antisense primers having appropriate restriction sequences at their 5'-end. It is recommended to use a high-fidelity DNA polymerase in PCR to reduce potential mutations and confirm the amplified sequence after cloning.
2. In general, 1 U of restriction enzyme can digest 1 μg of DNA at its optimum temperature in 1 hour. However, I often add more enzymes to achieve complete digestion. Most enzymes are stored in 50% glycerol, but they are usually less active in >5% glycerol. Therefore, it is not recommended to add more than 1 μL of enzyme in a 10-μL reaction. Although restriction enzymes are available from

many companies, using enzymes from one company makes easy selection of the appropriate buffer for double digestion because most companies already formulate different enzyme activities in different buffers.

3. The desired DNA fragment must be separated and purified from its associated vector sequence, which can be easily done by using a gel extraction procedure. Many DNA cleaning and gel extraction kits are available from various companies. No matter the type of kit used, it is better to elute DNA with water rather than with the elution buffer provided in the kits. Though the yield may be low, elution with water prevents possible inhibition of the following ligation reaction by an elution buffer.

4. The ratio of DNA to vector is critical for efficient ligation. In our experience, the ratio of 5:1–10:1 is suitable for a cohesive-end ligation, whereas a blunt-end ligation requires an even higher ratio ranging from 10:1 to 20:1.

5. Other types of competent cells like XL1-Blue (Stratagene), TOP10F', or DH10 (Invitrogen) can be used. Transformation efficiency for all the competent cells can be greatly reduced by repeating thaw-frozen cycles. Aliquot the unused cells, quickly freeze on dry ice and store at –80°C.

6. Any other kits or protocols for isolating plasmid DNAs can be used. It is highly recommended to confirm the clones through sequencing even if the result from restriction enzyme digestion has been satisfied.

7. The protocols for DEAE-dextran transfection and LipofectAmine transfection described in this chapter have been optimized in our CHO cells. However, if another cell line or a CHO cell line from a different source is used, the protocols may not be useful. It is highly recommended to optimize transfection conditions for each new cell line with a vector containing a reporter gene to determine the transfection efficiency. Luciferase and β-galactosidase (*LacZ*) are commonly used as the reporters. We use pCH110 vector containing a *LacZ* reporter under control of a SV40 promoter for optimization. Transfection efficiency can be easily determined by β-gal staining or by measuring β-gal activity with available kits (Promega and Boehringer Mannheim). The optimized conditions include the ratio and the amount of the DNA and its reactive reagents, the cell density reached before transfection, the incubation time after adding the DNA-reagent mixture, and the additional shock steps in DEAE-dextran transfection. DEAE-dextran transfection is suitable for transiently transfecting a large number of CHO cells, whereas LipofectAmine transfection is mainly used for obtaining stable clones. However, a small number of the cells from the transient transfection can also be used for selecting stable clones.

8. It is crucial to manipulate mammalian cells under strict sterile conditions to prevent contamination by bacteria or fungi. All materials including media, reagents, buffers and glassware should be sterilized by either standard autoclaving or filtering through a 0.22-μm filter. Standard hood operations and incubator maintenance should be strictly followed. The protocol described here is for transfecting 5 × 150 mm dishes. If more or less dishes are used, all the solutions and volumes can be multiplied or divided based upon their surface areas.

9. DMSO shock can increase transfection efficiency by 2–3 folds in our CHO cells, but it may not be necessary for other cell lines. The shock time, from 90–120 s, but no more than 120 s, should be followed to avoid overshocking the cells.
10. Many types of liposome-mediated transfection reagents are available from same or different companies. There are also several formulas even with the same type of lipid. For instance, LipofectAmine has three different formulas, LipofectAmine 2000, LipofectAmine Plus and LipofectAmine. In our CHO cells, transfection with LipofectAmine is better than that with LipofectAmine Plus or LipofectAmine 2000. However, in our HEK293 cells, transfection with LipofectAmine Plus is more efficient than that with LipofectAmine or LipofectAmine 2000.
11. Cell density can greatly influence the antibiotic sensitivity. If a selection starts with high cell density, cells may be killed by overcrowding rather than by antibiotics. Therefore, the optimum concentration of antibiotics should be selected under the cell density similar to that plated in actual stable selection.
12. Because the stable transfection with a small number of cells needs much less DNA than transient transfection, the DNA isolated from the miniprep is usually enough for the stable transfection. However, if the DNA concentration is too low, it is necessary to increase DNA concentration by either ethanol precipitation or by a DNA clean and concentrator kit.
13. Isolating individual colonies with a pipet is easier and faster than with traditional cloning cylinders. If the cell growth rate is slow, the lifted colony can be transferred into a smaller well (12-well or 24-well plate) so that the cells are not diluted too much.
14. Opioid receptor binding is very sensitive to trypsin. Do not lift the cells with trypsin when the cells are passed for binding.

Acknowledgments

References

1. Kieffer, B. L., Befort, K., Gaveriaux-Ruff, C., and Hirth, C. G. (1992) The δ-opioid receptor: Isolation of a cDNA by expression cloning and pharmacological characterization. *Proc. Nat. Acad. Sci. USA* **89,** 12048–12052.
2. Evans, C. J., Keith, D. E., Jr., Morrison, H., Magendzo, K., and Edwards, R. H. (1992) Cloning of a delta opioid receptor by functional expression. *Science* **258,** 1952–1955.
3. Chen, Y., Mestek, A., Liu, J., Hurley, J. A., and Yu, L. (1993) Molecular cloning and functional expression of a μ-opioid receptor from rat brain. *Mol. Pharmacol.* **44,** 8–12.
4. Wang, J. B., Imai, Y., Eppler, C. M., Gregor, P., Spivak, C. E., and Uhl, G. R. (1993) μ opiate receptor: cDNA cloning and expression. *Proceed. Nat. Acad. Sci. USA* **90,** 10,230–10,234.

5. Thompson, R. C., Mansour, A., Akil, H., and Watson, S. J. (1993) Cloning and pharmacological characterization of a rat μ opioid receptor. *Neuron* **11,** 903–913.

6. Minami, M., Toya, T., Katao, Y., Maekawa, K., Nakamura, S., Onogi, T., et al. (1993) Cloning and expression of a cDNA for the rat kappa-opioid receptor. *FEBS Lett*. **329,** 291–295.

7. Raynor, K., Kong, H., Chen, Y., Yasuda, K., Yu, L., Bell, G. I., et al. (1994) Pharmacological characterization of the cloned κ-, δ- , and μ-opioid receptors. *Mol. Pharmacol*. **45,** 330–334.

8. Chen, Y., Mestek, A., Liu, J., and Yu, L. (1993) Molecular cloning of a rat kappa opioid receptor reveals sequence similarities to the μ and δ opioid receptors. *Biochem. J*. **295,** 625–628.

9. Lai, J., Ma, S., Zhu, R.-H., Rothman, R. B., Lentes, K.-U., and Porreca, F. (1994) Pharmacological characterization of the cloned kappa opioid receptor as a kappa$_{1b}$ subtype. *Neuroreport* **5,** 2161–2164.

10. Pan, Y.-X., Cheng, J., Xu, J., Rossi, G. C., Jacobson, E., Ryan-Moro, J., et al. (1995) Cloning and functional characterization through antisense mapping of a kappa$_3$-related opioid receptor. *Molec. Pharmacol*. **47,** 1180–1188.

11. Chen, Y., Fan, Y., Liu, J., Mestek, A., Tian, M., Kozak, C. A., et al. (1994) Molecular cloning, tissue distribution and chromosomal localization of a novel member of the opioid receptor gene family. *FEBS Lett*. **347,** 279–283.

12. Lachowicz, J. E., Shen, Y., Monsma, F. J., Jr., and Sibley, D. R. (1995) Molecular cloning of a novel G protein-coupled receptor related to the opiate receptor family. *J. Neurochem*. **64,** 34–40.

13. Wick, M. J., Minnerath, S. R., Lin, X., Elde, R., Law, P.-Y., and Loh, H. H. (1994) Isolation of a novel cDNA encoding a putative membrane receptor with high homology to the cloned μ, δ, and kappa opioid receptors. *Molec. Brain Res*. **27,** 37–44.

14. Mollereau, C., Parmentier, M., Mailleux, P., Butour, J. L., Moisand, C., Chalon, P., et al. (1994) ORL-1, a novel member of the opioid family: cloning, functional expression and localization. *FEBS Lett*. **341,** 33–38.

15. Fukuda, K., Kato, S., Mori, K., Nishi, M., Takeshima, H., Iwabe, N., et al. (1994) cDNA cloning and regional distribution of a novel member of the opioid receptor family. *FEBS Lett*. **343,** 42–46.

16. Wang, J. B., Johnson, P. S., Imai, Y., Persico, A. M., Ozenberger, B. A., Eppler, C. M., et al. (1994) cDNA cloning of an orphan opiate receptor gene family member and its splice variant. *FEBS Lett*. **348,** 75–79.

17. Gavériaux-Ruff, C., Peluso, J., Befort, K., Simonin, F., Zilliox, C., and Kieffer, B. L. (1997) Detection of opioid receptor mRNA by RT-PCR reveals alternative splicing for the δ- and kappa-opioid receptors. *Molec. Brain Res*. **48,** 298–304.

18. Halford, W. P., Gebhardt, B. M., and Carr, D. J. J. (1995) Functional role and sequence analysis of a lymphocyte orphan opioid receptor. *J. Neuroimmunol*. **59,** 91–101.

19. Pan, Y. X., Xu, J., Wan, B. L., Zuckerman, A., and Pasternak, G. W. (1998) Identification and differential regional expression of KOR-3/ORL-1 gene splice variants in mouse brain. *FEBS Lett* **435,** 65–68.

20. Curro, D., Yoo, J. H., Anderson, M., Song, I., Del Valle, J., and Owyang, C. (2001) Molecular cloning of the orphanin FQ receptor gene and differential tissue expression of splice variants in rat. *Gene* **266,** 139–145.

21. Bare, L. A., Mansson, E., and Yang, D. (1994) Expression of two variants of the human μ opioid receptor mRNA in SK-N-SH cells and human brain. *FEBS Lett*. **354,** 213–216.

22. Zimprich, A., Simon, T., and Hollt, V. (1995) Cloning and expression of an isoform of the rat μ opioid receptor (rMOR 1 B) which differs in agonist induced desensitization from rMOR1. *FEBS Lett*. **359,** 142–146.

23. Pan, Y. X., Xu, J., Bolan, E. A., Abbadie, C., Chang, A., Zuckerman, A., et al. (1999) Identification and characterization of three new alternatively spliced mu opioid receptor isoforms. *Molec*. *Pharmacol*. **56,** 396–403.

24. Pan, Y.-X., Xu, J., Bolan, E. A., Chang, A., Mahurter, L., Rossi, G. C., et al. (2000) Isolation and expression of a novel alternatively spliced mu opioid receptor isoform, MOR-1F. *FEBS Lett*. **466,** 337–340.

25. Pan, Y.-X., Xu, J., Rossi, G., Bolan, E., Xu, M. M., Mahurter, L., et al. (2001) Generation of the mu opioid receptor (MOR-1) protein by three new splice variants of the *Oprm* gene. *Proc*. *Natl*. *Acad*. *Sci*. *USA* **98,** 14,084–14,089.

26. Kozak, M. (8-20-1987) At least six nucleotides preceding the AUG initiator codon enhance translation in mammalian cells. *J*. *Mol*. *Biol*. **196,** 947–950.

27. Sambook, J., Fritsh, E., and Maniatis, T. (1989) *Molecular Cloning: A Laboratory Manual*, 2nd Ed., Cold Spring Harbor Press, Cold Spring Harbor, NY.

28. Goldberg, I. E., Rossi, G. C., Letchworth, S. R., Mathis, J. P., Ryan-Moro, J., Leventhal, L., et al. (1998) Pharmacological characterization of endomorphin-1 and endomorphin-2 in mouse brain. *J*. *Pharmacol*. *Experiment*. *Therap*. **286,** 1007–1013.

29. Brown, G. P., Yang, K., Ouerfelli, O., Standifer, K. M., Byrd, D., and Pasternak, G. W. (1997) ^{3}H-morphine-6β-glucuronide binding in brain membranes and an MOR-1-transfected cell line. *J*. *Pharmacol*. *Experiment*. *Therap*. **282,** 1291–1297.

30. Pan, Y.-X., Xu, J., Ryan-Moro, J., Mathis, J., Hom, J. S. H., Mei, J. F., et al. (1996) Dissociation of affinity and efficacy in KOR-3 chimeras. *FEBS Lett*. **395,** 207–210.

31. Mathis, J. P., Ryan-Moro, J., Chang, A., Hom, J. S. H., Scheinberg, D. A., and Pasternak, G. W. (1997) Biochemical evidence for orphanin FQ/nociceptin receptor heterogeneity in mouse brain. *Biochem*. *Biophys*. *Res*. *Commun*. **230,** 462–465.

32. Pan, Y. X., Mei, J. F., Xu, J., Wan, B. L., Zuckerman, A., and Pasternak, G. W. (1998) Cloning and characterization of a σ1 receptor. *J*. *Neurochem*. **70,** 2279–2285.

33. Abbadie, C., Pan, Y.-X., and Pasternak, G. W. (2000) Differential distribution in rat brain of mu opioid receptor carboxy terminal splice variants MOR-1C and MOR-1-like immunoreactivity: Evidence for region-specific processing. *J*. *Compar*. *Neurol*. **419,** 244–256.

3

Assessing Opioid Regulation of Adenylyl Cyclase Activity in Intact Cells

Deepak R. Thakker, Hatice Z. Ozsoy, and Kelly M. Standifer

1. Introduction

Modulation of adenylyl cyclase activity constitutes one of the important intracellular signaling cascades by which many receptors, including opioid receptors, translate extracellular messages into cellular function. Following receptor activation, adenylyl cyclase is either activated or inhibited via the α-subunit of G_s or $G_{i/o}$ protein, respectively *(1)*. Regulation of adenylyl cyclase activity consequently leads to changes in intracellular levels of adenosine 3', 5'-cyclic monophosphate (cAMP), which, in turn, activates cAMP-dependent protein kinase *(2)*. Opioid receptor coupling to adenylyl cyclase is commonly exploited to study the responsiveness to opioid ligands at the cellular level. In most of the cell systems studied, acute activation of opioid receptors leads to inhibition of adenylyl cyclase activity and a decrease in intracellular cAMP levels *(3)*.

Several methods have been employed for assessing modulation of adenylyl cyclase activity in vitro. One of these methods is based on protein kinase-induced phosphorylation of exogenous substrates *(4)* wherein measuring the end result at the protein kinase level builds up an additional limiting factor to the accuracy of the assay. Another method used for measuring adenylyl cyclase activity is by quantifying the amount of cAMP synthesized from intracellular ATP pre-labeled with radioactive ^{32}P *(5)*. This method is limited by an additional time-consuming and laborious step of separating the radiolabeled cAMP from the non-metabolized, radiolabeled ATP, usually achieved by a two-step chromatography *(5)*. The method that is most extensively used involves a bind-

ing assay wherein intracellular cAMP produced after a reaction is allowed to compete with a known amount of radiolabeled cAMP for binding to a cAMP binding protein (a specific antibody or the regulatory subunit of cAMP-dependent protein kinase) *(6–9)*. Protein-bound cAMP (radiolabeled as well as unlabeled) is separated from free cAMP and the protein-bound radioactivity is determined. This radioactive count is compared to a standard curve, determined using different concentrations of unlabeled cAMP that compete with a known amount of radiolabeled cAMP for protein binding, and the amount of cAMP produced in the cell is extrapolated from this curve. We will illustrate this method in detail, utilizing [^{3}H]cAMP as the radiolabeled cAMP and an extract containing cAMP-dependent protein kinase as the cAMP binding protein, to assess the inhibition of adenylyl cyclase activity upon activation of µ opioid receptors endogenously expressed in BE(2)-C human neuroblastoma cells. This method offers numerous advantages including: 1) low cost; 2) rapidity of assaying a large number of samples in a small amount of time; 3) less laborious; 4) involves handling of ^{3}H as compared to other methods that use ^{125}I or ^{32}P; and 5) is suitable for an accurate analysis of cAMP levels as low as 0.15 pmol *(7)*.

2. Materials

1. BE(2)-C neuroblastoma cells (passages 19–49).
2. Phosphate-buffered saline (PBS), pH 7.4 at 4°C.
3. Hank's balanced salt solution (HBSS), pH 7.4, freshly prepared before use, containing 0.5 m*M* 3-isobutyl-1-methyl-xanthine (IBMX).
4. Forskolin: 24 m*M* stock prepared in dimethyl sulfoxide and stored in 50 µL aliquots at –20°C, light sensitive.
5. [D-Ala^2, N-methyl-Phe^4, Gly-ol^5]-enkephalin (DAMGO).
6. [^{3}H]cAMP: 35 Ci/mmol (Amersham Life Sciences, Arlington Heights, IL).
7. BSAT solution for [^{3}H]cAMP: Protease-free bovine serum albumin (BSA; 0.084%) and 31.2 m*M* theophylline in 25 m*M* Tris-HCl, pH 7.0 at 4°C.
8. cAMP.
9. Adrenal cortex extract (ACE): containing cAMP binding protein (Sigma-Aldrich, St. Louis, MO).
10. Buffer for ACE: 0.25 *M* sucrose, 10 m*M* ethylene diamine tetraacetic acid (EDTA), 250 m*M* NaCl, and 0.1% β-mercaptoethanol in 100 m*M* Tris-HCl, pH 7.0 at 4°C.
11. Hydroxyapatite: 25% solid suspension in 1 m*M* phosphate buffer, pH 6.8 (Sigma-Aldrich).
12. Semiautomatic cell harvester.
13. #34 glass-fiber filters (Schleicher & Schuell, Inc., Keene, NH) or GFC grade filters (Whatman, Inc., Clifton, NJ).
14. Liquiscint scintillation fluor (National Diagnostics, Atlanta, GA).
15. Beckman LS 6000 counter.

3. Methods

The methods described here outline the following major steps: 1) Preparation of supernatants containing intracellular cAMP following treatment of intact cells with drug and/or other agents; 2) Binding of unknown cAMP vs known [³H]cAMP to a binding protein and separation of protein-bound cAMP from free cAMP; and 3) Analysis of protein-bound cAMP and extrapolation of cAMP concentrations in samples from a standard curve.

3.1. cAMP-Containing Cell-Supernatant

The preparation of cAMP-containing cell-supernatants is described in **Subheadings 3.1.1.–3.1.2.** that include: 1) preparation of cell suspension for drug treatment; and 2) experimental incubations and termination of assay.

3.1.1. Preparation of Cell Suspension

1. Culture BE(2)-C cells in tissue culture flasks in a 1:1 mixture of Dulbecco's modified Eagle's minimum essential medium (DMEM) with nonessential amino acids and Ham's nutrient mixture F-12, supplemented with 10% fetal bovine serum (FBS), 100 U/mL penicillin G, and 0.1 mg/mL streptomycin sulfate.
2. Grow cells to 70–90% confluency (prelogarithmic phase) in 150 or 100 cm² dishes in a 6% CO_2-94% air-humidified atmosphere at 37°C.
3. For assaying, wash cell monolayers four times with ice-cold PBS and lift from substrate using PBS containing 1 m*M* EGTA (*see* **Note 1**).
4. Centrifuge the harvested cells at 1000 *g* for 5 min and gently resuspend the cell pellet in HBSS containing the phosphodiesterase inhibitor IBMX (0.5 m*M*).
5. Incubate the resuspended cells in the same buffer for 5 min at 37°C to allow permeabilization of IBMX into the intact cells. IBMX prevents the breakdown of any freshly synthesized cAMP by phosphodiesterases during the assay period.

3.1.2. Experimental Incubations and Termination of Assay

1. Set 1.5-mL microfuge tubes (in duplicate) in ice and divide in three groups: buffer alone, buffer + forskolin and buffer + forskolin + drug (*see* **Note 2**).
2. Add HBSS + IBMX to all tubes such that the final volume of reaction mixture is 500 μL.
3. Dissolve the experimental drug, in this case DAMGO (μ agonist), in the same buffer to make a 10× concentration and add 50 μL to the assay tubes, where appropriate.
4. Dilute forskolin in HBSS + IBMX and add to the assay tubes to give a final concentration of 10 μ*M*. To prevent any light-induced degradation, add forskolin to the assay tubes just before addition of cells for incubation.
5. Add cell suspension (0.1–0.4 mg protein determined by the method of Lowry for protein estimation *(10)* to the reaction mixture, close the tubes, and set them in a water bath at 37°C with mild agitation for 10 min.

6. Terminate the assay by incubating the tubes in a boiling water bath for 5 min (*see* **Note 3**).
7. Allow the assay tubes to cool at room temperature and store at –20°C for no more than one mo before advancing to the binding step of the assay.

3.2. [³H]cAMP Binding Assay

The binding assay constitutes several steps described in **Subheadings 3.2.1.–3.2.5.** These processes include: 1) dilution of [³H]cAMP in BSAT solution; 2) preparation of cAMP binding protein; 3) preparation of hydroxyapatite suspension; 4) performing the experimental incubations wherein unlabeled cAMP (in samples) competes with [³H]cAMP for binding to a protein in the ACE; and 5) separation of protein-bound cAMP from free cAMP.

3.2.1. [³H]cAMP

1. Depending on its specific activity, [³H]cAMP must be diluted so as to achieve a final concentration of 0.8 pmol/50 μL BSAT solution. For example, if the specific activity of a given stock of [³H]cAMP is 50 Ci/mmol, then a 50 μL dilution should contain $[(50 \text{ Ci/mmol}) \times (2.22 \times 10^{12} \text{ dpm/Ci}) \times (0.5 \text{ cpm/dpm}) \times (10^{-9} \text{ mmol/pmol}) \times 0.8 \text{ pmol}]$ 44,400 cpm as determined in a β-counter with 0.5 cpm/dpm efficiency.
2. Store diluted [³H]cAMP in aliquots at –20°C before use. Care must be taken to ensure that theophylline has completely dissolved in the BSAT solution before adding [³H]cAMP for dilution and also while thawing the diluted aliquot for use in assay. This can be accomplished by warming the solution to temperatures not more than 37°C and/or sonication.

3.2.2. cAMP Binding Protein

cAMP-dependent protein kinase from bovine adrenal cortices is used as the binding protein (*see* **Note 4**). This binding protein can be prepared either from bovine adrenals that are dissected free of subcapsular fat and medullar tissue *(7)*, or from commercially available, lyophilized crude adrenal cortex extract.

1. Homogenize bovine adrenals or extract powder in 10 volumes of freshly prepared buffer described in **Subheading 2.** Soaking the tissue protein in ice-cold buffer for approx 45 min prior to homogenization with intermittent stirring provides a better yield of soluble proteins.
2. Clear the homogenate from the greasy layer on top and the crude particulate matter by pouring through cheesecloth and centrifuge for 60 min (4°C) at 30,000*g*.
3. Pour the supernatant again through cheesecloth and adjust the final protein concentration to approx 6 mg/mL with ACE buffer.
4. Freeze this binding protein in 5–10 mL aliquots at –20°C. It is good for use for 1–2 yr.

3.2.3. Hydroxyapatite

Hydroxyapatite enables the separation of protein-bound cAMP by binding to the cAMP binding protein while filtering off the unbound cAMP (*see* **Note 5**).

1. Wash fresh hydroxyapatite three times with equal volumes of distilled water, allowing about 24 h between two washes for the resin to settle (4°C).
2. Pour off the supernatant after each wash and resuspend the resin in an equal volume of water.
3. At the end of three washes, prepare a suspension of 50% w/v hydroxyapatite using distilled water and store at 4°C (good for use for up to 6 mo). The occurrence of microbial growth in hydroxyapatite suspension may impede the binding of cAMP to the binding protein, and can be prevented by preparing a suspension of hydroxyapatite (50% w/v) in 25 m*M* Tris-HCl (pH 7.0) with 0.02% sodium azide or 0.02% thimerosal.

3.2.4. Binding of Unlabeled cAMP vs [^{3}H]cAMP to the Binding Protein

1. Thaw the assay tubes and centrifuge at 10,000 *g* for 5 min.
2. Add 50-µL aliquots of supernatant in duplicate glass tubes (12 × 75 mm) to give a total volume of 0.175 mL containing 25 m*M* Tris-HCl (pH 7.0) buffer and 0.8 pmol [^{3}H]cAMP. Take care not to disturb the pellet while pipeting out the supernatant to prevent any contaminating cAMP from the pellet. This can also be achieved by collecting the supernatant in a separate tube after centrifugation.
3. Set additional tubes in quadruplet containing buffer + [^{3}H]cAMP alone and buffer + [^{3}H]cAMP + a large excess of unlabeled cAMP (1 µ*M*); these will represent total and nonspecific binding of radioligand, respectively.
4. Add ACE (40–60 µg/tube) to all tubes and incubate for 60 min on ice to permit the binding of cAMP (from samples) and [^{3}H]cAMP to cAMP-dependent protein kinase in ACE.

3.2.5. Separation of Protein-Bound cAMP from Unbound cAMP

1. Following 1-h incubation with ACE, add 75 µL of hydroxyapatite suspension (well shaken before use) to the reaction mixture.
2. After swirling, incubate the tubes in ice for 6 min.
3. At the end of this incubation period, add 3 mL of ice-cold Tris-HCl buffer (10 m*M*, pH 7.0) to all tubes.
4. Filter the suspension onto #34 glass-fiber filters using a semiautomatic cell harvester and wash three times with the same buffer.
5. Allow the filters to dry and place them in vials with 5 mL Liquiscent (National Diagnostics).
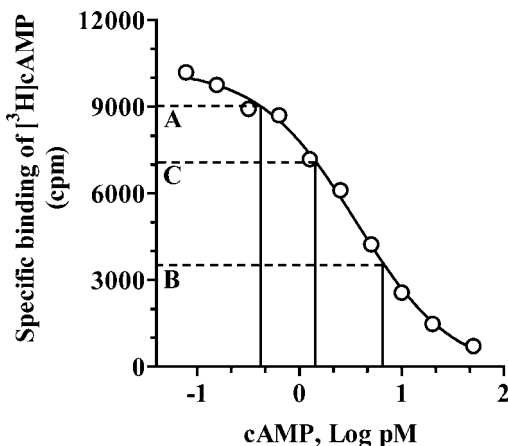6. Determine the radioactivity in vials by scintillation spectroscopy using a Beckman LS 6000 counter.

Fig. 1. cAMP standard curve. The cAMP assay was performed using 0.078–50 pmol of unlabeled cAMP to displace [^{3}H]cAMP (0.8 pmol) for binding to the cAMP binding protein in ACE. The radioactive counts obtained were normalized to determine the specific binding of [^{3}H]cAMP in cpm (10,182-713), and their log values were used to generate the standard curve in GraphPad Prism. The average counts for the three assay groups, namely (**A**) buffer alone, (**B**) buffer + forskolin, and (**C**) buffer + forskolin + DAMGO (1 μM) were 9000, 3600, and 7110, respectively. Using the standard curve, the cAMP levels for these three groups were determined to be 25.4, 201.2, and 71.5 pmol/mg protein, respectively. Subtracting basal values from all groups, we conclude that a 10-min incubation of BE(2)-C cells with DAMGO (1 μM) produced a 74% inhibition of forskolin (10 μM)-stimulated cAMP accumulation.

3.3. Determination of cAMP Concentrations in Samples

The radioactive count on the filter from each tube represents the remaining amount of [^{3}H]cAMP bound to the protein after being displaced by cAMP in the samples. The amount of cAMP in samples that could displace [^{3}H]cAMP binding is determined using a standard curve.

1. To construct the standard curve, perform the same assay in triplicate as described earlier, using a known range of cAMP concentrations (0.078–50 pmol) to compete with [^{3}H]cAMP for protein binding.
2. Use the radioactive counts obtained to prepare a standard curve in GraphPad Prism version 3.00 for Windows 95/98 (GraphPad Software, San Diego, CA). This software provides a template for analysis in radioimmunoassays where a standard curve is generated using values as described above and unknown concentrations of cAMP (in samples) are extrapolated from this standard curve using radioactive counts obtained for each treatment (*see* **Fig. 1**).

4. Notes

1. Adenylyl cyclase assays can also be performed using membranes instead of in-tact cells. Cell membranes can be prepared ahead of time and provide an advan-tage of conducting this assay with several sets of membranes at a convenient time. However, these experiments require additional components (such as an ATP regenerating system) to be supplemented in the assay buffer along with radiola-beled ATP as a substrate for membrane-bound adenylyl cyclase *(11)*. Further-more, several studies have reported a striking limitation that the drug potency for inhibiting adenylyl cyclase activity in membranes is much lower compared to that in intact cells *(11,12)*. Although some studies report receptor-G protein un-coupling during preparation of membranes *(13)*, others propose the requirement of an unknown amplification factor that does not operate under assay conditions using isolated membranes *(11)*.

   Cells such as the Chinese hamster ovary or human embryonic kidney cells are difficult to lift from substrate unless trypsin is used in this process. In this case, intact cell assays are performed while these cells are still attached to the sub-strate. Cells are seeded in 6- to 96-well dishes and allowed to grow until a desired confluency is attained. Cell monolayers are washed, and the assay buffer and other components are added for incubation in wells.

2. Depending on the cell type studied, opioid receptors are demonstrated to couple to both G_s and/or $G_{i/o}$ proteins, ultimately leading to either stimulation or inhibi-tion of adenylyl cyclase *(14,15)*. Although activation of opioid receptors may result in inhibition of adenylyl cyclase activity in most cells, unless basal activity is high, an accurate assessment of this response is usually difficult. Therefore, we utilize a submaximal concentration of forskolin to stimulate adenylyl cyclase activity to accurately assess the inhibitory response of opioids with good repro-ducibility. Forskolin, a direct activator of adenylyl cyclase *(16)*, is used instead of agents such as prostaglandin E1 or adenosine *(17)* as they indirectly activate the adenylyl cyclase enzyme by initiating receptor-mediated signaling cascades, and may increase the number of limiting factors in the assay.

3. The time for incubating the cells with drug and/or other agents for cAMP assay is determined after performing a detailed time course to evaluate the time required for obtaining a maximal cAMP accumulation under the same conditions. Our preliminary studies reveal that the response of μ agonists plateaus by 7–10 min; therefore, the time for conducting this assay was set to 10 min.

   Termination of assays performed in 6- to 96-well dishes can be achieved by quickly aspirating the incubation mixture followed by addition of boiling Tris-HCl (25 m*M*, pH 7.0 at 4°C) to lyse the cells. Alternative methods for terminat-ing the reaction include addition of acids like perchloric acid *(7)*, trichloroacetic acid *(18)*, or HCl *(11)* that extract the cAMP produced at the end of the reaction. These acids are then neutralized by KOH/Tris base after centrifuging the samples. Another method used for terminating the reaction and cAMP extraction involves

addition of a 1:1 mixture of methanol/chloroform *(19)*. None of these methods impedes the sensitivity of this assay or the functionality of any agents used in this assay.

4. Although the binding protein used in this assay is a crude protein kinase preparation, it binds to cAMP with high specificity and with negligible specificity to endogenous adenine compounds or other cyclic nucleotides *(8)*. However, the sensitivity of this assay is limited to cAMP levels not less than 0.15 pmol/tube. For analyzing samples with cAMP levels lower than 0.15 pmol/tube, antibodies generated against the succinylated or acetylated forms of cAMP are recommended for use as the cAMP binding protein *(6,7)*. In this method, intracellular cAMP produced after a reaction is subjected to a succinylation or acetylation reaction and the derivatized cAMP then competes with a known amount of ^{125}I-succinylated or ^{125}I-acetylated cAMP for binding to the antibody. This method in turn suffers from drawbacks of high cost and labor for generating antibodies in the laboratory, and synthesizing and iodinating the succinyl or acetyl derivatives of cAMP.

5. Separation of protein-bound cAMP from free cAMP can also be achieved using albumin-saturated charcoal *(8)* or ammonium sulfate *(9)* followed by centrifugation. These methods are time- and labor-consuming and not suitable for analysis of large number of samples. These disadvantages are overcome by using the semi-automatic method of separation described in this chapter.

Acknowledgment

References

1. Gilman, A. G. (1987) G proteins: transducers of receptor-generated signals. *Annu. Rev. Biochem.* **56,** 615–649.
2. Krebs, E. G. (1989) The Albert Lasker Medical Awards. Role of the cyclic AMP-dependent protein kinase in signal transduction. *JAMA* **262,** 1815–1818.
3. Law, P. Y., Wong, Y. H., and Loh, H. H. (2000) Molecular mechanisms and regulation of opioid receptor signaling. *Annu. Rev. Pharmacol. Toxicol* **40,** 389–430.
4. Kuo, J. F. and Greengard, P. (1972) An assay method for cyclic AMP and cyclic GMP based upon their abilities to activate cyclic AMP-dependent and cyclic GMP-dependent protein kinases. *Adv. Cyclic Nucleotide Res.* **2,** 41–50.
5. Salomon, Y., Londos, C., and Rodbell, M. (1974) A highly sensitive adenylate cyclase assay. *Anal. Biochem.* **58,** 541–548.
6. Brooker, G., Harper, J. F., Terasaki, W. L., and Moylan, R. D. (1979) Radioimmunoassay of cyclic AMP and cyclic GMP. *Adv. Cyclic Nucleotide Res.* **10,** 1–33.
7. Nordstedt, C. and Fredholm, B. B. (1990) A modification of a protein-binding method for rapid quantification of cAMP in cell-culture supernatants and body fluid. *Anal. Biochem.* **189,** 231–234.

8. Brown, B. L., Albano, J. D., Ekins R. P., Sgherzi, A. M., and Tampion, W. (1971) A simple and sensitive saturation assay method for the measurement of adenosine 3':5'-cyclic monophosphate. *Biochem. J.* **121,** 561–562.

9. Doskeland, S. O., Ueland, P. M., and Haga, H. J. (1977) Factors affecting the binding of [³H]adenosine 3':5'-cyclic monophosphate to protein kinase from bovine adrenal cortex. *Biochem. J.* **161,** 653–665.

10. Lowry, O. H., Rosebrough, N. J., Farr, A. L., and Randall, R. J. (1951) Protein measurement with the Folin phenol reagent. *J. Biol. Chem.* 193, 265–275.

11. Costa, T., Klinz, F. J., Vachon, L., and Herz, A. (1988) Opioid receptors are coupled tightly to G proteins but loosely to adenylate cyclase in NG108-15 cell membranes. *Mol. Pharmacol.* **34,** 744–754.

12. Mathis, J. P., Mandyam, C. D., Altememi, G. F., Pasternak, G. W., and Standifer, K. M. (2001) Orphanin FQ/nociceptin and naloxone benzoylhydrazone activate distinct receptors in BE(2)-C human neuroblastoma cells. *Neurosci. Lett.* **299,** 173–176.

13. Okawa, H., Hirst, R. A., Smart, D., McKnight, A. T. and Lambert, D. G. (1998) Rat central ORL-1 receptor uncouples from adenylyl cyclase during membrane preparation. *Neurosci. Lett.* **246,** 49–52.

14. Wang, L. and Gintzler, A. R. (1994) Bimodal opioid regulation of cyclic AMP formation: implications for positive and negative coupling of opiate receptors to adenylyl cyclase. *J. Neurochem.* **63,** 1726–1730.

15. Cruciani, R. A., Dvorkin, B., Morris, S. A., Crain, S. M., and Makman, M. H. (1993) Direct coupling of opioid receptors to both stimulatory and inhibitory guanine nucleotide-binding proteins in F-11 neuroblastoma-sensory neuron hybrid cells. *Proc. Natl. Acad. Sci. USA* **90,** 3019–3023.

16. Zahler, W. L. (1983) Evidence for multiple interconvertible forms of adenylate cyclase detected by forskolin activation. *J. Cyclic Nucleotide Protein Phosphor. Res.* **9,** 221–230.

17. Sharma, S. K., Klee, W. A. and Nirenberg, M. (1975) Dual regulation of adenylate cyclase accounts for narcotic dependence and tolerance. *Proc. Natl. Acad. Sci. USA* **72,** 3092–3096.

18. Kazmi, S. M. I. and Mishra, R. K. (1987) Comparative pharmacological properties and functional coupling of μ and δ opioid receptor sites in human neuroblastoma SH-SY5Y cells. *Mol. Pharmacol.* **32,** 109–118.

19. Voss, T. and Wallner, E. (1992) An easy cAMP extraction method facilitating adenylyl cyclase assays. *Anal. Biochem.* **207,** 40–43.

4

Analysis of Opioid-Induced Kinase Activation

Lan Ma

1. Introduction

Phosphorylation is the most important and common way of regulation of protein functions. It offers rapid and reversible regulation. Protein kinases catalyze phosphorylation of a protein and transfer the γ-phosphate of adenosine triphosphate (ATP) onto the serine, threonine, or tyrosine residue. It has been shown that stimulation of opioid receptors regulates activities of numerous protein kinases including protein kinase C (PKC), cAMP-dependent protein kinase (PKA), Ca^{2+}/calmodulin-dependent protein kinase II (CamK II), mitogin-activated protein kinases (MAPKs), and G protein coupled receptor kinases *(1–7)*. Kinases activated by opioids play an important role in regulation of opioid signaling, including homologous desensitization of opioid receptors. Studies have demonstrated that activation of these kinases that are key players in opioid signaling cascades also results in crosstalk of opioid signaling to other signal pathways. Furthermore, protein kinases activated by nonopioid signal pathways play important roles in heterologous regulation of opioid functions. Therefore, opioid researchers often face the challenge of determining changes in the activities of protein kinases in study of opioid signal transduction. Kinase assays have become a very common and useful tool in opioid research. This chapter describes practical protocols for measuring activities of CamKII *(6,8,9)*, PKC *(2,3,10)*, PKA *(2,11–13)*, and MAPK *(14–16)* using radioactive or nonradioactive methods.

2. Materials
2.1. CamKII Assay

1. Lysis buffer: 20 m*M* Tris-HCl, pH 7.5, 0.5 m*M* ethylene diamine tetraacetic acid (EDTA), 0.5 m*M* EGTA, 0.4 m*M* molybdate, 1 m*M* dithiothreitol (DTT), 1 m*M*

phenylmethylsulfonyl fluoride (PMSF), 20 µg/mL leupeptin, 10 µ*M* sodium pyrophosphate, and 10 µg/mL aprotinin. (*see* **Note 1**).
2. [γ-^{32}P]ATP: 3000 Ci/mmol, 10 µCi/µL (Du Pont-New England Nuclear).
3. [γ-^{32}P]ATP/ATP solution: 1 m*M* ATP containing 0.2 µCi/µL [γ-^{32}P]ATP.
4. Stock solution I: 80 m*M* 1,4-piperazinediethanesulfonic acid (PIPES), pH 7.5, 16 m*M* MgCl$_2$, 0.96 m*M* EGTA, 0.32 m*M* EDTA, 160 µg/mL BSA, and 0.64 m*M* DTT.
5. Stock solution II: 80 m*M* PIPES, pH 7.5, 16 m*M* MgCl$_2$, 0.8 m*M* Ca$_2$Cl$_2$, 160 µg/mL BSA, 0.64 m*M* DTT, and 20 µg/µL calmodulin in stock solution I.
6. Substrate solution: 200 µ*M* autocamtide-2 (KKALRRQETVDAL) in 50 m*M* PIPES (pH 7.5).
7. P81 phosphocellulose paper (Whatman).
8. 75 m*M* H$_3$PO$_4$.

2.2. PKC Assay

1. Lysis buffer: 25 m*M* Tris-HCl, pH 7.4, 10 m*M* EGTA, 2 m*M* EDTA, 10 m*M* β-mercaptoethanol, 1 µg/mL leupeptin, 1µg/mL aprotinin, and 1 m*M* PMSF (*see* **Note 1**).
2. [γ-^{32}P]ATP: 3000 Ci/mmol, 10 µCi/µL.
3. [γ-^{32}P]ATP/ATP solution: 1 m*M* ATP containing 0.2 µCi/µL [γ-^{32}P]ATP.
4. Reaction stock solution I: 250 m*M* Tris-HCl, 7.5 m*M* CaCl$_2$, 5 m*M* MgCl$_2$, and 2.5 m*M* DTT.
5. Reaction stock solution II: 50 m*M* Tris-HCl, pH 7.4, 0.25 mg/mL phosphatidylserine, and 0.05 mg/mL diolein.
6. Substrate solution: 5 mg/mL PKC substrate peptide KRTLRR in 20 m*M* Tris-HCl (pH 7.4).
7. P81 phosphocellulose paper (Whatman).
8. 75 m*M* H$_3$PO$_4$.

2.3. PKA Assay

1. Homogenization buffer (for tissue): 20 m*M* Tris-HCl, pH 7.5, 10 m*M* EGTA, 2 m*M* EDTA, 5 m*M* DTT, 1 m*M* PMSF, 10 µg/mL aprotinin, and 10 µg/mL leupeptin.
2. Homogenization buffer (for cultured cells): 0.2 % Triton X-100, 10 m*M* NaH$_2$PO$_4$, pH 6.8, 10 m*M* EDTA, 50 m*M* NaCl, and 0.5 m*M* 3-isobutyl-1-methyl-xanthine.
3. PKA dilution buffer: 350 m*M* KH$_2$PO$_4$, pH 7.5, and 0.1 m*M* DTT.
4. 80% glycerol.
5. 50 m*M* Tris-HCl, pH 8.0.
6. Nonradioactive cAMP-dependent protein kinase assay kit (Promega): (1) PepTag PKA reaction 5X buffer (100 m*M* Tris-HCl, pH 7.4, 50 m*M* MgCl$_2$, and 5 m*M* ATP). (2) PKA activator 5X solution (5 µ*M* cAMP). (3) PepTag A1 peptide (PKA substrate peptide Kemptide carrying a fluorescent tag, 0.4 µg/µL). (4) PKA catalytic subunit.
7. Horizontal agarose gel apparatus.

2.4. MAPK Assay

1. Lysis buffer: 50 mM Tris-HCl, pH 7.5, 1 % Triton X-100, 100 mM NaCl, 5 mM EDTA, 1 mM DTT, 40 mM sodium pyrophosphate, 0.1 mM PMSF, 1 μg/mL pepstatin A, 2 μg/mL leupeptin, and 4 μg/ml aprotinin.
2. Kinase buffer: 40 mM HEPES, pH 7.5, 5 mM MgCl$_2$, 2 mM DTT, and 1 mM EGTA.
3. Melin basic protein (MBP, Sigma).
4. ATP solution: 500 μM [γ-^{32}P]ATP/ATP containing 0.1 μCi/μL [γ-^{32}P]ATP.
5. MAPK antiserum (New England Biolabs).
6. Protein A-agarose.
7. P81 phosphocellulose paper (Whatman).

3. Methods

3.1. CamK II Assay

1. Homogenize brain tissue or cultured cells in a Dounce homogenizer by brief soni-cation (10 s) in ice-cold lysis buffer.
2. Centrifuge the lysate at 4°C at 12,000 *g* for 10 min. The resulting supernatant is ready for assay for CamK II activity (*see* **Note 2**).
3. Prepare 1 mM [γ-^{32}P]ATP/ATP solution.
4. Label 0.5-mL microcentrifuge tubes and P81 membrane (cut into squares of 1–2 cm × 1–2 cm). For each sample to be tested for CamK II kinase activity, four tubes are needed and they can be labeled as 1A, 1B, 1C, 1D, 2A, and so on. Label the P81 membranes accordingly. In addition, prepare two extra pieces of P81 membrane labeled as "0".
5. Test each lysate sample (containing 5–50 μg protein) for Ca^{2+}/calmodulin-dependent and Ca^{2+}/calmodulin-independent activities with minus substrate con-trol. Each reaction contains 50 mM PIPES, 1 mM DTT, 0.25 mM EGTA, 20 μM autocamtide-2100 μM ATP, 2 μCi of [γ-^{32}P]ATP, 20 μg/mL calmodulin, and 0.75 mM CaCl$_2$.
6. To measure the Ca^{2+}/calmodulin-independent protein kinase activity of CaMK II, perform reactions in the absence of Ca^{2+} and calmodulin and in the presence of 1 mM EGTA.
7. Set up four reaction mixtures (A-D) for each sample tested. Assemble the four assay reaction mixtures for each sample in 0.5-mL microcentrifuge tubes on ice as following: add 70 μL stock solution I to tubes A and B and 70 μL stock solu-tion II to C and D, 10 μL 50 mM PIPES to A and C and 10 μL substrate solution to tubes B and D, and 10 μL of 1 mM [γ-^{32}P]ATP/ATP to A–D.
8. Take one reaction mixture assembled as above, add 10 μL sample to it (final reaction volume = 100 μL; reaction volume can be reduced to 50 μL), and tap the tube gently to mix.
9. Incubate the tube in 30°C water bath for 30 s (precisely).
10. After incubation, immediately take 75 μL from the tube, spot onto P81 mem-brane and immerse the membrane immediately in 75 mM H$_3$PO$_4$ to stop the reac-tion. Repeat this step for each reaction. (Because the reaction is very fast, this step has to be done tube by tube, *see* **Note 3**.)

11. Take 10 μL each from the reaction mixture remained from any two reaction tubes and spot onto P81 membrane labeled as "0" for determination of specificity of [γ-^{32}P]ATP in the reaction.
12. Wash the P81 membranes in 75 m*M* H$_3$PO$_4$ for 5 min and repeat twice. Monitor the radioactivity reading with a handhold radioactivity moniter. Stop washing when the reading drops to approx 2000 cpm.
13. Put the membranes on a filter paper and let them air-dry.
14. Determine the radioactivity on the P81 membranes in a liquid scintillation counter. The background readings are usually between 2000–3000 cpm.
15. The CamK II activity in the sample can be calculated according to the following equation:

$$\text{Activity (pmol/min/}\mu\text{g)} = \frac{\text{cpm}_{\text{(with substrate)}} - \text{cpm}_{\text{(without substrate)}}}{0.5\ \text{min} \times \mu\text{g of protein on the membrane} \times \text{cpm/pmol ATP in the reaction}}$$

3.2. PKC Assay

1. Wash the cells twice with PBS and sonicate in lysis buffer for 10 s on ice.
2. Centrifuge the cell lysate at 100,000*g* for 30 min at 4°C. Collect the supernatant and use it as cytosolic fraction (*see* **Note 2**).
3. Resuspend the pellet in lysis buffer containing 0.5% triton X-100, homogenized in a Dounce homogenizer, and placed at 4°C for 1 h.
4. Centrifuge at 100,000*g* for 30 min at 4°C . Use the resultant supernatant containing the solubilized membranes as membrane fractions (*see* **Note 2**).
5. Prepare 1 m*M* [γ-^{32}P]ATP/ATP solution.
6. Label 0.5 mL microcentrifuge tubes and P81 membrane (cut into squares of 1–2 cm × 1–2 cm). In addition, prepare two extra pieces of P81 membrane labeled as "0".
7. Test each membrane of cytosol lysate sample (containing 5–50 μg protein) for phospholipid-dependent and phospholipid-independent (control) activities. Each reaction contains 50 m*M* Tris-HCl, pH. 7.4, 0.5 m*M* DTT, 1 m*M* MgCl$_2$, 1.5 m*M* CaCl$_2$, 0.5 mg/mL PKC substrate peptide, 100 μ*M* [γ-32P]ATP (200-400 cpm/ pmol), 25 μg/mL phosphatidylserine, and 0.5 mg/mL diolein.
8. Assemble the assay reaction mixtures in 0.5-mL microcentrifuge tubes on ice as following: add 10 μL stock solution I, 5 μL stock solution II (or 5 μL 20 m*M* Tris-HCl as control), 5 μL substrate solution, 10 μL H$_2$O, and 5 μL of 1 m*M* [γ-^{32}P]ATP/ATP.
9. Take one reaction mixture assembled as above, add 5-μL sample to it (the final reaction volume = 50 μL), and tap the tube gently to mix.
10. Incubate the tube in 30°C water bath for 3 min. After incubation, immediately take 30 μL from the tube, spot onto P81 membrane, and immerge the membrane immediately in 75 m*M* H$_3$PO$_4$ to stop the reaction. Repeat this step for each reaction (*see* **Note 3**).
11. Take 10 μL each from the reaction mixture remained from any two reaction tubes and spot onto P81 membrane labeled as "0" for determination of specificity of [γ-^{32}P]ATP in the reaction.

12. Wash the P81 membranes in 75 mM H$_3$PO$_4$ for 5 min and repeat twice.
13. Put the membranes on a filter paper and let air-dry.
14. Determine the radioactivity on the P81 membranes in a liquid scintillation counter (*see* **Note 4**).
15. The PKC activity in the sample can be calculated by the following the equation:

$$\text{Activity (pmol/min/µg)} = \frac{\text{cpm}_{\text{(with phospholipids)}} - \text{cpm}_{\text{(without phospholipids)}}}{3 \text{ min} \times \text{µg of protein on the p81 membrane} \times \text{cpm/pmol } [\gamma\text{-}^{32}\text{P}]\text{ATP in the reaction}}$$

3.3. PKA Assay

1. Homogenize brain tissues or cultured cells in ice-cold homogenization buffer and centrifuge at 4°C at 20,000g for 5 min. The resulting supernatant is ready for assay for PKA activity.
2. Take appropriate amount of PKA catalytic subunit and dilute to 2 µg/mL in PKA dilution buffer (*see* **Note 5**).
3. Assemble the assay reaction mixture on ice. Mix 5 µL PKA reaction 5 × buffer, 5 µL PepTag A1 PepTag, 5 µL PKA activator 5 × solution, and 5 µL dH$_2$O in a 0.5 µL microcentrifuge tube.
4. Remove the tube from ice and incubate at 30°C for 1 min.
5. Add 5 µL sample to be tested (or the same volume of lysis buffer/PKA catalytic subunit as negative/positive control) and incubate at 30°C for 30 min.
6. Stop the reaction by placing the tube in a 95°C water bath for 10 min. The sample can be stored at ≤4°C in dark until use.
7. Prepare a 0.8% agarose gel in 50 mM Tris-HCl, pH 8.0.
8. Add 1 µL 80% glycerol to the sample to facilitate loading. Load samples without pause and start the gel immediately after loding the last sample.
9. Run the gel at 100 V for 15–18 min or until apparent separation of bands (*see* **Notes 6** and **7**).
10. When electrophoresis is complete, remove the gel from the chamber and photograph immediately. For better sensitivity, photograph the gel under ultraviolet (UV) light. A qualitative estimate of the relative amounts of PKA activity in the samples can be made by densitometry and spectrofluorometry (*see* **Note 8**). A gel picture is shown in **Fig. 1.**

3.4. MAPK Assay

1. Lyse cells in 400 µL cold lysis buffer and let stand on ice for 20 min.
2. Let the cell lysate pass through a small needle (six times) using an insulin syringe.
3. Centrifuge at 12,000g for 15 min to remove insoluble materials.
4. Collect the supernatant in a 1.5-mL microcentrifuge tube and add 2 µL (approx 1 µg) p44/p42 MAPK polyclonal antibody against total MAPK.
5. Rock at 4°C for 2 h to allow the formation of immune complex.
6. Add 20 µL of protein A-agarose (50% slurry) and incubate for an additional 2 h with occasional shaking.
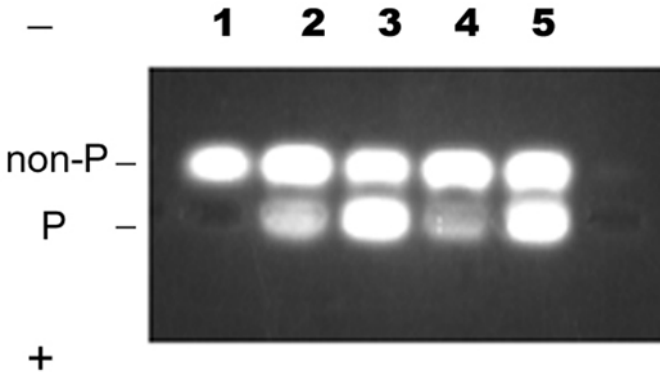
Fig. 1. Activation of PKA. The assay for PKA activity was carried out as described in **Subheading 3.3**. After reaction, the samples were loaded onto 0.8% agarose gel to separate the phosphorylated and unphosphorylated substrates. Lane 1: vehicle control, lanes 2 and 4: 10 μg cell lysate; lanes 3 and 5: 50 μg cell lysate.

7. Spin at aprrox 3000g for 1 min. Wash the pellets three times in lysis buffer, and then twice in Kinase Buffer.
8. Resuspend the pellets in 50 μL kinase buffer supplemented with 250 μg/mL melin basic protein.
9. Add 5 μL ATP solution (500 μM ATP containing 0.1 μCi/μL [γ-^{32}P]ATP) to each tube and incubate at 30°C for 30 min with occasional shaking.
10. Add 5 μL 88% formic acid to terminate the reaction. Centrifuge at approx 3000g for 1 min.
11. Take 30 μL supernatant and spot onto Whatman P81 paper.
12. Wash the P81 filter paper four times in 150 mM phosphoric acid to remove unbound [γ-^{32}P]ATP.
13. Measure the radioactivity incorporated into MBP on the P81 paper by scintillation counting. Correct results by subtraction of the average value of control samples containing no MAPK antibodies.
14. Phosphorylation of MBP by MAPK can also be quantified by autoradiography following sodium dodecyl suylfate-polyacrylamide gel electorphoreois (SDS-PAGE). After completing step 9, terminate the reaction with 6 × SDS-PAGE sample buffer and run the samples on a 15% SDS polyacrylamide gel. Dry the gel and expose to X-ray films or subject to phosphor imaging.
15. Assay for p38 MAPK activity can be done using similar methodology (*see* **Note 9**).

4. Notes

1. DTT, PMSF, protease inhibitors, and ATP stock solution should be stored at –20°C and added just before use.
2. Keep the samples and the reagents on ice when possible to avoid inactivating the enzyme.

3. Perform this step consistently for each reaction because the reaction goes very fast. For example, tap the tube exactly the same number of times when mixing the reaction for each sample.

4. The activity of PKC can also be determined using a nonradioactive method. A nonradioactive PKC assay kit is available from Promega *(13)*.

5. Dilute PKA just before use. PKA is labile at 30°C. The reaction time should be kept to a minimum.

6. The assay is based on the changes in the net charge of the PKA substrates before and after phosphorylation. Phosphorylation by PKA of PKA specific substrate (LRRASLG) alters the peptide's net charge from positve to negative. This allows the separation of phosphorylated and nonphosphorylated substrate by electrophoresis on an agarose gel at neutral pH. The phosphorylated species migrates toward the positive electrode (the same direction as DNA moves during electrophoresis) while the nonphosphorylated substrate migrates toward the negative electrode (opposite to the direction DNA moves). The fluorescent tag attached to the PKA substrate facilitates the visualization of the phosphorylated and unphosphorylated substrates. The fluorescence intensity of phosphorylated peptides reflects the activity of PKA.

7. Put the comb in the center of the gel when pouring the gel (do not put it at one end as usual).

8. Stop running when the two bands get good separation and photograph it immediately.

9. *p*38 MAPK in cell lysate can be precipitated with *p*38 antibodies and kinase activity of *p*38 toward its specific substrate ATF-2 is determined. A nonradioactive p38 kinase assay kit is available commercially (New England Biolabs).

Acknowledgment

References

1. Mayer, D. J., Mao, J., and Price, D. D. (1995) The development of morphine tolerance and dependence is associated with translocation of protein kinase C. *Pain* **61,** 365–374.

2. Lou, L.-G. and Pei, G. (1997) Modulation of protein kinase C and cAMP-dependent protein kinase by δ-opioid. *Biochem. Biophys. Res. Commun.* **236,** 626–629.

3. Lou, L.-G., Ma, L., and Pei, G. (1997) Nociceptin/orphanin FQ activates protein kinase C, and this is mediated through phospholipase C/Ca^{2+} phathway. *Biochem. Biophys. Res. Commun.* **240,** 304–308.

4. Burt, A. R., Carr, I. C., Mullaney, I., Anderson, N. G., and Milligan, G. (1996) Agonist activation of p42 and p44 mitogen-activated protein kinases following expression of the mouse δ opioid receptor in Rat-1 fibroblasts: effects of receptor expression levels and comparisons with g-protein activation. *Biochem. J.* **320,** 227–235.

5. Fukuda, K., Kato, S., Morikawa, H., Shoda, T., and Mori, K. (1996) Functional coupling of the delta-, mu-, and kappa-opioid receptors to mitogen-activated protein kinase and arachidonate release in Chinese hamster ovary cells. *J. Neurochem.* **67,** 1309–1316.

6. Lou, L.-G., Zhou, T.-H., Wang, P., and Pei, G. (1999) Modulation of Ca^{2+}/calmodulin-dependent protein kinase II activity by acute and chronic morphine administration in rat hippocampus: Differential regulation of α and β forms. *Mol. Pharmacol.* **55,** 557–563.

7. Guo, J., Wu, Y.-L., Zhang, W.-B., Zhao, J., Devi, L..A., Pei, G., et al. (2000) Identification of G protein-coupled receptor kinase 2 phosphorylation sites responsible for agonist-stimulated delta-opioid receptor phosphorylation. *Mol. Pharmacol.* **58,** 1050–1056

8. Occur, K. A. and Schulman, H. (1991) Activation of multifunctional Ca^{2+}/calmodulin-dependent kinase in intact hippocampal slices. *Neuron* **6,** 907–914.

9. Wang, P., Wu, Y.-L., Zhou, T.-H., Sun, Y., and Pei, G. (2000) Identification of alternative splicing variants of the β subunit of human Ca^{2+}/calmodulin-dependent protein kinase II with different activities. *FEBS Lett.* **475,** 107–110.

10. Davis, R. J. and Czech, M. P. (1987) Stimulation of epidermal growth factor receptor threonine 654 phosphorylation by platelet-derived growth factor in protein kinase C-deficient human fibroblasts. *J. Biol. Chem.* **262,** 6832–6841.

11. Karege, F., Schwald, M., Lambercy, C., Murama, J. J., Cisse, M., and Malafosse, A. (2001) A non-radioactive assay for the cAMP-dependent protein kinase activity in rat brain homogenates and age-related changes in hippocampus and cortex. *Brain Res.* **903,** 86–93.

12. Lutz, M. P., Pinon, D. I., and Miller, L. J. (1994) A nonradioactive fluorescent gel-shift assay for the analysis of protein phosphatase and kinase activities toward protein-specific peptide substrates. *Anal. Biochem.* **220,** 268–274.

13. Promega Corp. (2001) PepTag Assay for non-radioactive detection of protein kinase C or cAMP-dependent protein kinase. *Technical Bulletin No 132*.

14. Faure, M., Voyno-Yasenetskaya, T. A., and Bourne, H. R. (1994) cAMP and $\beta\gamma$ subunits of heterotrimetic G proteins stimulate the mitogen-activated protein kinase pathway in COS-7 cells. *J. Biol. Chem.* **269,** 7851–7854.

15. Lou, L. G., Zhang, Z., Ma, L., and Pei, G. (1998) Nociceptin/orphanin FQ activates mitogen-activated protein kinase in Chinese hamster ovary cells expressing opioid receptor-like receptors. *J. Neurochem.* **70,** 1316–1322.

16. Zhang, Z., Xin, S.-M., Wu, G.-X., Zhang, W.-B., Ma, L., and Pei G. (1999) Endogenous delta-opioid and ORL1 receptors couple to phosphorylation and activation of p38 MAPK in NG108-15 cells and this is regulated by protein kinase A and protein kinase C. *J Neurochem.* **73,** 1502–1509.

5

Study of Opioid Receptor Phosphorylation Using Cell-Labeling Method with ^{32}P-Orthrophosphate

Jia Bei Wang

1. Introduction

Phosphorylation is a posttranslational modification used to regulate the functions of a variety of proteins, including neurotransmitter receptors. Protein phosphorylation is catalyzed by protein kinases transferring a phosphate molecule from ATP to a protein substrate. The addition of the negatively charged phosphate group alters the structure of the protein and regulates its functional properties. Protein phosphorylation is a highly regulated reversible process and thus the level of receptor phosphorylation in neurons is constantly modified by neurotransmitters and other cellular signals released by surrounding neurons.

A prominent characteristic of morphine-like opioid drugs is their ability to induce tolerance and dependence in humans *(1)*. Opioid receptor desensitization is one of the cellular mechanisms that could have a significant role in this neuroadaptive process *(2)*. It is hypothesized that opioid receptor phosphorylation plays a role in the development of receptor desensitization. Identification and isolation of the phosphorylated receptor has become increasingly more important in understanding of the relationship between phosphorylation and receptor desensitization and the mechanism underlying the development of tolerance and dependence of opioid drugs. Such an understanding is fundamental to the pharmacological segregation of the analgesic and addictive effects of opioid drugs and to the development of better therapeutic agents for pain and for prevention and treatment of drug addiction.

A common method used to identify phosphorylated opioid receptors is the cell-labeling technique, which labels the intracellular ATP-pool with

^{32}P-orthrophosphate *(3–6)*. Once the receptor phosphorylation takes place, a ^{32}P-labeled γ-phosphoryl group of ATP is transferred to specific residues in the receptor by a protein kinase. Subsequently, a phosphorylated opioid receptor can be identified by autoradiography following purification from nonreceptor proteins via immunoprecipitation and separation by sodium dodecyl sulfite-polyacrylamide gel electrophoresis (SDS-PAGE). This technique can be utilized to study receptor phosphorylation as a consequence of drug action *(7)*, correlations between receptor phosphorylation and other intracellular signal transduction pathways *(6)*, and characteization of phosphorylation sites on the receptor when combined with site-directed mutagenesis *(8)*. It also has been used as a preparatory step for phosphopeptide mapping and phosphorylation site determination of the receptor (Wang, J.B., unpublished data).

   The advantage of ^{32}P-cell labeling is that this approach can detect the phosphorylation events on the receptor proteins without any knowledge of which protein kniases are involved, which often may be the case in preliminary investigations. This technique also generates direct information on the receptor protein phosphorylation . The method has been used mostly on cultured cells *(3–5)*; however, it also can be applied to tissues if used appropriately *(9)*. In this chapter, we present the optimal conditions used for the assessment of human mu opioid receptor phosphorylation by modifications of the cell labeling method described by Pei et al. *(3)*.

2. Materials

1. ^{32}P-orthophosphate (8500 Ci/mmole, NEX-053H, DuPont NEN).
2. Dulbecco's modified Eagle's medium (DMEM) with 100 u/L penicillin and 100 mg/L streptomycin and 10% fetal calf serum (FCS).
3. DMEM without sodium phosphate (GIBCO, 21075-015): 100 u/L penicillin and 100 mg/mL streptomycin in 20 mM HEPES, pH 7.4.
4. RIPA$^+$ buffer: 1% NP40, 0.5% Na$_2$ deoxycholate, 0.1% SDS, 5 MM EDTA in PBS (pH 7.4), 10 MM NaF, 10 MM Na$_2$ Pyrophosphate, 1 μM okadaic acid (phosphatase inhibitor), and protease inhibitors: 0.1 MM PMSF, 10 μg/mL benzamidine, 10 μg/mL leupeptin, and 1 μg/mL pepstatin A.
5. Protein A / Sepharose CL-4B (Pharmacia), presoaked with 10% (v/v) in RIPA$^+$ buffer, 3% (w/v) BSA (Sigma, fraction V).
6. Anti-mu antibody, custom-made against the mu opioid receptor's C-terminal 18 amnio acids.
7. 8% SDS-PAGE gel.
8. SDS-PAGE loading buffer: 4% SDS, 25 MM Tris-HCl, pH 6.8, 5% glycerol, 0.5% 2-methanol, and 0.005% bromophenol blue.
9. PhosphoImager cassettes or Hyperfilm-MP (Amersham) with intensifying screens.

3. Methods

3.1. Day 1

1. Plate nontransfected Chinese hamster ovary (CHO) cells (as a control) and the CHO cells stably expressing human mu opioid receptors (HµCHO) at 80% confluence (approx 1×10^6 cells/well) in six-well plates.
2. Grow the cells for 24–72 h in DMEM containing 10% FCS, 100 u/L penicillin, and 100 mg/L streptomycin (*see* **Notes 1** and **2**).

3.2. Day 2–3

1. Remove the DMEM medium and wash the cells twice with phosphate-free DMEM.
2. To label the intracellular ATP with ^{32}P- orthophosphate, add 0.5 ml/well of labeling medium (phosphate-free DMEM with 300 µCi/mL [^{32}P] orthophosphate) to the cells and incubate at 37°C in 5% CO_2 for 2 h (rock the plates every 15 min) (*see* **Note 3**).
3. Expose the labeled cells to treatments with varied times and concentrations as required in individual experiments.
4. Place the 6-well dish on a slide-warmed tray at 37°C.
5. To each well add 0.5 mL of pre-warmed medium containing treatment drug (or control) at 2× the desired final concentration and incubate for 5–20 min.
6. Following removal of the medium, cool the cells to 4°C by washing the cell twice with ice-cold phosphate-buffered saline (PBS).
7. Carry out all subsequent procedures at 4°C.
8. Extract proteins by adding 0.5 mL/well of ice-cold "RIPA$^+$" buffer to the cells. Scrape the cells free with a disposable cell scraper.
9. Agitate the dissolved cells and transfer to a 1.5-mL screw-cap tube.
10. Wash each well with an additional 0.3 mL of ice-cold RIPA$^+$ buffer and transfer the wash solution to the 1.5 mL screw-cap tube and place on ice.
11. Solubilize the membrane proteins on ice for 60 min.
12. Briefly spin tubes for 10 s at 4°C, and transfer the tube contents (including unsolubilized membrane) to precooled Beckman centrifuge tubes.
13. Spin the samples in a Beckman SW50.1 rotor at 150,000g for 15 min at 4°C.
14. Transfer the supernatant (approx 700 µL/reaction) to fresh 1.5 mL-tubes containing pre-chilled protein A/Sepharose CL-4B (120 µL), and incubate at 4°C for 1 h. Save 30 µL of the supernatant for a subsequent protein concentration measurement (*see* **Note 4**).
15. Microcentrifuge at maximum speed for 20 s at 4°C.
16. Incubate the supernatant from the preabsorption step with antiserum directed against the µ opioid receptor for 2 h.
17. Carefully transfer all of the supernatant to a fresh 1.5-mL tube preloaded with antibody diluted with RIPA$^+$ buffer (100 µL RIPA$^+$ buffer with 2 µL antiserum of the above).

18. Add 120 µL protein A/Sepharose CL-4B to each tube, cap the tube, and incubate at 4°C for 2 h with gentle agitation.
19. Microcentrifuge the tubes at maximum speed at 4°C for 20 s.
20. Discard the supernatant and wash the beads three times by resuspending in 1 mL RIPA+ followed by microcentrifugation. At this point, the experiment can proceed to the next step or the pelleted beads can be stored at –80°C over night.
21. Dissociate the immunoprecipitated proteins from beads by adding 60 µL of SDS-PAGE gel loading buffer and incubating at 65°C (water bath) for 10 min.
22. Microcentrifuge at maximum speed for 20 s at room temperature.
23. Transfer the supernatant to fresh tubes, and analyse by SDS-PAGE. Run 20–30 µL/per lane of the immunoprecipitated proteins with pre-stained molecular mass standards (Amersham) in an adjacent lane.
24. Dry the SDS-PAGE gel on a slab gel dryer for 1 h, and expose the dried gel to phosphoimager cassettes (Molecular Dynamics) or Hyperfilm-MP (Amersham) with intensifying screens for 1–3 d.
25. Scan the results on phosphoimager or develop the film. The densities of bands of interest can be quantified with IMAGEQUANT software or by scanning densitometry, and normalized to the amounts of extracted cell protein subjected to immunoprecipitation.

4. Notes

1. The level of receptor expression is key to the success in detection of the phosphorylated opioid receptor protein in the cell labeling method. The rule of thumb is that an expression level of 1 pmol receptor/mg protein or more is required, which can usually be achieved by using a transfected cell line that stably expresses the receptor. For samples that have less receptor expression, such as brain tissues, you may have to increase the amount of ^{32}P in the labeling medium and film exposure time in order to detect the phosphorylated receptor protein.
2. Beware that different cell types and growth conditions may yield different results on receptor phosphorylation. For example, morphine can induce a significant mu opiod receptor phosphorylation in transfected CHO cells but poorly in HEK293 cells *(7,10)* even with the similar expression level of the receptor.
3. Because of the relatively high dose of ^{32}P-orthophosphate used in this method, extra caution is needed in handling of radioactive materials during the labeling procedure. Make sure you have all the necessary beta radiation shields and protective tools (benchtop shield, waste container and shield, storage box, covered microtube racks, and goggles) for environmental and personal safety before you start the experiment. After each experiment, check all working areas for contamination including centrifuge rotors.
4. It is important to store the presoaked protein A/Sepharose CL-4B beads and antiserum in suitable conditions. Before use, store the antibody at –80°C, and make small aliqots of antibody to avoid multiple thaw/ freeze cycle. Presoaked protein A/Sepharose CL-4B beads can be prepared in advance. Try to prepare the correct amount of beads enough for just a week of use and store them at 4°C to prevent microbial growth, which can cause the loss of protein A function.

References

1. Reisine, T. and Pasternak, G. (1996) Opioid analgesics and antagonists, in *Goodman & Gilman's the pharmacological basis of therapeutics* (Hardman, J.G. and Limbird, L.E., eds.), McGraw-Hill, New York, pp. 521–555.
2. Nestler, E. J., Hope, B.T., and Widnell, K.L. (1993) Drug addiction: a model for the molecular basis of neural plasticity. *Neuron* **11,** 995–1006.
3. Pei, G., Kieffer B.L., Lefkowitz, R.J., and Freedman, N.J. (1995) Agonist-dependent phosphorylation of the mouse delta-opioid receptor: involvement of G protein-coupled receptor kinases but not protein kinase C. *Mol. Pharmacol.* **48(2),** 173–177.
4. Zhang, L., Yu, Y., Mackin, S., Weight, F.F., Uhl, G.R., and Wang, J.B. (1996) Differential mu opiate receptor phosphorylation and desenstization induced by agonist and phorbol esters. *J. Biol. Chem.* **271,** 11,449–11,454.
5. Arden, J.R., Segredo, V., Wang, Z., Lameh, J., and Sadee W. (1995) Phosphorylation and agonist-specific intracellular trafficking of an epitope-tagged mu-opioid receptor expressed in HEK 293 cells. *J. Neurochem.* **65(4),** 1636–1645.
6. Schmidt, H., Schulz, S., Klutzny, M., Koch, T., Handel, M., and Hollt. V. (2000) Involvement of mitogen-activated protein kinase in agonist-induced phosphorylation of the mu-opioid receptor in HEK 293 cells. *J. Neurochem.* **74(1),** 414–422.
7. Yu, Y., Zhang, L., Yin, X., Sun, H., Uhl, G.R., and Wang, J.B. (1977) Mu opiate receptor phosphorylation, desenstization and ligand efficacy. *J. Biol. Chem.* **272,** 28,869–28,874.
8. Deng, H.B., Yu, Y., Pak, Y., O'Dowd, B.F., George, S.R., Surratt., C.K., et al. (2000) A role for the C-terminus in agonist-induced mu opioid receptor phosphorylation and desensitization. *Biochemistry* **39(18),** 5492–5499.
9. Deng, H.B., Yu, Y., and Wang, J.B. (2001) Agonist-induced mu opioid receptor phosphorylation and functional desensitization in rat thalamus. *Brain Res,* **898,** 204–214.
10. Zhang, J., Ferguson, S.S., Barak, L.S., Bodduluri, S.R., Laporte, S.A., Law, P.Y., et al. (1998) Role for G protein-coupled receptor kinase in agonist-specific regulation of mu-opioid receptor responsiveness. *Proc. Natl. Acad. Sci. USA* **95(12),** 7157–7162.

6

Opioid Receptor Coupling to GIRK Channels

In Vitro Studies Using a Xenopus *Oocyte Expression System and In Vivo Studies on* Weaver *Mutant Mice*

Kazutaka Ikeda, Mitsunobu Yoshii, Ichiro Sora, and Toru Kobayashi

1. Introduction

Opioid receptors are coupled to a variety of effectors, including G protein-activated inwardly rectifying potassium (GIRK) channels (also known as Kir3), adenylyl cyclases, and voltage-dependent calcium channels *(1)*. GIRK channels have been shown to be involved in opioid-induced analgesia *(2)*. These channels are activated by G protein-coupled receptors (GPCRs) such as opioid, nociceptin/orphanin FQ, M2 muscarinic, α_2 adrenergic, and D_2 dopaminergic receptors via the βγ subunits of G proteins (Gβγ) (*see* **Fig. 1**) *(3–7)*. Activation of GIRK channels induces membrane hyperpolarization of the neurons via efflux of potassium ions, ultimately reducing neural excitability and heart rate *(3,8–10)*. GIRK channels are members of a family of inwardly rectifying potassium (IRK) channels which have two transmembrane regions and one pore-forming region (*see* **Fig. 2**). The cDNAs for four GIRK channel subunits have been cloned from mammalian tissues *(11–13)*. Neuronal GIRK channels in most regions of the central nervous system (CNS) are predominant heteromultimers consisting of GIRK1 and GIRK2 subunits *(14–16)*, whereas atrial GIRK channels are heteromultimers consisting of GIRK1 and GIRK4 subunits *(17)*. The GIRK1, GIRK2, and GIRK3 subunits are widely and distinctively expressed in the CNS *(14,16,18)*, suggesting that they are involved in diverse functions of the CNS such as cognition, memory, emotion, and motor coordination. In many neurons, GIRK channels are coexpressed with opioid receptors *(6)*. For investigation of opioid-receptor
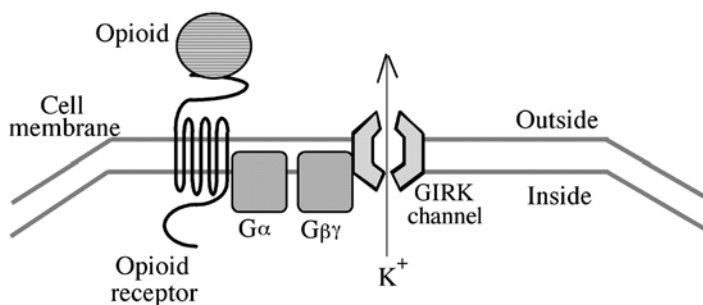
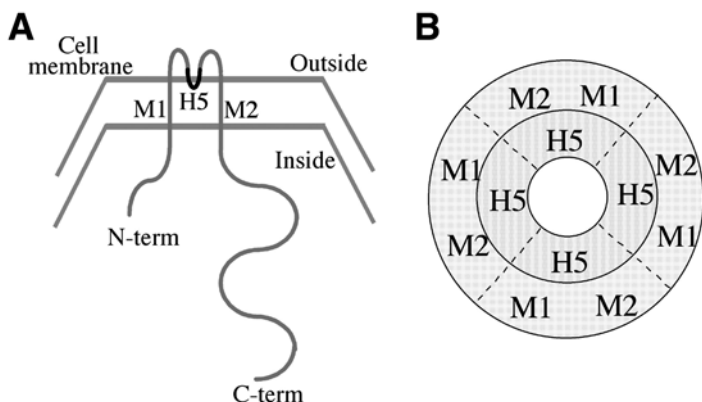Fig. 1. Schematic drawing of opioid receptor and GIRK channel coupling.

Fig. 2. Schematic drawings of a GIRK channel. **(A)** Schematic drawing of GIRK subunit structure. **(B)** Schematic drawing of GIRK channel structure. A GIRK channel is composed of 4 GIRK subunits. M1, M2: transmembrane domains 1, 2. H5: pore-forming region.

functions in vitro, especially coupling of opioid receptors to GIRK channels, the *Xenopus* oocyte expression system is sensitive and valuable in generating functional analyses and physiological significance. Functions of the opioid system, including analgesia and reward, can be analyzed only in animals, not in individual cells. The *weaver* mutant mouse serves as an ideal animal model for studying the role of the GIRK channel in vivo because of the impaired couplings of opioid receptors to GIRK channels *(19)*.

2. Materials

1. First strand cDNA (e.g., mouse brain cDNA).
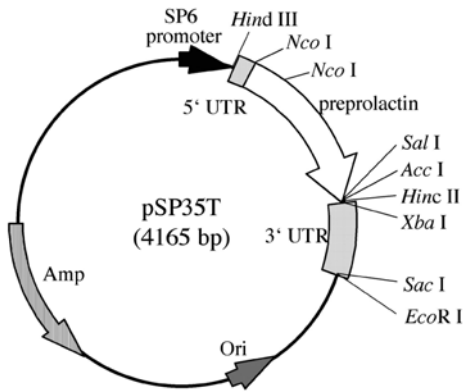2. Expression vector [e.g., pSP35T *(20)* (*see* **Fig. 3**)].

Fig. 3. Schematic drawing of pSP35T expression plasmid. 5' UTR: the 5' untranslated region of *Xenopus* β-globin. 3' UTR: the 3' untranslated region of *Xenopus* β-globin. Preprolactin can be substituted by cDNA for receptor or channel. Amp: ampicillin resistant gene. Ori: origin of replication.

3. DNA polymerase (e.g., *Pfu* DNA polymerase; Stratagene; La Jolla, CA).
4. mRNA synthesis kit (e.g., mMESSAGEmMACHINE; Ambion, Austin, TX).
5. STE solution: 150 mM NaCl, 10 mM Tris-HCl, pH 7.5, 1 mM EDTA.
6. cDNA spun column (e.g., Sephacryl S-300; Amersham Pharmacia Biotech, Buckinghamshire, U.K.).
7. Adult female South African clawed frogs (*Xenopus laevis*) (e.g., Copacetic, Aomori, Japan).
8. 100X Tris-Calcium Solution: 750 mM Tris-HCl, pH 7.4, 33 mM Ca(NO$_3$)$_2$, 41 mM CaCl$_2$ (Autoclaved).
9. Calcium-free ND96 solution: 96 mM NaCl, 2 mM KCl, 2 mM MgCl$_2$, 5 mM HEPES, adjust pH to 7.5 with NaOH.
10. 50X Salts Solution: 4.4 M NaCl, 50 mM KCl, 41 mM MgSO$_4$ (Autoclaved).
11. Gentamicin sulfate (e.g., Wako Pure Chemical Industries, Ltd., Osaka, Japan).
12. Barth's solution: 1 X Tris-Calcium Solution, 1x Salts Solution, 2.4 mM NaHCO$_3$, 0.1 mg/mL gentamicin in autoclaved distilled water.
13. Electrode puller (e.g., PN-3; Narishige, Tokyo, Japan).
14. Microforge (e.g., MF-83; Narishige, Tokyo, Japan).
15. Microinjector (e.g., IM-50B; Narishige, Tokyo, Japan; and Nano liter injector A203XVY model; World Precision Instruments, Inc., Sarasota, FL).
16. Collagenase (e.g., Collagenase Type I; Wako Pure Chemical Industries, Ltd., Osaka, Japan).
17. Perfusion medium, e.g., high potassium solution (HKS): 96 mM KCl, 2 mM NaCl, 1 mM MgCl$_2$, 1.5 mM CaCl$_2$.
18. Electrophysiological setup for two-microelectrode voltage clamp.
19. *Weaver* mutant mice (The Jackson Laboratory, Bar Harbor, ME, or our laboratory for C3H-backcrossed mice).
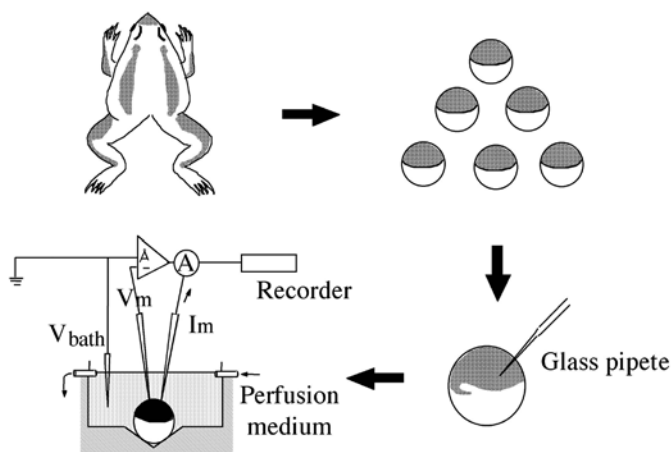
Fig. 4. Experimental procedure for the *Xenopus* oocyte expression system. A: amplifier.

20. Tail-flick test apparatus (e.g., MK-330B; Muromachi Kikai Co., Ltd., Tokyo, Japan).
21. Hot-plate test apparatus (e.g., MK-350B; Muromachi Kikai Co., Ltd.).
22. Open-field test apparatus (e.g., X-Y-Z; Muromachi Kikai Co., Ltd., Tokyo, Japan).
23. Morphine chloride.
24. (–)–U50488 hydrochloride.

3. Methods

3.1. Xenopus Oocyte Expression System (see Fig. 4)

Xenopus laevis oocytes have been widely used in studies on the function and regulation of a variety of ion channels and receptors *(21)*. They are unfertilized eggs that install all biochemical machinery necessary for translating mRNA, for transporting the resulting protein, and for inserting it correctly in the plasma membrane *(22)*. Detailed understanding of the physiological characteristics of oocyte plasma membrane has enabled the characterization of proteins translated from foreign mRNAs *(22)*. *Xenopus* oocytes possess an endogenous GIRK subunit (XIR) which forms a heteromultimer channel with an exogenously expressed GIRK1 subunit *(23,24)*. No endogenous opioid receptor has been found in *Xenopus* oocytes. The *Xenopus* oocyte expression system is superior to ligand binding methods because it allows the activation and inhibition of receptors to be studied under physiological conditions *(25,26)*.

Sensitivity of the system is superior to conventional ligand binding methods and cAMP accumulation methods. Because opioid receptors are functionally coupled to GIRK channels via Gi/o proteins, investigations using the *Xenopus* oocyte expression system with these molecules should provide more physiologically relevant information than the Fluorometric Imaging Plate Reader (FLIPR) system with Gi/Gq chimeric G proteins *(27)*.

3.1.1. Construction of Expression Vectors

The pSP35T (*see* **Fig. 3**) expression system developed by Amaya *(20)* is highly effective in producing recombinant receptors and channels (e.g., mu-opioid receptor and GIRK channel) in *Xenopus* oocytes. This is because it contains those nucleotide sequences that correspond to the untranslated regions of *Xenopus* oocyte β-globin mRNA. Other expression vectors can also be used (e.g., pBKSA) *(28)* (*see* **Note 1**). The procedure is as follows:

1. Synthesize the first strand cDNA using template mRNA (e.g., mouse brain mRNA).
2. Synthesize a pair of oligonucleotide primers containing nucleotide sequences corresponding to the initiating methionine and stop codon. In the case of pSP35T vector, preferable sites for recombination are *Nco* I and *Xba* I sites (*see* **Note 2**).
3. Amplify the cDNA for the receptor or channel by PCR with *Pfu* DNA polymerase, with the first strand cDNA as a template and with the primers.
4. Insert the cDNA at the appropriate site of the pSP35T vector (*see* **Note 3**).
5. Amplify the recombinant vector plasmid using *Escherichia coli*.
6. Purify the plasmid (e.g., Qiagen plasmid purification kit).
7. Linearize the plasmid with an appropriate restriction enzyme (*Eco*R I or *Sac* I in the case of pSP35T).
8. Purify the linearized plasmid with conventional phenol/chloroform treatment.
9. Dissolve the plasmid with RNase-free distilled water at 0.5 mg/mL.

3.1.2. mRNA Synthesis

1. Synthesize mRNA using an RNA synthesis kit (e.g., mMESSAGEmMACHINE) with the linearized plasmid as template.
2. Degrade the template DNA with RNase-free DNase I.
3. Purify the mRNA with conventional phenol/chloroform treatment.
4. Remove chloroform completely by diethylether treatment (twice).
5. Purify the mRNA by gel-chromatography using cDNA spun columns buffered with STE solution.
6. Measure the mRNA concentration.
7. Add 1/19 vol of 3 *M* sodium acetate.
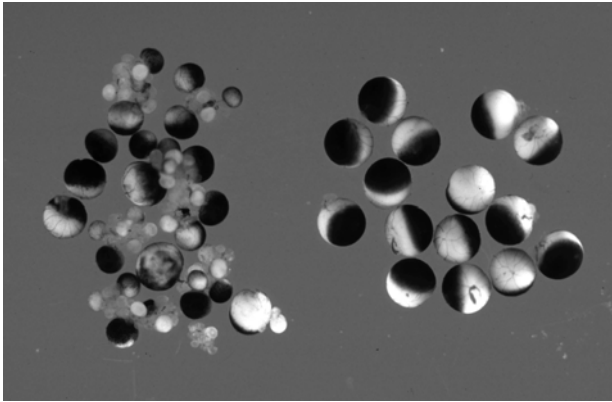8. Add 2.5 vol of ethanol.
9. Store at –80°C.

Figure 5. *Xenopus* oocytes. Left, oocytes inappropriate for experiment. These are too small or dying. Right, mature oocytes (Stage V and VI) as used in experiments. It is useful to leave a small amount of connective tissue or follicle cell layer surrounding the oocytes for removal of the follicle cell layer after collagenase treatment.

3.1.3. Oocyte Preparation

1. Maintain adult female South African clawed frogs at 19°C (*see* **Note 4**).
2. Anesthetize the frog by immersion in water containing 0.15% tricaine.
3. Remove several ovarian lobes from the abdomen, and immerse these in Barth's solution.
4. Isolate mature oocytes suitable for experiments, using spring scissors and forceps (*see* **Fig. 5**).

3.1.4. Injection and Collagenase Treatment

1. Prepare injection pipets from glass tubes using a puller, a microforge (*see* **Fig. 6**) and a sterilizing oven (200°C for 8 h).
2. Centrifuge an appropriate volume of mRNA(s) (ethanol suspension) and remove the supernatant.
3. Dissolve the mRNA(s) in 10 µL distilled water (approx 10 pmol/mL).
4. Inject the mRNA solution into approx 100 oocytes using the glass pipet and the microinjector.
5. Incubate the injected oocytes in Barth's solution for 2 d at 19°C.
6. Treat the oocytes with collagenase (1 mg/mL) dissolved in calcium-free ND96 solution for 1 h at 19°C.
7. Remove the follicle cell layer from the oocytes using forceps and maintain the oocytes in Barth's solution.

3.1.5. Voltage Clamp Recording

1. Prepare HKS or other perfusion medium.
2. Fill the micropipet electrode with 3 *M* KCl. The resistance of the current-injecting
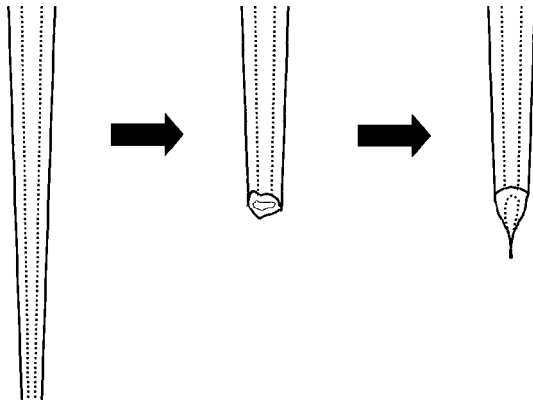
Fig. 6. Preparation of injection pipets. A glass pipet is prepared using the puller. After breaking off the pipet tip, the shape of the tip is changed using a microforge.

   electrode (*Im*) should be approx 1 *M*Ω and the resistance of the potential electrode (*Vm*) approx 5 MΩ.
3. Measure the bath potential (*V*bath) with the potential electrode and adjust it to zero.
4. Insert the potential electrode into the oocyte using a micromanipulator and measure the resting potential.
5. Insert the current electrode. Clamp the membrane at –70 mV and wait until the current becomes stable (*see* **Note 5**).
6. Apply drugs to perfusion medium in sequence and record the membrane currents as responses to the drugs (*see* **Note 6**).

3.2. Weaver *Mutant Mice*

   To understand actions of the opioid system in vivo, including analgesia, euphoria, and dependence, animal experiments are necessary. The *weaver* mutant mouse is a valuable animal model because the coupling of opioid receptors to GIRK channels is impaired and no specific activators or blockers of GIRK channels has yet been found. The mutant mice possess a missense point mutation in the pore-forming region of the GIRK2 subunit *(29)* (*see* **Fig. 7**). The activity of the mutant GIRK channel is not regulated by G proteins *(19)*, implying that the pathway of opioid signaling via GIRK channels is impaired in weaver mutant mice. Interestingly, *weaver* mutant mice show reduced analgesia after administration of either morphine or kappa-opioid receptor agonists *(30)*, although a nonsteroidal antiinflammatory drug (NSAID) induces analgesia normally *(31)*. These results suggest the involvement of GIRK channels in opioid-induced analgesia. Further investigation using *weaver* mutant mice promises a better understanding of opioid functions in vivo.

	ACA GAA ACC ACC ATC G|GT TAT GGC TAC CGG
Wild type	Thr Glu Thr Thr Ile Gly Tyr Gly Tyr Arg
	ACA GAA ACC ACC ATC A|GT TAT GGC TAC CGG
Weaver	Thr Glu Thr Thr Ile Ser Tyr Gly Tyr Arg

Amino-acid No.   151   152   153   154   155   156   157   158   159   160

Fig. 7. A missense point mutation in a gene encoding the GIRK2 subunit in *weaver* mutant mice.
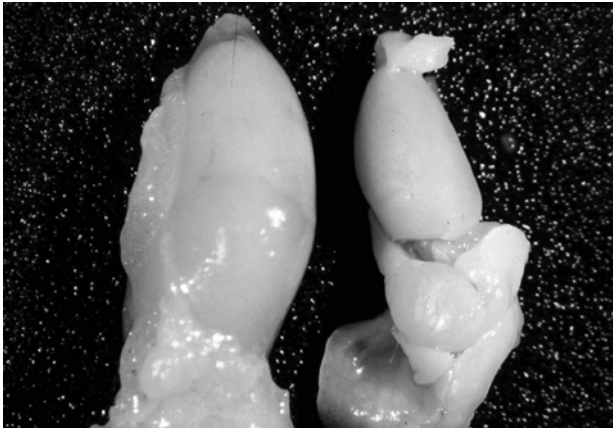
Fig. 8. Testes of C3H (left) and *weaver* mutant (right) mice.

3.2.1. Breeding

Weaver mutant mice with genetic background C57BL/6 can be purchased from the Jackson Laboratory. Breeding of the homozygous mice is difficult due to impaired testicular development (*see* **Fig. 8**). Homozygous mutant mice can be obtained efficiently by mating heterozygous male and homozygous female mice. Homozygous *weaver* mutant mice with genetic background C3H are readily bred *(31)* (*see* **Note 7**).

3.2.2. Genotyping

1. Cut the tip (approx 5 mm) of the mouse tail.
2. Prepare the genomic DNA by conventional methods.
3. Amplify the DNA fragment using the PCR method with the following pair of primers:
   5'-ATGATCTGGTGGCTGATTGC-3', 5'-TTGGGATATTTTCACAAACA-3'
4. Analyze the nucleotide sequence of the DNA fragment (*see* **Fig. 7**).

3.2.3. Behavioral Analyses

Opioid-induced analgesia can be evaluated by the tail-flick test or the hotplate test *(30)*. Examination of locomotor activity is necessary when analyzing the behavior of the *weaver* mutant mouse because these mice display motor ataxia and hyperactivity. Experiments should also be carefully designed (*see* **Note 8**).

4. Notes

1. Either receptors or channels can be expressed in the cell membrane of *Xenopus* oocytes using vector systems possessing appropriate promoters (e.g., pCDNA) when the vectors are injected in the nuclei of oocytes *(32)*. The size of the nucleus is approx one-fourth of the oocyte diameter.
2. It is recommended that GC sequence is added at the 5' end of each nucleotide oligomer. The sequence can be removed when the PCR fragment is digested with restriction enzyme.
3. If recombination of the vector at the *Nco* I site is difficult, a cDNA fragment can be connected at *Hin*d III site (removal of the 5' untranslated region of β-globin mRNA), although the amount of expression will be reduced.
4. It is known that stretch activated channels are expressed in *Xenopus* oocytes when the frogs are kept in a warm room. The stretch activated channels make the experiments more difficult.
5. If the holding current does not stabilize within approx 10 min, the oocyte should be discarded.
6. Oocytes can be analyzed several times if they are incubated in Barth's solution after each analysis.
7. Mashed food is better for raising homozygous *weaver* mutant mice. The floor chip in the cage should not be changed during the first week after birth.
8. In weaver mutant mice, neuronal degeneration is observed in the granule cell layer of the cerebellum, the substantia nigra and the pontine nucleus *(33)*. *Weaver* mouse brain is shown in **Fig. 9**.

Acknowledgments
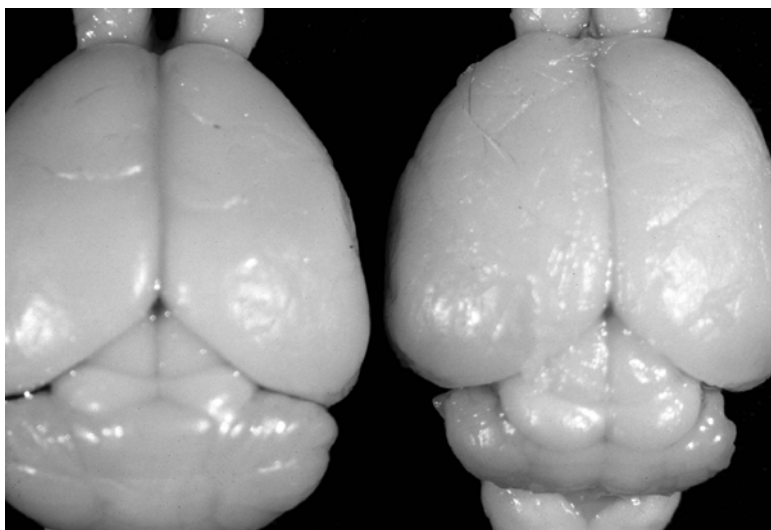
Fig. 9. Brains of C3H (left) and *weaver* mutant (right) mice.

References

1. Law, P. Y., Wong, Y. H., and Loh, H. H. (2000) Molecular mechanisms and regulation of opioid receptor signaling. *Annu. Rev. Pharmacol. Toxicol.* **40,** 389–430.
2. Ikeda, K., Kobayashi, T., Kumanishi, T., Yano, R., Sora, I., and Niki, H. (2002) Molecular mechanisms of analgesia induced by opioids and ethanol: is the GIRK channel the key? *Neurosci. Res.* **44,** 121–131.
3. North, R. A. (1989) Drug receptors and the inhibition of nerve cells. *Br. J. Pharmacol.* **98,** 13–28.
4. Takao, K., Yoshii, M., Kanda, A., Kokubun, S., and Nukada, T. (1994) A region of the muscarinic-gated atrial K^+ channel critical for activation by G protein beta gamma subunits. *Neuron* **13,** 747–755.
5. Ikeda, K., Kobayashi, K., Kobayashi, T., Ichikawa, T., Kumanishi, T., Kishida, H., et al. (1997) Functional coupling of the nociceptin/orphanin FQ receptor with the G-protein-activated K^+ (GIRK) channel. *Brain Res Mol. Brain Res.* **45,** 117–126.
6. Ikeda, K., Kobayashi, T., Ichikawa, T., Usui, H., Abe, S., and Kumanishi, T. (1996) Comparison of the three mouse G-protein-activated K^+ (GIRK) channels and functional couplings of the opioid receptors with the GIRK1 channel. *Ann. NY Acad. Sci.* **801,** 95–109.
7. Ikeda, K., Kobayashi, T., Ichikawa, T., Usui, H., and Kumanishi, T. (1995) Functional couplings of the d- and the k-opioid receptors with the G-protein-activated K^+ channel. *Biochem. Biophys. Res. Commun.* **208,** 302–308.

8. Brown, A. M. and Birnbaumer, L. (1990) Ionic channels and their regulation by G protein subunits. *Annu. Rev. Physiol.* **52,** 197–213.

9. Signorini, S., Liao, Y. J., Duncan, S. A., Jan, L. Y., and Stoffel, M. (1997) Normal cerebellar development but susceptibility to seizures in mice lacking G protein-coupled, inwardly rectifying K$^+$ channel GIRK2. *Proc. Natl. Acad. Sci. USA* **94,** 923–927.

10. Wickman, K., Nemec, J., Gendler, S. J., and Clapham, D. E. (1998) Abnormal heart rate regulation in GIRK4 knockout mice. *Neuron* **20,** 103–114.

11. Kubo, Y., Reuveny, E., Slesinger, P. A., Jan, Y. N., and Jan, L. Y. (1993) Primary structure and functional expression of a rat G-protein-coupled muscarinic potassium channel. *Nature* **364,** 802–806.

12. Doupnik, C. A., Davidson, N., and Lester, H. A. (1995) The inward rectifier potassium channel family. *Curr. Opin. Neurobiol.* **5,** 268–277.

13. Reimann, F. and Ashcroft, F. M. (1999) Inwardly rectifying potassium channels. *Curr. Opin. Cell Biol.* **11,** 503–508.

14. Kobayashi, T., Ikeda, K., Ichikawa, T., Abe, S., Togashi, S., and Kumanishi, T. (1995) Molecular cloning of a mouse G-protein-activated K$^+$ channel (mGIRK1) and distinct distributions of three GIRK (GIRK1, 2 and 3) mRNAs in mouse brain. *Biochem. Biophys. Res. Commun.* **208,** 1166–1173.

15. Lesage, F., Guillemare, E., Fink, M., Duprat, F., Heurteaux, C., Fosset, M., et al. (1995) Molecular properties of neuronal G-protein-activated inwardly rectifying K$^+$ channels. *J. Biol. Chem.* **270,** 28,660–28,667.

16. Liao, Y. J., Jan, Y. N., and Jan, L. Y. (1996) Heteromultimerization of G-protein-gated inwardly rectifying K$^+$ channel proteins GIRK1 and GIRK2 and their altered expression in weaver brain. *J Neurosci* **16,** 7137–7150.

17. Krapivinsky, G., Gordon, E. A., Wickman, K., Velimirovic, B., Krapivinsky, L., and Clapham, D. E. (1995) The G-protein-gated atrial K$^+$ channel IKACh is a heteromultimer of two inwardly rectifying K$^+$-channel proteins. *Nature* **374,** 135–141.

18. Karschin, C., Dissmann, E., Stuhmer, W., and Karschin, A. (1996) IRK(1-3) and GIRK(1-4) inwardly rectifying K$^+$ channel mRNAs are differentially expressed in the adult rat brain. *J. Neurosci.* **16,** 3559–3570.

19. Navarro, B., Kennedy, M. E., Velimirovic, B., Bhat, D., Peterson, A. S., and Clapham, D. E. (1996) Nonselective and G$\beta\gamma$-insensitive weaver K$^+$ channels. *Science* **272,** 1950–1953.

20. Amaya, E., Musci, T. J., and Kirschner, M. W. (1991) Expression of a dominant negative mutant of the FGF receptor disrupts mesoderm formation in *Xenopus* embryos. *Cell* **66,** 257–270.

21. Dascal, N. (1987) The use of *Xenopus* oocytes for the study of ion channels. *CRC Crit. Rev. Biochem.* **22,** 317–387.

22. Fraser, S. P. and Djamgoz, M. B. A. (1992) *Xenopus* oocytes: endogenous electrophysiological characteristics, in *Current Aspects of the Neurosciences*, (Osborne, N. N., ed.), Macmillan Basingstoke, Hampshire, UK, vol. 4, pp. 267–315.

23. Duprat, F., Lesage, F. Guillemare, E., Fink, M., Hugnot, J. P., Bigay, J., et al. (1995) Heterologous multimeric assembly is essential for K$^+$ channel activity of

neuronal and cardiac G-protein-activated inward rectifiers. *Biochem. Biophys. Res. Commun.* **212,** 657–663.

24. Hedin, K. E., Lim, N. F., and Clapham, D. E. (1996) Cloning of a *Xenopus laevis* inwardly rectifying K⁺ channel subunit that permits GIRK1 expression of IKACh currents in oocytes. *Neuron* **16,** 423–429.

25. Kobayashi, T., Ikeda, K., Ichikawa, T., Togashi, S., and Kumanishi, T. (1996) Effects of sigma ligands on the cloned μ-, δ- and κ-opioid receptors co-expressed with G-protein-activated K⁺ (GIRK) channel in *Xenopus* oocytes. *Br. J. Pharmacol.* **119,** 73–80.

26. Kobayashi, T., Ikeda, K., and Kumanishi, T. (1998) Effects of clozapine on the δ- and κ-opioid receptors and the G-protein-activated K⁺ (GIRK) channel expressed in *Xenopus* oocytes. *Br. J. Pharmacol.* **123,** 421–426.

27. Coward, P., Wada, H. G., Falk, M. S., Chan, S. D., Meng, F., Akil, H., and Conklin, B. R. (1998) Controlling signaling with a specifically designed Gi-coupled receptor. *Proc. Natl. Acad. Sci. USA* **95,** 352–357.

28. Yamazaki, M., Mori, H., Araki, K., Mori, K. J., and Mishina, M. (1992) Cloning, expression and modulation of a mouse NMDA receptor subunit. *FEBS Lett.* **300,** 39–45.

29. Patil, N., Cox, D. R., Bhat, D., Faham, M., Myers, R. M., and Peterson, A. S. (1995) A potassium channel mutation in *weaver* mice implicates membrane excitability in granule cell differentiation. *Nat. Genet.* **11,** 126–129.

30. Ikeda, K., Kobayashi, T., Kumanishi, T., Niki, H., and Yano, R. (2000) Involvement of G-protein-activated inwardly rectifying K⁺ (GIRK) channels in opioid-induced analgesia. *Neurosci. Res.* **38,** 113–116.

31. Kobayashi, T., Ikeda, K., Kojima, H., Niki, H., Yano, R., Yoshioka, T., and Kumanishi, T. (1999) Ethanol opens G-protein-activated inwardly rectifying K⁺ channels. *Nat. Neurosci.* **2,** 1091–1097.

32. Swick, A. G., Janicot, M., Cheneval-Kastelic, T., McLenithan, J. C., and Lane, M. D. (1992) Promoter-cDNA-directed heterologous protein expression in Xenopus laevis oocytes. *Proc. Natl. Acad. Sci. USA* **89,** 1812–1816.

33. Ozaki, M., Hashikawa, T., Ikeda, K., et al. (2002) Degeneration of pontine mossy fibres during cerebellar development in weaver mutant mice. *Eur. J. Neurosci.* **16,** 565–574.

7

Identification of Alternatively Spliced Variants from Opioid Receptor Genes

Ying-Xian Pan

1. Introduction

Alternative splicing is commonly used in eucaryotic gene regulation. A single mouse μ opioid receptor gene (*Oprm*) can generate 15 spliced variants by alternative splicing of its 14 exons *(1–6)*. Furthermore, the region-specific expression of the splice variants suggests an important role of alternative splicing in regulating gene functions *(4–8)*. Genomic sequences from various species are available from many genome projects, but it is still challenging to directly identify splice variants from a given gene sequence through sequence analysis, particularly for those with cryptic splice sites. Since some of the variants are expressed at a lower level, traditional library screening often fails to identify such variants. Rapid development of polymerase chain reaction (PCR) technology provides a powerful tool of isolating low-level splice variants with great sensitivity and specificity. There are several common patterns of alternative splicing including exon skipping, intron retention, and exon recruiting. This chapter describes three similar, but distinct approaches of identifying the potential low-level splice variants: 1) a modified rapid amplification of cDNA 5'- end (5'RACE) approach used to isolate the variants with new exons at the 5'-end; 2) a modified 3' RACE approach used to obtain the variants with new exons at the 3'-end; and 3) an internal exon-scanning reverse transcriptase (RT)-PCR approach used to identify the variants with new exons from the introns or with exon skipping.

2. Materials

1. RNeasy Mini kit (Qiagen).
2. Mini Oligotex Direct mRNA kit (Qiagen).
3. Superscript II RNase H$^-$ reverse transcriptase, 200 U/µL (Invitrogen).
4. Random Hexamer (Amersham).
5. RNaseOUT, 40 U/µL (Invitrogen).
6. dNTP, 10 m*M* each of dATP, dGTP, dCTP, and dTTP in H_2O.
7. 5'-biotinylated primers.
8. RNase H, 2 U/µL (Invitroge).
9. RNase A (Qiagen).
10. Magnetic beads M280 coupled with streptavidin (M280-S), 10 mg/mL (Dynal).
11. Magnetic Particle Concentrator (MPC) (Dynal).
12. 2 x Buffer A: 10 m*M* Tris-HCl, pH 7.5, 1 m*M* ethylenediamine tetraacetic acid (EDTA), and 2 *M* NaCl.
13. Adapter: 5'(Phosphate)-CCCTTCTGTCGTCTTCTCGCAGCCGTA-3'(NH$_2$) (*see* **Note 1**).
14. Anchor sense primer: 5'-TACGGCTGCGAGAAGACGACAGAAGGG-3'.
15. Oligo d(T) $_{30}$VN (V = A, C, or G; N = A, C, G, or T).
16. T$_4$ RNA ligase (New England BioLab), 5 × T$_4$ RNA ligase buffer, 250 m*M* Tris-HCl, pH 8.0, 50 m*M* MgCl$_2$, 5 m*M* Hexammine cobalt chloride (HCC), 100 µ*M* ATP, and 50 µg/mL BSA in H_2O.
17. 50% PEG8000: Dissolve 25 g of polyethylene glycol (PEG, Mw. 8000) in H_2O. and store at –20°C.
18. Platinum Taq DNA polymerase, 5 U/µL (Invitrogen).
19. pCRII-TOPO vector (Invitrogen).
20. TOP10F' competent cells (Invitrogen).
21. Luria-Bertani (LB) broth: Dissolve 10 g of Bacto tryptone, 5 g of Bacto yeast extract, and 5 g of NaCl in 800 mL H_2O. Adjust the pH to 7.2 with 1 *M* NaOH and bring the volume to 1 L. Sterilize the medium by autoclaving.
22. 100 m*M* IPTG stock: Dissolve 1.19 g isopropyl-β-D-thio-galactopyranoside (IPTG) in 50 mL of H_2O. Filtrate the solution through a 0.22-µm filter and store at –20°C.
23. 2% X-gal stock: Dissolve 1 g 5-bromo-4-chloro-3-indoyl-β-D-galactopyranoside (X-gal) in 50 mL of dimethylform amide. Store in a foil-wrapped tube at –20°C.
24. 50 mg/mL Ampicillin stock: Dissolve 2 g ampicillin in 40 mL of H_2O. Filtrate the solution through a 0.22-µm filter and store at –20°C.
25. LB/IPTG/X-gal/ampicillin plates: Add 4 g agar in 330 mL of LB broth (1.2% agar). Autoclave and cool the medium to 50°C. Add 0.2 m*M*/mL IPTG, 0.008% X-gal and 100 µg/mL ampicillin into the medium and pour into 15 × 100 mm sterile polystyrene plates (approx 30 mL per plate). Cool the plates at room temperature and store in dark at 4°C.
26. SOC medium: Dissolve 20 g of Bacto tryptone and 5 g of Bacto yeast extract in 800 mL of H_2O. Add 2 mL of 5 *M* NaCl and 2.5 mL of 1 *M* KCl. Bring the volume to 1 L and autoclave the medium. For 50 mL SOC medium, add 1 mL of

20% glucose, 0.5 mL of 1M $MgSO_4$, and 0.5 mL of $MgCl_2$ into 48 mL SOB medium.

3. Methods

3.1. 5' RACE (see *Fig. 1*)

3.1.1. RT Reaction with Superscript II RNase H⁻ Reverse Transcriptase (see **Note 2**, **Fig. 1**, **step 1**)

1. RNA isolation (*see* **Note 3**). Isolate total RNA or mRNA from 20–30 mg of tissues or 10^6–10^7 cultured cells by using a RNeasy mini kit or a mini Oligotex Direct mRNA kit. Estimate the RNA concentrations by an UV spectrophotometer at OD_{260}.
2. RT reaction with random hexamers, $pd(N)_6$ (*see* **Fig.1A**). Add 20 µg of total RNA or 1 µg of mRNA and 0.8 µg of random hexamers into a 1.5-mL tube, and bring volume to 11 µL with water.
3. Heat the tube at 70°C for 10 min, quickly cool it on ice for 2 min, and briefly spin it for a few seconds to bring evaporated moisture down.
4. Add 4 µL of 5 × RT reaction buffer, 2 µL of 0.1 *M* dithiothreitol (DTT), 1 µL of 10 m*M* deoxynucleotide 5'-triphosphate (dNTP), and 1 µL of RNaseOUT (40 U) into the tube containing the RNA and hexamers.
5. Mix the mixture by gently vortexing and incubate the tube at 37°C for 2 min.
6. Add 1 µL of Superscript II RT (200 U) into the mixture and incubate the tube at room temperature for 10 min, then at 37°C for 10 min, and finally at 42°C for 1 h.
7. Heat-inactivate the enzyme at 70°C for 5 min and store the tube at –20°C if not proceeding the next step.
8. RT reaction with a gene-specific antisense primer with a 5' biotinylation modification (*see* **Note 4** and **Fig.1B**). Perform the same reaction as described earlier except for using 1 µL of 20 µ*M* the 5' biotinylated primer stock instead of 0.8 µg of the hexamers and for directly incubating the tube at 42°C for 1 h after adding the enzyme.
9. Removal of mRNA from DNA/RNA hybrid with RNase H (*see* **Fig. 1**, **step 2**). Add 4 U of RNase H and 1 µg of RNase A into the RT tube. Incubate the tube at 37°C for 30 min, and then 70°C for 5 min.

3.1.2. Hybridization, Purification, and Ligation

1. Hybridization of a gene-specific sense primer carrying a biotin at its 5'-end with the first-strand cDNA reverse-transcribed with the hexamers (*see* **Fig. 1**, **step 3**). Mix 1 µL of 20 µ*M* 5' biotinylated sense primer stock with the RT reaction with the hexamers in a PCR tube. Perform three thermal cycles with each cycle consisting of a 30-s melting step at 94°C and a 5 min annealing step at 60°C. Then cool down the tube to 4°C.
2. Purification of the biotinylated primers and their associated cDNA fragments with magnetic beads covalently coupled to streptavidin (M280-S) (*see* **Note 5**, **Fig. 1**, **step 4**). Prepare 30 µL of M280-S (10 mg/mL) for each 20 µL of RT
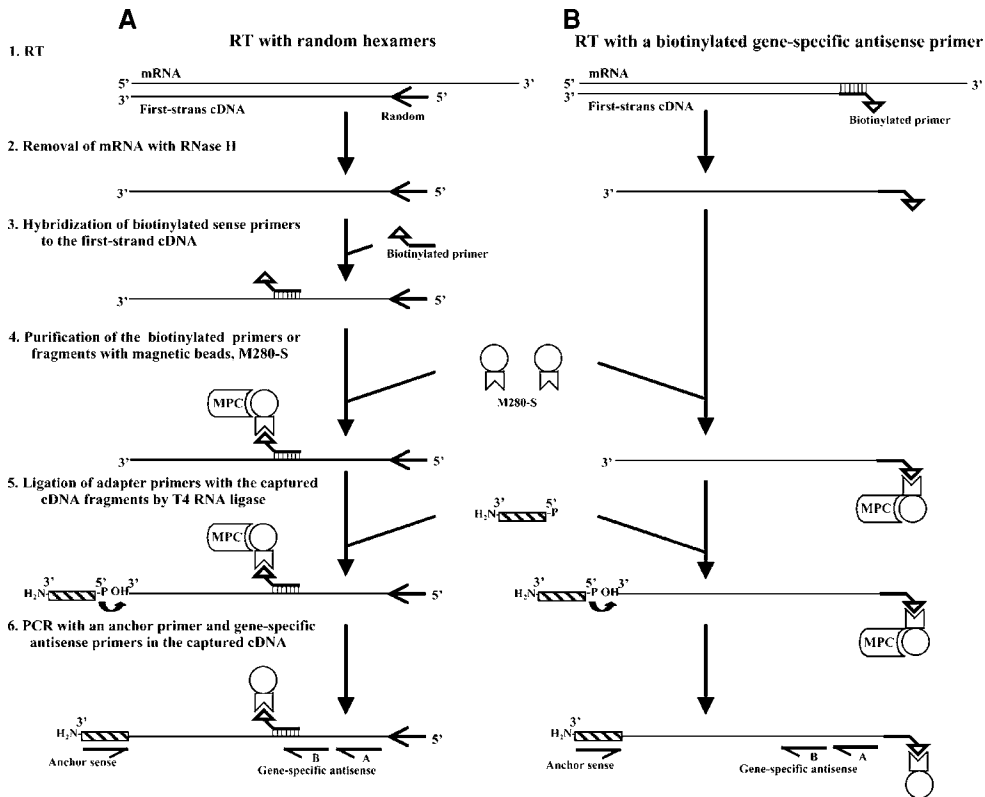
Fig. 1. Scheme of a modified 5' RACE approach. **(A)** Start a RT reaction with random hexamers. **(B)** Start a RT reaction with a 5'-biotinylated gene-specific antisense primer. M280-S, Magnetic beads M280 coupled with streptavidin. MPC, magnetic particle concentrator.

reaction. For one capture reaction, transfer 30 μL of well-mixed M280-S to a 1.5-mL tube.

3. Wash the beads with 90 μL of 2 × Buffer A at room temperature for three times by using a Magnetic Particle Concentrator (MPC). In each washing, resuspend the beads by gently vortexing, place the tube on MPC for 1 min to separate the beads from the buffer, and carefully remove the buffer by using a pipet. After the final washing, resuspend the beads in 22 μL of 2 × Buffer A.

4. Mix 22 μL of the prepared M280-S with 22 μL of the RT reaction mixture containing the biotinylated primers or their associated cDNA fragments (1 × Buffer A in the final concentration). Incubate the tube at 43°C for 1 h to allow binding of the biotinylated primers and its associated fragments to the beads. Gently vortex the tube to resuspend the beads every 8–10 min during the incubation.

5. Wash the beads at room temperature for three times with 100 μL of 1 × Buffer A as described earlier. After the final washing, perform ligation reaction immediately as described later.

6. Ligation of an adapter primer to the 3'-end of the first-strand cDNA with T_4 RNA ligase (*see* **Note 1**, **Fig. 1**, **step 5**). For one ligation reaction, make a ligation mixture by mixing 4 μL of 5 × T_4 RNA ligase buffer, 1 μL of 20 μ*M* adapter, 0.5 μL of T_4 RNA ligase and 4.5 μL of water in a separate tube. Resuspend the washed beads with 10 μL of the ligation mixture.

7. Mix 10 μL of 50% PEG8000 with the ligation mixture containing the beads by gently pipeting.

8. Incubate the tube at 25°C overnight.

3.1.3. PCR (see **Note 6**, **Fig. 1**, **step 6**)

1. Perform a two-step PCR with an anchor sense primer whose sequence is complementary to the adapter sequence and a gene-specific antisense primer by using the earlier ligation reaction as template.

2. In a PCR tube, add 10 μL of 10× reaction buffer without $MgCl_2$, 3 μL of 50 m*M* $MgCl_2$, 2 μL of 10 m*M* dNTP, 1 μL of 20 μ*M* anchor sense primer, 1 μL of 20 μ*M* antisense primer, 5 μL of the ligation mixture containing the beads and 5 U of Platinum Taq DNA polymerase.

3. Bring the volume to 100 μL with H_2O.

4. Perform PCR with an initial 2 min denaturing at 94°C and then 35 thermal cycles, each cycle consisting of a 20-s melting step at 94°C, a 2–5 min annealing/extension step at 68°C and a final 5 min extension at 72°C.

5. Analyze 10 μL of the PCR products on 1% agarose gel with 0.2 μg/mL ethidium bromide.

3.1.4. Cloning and Sequencing PCR Fragments

1. Ligate the PCR fragment into pCRII-TOPO vector. Incubate 1–4 μL (5–50 ng) of the PCR mixture with 1 μL of pCRII-TOPO vector in 5 μL of the total volume at room temperature for 5 min, and then store the tube on ice.

2. Transform the ligation products into one shot TOP10F' competent cells. Mix 2 μL of the ligation mixture with 100 μL of the TOP10F' competent cells thawed on ice. Incubate the tube on ice for 30 min, heat-shock the tube in a 42°C water bath for 45 s and then put the tube on ice for 2 min, followed by adding 250 μL of SOC medium.

3. Incubate the tube at 37°C for 1 h with shaking and plate 150 μL of the cells onto a LB/IPTG/X-gal/ampicillin plate.

4. Incubate the plate at 37°C overnight.

5. Pick up white colonies for plasmid DNA isolation.

6. Pick up individual white colonies in 5 mL of LB media containing 100 μg/mL ampicillin, grow them at 37°C overnight, and isolate the plasmid DNA by using a Plasmid Miniprep kit.

7. Sequence the DNA inserts containing the 5'RACE products in the plasmids with T7 primer and/or M13 Reverse primer.

8. Analyze the sequences to see if a new sequence is linked to the 5'-end of the predicated exon sequences.

9. Isolation of the full length of cDNAs. If the new 5'-end sequence is identified, perform PCR with the sense primers from the new sequence and the antisense primers from the downstream exons to obtain the full length of the cDNAs; or screen cDNA libraries by using the new sequence as the probe.

3.2. 3' RACE (see *Fig. 2;* see *Note 7*)

1. RNA isolation. Isolate total RNA as described in **Subheading 3.1.1.**, **step 1**.

2. RT reaction with Superscript II RNase H⁻ reverse transcriptase (*see* **Fig. 2**, **step 1**). Perform the same RT reaction as described in **Subheading 3.1.1.**, **step 8** except for using 0.8 μg of an oligo d(T)$_{30}$VN (V = A, C, or G; N = A, C, G, or T).

3. Removal of mRNA from DNA/RNA hybrid with RNase H (*see* **Fig. 2**, **step 2**). Perform the same reaction as described in **Subheading 3.1.1., step 9**.

4. Hybridization of a gene-specific sense primer carrying a biotin at its 5'-end with the first-strand cDNA reverse-transcribed with the oligo d(T)$_{30}$VN primer (*see* **Fig. 2**, **step 3**). Perform the same procedures as described in **Subheading 3.1.2.**, **step 1**.

5. Perform the same capture procedures as described in **Subheading 3.1.2.**, **steps 2–5** (*see* **Fig. 2**, **step 4**).

6. Perform the same PCR as described in **Subheading 3.1.3.** with the same thermal cycling profile except for using a gene-specific sense primer and the oligo d(T)$_{30}$VN primer as antisense primer, and the captured cDNA or the above RT reaction as the template (*see* **Fig. 2**, **step 5**) (*see* **Note 6**).

7. Cloning and sequencing the PCR fragments. Perform the same procedures as described in **Subheading 3.1.4.**

8. Isolation of the full length of cDNA. If the new 3'-end sequence is obtained, perform PCR with the further upstream sense primers and the antisense primers from the new sequence to obtain the full length of the cDNAs; or screen cDNA libraries by using the new sequence as the probe.
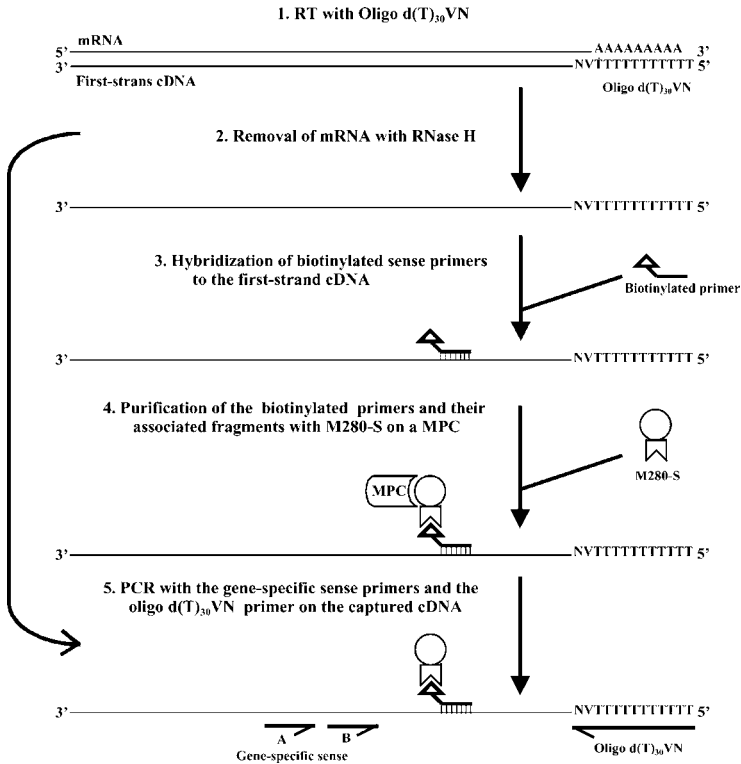
Fig. 2. Schematic illustration of a modified 3' RACE approach. M280-S, Magnetic beads M280 coupled with streptavidin. MPC, magnetic particle concentrator.

3.3. Internal Exon-Scanning RT-PCR (see *Fig. 3, Note 7*)

1. Perform RNA isolation as described in **Subheading 3.1.1.**, **step 1**.
2. Perform RT reaction as described in **Subheading 3.1.1.**, **steps 2–8** (*see* **Fig. 3**, **step 1**).
3. Removal of mRNA from DNA/RNA hybrid with RNase H as described in **Subheading 3.1.1**, **step 9** (*see* **Fig. 3**, **step 2**).
4. Hybridize a gene-specific sense primer carrying a biotin at its 5'-end with the first-strand cDNA reverse-transcribed with the random hexamers as described in **Subheading 3.1.2.**, **step 1** (*see* **Fig. 3, step 3**).
5. Purify the biotinylated primers and their associated cDNA fragments with the magnetic beads, M280-S, as described in **Subheading 3.1.2., steps 2–5** (*see* **Fig. 3, step 4**).
6. Perform a two-step PCR with both the gene-specific sense and antisense primers by using the captured products as the template, as described in **Subheading 3.1.3.** (*see* **Fig. 3, step 5**).
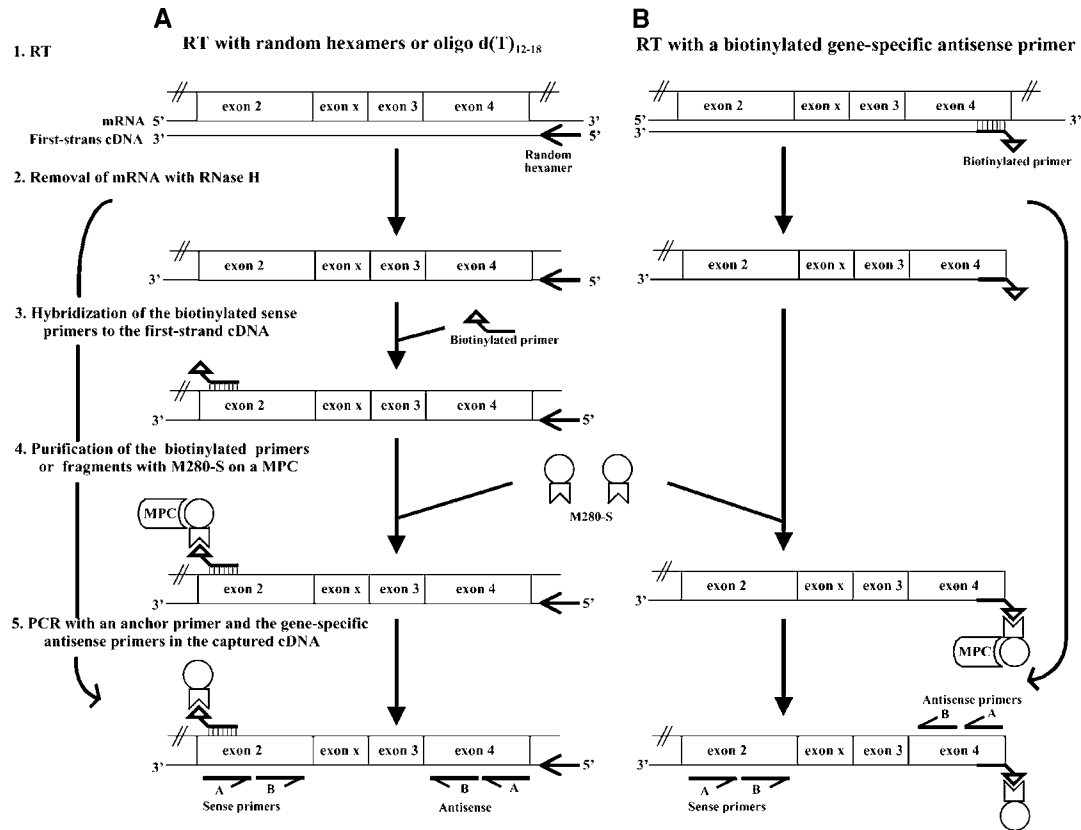
Fig. 3. Schematic illustration of an internal exon-scanning RT-PCR. M280-S, Magnetic beads M280 coupled with streptavidin. MPC, magnetic particle concentrator. (**A**) Start a RT reaction with random hexamers or oligo d(T)$_{12-18}$. (**B**) Start a RT reaction with a 5-biotinylated gene-specific antisense primer.

7. Clone and sequence the PCR fragments as described in **Subheading 3.1.4**.
8. Isolation of the full length of cDNA. If a new exon is identified, a 5'-biotinylated sense primer designed from the new exon sequence can be used to capture the targets from the first-strand cDNA. Then perform PCR with the sense and antisense primers from both the 5'- and 3'-ends of the cDNA by using the captured cDNAs as the template.

4. Notes

1. A regular primer does not contain a phosphate group on its 5'-end. In order to efficiently and unidirectionally ligate the adapter primer to the 3'-end of the single-strand cDNA, the adapter should be synthesized in such a way that it contains not only a 5'-phosphoryl terminal to provide the substrate for T4 RNA ligase, but also a 3'-amino group to avoid primer-primer self-ligation. Optimized condition for T4 RNA ligase is described by Tessier et al. and Troutt et al. *(10,11)*.
2. Superscript II RNase H⁻ reverse transcriptase is favored because of its high activity and good performance at higher temperatures (48–50°C). Instead of random hexamers, oligo $d(T)_{12-18}$ (0.5 μg) can also be used in the same RT reaction. Sometimes both random hexamers (0.4 μg) and oligo $d(T)_{12-18}$ (0.25 μg) can be applied together in the same RT reaction. There are no specific rules in choosing which primer to use, but random hexamers are favored in a 5'RACE reaction, probably because of its potential to produce cDNAs toward the 5'-end more efficiently than that of an oligo d(T) primer.
3. Both poly(A)+ RNAs and total RNAs can be used, but I prefer using total RNAs in 5'RACE because some mRNAs, especially those at a lower abundance, might lack poly(A) tracks as a result of its rapid degradation from their 3'-end. It is critical to obtain high-quality RNAs for the RACE reactions. Various methods have been developed to isolate RNAs from different tissues and cells. The mini RNeasy kit from Qiagen provides an easy and efficient tool to isolate total RNAs from a small amount of tissues or cells. If a large amount of total RNAs is required, a simple method by Acid Guanidine Isothiocyanate-Phenol-Chloroform extraction, developed by Chomczynski and Sacchi *(9)*, can be used because the extra phenol-chloroform extraction will help to completely deplete proteins and lipids. mRNA can be directly isolated from tissues and cells without purifying the total RNA by using the mini Oligotex Direct mRNA kit. Alternatively, mRNA can be purified from the total RNA by using an Oligotex mRNA kit. A major problem in RNA isolations is RNase contamination. Several precautions can be taken to avoid the problem: 1) always wear gloves when performing procedures; 2) use RNase-free containers, materials and reagents; 3) perform all procedures as quickly as possible, especially for tissue dissection, lysis, and homogenization steps, to minimize the activity of the endogenous RNases; and 4) store purified RNAs in 70% alcohol at –80°C. The quality of the total RNA is estimated by measuring ratio of OD_{260}/OD_{280} and visualized on the RNA agarose gel. A 1.8–2.0 of OD_{260}/OD_{280} ratio in 10 m*M* Tris-HCl, pH7.5 and sharp bands of both 28S and 18S RNAs on the gel are good indications of a purified RNA.

4. The gene-specific antisense primer should be designed close to the 5'-end of the known sequence to increase the chance of further 5' extension. The 5' biotinylation of the primer can be easily made during the primer synthesis. It is recommended to purify the biotinylated primer by PAGE or HPLC to obtain high-quality primers for efficient binding. When the 5' biotinylated gene-specific primer is used, the RT reaction temperature is set at 42°C, which can increase the specificity of the reaction.

5. Streptavidin is composed of four identical subunits, each having a binding site for biotin with high affinity ($K_D = 10^{-15} M$). Streptavidin-coupled magnetic beads have been widely used in nucleic acid and protein purifications and are available from several companies such as Dynal and CPG, Inc. The advantage of using the magnetic beads is that they simplify purification procedures, allowing the performance of several sequential reactions in a single tube without phenol-chloroform treatment and ethanol precipitation. Another advantage is that the magnetic beads capture low abundant mRNAs from a large amount of RNA samples.

6. It is recommended to design the gene-specific primers containing higher melting temperature (Tm) (>70°C) so that a two-step PCR can be performed in which the annealing and extension steps are combined into one step at 68°C after the first denaturing step at 94°C. The two-step PCR can improve specificity and reduce background of the PCR. In the PCR using the template from the RT reactions with the random hexamers, the gene-specific antisense primers used should be designed close to the 5'-end of the known sequence to maximize the 5' extension potential. If the template from the RT reactions with the biotinylated antisense primer is used, the nested antisense primers relative to the biotinylated primer also should be used in PCR. Extension time is usually set for 5 min for amplifying the fragments less than 5 kb when Platinum Taq DNA polymerase is used. However, if a longer product is expected, a longer PCR with a reading-proof DNA polymerase should be used. Advantage 2 PCR system (CloTech), EXL DNA polymerase (Stratagene) and DNA polymerase mixture for long template (Roche Applied Science) can be used. If there are very faint bands or no visible bands on the agarose gel during analysis of the PCR products, a nested (second round) PCR should be carried out by using the first PCR product as the template with a nested gene-specific antisense primer and the same anchor sense primer A (*see* **Fig. 1**, **step 6**).

7. Once the first-strand cDNA is synthesized, PCR can be directly performed like traditional 3'RACE or RT-PCR with the gene-specific primers and oligo $d(T)_{30}VN$ primer by skipping the middle purification steps (*see* **Figs. 2** and **3**). Some premade 5' and 3' RACE-ready cDNAs are also available from several companies such as ClonTech, Ambion, and OriGene. In these cDNAs, the double-strand cDNAs containing the adapters at both their 5'- and 3'-ends and their anchor primers are provided. 5'RACE or 3'RACE is easily performed by direct PCR on these templates. However, the biotinylated primer/M280-S purification described here can specifically concentrate the targeted sequences on the beads from a large pool of cDNAs, and thus greatly enhance the opportunity of identifying the low-abundance variants.

Acknowledgment

I would like to thank Jin Xu and Loriann Mahurter for their contribution to the procedures described here and Dr. Gavril W. Pasternak for his support.

References

1. Chen, Y., Mestek, A., Liu, J., Hurley, J. A., and Yu, L. (1993) Molecular cloning and functional expression of a μ-opioid receptor from rat brain. *Mol. Pharmacol.* **44,** 8–12.
2. Bare, L. A., Mansson, E., and Yang, D. (1994) Expression of two variants of the human μ opioid receptor mRNA in SK-N-SH cells and human brain. *FEBS Lett.* **354,** 213–216.
3. Zimprich, A., Simon, T., and Hollt, V. (1995) Cloning and expression of an isoform of the rat μ opioid receptor (rMOR 1 B) which differs in agonist induced desensitization from rMOR1. *FEBS Lett.* **359,** 142–146.
4. Pan, Y. X., Xu, J., Bolan, E. A., Abbadie, C., Chang, A., Zuckerman, A., et al. (1999) Identification and characterization of three new alternatively spliced μ opioid receptor isoforms. *Mol. Pharmacol.* **56,** 396–403.
5. Pan, Y.-X., Xu, J., Bolan, E. A., Chang, A., Mahurter, L., Rossi, G. C., et al. (2000) Isolation and expression of a novel alternatively spliced mu opioid receptor isoform, MOR-1F. *FEBS Lett.* **466,** 337–340.
6. Pan, Y.-X., Xu, J., Rossi, G., Bolan, E., Xu, M. M., Mahurter, L., et al. (2001) Generation of the mu opioid receptor (MOR-1) protein by three new splice variants of the Oprm gene. *Proc. Natl. Acad. Sci. USA* **98,** 14,084–14,089.
7. Abbadie, C., Pan, Y.-X., and Pasternak, G. W. (2000) Differential distribution in rat brain of mu opioid receptor carboxy terminal splice variants MOR-1C and MOR-1-like immunoreactivity: Evidence for region-specific processing. *J. Compar Neurol.* **419,** 244–256.
8. Abbadie, C., Pan, Y.-X., Drake, C. T., and Pasternak, G. W. (2000) Comparative immunohistochemical distributions of carboxy terminus epitopes from the mu opioid receptor splice variants MOR-1D, MOR-1 and MOR-1C in the mouse and rat central nervous systems. *Neuroscience* **100,** 141–153.
9. Chomczynski, P. and Sacchi, N. (1987) Single-step method of RNA isolation by acid guanidinium thiocyanate-phenol-chloroform extraction. *Analyt. Biochem.* **162,** 156–159.
10. Tessier, D. C., Brousseau, R., and Vernet, T. (1986) Ligation of single-stranded oligodeoxyribonucleotides by T4 RNA ligase. *Analyt. Biochem.* **158,** 171–178.
11. Troutt, A. B., McHeyzer-Williams, M. G., Pulendran, B., and Nossal, G. J. (1992) Ligation-anchored PCR: a simple amplification technique with single- sided specificity. *Proc. Natl. Acad. Sci. USA* **89,** 9823–9825.

8

Immunohistochemical Localization of μ-, δ- and κ-Opioid Receptors Within the Antinociceptive Brainstem Circuits

Alexander E. Kalyuzhny

1. Introduction

Three functionally linked units, periaqueductal gray (PAG), rostral ventromedial medulla (RVM), and spinal cord dorsal horn are thought to comprise supraspinal pain suppression system. As it has been suggested, the activation of neurons in PAG excites RVM-spinal cord projecting neurons which results in the inhibition of nociceptive cells in the spinal cord *(1–3)*. PAG-RVM-spinal cord descending pathway is one of the targets of opiates mediating antinociception. It has been hypothesized that the analgesic effects of opiates are mediated indirectly through inhibition of inhibitory GABAergic neurons within the PAG-RVM-spinal cord circuit *(2,4–6)*.

After opioid receptors were cloned *(7–14)*, it became possible to localize them immunocytochemically *(15–24)*. The advantage of using immunohistochemical (IHC) approach to detect opioid receptors over *in situ* hybridization is that IHC allows simultaneous detection of multiple targets such as μ-, δ-, and κ-opioid receptors and GABA or glutamic acid decarboxylase (GAD-65) within the same anatomical profiles.

In this chapter, we describe immunohistochemistry techniques to localize opioid receptors within the antinociceptive brainstem circuits including the PAG, RVM, and spinal cord dorsal horn. Immunohistochemical localization of opioid receptors and GABAergic cells is a valuable technique in identifying various types of neurons within the anatomical regions that include antinociceptive brainstem circuits *(25,26)*. However, immunohistochemistry

alone is not sufficient to identify neurons comprising such circuits and has to be combined with tract-tracing techniques. In this chapter, we describe protocols which combine retrograde tract-tracing techniques with fluorescence immunohistochemistry allowing co-localization of one of μ-, δ- or κ-opioid receptors with GABA and GAD-65 in neurons projecting from PAG to RVM and from RVM to spinal cord dorsal horn. First, projection neurons are labeled using retrograde tract-tracer Fluoro-Gold and then these tissue sections are stained with antibodies raised against opioid receptors, and GABA or GAD-65. Techniques described here can be used alone as well as combined with molecular biology techniques including *in situ* hybridization and receptor autoradiography.

2. Materials

1. Animals: 100–120 g, Sprague-Dawley rats.
2. Anesthetics: mixture of ketamine (75 mg/kg), xylazine (5 mg/kg), and acepromazine (1 mg/kg) can be used to anesthetize rats. Administer the mixture by intramuscular injection.
3. Retrograde tract-tracer: Fluoro-Gold (FG, Fluorochrome, Inc., Englewood, CO) *(27)* to label neurons projecting from PAG to RVM and from RVM to spinal cord.
4. GABA-transaminase inhibitor: 100 mg/kg intraperitoneal of (aminooxy) acetic acid (AOAA, ICN Biomedicals, Inc., Aurora, OH) to prevent enzymatic reduction of GABA. This approach allows to improve the intensity of GABAergic somata labeling *(28)*.
5. Calcium-free Tyrodes solution: this solution is used to clear rats' vasculature from blood during transcardial perfusion. To 500 mL of distilled water, add 6.8 g NaCl, 0.4 g KCl, 0.32 g $MgCl_2 \cdot 6H_2O$, 0.1 g $MgSO_4 \cdot 7 H_2O$, 0.17 g $NaH_2PO_4 \cdot H_2O$, 1.0 g glucose, and 2.2 g $NaHCO_3$. Adjust volume to 1 L. Store at 4°C. Immediately before use, gas the solution with 95% O_2 and 5% CO_2 gas mixture for 20 min.
6. Sucrose solution (for cryoprotection of tissues):

   a. Sorenson's buffer (0.2*M*): To 400 mL of distilled water, add 4 g KH_2PO_4 (anhydrous) and 18.9 g Na_2HPO_4. Adjust volume to 500 mL with distilled water and adjust pH to 7.2 with 1*M* NaOH.

   b. To 500 mL of Sorenson's buffer, add 100 g Sucrose, 100 g NaN_2 and 0.2 g Bacitracin. Adjust volume to 1 L and mix for about 1 h on a stir plate.

7. Lana's fixative: this soultion is used to fix brain tissues by transcardial perfusion. Wear mask and gloves and use the hood when preparing paraformaldehyde fixative.

   a. Solution A [0.4*M* phosphate buffered saline (PBS)]: Fill 1-L beaker with 900 mL of distilled water and dissolve 25.6 g of KH_2PO_4 (anhydrous) and 56.8 g $Na_2HPO_4 \cdot 7H_2O$. Add distilled water to 1 L and adjust pH to 6.9 with 1*M* NaOH.

b. Solution B (16% paraformaldehyde): Dissolve 16 g paraformaldehyde powder in 100 mL of distilled water using heating stir plate. Slowly heat this solution while stirring. After temperature reaches 56–58°C, turn the heat off and add 1–2 drops of 1*M* NaOH to clear this solution. Continue stirring for another 20–30 min and then filter the fixative solution through regular filter paper (i.e., Whatman #1). It is strongly recommended to monitor the temperature of the paraformaldehyde solution to avoid its heating above 58°C. If overheated, discard it and make a new one;

c. Fixing solution (4% paraformaldehyde): Prepare this solution by mixing 100 mL of Solution A with 160 mL of Solution B and 56 mL of saturated filtered Picric acid (approx 3%). Add 0.4 *M* PBS to 400 mL and adjust pH to 6.9 with 1*M* NaOH. This solution is stable up to three weeks at room temperature.

8. Wash buffer (PBS): Fill 1-L beaker with 900 mL of distilled water and dissolve 0.23 g NaH_2PO_4 (anhydrous), 1.15 g Na_2HPO_4 (anhydrous) and 9 g NaCl. Adjust to pH 7.4 using 1 *M* NaOH and/or 1*M* HCl.

9. High-compliance current source: Model CS-3 (Stoelting, Chicago, IL). This instrument is used for FG injections into the RVM.

10. Cryostat: Bright cryostat (Huntington, U.K.). To cut rat brain sections for immunohistochemistry.

11. Dilution buffer: PBS (same as in **Subheading 2.**, **step 8**) containing 1% bovine serum albumin (BSA), 0.3% Triton X-100 (v/v), and 0.01% sodium azide.

12. Primary antibodies against opioid receptors: Make working dilution within the range 1:600–1:5000 of rabbit polyclonal anti-μ- (Cat no. RA10104, Neuromics, Inc., Minneapolis, MN), or anti-δ- (Cat no. RA10100, Neuromics, Inc., Minneapolis, MN), or anti-κ (Cat#RA10103, Neuromics, Inc.) opioid receptor antibodies in dilution buffer. Antibody solutions may be stored for 1–3 mon at 4°C.

13. Anti-GABA antibodies: Mouse monoclonal antibodies (IgG1 isotype, clone GB-69; Sigma Immunochemicals, St. Louis, MO) diluted 1:1000.

14. Anti-glutamic acid decarboxylase antibodies: Mouse monoclonal anti-GAD-65 antibody (produced and distributed by Developmental Studies Hybridoma Bank, maintained by the Department of Pharmacology and Molecular Sciences, John Hopkins University School of Medicine, Baltimore, MD, and the Department of Biological Sciences, University of Iowa, Iowa City, under Contract N01-HD-6-2915 from the NICHD) diluted 1:100–1:200.

15. Fluorescent secondary antibodies: Donkey antimouse antibodies conjugated with fluorescein isothiocyanate (FITC; Jackson ImmunoResearch Laboratories, West Grove, PA) to detect GABA or GAD-65; Donkey antirabbit antibodies conjugated with cyanine 3.18 (Cy3; Jackson ImmunoResearch Laboratories, West Grove, PA) to detect opioid receptors. To make working dilutions, dilute secondary antibodies 1:100 with dilution buffer. Diluted secondary antibodies may be stored at 4°C for 1–3 mo.

16. Mounting medium for fluorescent labels: ProLong antifade kit (Molecular Probes, Eugene, OR). This medium minimizes loss of fluorescence by FITC and Cy3

because of photobleaching during examination under the fluorescence micro-scope. Alternatively, a PBS/glycerol solution containing 0.1% phenylenediamine (Sigma) can be used to reduce fading *(29)*.

17. Wax pen (ImmEdge pen, Vector Laboratories, Burlingame, CA): to draw circles around tissue section on the histological slide. Use this pen to create a hydropho-bic barrier around the tissue section to keep incubation reagents on the tissue.
18. Humidity incubation chamber: Staining tray with humidity cover (Signet Labo-ratories, Dedham, MA) allowing incubation of up to five slides with primary and secondary antibodies.
19. Stereo-microscope with magnification range from 1.8–50: to perform surgical procedures and to apply Fluoro-Gold.
20. Image acquisition systems:

   a. Fluorescence microscope (Provis; Olympus, Melville, NY) equipped with cooled CCD color digital camera (Spot; Diagnostic Instruments, Sterling Heights, MI) and fluorescence filter set to visualize FITC (460–490 nm exci-tation and 510–550 nm emission), Cy3 (541–551 nm excitation and 572–607 nm emission), and Fluoro-Gold (330–390 nm excitation and 420–480 nm emission).
   b. Confocal microscope. Any type of confocal microscope can be used to collect images of fluorescence labeling. We had a every good experience using Bio-Rad MRC 1024 confocal scanning laser microscope equipped with a Kr/Ar-ion laser. It is required to have a set of filters on the microscope to visualize FITC, Cy3 and Fluoro-Gold (see earlier) and such objectives as 4× (na 0.16), 10× (na 0.5), 20× (na 0.75), and 60× (na 1.4).

3. Methods

All surgical and immunohistochemistry procedures are done at room tem-perature, unless stated otherwise. If protocol calls for incubation at room tem-perature, reagents stored in the cold room at 4°C should be allowed to adjust to room temperature before their use. It is recommended to perform each staining experiment in duplicate or triplicate in case some tissue samples are damaged or will dry out during the incubation and are excluded from the experiment.

3.1. Labeling of Neurons Using Retrograde Tract-Tracer Fluoro-Gold

Retrograde tract-tracing (*see* **Figs. 1** and **2**) has to be done on deeply anes-thetized animals (*see* **Note 1**). If, during a surgical procedure, an animal starts waking up, interrupt surgery immediately and inject additional amount of anesthetic equal to 20% of original dose. Wait 5–10 min to be sure that the animal is sedated adequately. If the animal is not fully anesthetized yet, inject additional amount of anesthetic, but do not exceed 20% of the original dose.
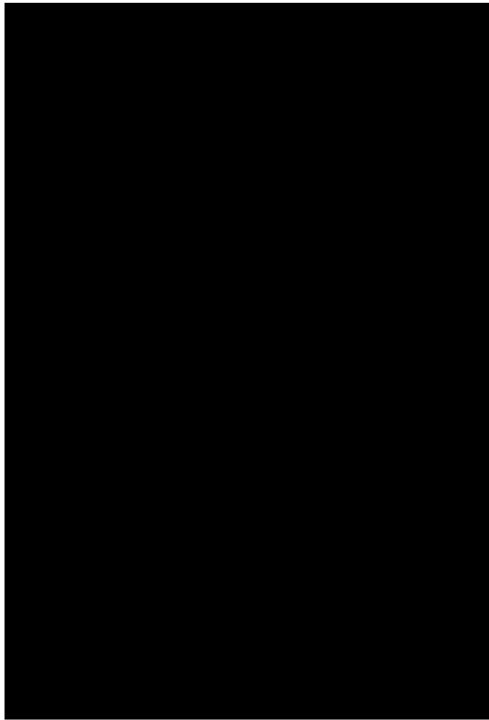
Fig. 1. Fluor-Gold injection sites in the RVM to label projection neurons in the PAG. The upper panel shows the largest extent in the coronal plane of the injection; the dashed line represents the borders of the pyramidal tract. The line drawing on the bottom panel reconstructs the rostrocaudal extent of the injection. Scale bar on bottom panel (line drawing) = 1 mm. pt: pyramidal tract. (From Kalyuzhny and Wessendorf, *J.Compar. Neurol.*,© 1998 Wiley-Liss, Inc., reprinted by permission of Wiley-Liss, Inc., a subsidiary of John Wiley & Sons, Inc.)

Injections of small amounts allow avoiding an overdose, which may cause death of the animal.

3.1.1. Labeling of RVM-Spinal Cord Projecting Neurons

Two approaches may be used to label neurons projecting from RVM to spinal cord: by either injecting tract-tracer into spinal cord dorsal horn using glass micropipet, or placing onto the dorsal portion of the spinal cord a piece of minisponge soaked with tract-tracer. Injections are more difficult to perform than using such minisponge material as gelfoam described here. Even though Fluoro-Gold is soluble in aqueous solutions, it is recommended to dissolve it in dimethylsulphoxide (DMSO) to facilitate the penetration of Fluoro-Gold into the tissue (*see* **Note 2**). Strong labeling of RVM-spinal cord projecting neurons
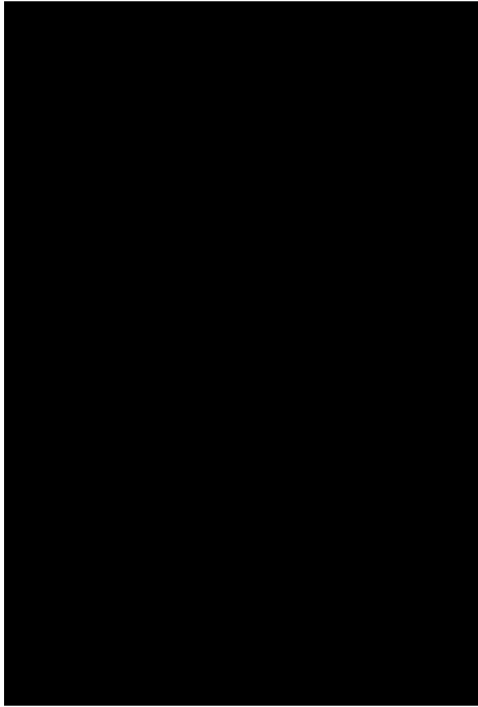
Fig. 2. Fluoro-Gold application site in the lumbar spinal cord to label bulbospinal neurons. The upper panel shows the largest extent in the coronal plane of the Fluoro-Fold application. The line drawing on the bottom panel reconstructs the rostrocaudal extent of the Fluoro-Gold application. Scale bars: on upper panel = 250 μm; on line drawing = 1 mm. (From Kalyuzhny and Wessendorf, *J. Compar. Neurol.*,© 1998 Wiley-Liss, Inc., reprinted by permission of Wiley-Liss, Inc., a subsidiary of John Wiley & Sons, Inc.)

may be accomplished by placing the gelfoam on the surface of the lumbar spinal cord (*see* **Fig. 2**) at the level of the 13th rib *(23)*.

1. Anesthetize rats by subcutaneous injection of a mixture of ketamine (75 mg/kg), xylazine (5 mg/kg) and acepromazine (1 mg/kg).
2. Shave the back of the rat and open the skin by making an incision (approx 1-in long) in the rostro-caudal direction alone the spine at the level of the 13th rib. Under the stereo microscope perform laminectomy to make a 3 × 3 mm opening and then open the dura matter to expose spinal cord.
3. Presoak a piece of gelfoam (approx 2 mm^3) in 2 μL of 5% Fluoro-Gold in DMSO. To facilitate absorption of Fluor-Gold by the tissue, gently abrade the exposed dorsal side of the spinal cord with the sharpened end of a wooden swab.

4. Place the gelfoam presoaked with Fluoro-Gold onto the dorsal spinal cord, leave it there and close the wound.
5. Place the operated rat back into the cage and create comfortable conditions for animal recovery according to accepted veterinary service recommendations.

3.1.2. Retrograde Labeling of Neurons Projecting from the PAG to Nucleus Raphe Magnus (NRM) (23)

Follow recommendations described in **Subheading 3.1.1.**

1. Anesthetize rats by subcutaneous injection of a mixture of ketamine (75 mg/kg), xylazine (5 mg/kg), and acepromazine (1 mg/kg).
2. Shave the back of the head and make an incision (approx 1/2 in) over cisterna magna.
3. Cut a hole (approx 3 mm wide and 7 mm long) on the caudal midline of the occipital plate using bone rongeurs.
4. Immobilize the rat's head using ear bars on the stereotaxis apparatus.
5. Under the stereo microscope open the dura matter to expose the obex, which will serve as a tissue landmark.
6. Gently displace the caudal-most portion of the cerebellar vermis rostrally.
7. Fill a glass micropipette (tip diameter about 30 μm) with 3% of Fluoro-Gold in 0.9% NaCl and advance it at a 15° angle through the cerebellum into NRM using coordinates of 3.5 mm rostral and 4.0 mm ventral to the obex. Monitor advancement of the glass micropipet into the brain using stereo microscope.
8. Inject Fluoro-Gold using a constant positive current (approx 7 μA) applied for 10 min by a high-compliance current source.
9. Switch off the high-compliance source and withdraw the glass pipette with Fluoro-Gold from the tissue.
10. Close the wound, place the operated rat back into the cage and create comfortable conditions for animal recovery according to accepted veterinary service recommendations.

3.2. Double-Labeling for Opioid Receptors and GABA

Immunofluorescence protocol utilizing two-color labeling is more convenient than the chromogenic one. It is shorter and results in unambiguous separation of colors (*see* **Fig. 3–6**). However, the older the rats, the stronger the autofluorescence of lipofuscin (age pigment) represented by granules of various size that are distributed in the neuropile and within neuronal cell (*see* **Note 1**). Rats are allowed to survive 4–6 d before they are killed to allow Fluoro-Gold accumulate within the projecting neurons.

1. Two-and-a-half hours prior to euthanasia, inject the operated rats ip with 100 mg/kg of the GABA-transaminase inhibitor AOAA to improve the intensity of staining in GABAergic somata *(28)*.
2. Deeply anesthetize the rat and fix it by vascular perfusion with 500–700 mL of fixative, followed by 400 mL of 10 % sucrose solution in 0.1 *M* phosphate buffer (pH 7.2).
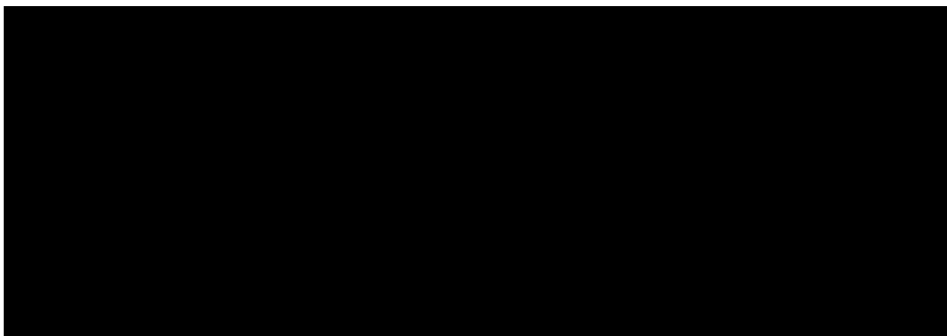
Fig. 3. Double-labeling for GABA and δ-opioid receptor (DOR1). Confocal images showing the relationship of varicosities (pointed by arrows) labeled for the cloned δ-opioid receptor (DOR1-ir) to neurons labeled for γ-aminobutiric acid (GABA-ir) in the rat spinal cord dorsal horn. (From Kalyuzhny and Wessendorf, *J. Compar. Neurol.*, ©1998 Wiley-Liss, Inc., reprinted by permission of Wiley-Liss, Inc., a subsidiary of John Wiley & Sons, Inc.)
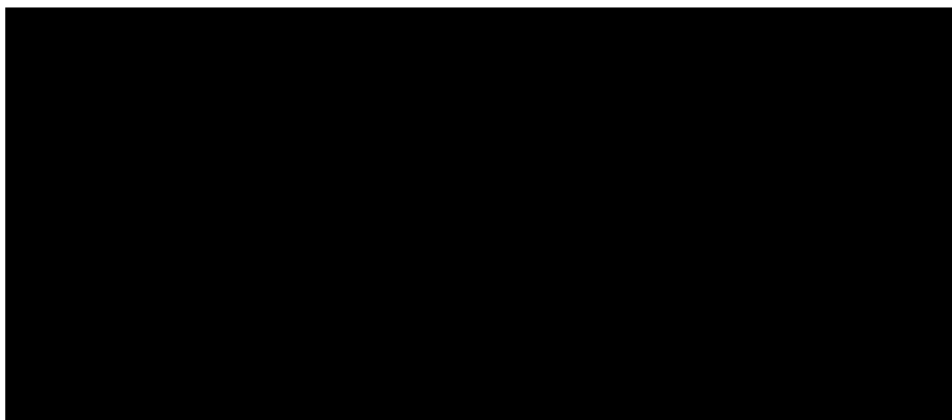
Fig. 4. Double-labeling for δ-opioid receptor (DOR1) and GAD-65. Images of a single section stained for both the cloned δ-opioid receptors (DOR-ir) and glutamic acid decarboxylase (GAD-65-ir) in the nucleus raphe magnus of rostral ventromedial medulla (RVM). Note that structures immunoreactive for DOR (arrows) are not immunoreactive for GAD-65 (arrowheads). (From Kalyuzhny and Wessendorf, *J. Compar. Neurol.*,© 1998 Wiley-Liss, Inc., reprinted by permission of Wiley-Liss, Inc., a subsidiary of John Wiley & Sons, Inc.)

3. Dissect the brain and spinal cord, freeze them and cut 5–7-μm-thick tissue sections using the cryostat (but *see* **Note 3**). Store slides with sections in the slide storage box at –20°C before use. Slides may be stored for up to 6 mo.
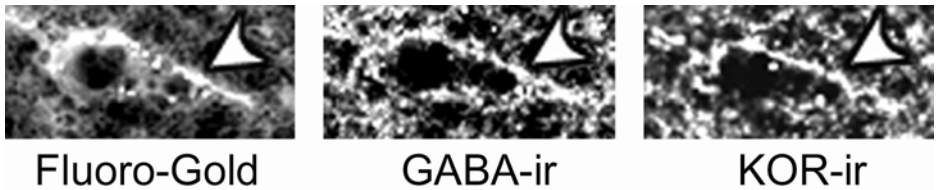
Fig. 5. Expression of κ-opioid receptor (KOR1) by GABAergic neurons projecting from the PAG to the RVM. A single section at the level of PAG containing Fluoro-Gold filled cells was stained for both γ-aminobutiric acid (GABA-ir) and the cloned κ-opioid receptor (KOR-ir). Arrows points to a Fluoro-Gold labeled neuron that was also immunoreactive for GABA and κ-opioid receptors.
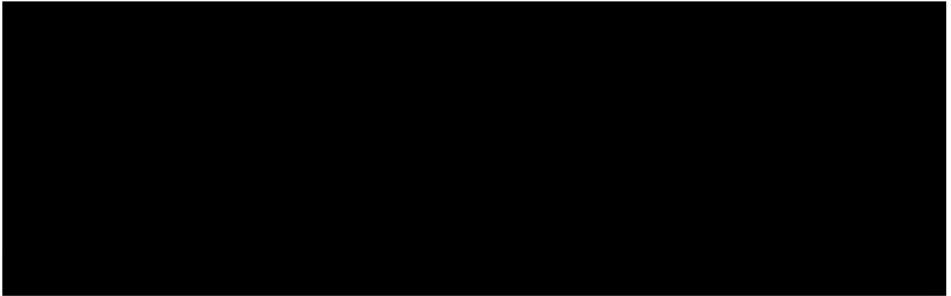
Fig. 6. Expression of μ-opioid receptor (MOR) by GABAergic neurons projecting from the RVM to the spinal cord dorsal horn. Arrows depict a bulbospinal neuron in the RVM that was double-labeled for the cloned μ-opioid receptor (MOR-ir) and GABA-ir. (From Kalyuzhny and Wessendorf, *J. Compar. Neurol.*,© 1998 Wiley-Liss, Inc., reprinted by permission of Wiley-Liss, Inc., a subsidiary of John Wiley & Sons, Inc.)

4. Bring the box with tissue slides from the freezer into a room and let it sit for 20–30 min to adjust to room temperature.
5. Label the slides with tissues. This information may include the date, type of primary and secondary antibodies, and their concentration and whether the slide is used for absorption control. If the slide is used as a control, it is advisable to indicate the type of control (*see* **Note 4**).
6. Draw a circle around the tissue section with ImmEdge pen. The gap between the tissue and the ImmEdge pen line should not be smaller than 2–3 mm. Let the ImmEdge pen line to dry for at least 5 min. If reagents are added before the the ImmEdge line is completely dry, it may come off the slide.
7. Rehydrate the tissue sections with wash buffer. This may be done by either: 1) incubating slides in a glass Coplin jar; or 2) placing slides horizontally into a humid chamber and adding 0.1–0.3 μL of wash buffer onto the tissue section. Incubate for 5 min.

8. Remove the slides from the humid chamber or Coplin jar, shake excess wash buffer, place the slides horizontally and add 50–200 μL of the mixture of primary antibodies in diluent. Before adding primary antibodies calculate the volume of antibodies' working solution, given that 100–200 μL is required to cover 2×1 cm^2 of tissue area. After adding primary antibodies put the humidity chamber with slides into the cold room or refridgerator. Incubate for 16–24 h (*see* **Note 5**).
9. Wash the tissues 3×15 min with wash buffer in the Coplin Jar.
10. Remove the slides from the Coplin jar, shake excess wash buffer, place the slides horizontally and add 50–200 μL of the secondary antibodies in diluent (*see* **Note 6**). Before adding primary antibodies calculate the volume of antibodies' working solution as described in **step 8**. Incubate the slides in the humid chamber for 60 min.
11. Repeat **step 9**.
12. Remove the slides from the Coplin jar, shake excess wash buffer, place the slides horisontally and add 30–50 μL of the mounting medium for fluorescent labels. Cover tissue section with coverslips of appropriate size. Place the slides vertically onto a paper towel to drain excess of mounting medium. Examine the slides using fluorescence or confocal microscopy (*see* **Notes 7** and **8**).

4. Notes

1. It is recommended to use younger rats, not exceeding 100–120 g in body weight. First of all smaller rats are easier to handle and perform surgical procedures requiring partial removal of bones (i.e., scull and spine). Second, during aging, a fluorescent pigment lypofuscin accumulates in the cytolpasm of neuronal cells *(30, 31)* which, due to the broad emission spectra *(32–34)*, will overlap with that one of fluorophores used as reporter molecules and obscure their identification *(26,35,36)*. If the only choice is to use older animals, then the autofluoresecence of lipofuscin can be reduced or quenched by incubating tissue sections with 1–10 m*M* CuSO4 in 50 m*M* ammonium acetate buffer (pH 5.0) or 1% Sudan Black B (SB) in 70% ethanol *(37)*.
2. The advantage of using a Fluoro-Gold is that it is easily absorbed by tissues, has a fast tract-tracing rate and produces intense labeling that can be detected using low magnification lenses under UV light. The drawback of using Fluoro-Gold is its rapid fading under the strong UV illumination that may challenge image acquisition. The way to avoid fast Fluoro-Gold fading is to reduce intensity of UV illumination using neutral density filters when evaluating labeled tissues: the intensity should be just enough to identify labeled cells and their processes. If brightness of Fluoro-Gold drops below the sensitivity of charge coupled device (CCD) camera, ultraviolet (UV) light intensity may be increased during image capturing. It is also advisable to have stained adjacent tissue sections to compensate for losses of primary data caused by Fluoro-Gold fading.
3. We found that labeling of cell somata for both MOR and GABA can be improved by staining 2-μm-thick cryostat sections. To cut such thin sections, it is necessary to use sharp cutting knife which is free of any defects on its cutting edge. Unlike

thicker sections, 2-μm sections should be cut without using an antiroll plate, which will cause jamming of the tissue sections. We recommend cutting sections with cryostat temperature set between –20 and –25°C.

4. Various types of controls should be used to prove the specificity of the immuno-histochemical labeling. Four types of controls may be used as follows:

   a. *Secondary antibodies control*. This control addresses the question whether secondary antibodies conjugated to fluorescent probes bind to tissues *per se*. The easiest way to solve this issue is to incubate tissue sections with antibody diluent instead of primary antibodies and lack of labeling will indicate that there is no nonspecific binding of secondary antibodies to tissues. However, if nonspecific labeling is observed, additional steps are required to reduce it. For example, nonspecific labeling may be caused by nonreduced aldehyde groups of the paraformaldehyde-based fixative. Aldehyde groups may "crosslink" secondary antibodies to tissues. As a remedy it is suggested to incubate tissues before adding primary antibodies with 0.5 mg/mL of sodium borohydrate (NaBH4) for 10–20 min at room temperature. Alternatively, before adding primary antibodies, non-specific tissue binding sites may be blocked by incubating tissues with 10% normal serum (horse, swine or donkey) for 5–30 min at room temperature. It is of critical importance to use blocking normal serum from species other than the host of primary antibodies, otherwise, secondary antibodies will crossreact with blocking serum retained by tissues, causing nonspecific labeling.

   b. *Tissue negative control*. This control addresses the issue of antibodies' crossreactivity with targets other than opioid receptors. This may be done by staining brain regions known for their lack of opioid receptors. For example, rat cerebellum may be used as a negative control since this part of the brain is known for its lack of expression of opioid receptors (*see* **Fig. 7**).

   c. *Tissue positive control*. Unlike negative control, positive control should include brain regions where expression of opioid receptors is well documented. We recommend to use coronal sections of the spinal cord where opioid receptors are known to be localized in the dorsal horn.

   d. *Absorption control*. The purpose of determining the immunonological specificity of anti-opioid receptor antibodies is to demonstrate that tissue labeling occurrs as a result of the antigen-antibody interaction rather than is caused by crossreactivity of antibodies with nonspecific tissues targets. The way to study immunological specificity is to employ a so-called absorption control: mix antibodies (taken in 1:600 working dilution) with the peptide used as immunogen taken in concentration of 10 μg/mL. Specific labeling is expected to be either reduced or abolished after incubating tissue sections with antibody-peptide mixture (*see* **Fig. 7**).

5. Avoid drying tissue sections during the incubation since this may cause high background and even false-positive labeling owing to adsorption of reagents by the tissue. Do not try to rehydrate dry tissues but discard them. Also watch for drying of tissue section margins which may appear labeled stronger but not nec-
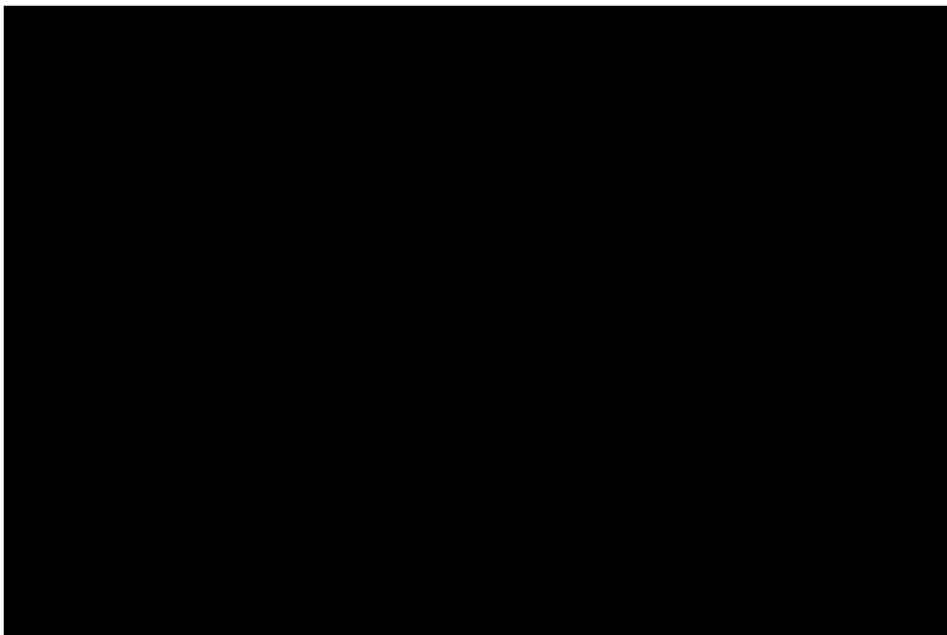
Fig. 7. Tissue negative and absorption controls. Labeling for MOR and GABA in cerebellum. When we attempted to stain sections for MOR1 and GABA, only labeling for GABA was observed **(A,C)**. Labeling for MOR was not observed **(B)**; fluorescence for MOR appeared to be of the same low intensity as observed in an absorption control on an adjacent section **(D)**. Scale bar = 30 μm. (From Kalyuzhny and Wessendorf, *J. Compar. Neurol.*, © 1998 Wiley-Liss, Inc., reprinted by permission of Wiley-Liss, Inc., a subsidiary of John Wiley & Sons, Inc.)

essarily specific. Because partial drying may be sometimes unnoticed, it is recommended to interpret labeling on tissue margins with caution.

6. Double-labeling (i.e., for either μ-, δ-, or κ-opioid receptors and GABA or GAD-65) can be done by incubating tissue sections with two antibodies mixed together. It makes sense to mix only antibodies raised in different species: for example rabbit anti-MOR and mouse anti-GABA. Detection, in turn, can be done by incubating tissues with secondary antirabbit and antimouse antibodies mixed together. Use secondary antibodies conjugated to different fluorescence probes, i.e., Cy3 and FITC that have nonoverlapping emission spectra.

7. Since Fluoro-Gold is a fast fading tract-tracer (*see* **Note 2**) its illumination with UV light during image collection will make Fluoro-Gold labeled cells difficult or even impossible to visualize. Thus, it is recommended to collect first images of labeling for opioid receptors and GABA or GAD-65 using confocal microscope and then collect images of Fluoro-Gold labeled cells using fluorescence microscope.

8. When manipulating digital images, adjust brightness and contrast simultaneously on images depicting specific labeling and control to ensure accurate comparison of labeling.

References

1. Basbaum, A. I., Clanton, C. H., and Fields, H. L. (1978) Three bulbospinal pathways from the rostral medulla of the cat: an autoradiographic study of pain modulating systems. *J. Comparitive Neurol.* **178(2),** 209–224.
2. Basbaum, A. I. and Fields, H. L. (1984) Endogenous pain control systems: brainstem spinal pathways and endorphin circuitry. *Ann. Rev. Neurosci.* **7** 309–338.
3. Fields, H. L. and Basbaum, A. I. (1978) Brainstem control of spinal pain-transmission neurons. *Ann. Rev. Physiol.* **40,** 217–248.
4. Pan, Z. Z., Williams, J. T., and Osborne, P. (1990) Opioid actions on single nucleus raphe magnus neurons from rat and guinea pig in vitro. *J. Physiol. (Lond.)* **427,** 519–532.
5. Fields, H. L., Heinricher, M. M., and Mason, P. (1991) Neurotransmitters in nociceptive modulatory circuits. *Ann. Rev. Neurosci.* **14,** 219–245.
6. Chieng, B. and Christie, M. J. (1994) Inhibition by opioids acting on mu-receptors of GABAergic and glutamatergic postsynaptic potentials in single rat periaqueductal gray neurones in vitro. *Br. J. Pharmacol.* **113(1),** 303–309.
7. Evans, C. J., Keith, D. J., Jr., Morrison, H., Magendzo, K., and Edwards, R. H. (1992) Cloning of a delta opioid receptor by functional expression. *Science* **258,** 1952–1955.
8. Kieffer, B. L., Befort, K., Gaveriaux, R. C., and Hirth, C. G. (1992) The delta-opioid receptor: isolation of a cDNA by expression cloning and pharmacological characterization. *Proc. Natl. Acad. Sci. USA* **89(24),** 12,048–12,052.
9. Chen, Y., Mestek, A., Liu, J., Hurley, J. A., and Yu, L. (1993) Molecular cloning and functional expression of a mu-opioid receptor from rat brain. *Mol. Pharmacol.* **44(1),** 8–12.
10. Meng, F., Xie, G. X., Thompson, R. C., Mansour, A., Goldstein, A., Watson, S. J., and Akil, H. (1993) Cloning and pharmacological characterization of a rat kappa opioid receptor. *Proc. Natl. Acad. Sci. USA* **90(21),** 9954–9958.
11. Nishi, M., Takeshima, H., Fukuda, K., Kato, S., and Mori, K. (1993) cDNA cloning and pharmacological characterization of an opioid receptor with high affinities for kappa-subtype-selective ligands. *Febs. Lett.* **330(1),** 77–80.
12. Thompson, R. C., Mansour, A., Akil, H., and Watson, S. J. (1993) Cloning and pharmacological characterization of a rat mu opioid receptor. *Neuron* **11(5),** 903–913.
13. Yasuda, K., Raynor, K., Kong, H., Breder, C. D., Takeda, J., Reisine, T., and Bell, G. I. (1993) Cloning and functional comparison of kappa and delta opioid receptors from mouse brain. *Proc. Natl. Acad. Sci. USA* **90(14),** 6736–6740.
14. Knapp, R. J., Malatynska, E., Fang, L., Li, X., Babin, E., Nguyen, M., et al. (1994) Identification of a human delta opioid receptor: cloning and expression. *Life Sci.* **54(25),** 463–469.

15. Koulen, P., Sassoe-Pognetto, M., Grunert, U., and Wassle, H. (1996) Selective clustering of GABA(A) and glycine receptors in the mammalian retina. *J. Neurosci.* **16(6),** 2127–2140.

16. Dado, R. J., Law, P. Y., Loh, H. H., and Elde, R. (1993) Immunofluorescent identification of a delta (delta)-opioid receptor on primary afferent nerve terminals. *Neuroreport* **5(3),** 341–344.

17. Arvidsson, U., Riedl, M., Chakrabarti, S., Lee, J.-H., Nakano, A. H., Dado, R., et al. (1995) Distribution and targeting of a μ-opioid receptor (MOR1) in brain and spinal cord. *J. Neurosci.* **15,** 3328–3341.

18. Arvidsson, U., Dado, R. J., Law, P.-Y., Loh, H. H., Elde, R., and Wessendorf, M. W. (1995) Delta δ-opioid receptor immunoreactivity: distribution in brain stem and spinal cord and relationship to biogenic amines and enkephalin. *J. Neurosci.* **15,** 1215–1235.

19. Arvidsson, U., Riedl, M., Chakrabarti, S., Vulchanova, L., Lee, J.-H., Nakano, A. H., et al. (1995) The κ-opioid receptor (KOR1) is primarily postsynaptic: combined immunohistochemical localization of the receptor and endogenous opioids. *Proc. Natl. Acad. Sci. USA* **92,** 5062–5066.

20. Bausch, S. B., Patterson, T. A., Appleyard, S. M., and Chavkin, C. (1995) Immunocytochemical localization of delta opioid receptors in mouse brain. *J. Chem. Neuroanat.* **8(3),** 175–189.

21. Mansour, A., C.A., F., Burke, S., Akil, H., and Watson, S. J. (1995) Immunocytochemical localization of the cloned mu opioid receptor in the rat CNS. *J. Chem. Neuroanat.* **8(4),** 283–305.

22. Ding, Y.-Q., Kaneko, T., Nomura, S., and Mizuno, N. (1996) Immunohistochemical localization of μ-opioid receptors in the central nervous system of the rat. *J. Compar. Neurol.* **367,** 375–402.

23. Kalyuzhny, A. E., Arvidsson, U., Wei W., and Wessendorf, M. (1996) μ-opioid and κ-opioid receptors are expressed in brainstem antinocecptive curcuits: studies using immunocytochemistry and retrograde tract-tracing. *J. Neurosci.* **16(20),** 6490–6503.

24. Svingos, A. L., Moriwaki, A., Wang, J. B., Uhl, G. R., and Pickel, V. M. (1997) μ-opioid receptors are localized to extrasynaptic plasma membranes of GABAergic neurons and their targets in the rat nucleus accumbens. *J. Neurosci.* **17(7),** 2585–2594.

25. Kalyuzhny, A. E. and Wessendorf, M. W. (1997) CNS GABA neurons express the μ-opioid receptor: immunocytochemical studies. *NeuroReport* **8,** in press.

26. Kalyuzhny, A. E. and Wessendorf, M. W. (1998) Relationship of μ- and κ-opioid receptors to GABAergic neurons in the CNS, including antinociceptive brainstem circuits. *J. Compar. Neurol.* **392(4),** 528–547.

27. Schmued, L. C. and Fallon, J. H. (1986) Fluoro-Gold: a new fluorescent retrograde axonal tracer with numerous unique properties. *Brain Res.* **377(1),** 147–154.

28. Palmi, M., Brooke, S., Smith, A. D., and Bolam, J. P. (1991) GABA-like immunoreactivity in different cellular populations of cerebellar cortex of rats before and after treatment with amino-oxyacetic acid. *Brain Res.* **543(2),** 277–286.

29. Johnson, D. G. and de C Nogueria Araujo, G. M. (1981) A simple method of reducing the fading of immunofluorescence during microscopy. J. Immunol. *Meth.* **43,** 349–350.

30. Brizzee, K. R., Ordy, J. M., and Kaack, B. (1974) Early appearance and regional differences in intraneuronal and extraneuronal lipofuscin accumulation with age in the brain of a nonhuman primate (Macaca mulatta). *J. Gerontol.* **29(4),** 366–381.

31. Dowson, J. H. (1982) Neuronal lipofuscin accumulation in ageing and alzheimer dementia: a pathogenic mechanism? *Br. J. Psych.* **140,** 142–148.

32. Barden, H. (1980) Interference filter microfluorometry of neuromelanin and lipofuscin in human brain. *J. Neuropathol. Exp. Neurol.* **39(5),** 598–605.

33. Dowson, J. H. (1982) The evaluation of autofluorescence emission spectra derived from neuronal lipopigment. *J. Microsc.* **128(PT 3),** 261–270.

34. Dowson, J. H., Armstrong, D., Koppang, N., Lake, B. D., and Jolly, R. D. (1982) Autofluorescence emission spectra of neuronal lipopigment in animal and human ceroidoses (ceroid-lipofuscinoses). *Acta Neuropathol. (Berlin)* **58(2),** 152–156.

35. Correa, F. M., Innis, R. B., Rouot, B., Pasternak, G. W., and Snyder, S. H. (1980) Fluorescent probes of alpha- and beta-adrenergic and opiate receptors: biochemical and histochemical evaluation. *Neurosci. Lett.* **16(1),** 47–53.

36. Partanen, M., Santer, R. M., and Hervonen, A. (1980) The effect of ageing on the histochemically demonstrable catecholamines in the hypogastric (main pelvic) ganglion of the rat. *Histochem. J.* **12(5),** 527–535.

37. Schnell, S. A., Staines, W. A., and Wessendorf, M. W. (1999) Reduction of lipofuscin-like autofluorescence in fluorescently labeled tissue. *J. Histochem. Cytochem.* **47(6),** 719–730.

9

In Situ Hybridization in Neural Tissues

Howard B. Gutstein

1. Introduction

Concomitant developments in molecular biology and neuroanatomy have permitted the development of techniques to visualize the expression of messenger RNA (mRNA) of interest in its neuroanatomical context and in a relatively quantitative manner. *In situ* hybridization can be performed using either radioactive or nonradioactive techniques and quantitated using specialized image analysis programs. This chapter will describe a sensitive radioactive method of *in situ* hybridization, with references given to other variants in technique.

2. Materials
2.1. General Materials

1. Fresh frozen brain or spinal cord sections (10–15-μm thick) mounted on polylysine-coated slides.
2. Linearized sense (and antisense) plasmids for the molecule of interest for riboprobe   synthesis, inserted downstream of an RNA polymerase promoter.
3. Glass staining dishes and glass or plastic slide carriers.
4. Whatman #2 filter paper, cover slips, and permount.
5. Nunc square hybridization dishes, with plastic supports for slides (tongue blades will do).
6. Scintillation vials.
7. Access to light-tight darkroom.

2.2. In Situ *Hybridization*

1. Sodium phosphate buffer (0.2 *M*): 11.04 g $NaH_2PO_4 \cdot H_2O$, 45.44 g $Na_2HPO_4 \cdot 2H_2O$, dissolve in 2 L distilled (dd) H_2O.
2. Paraformaldehyde (Paraformaldehyde is a toxic powder and should be kept under a hood until it is safely dissolved in water).

3. Proteinase K stocks: 10 mg proteinase K (PK), 1 mL dd H_2O, save aliquot at –20°C.
4. Proteinase K Buffer: per 200 mL, 2.42 g Tris Base, 3.8 g Na_4EDTA [tetra sodium ethylenediamine tetraacetic acid (EDTA)], pH 8.0 with HCl, add 2 µL PK (10µg/µL); per liter, 12.1 g Tris Base, 19 g Na_4EDTA, 19 g Na_4EDTA, and 10 µL PK. Stir at room temperature, add to desired volume (200 mL or 1 L) with dd H_2O, final PK concentration = 0.1 µg/mL.
5. Triethanolamine (TEA, 1M): 13.3 mL TEA (7.53M), dilute to <1 L with dd H_2O, pH 8.0 (pH with HCl, then bring it up to full volume).
6. G50/50 Buffer: 6.05 g Tris-HCl, pH 7.5 (0.1 M), 2.375 g Na EDTA(4) (12.5 mM), 4.35 g Na Cl (0.15 M), dissolve in 500 mL dd sterile filtered water. Divide into two autoclavable containers. Add 5–10 g of G 50/50 sephadex to one container. Autoclave both. When cool, add 0.2% sterile sodium dodecyl sulfate (SDS) (5 mL of 10% SDS/container).
7. 5X transcription buffer: 200 mM Tris-HCl, pH 7.5 at 37°C, 30 mM $MgCl_2$, 10 mM spermidine HCl, 25 mM NaCl.
8. Stock of 50% hybridization buffer: 5 mL formamide (50% final concentration), 2.5 mL sterile filtered H_2O, 1.5 mL 20×- sodium chloride/sodium citrate (SSC) (3X), 200 µL 50X Denhardts (1X), 500 µL 1 M NaPhosphate, pH 7.4 (50 mM), 100 µL 10 mg/mL yeast tRNA (0.1 mg/mL), 1 g dextran sulfate (10%), rotate on nutator in 37°C oven overnight.
9. Hybridization dish buffer: per 100 mL, 50 mL formamide, 25 mL dd H_2O, 15 mL 20X-SSC, and 5 mL 1M NaPhosphate, pH 7.4; per 30 mL, 15 mL formamide, 7.6 mL dd H_2O, 5 mL 20X-D SSC, and 1.5 mL 1 M NaPhosphate, pH 7.4.
10. RNase Buffer (reusable until cloudy, keep refrigerated): 1.21 g Tris-HCl base (10 mM), 29 g NaCl (500 mM), pH 8.0, diluted to 1 L with dd H_2O, add 200 mg RNase A to 1 L buffer while stirring.

2.3. Nissl Staining of Slides

1. Cresyl violet acetate.
2. Glacial acetic acid.

3. Methods

3.1. Preparing Solutions

3.1.1. 4% Paraformaldehyde (4 L Family Size)

1. Heat 1600 mL water to 60°C.
2. Add 160 g paraformaldehyde (weigh this out using a balance in the hood).
3. While stirring, add drops of 10 N NaOH until solution clears (approx 50 drops).
4. Add 0.2 M phosphate buffer.
5. Let cool and filter with Whatman #2 filter paper.
6. Check pH with pH paper and, if necessary, adjust to pH 7.0–7.4.
7. Store at 4°C, reusable until it looks bad or until you lose signal in your *in situs*!

3.1.2. Cresyl Violet Stain (per 250 mL)

1. Get a 500-mL Erlenmeyer flask and add the following: 2.5 g cresyl violet acetate (add this first), 2.5 mL glacial acetic acid, and 247.5 mL dd H_2O (250 mL total volume).
2. Parafilm the flask and shake in 37°C incubator for 1 h.
3. Filter the stain using #2 Whatman filter paper, a large ceramic funnel, a 500-mL filter flask, and a vacuum pump next to the Watson hood.
4. Use the stain or store it at room temperature. When you need to use the cresyl violet again, repeat **steps 2–4**. Always test your stain because it can and will eventually go bad. Usually, the bad stain will precipitate onto your slide, making it look splotchy.

3.2. Fixing Tissue and Pre-Hybridization

1. Clean glass staining dishes with soapy water, then distilled water.
2. Fill clean (RNAse free) dishes with 4% paraformaldehyde (reuse until smell is no longer potent) Aldehydes provide for good retention of cellular RNA.
3. Load slides in carriers, fix in paraformaldehyde for 60 min at room temperature.
4. Put control slides into a separate gray carrier and incubate in RNase A at 37°C for 60 min. Keep these slides separate from other slides until day 2. This is a negative control (*see* **Note 1**).
5. Heat PK solution to 37°C in glass staining dishes. PK deproteination opens the tissue so probe can reach the mRNA in the cell.
6. Dilute approx 1.5 L–2 L 2X SSC for each dish. If you feel that you have enough time here, you may begin the labeling reaction which requires 90 min of incubation.
7. Dump formaldehyde back in jug and rinse sections in 2X-SSC 3 times.
8. Incubate the sections in PK solution for 10 min at 37°C.
9. Rinse once with 2X SSC.
10. Rinse for 1 min in dd H_2O at room temperature.
11. Fill clean glass staining dishes with 200 mL of fresh 0.1 *M* TEA.
12. While stirring with magnetic stir bar, add 500 µL acetic anhydride per dish. This can be hard to get in solution. This step acetylates amino groups in the tissue and reduces nonspecific electrostatic probe binding.
13. Put spacers in baths and stir slides for 10 min at room temperature.
14. Rinse for 5 min in 2X-SSC.
15. Dehydrate sections in graded alcohols (50% to 100% EtOH), 30 s in each solution, then air-dry.

3.3. Probe Labeling Reaction

Each transcription reaction will label about 100 slides. If you need to do more, run two identical reactions. Below are protocols for both single-label and double-label reactions (*see* **Notes 2** and **3).**

1. Combine the following in an eppendorf tube: for single label, 5 μL 5X transcription buffer, 4.5 μL sterile filtered H_2O, 2 μL 0.1 *M* DTT, 1 μL linearized plasmid, 1 μL 10 m*M* adenosine triphosphate (ATP), 1 μL 10 m*M* GTP, 1 μL 10 m*M* CTP, and 7.5 μL ^{35}S-UTP; for double label, 5 μL 5X transcription buffer, 6.75 μL sterile filtered H_2O, 2 μL 0.1 *M* DTT, 1 μL linearized plasmid, 1 μL 10 m*M* ATP, 1 μL 10 m*M* GTP, 2.5μL ^{35}S-CTP, and 3.75 μL 35S-UTP.

2. For both single and double label, add 1 μL RNasIN (RNase Inhibitor).

3. Spin down.

4. Add 1 μL T7 RNA polymerase (or appropriate polymerase for your plasmid), mix by pipeting up and down.

5. Incubate for 90 min at 37°C in floater (this is the transcription reaction).

6. Make a G50/50 Sephadex column.
   a. Set up brace and stand.
   b. Push a bit of sterile glass wool into tip of 1cm^3 syringe.
   c. load mixture of Sephadex and G50/50 buffer into column until it reaches the 1 cc mark. This step can be done during the 90-min incubation time as long as it is ready when the labeling reaction is completed. Be careful not to let the column dry out.

7. Add 1 μL RNase-free DNase to eppendorf (labeling reaction), incubate 15 min at room temperature.

8. Let 100 μL G50/50 buffer run through sephadex column (fraction 1).

9. Dilute the transcription reaction with 75 μL G50/50 buffer and load this into the column (fraction #2).

10. Load 100 μL G50/50 buffer, and wait for it to pass through column (fraction 3).

11. Continue loading 100 μL aliquot of G50/50 buffer except collect fractions 4 through 8 in labeled Eppendorf tubes.

12. Freeze fractions with 1 μL 1*M* DTT. This protects thiol groups from being oxidized, and breaking the backbone of the probe (*see* **Note 4**).

3.4. Hybridization

1. Count 1 μL of each fraction in Beta Counter (with an appropriate volume of scintillation fluid). We want to apply approx 1.5 million counts/slide. Save any fraction >1 million counts. Any fraction over 100 counts is considered "hot."

2. Make enough probe to use 30 μL per slide for 1 1/2 times the number of slides you have hybridization buffer + hot fraction + DTT = probe. Vortex well because the probe is hard to mix.

3. Calculate how much hot fraction you will need to get 1.5 million counts/slide, then add 25% because it is always colder than you think it is.

4. Add 1 *M* DTT in a ratio of 1:100 (final concentration 10 m*M*). So, 900 μL hybridization buffer would require 9 μL DTT. This protects thiol groups on probe form being oxidized, which would break the backbone of the probe.

5. Count 30 μL probe in Beta Counter to make sure it is at least 1.5 million counts.

6. Line square plastic Nunc hybridization dishes with whatman filter paper and wet with 30 mL of hybridization dish buffer.

7. Drop 30 µL probe onto each 22 × 22 cover slip using P200 pipet. Pick up cover slips with slides, being extremely careful to avoid bubbles.
8. Put slides in dish on plastic stick supports –20 slides/dish. Do not let slides touch each other. The coverslips tend to cause a capillary action effect that causes the slides to dry out which also increases tissue background.
9. Seal box thoroughly with tin foil and scotch tape.
10. Incubate in oven at 55°C overnight (12–16 h). Store any extra probe at –80°C.

3.5. Posthybridization or "Taking it Down"

RNase A digestion is required for RNA probes to remove free cRNA (and mRNA) in the tissue. This reduces nonspecific signal. To reduce background and remove unbound probe, sections are washed in decreasing salt concentrations.

1. Heat RNase A in glass dishes to 37°C.
2. Soak off cover slips in 2X-SSC (this waste is radioactive).
3. Load slides into plastic carriers and incubate in RNase A for 60 min at 37°C. Clean glassware very carefully after this step.
4. Wash sections in decreasing strength SSC: 2X, 1X, 0.5X, 0.25X, and then 0.1X-SSC (5 mL 20X/1 L) at room temperature.
5. Incubate in 0.1X-SSC for 60 min at 65°C.
6. Transfer back to cool 0.1X-SSC, rinse 2 or 3 times.
7. Rinse with dd H$_2$O at least 1 min.
8. Dehydrate sections in graded alcohols (50% to 100% EtOH) and air-dry.
9. Load slides into X-ray cassettes—30 slides per cassette.
10. Put film (Kodak XAR–5) in cassettes in darkroom and place in a light-tight drawer for 3–5 d.
11. Bend corner and mark with magic marker so you do not lose orientation or number of film.
12. Load film into light-tight sleeves, wrap in foil, and develop in darkroom.
13. Mark X-ray films with slide numbers; then load slides into large slide boxes for dipping (*see* **Note 5**).

3.6. Dipping Slides in Photographic Emulsion

Set up everything beforehand, and make sure you know where everything is, so that you can find it in the dark. Do not expose emulsion to light. Emulsion is expensive, so do not waste it. Maintain a completely light-tight darkroom with emulsion-safe "safe" light, which is needed for these procedures.

3.6.1. Setting Up

1. Fill water bath and plug it in. It should already be adjusted to 39–42°C, but check it with a meat thermometer.

2. Put a plastic beaker into the water bath and fill part way with water. Be careful that the emulsion container does not sink too far—water can seep in under the cap.
3. Place the emulsion container somewhere you can reach it—you will need it later, when it is dark.
4. Place the following items near the water bath: scintillation vials and caps (in the cardboard rack), a 25-mL pipet and pipetor, a box of Kimwipes, a box of blank slides, and some aluminum foil.

3.6.2. Making Emulsion

1. Heat emulsion in water bath (38–42°C) for 45–60 min; this melts the emulsion, which is a gelatinous solid. Do not open the emulsion box until you are in the darkroom.
2. Heat a 500-mL Erlenmeyer flask filled with 118 mL of Milli-Q water (38–42°C water bath)—use a red rubber-coated lead ring to weight it down.
3. Tilt the flask and pour the molten emulsion in, pouring down the side of the flask to avoid bubbles. Bubbles are difficult to get rid of and can ruin dipped slides.
4. Gently swirl the flask in the bath for several minutes (approx 3 min). Swirl slowly, so that you do not create any bubbles.
5. Let the mixed emulsion sit for 30 min to settle.
6. Aliquot emulsion out into scintillation vials, approx 25 mL per vial. Use a 25 mL pipet and a red pipetor, and fill the vials over the mouth of the emulsion flask—any spills or overflows are not wasted that way.
7. Fill the vial down the side; getting the right volume will require practice—pull up the maximum volume (approx 30 mL) then move the plunger down a thumb length or so. Reproducible and accurate pipeting will be better than guessing here.
8. Cap and wrap vial in foil.
9. The last vial is probably only partially filled. Set it aside for now.
10. Pour the contents of the last vial (if fairly full) or the second-to-last vial into the dipping chamber. Pour down the side of the chamber to avoid bubbles.
11. Tap the chamber on the bath and let it sit in the bath for 30 min.
12. Dip a blank test slide into your dipping chamber and wipe off the nonfrosted side with a Kimwipe.
13. Examine the slide in another room. Look for microbubbles; if there are any, let the dipping chamber sit for another 30 min and try again. Gently tapping the chamber on the water bath may help dislodge bubbles.
14. If the slide appears to be bubble-free, then dip your test sections into the chamber. Remember not to dip too deep, as this will waste expensive emulsion. The entire specimen must be covered, however. When in doubt, dip a blank slide and use that as a guide. Holding dipped slides up to the safe-light will expose them, so do not do it.
15. Wipe off the nonspecimen (nonfrosted) side of the slide, and let dry in a scintillation vial rack in a light-tight location for at least 2 h. The lights must remain off.
16. After the slides are dipped, carefully pour the remaining emulsion out of the dipping chamber and back into the scintillation vial. Cap and wrap it in three layers of foil.

17. Put the foil-wrapped emulsion vials into small boxes, five or six each box. If you did not get a full 25 mL into the last vial, put it in a separate box.
18. Wrap the boxes in three layers of foil. Label the foil well (initials, date, number of vials) and place in the refrigerator.
19. After 2 h, put the dipped slides into a slide box and wrap it in three layers of foil. Refrigerate these slides and develop them in 1–2 d. These slides will indicate whether the emulsion is working properly.

3.6.3. Dipping Slides in Photographic Emulsion

1. Set up as in **Subheading 3.6.1.**
2. Use a foil-wrapped box of diluted and tested emulsion. Never use untested emulsion. Note that one vial will be enough for about 100 slides.
3. In the dark, unwrap the emulsion and put it in the already warm water bath (in the beaker) for 30–45 min.
4. If you are going to be dipping more than 100 slides, calculate how much extra emulsion you will need and set it aside.
5. Rewrap the remaining emulsion in the box (three layers of foil) and store at 4°C. Label the emulsion you return (number of vials, date, and so on).
6. Carefully pour the emulsion into the dipping chamber; tilt both vial and chamber toward each other. Bubbles are difficult to get rid of. Do this over the water bath so that spill cleanup is easier. If the chamber begins to overflow, stop pouring.
7. Gently tap the filled dipping chamber on the bath to dislodge any bubbles; let it sit in the bath for 30 min.
8. If dipping more than 100 slides, put the next vial of emulsion into the water bath now.
9. Dip a blank slide into the emulsion and wipe off the nonfrosted side with a Kimwipe.
10. Examine the slide in the other darkroom near the yellow safety light. Look for microbubbles; if there are any, let the dipping chamber sit for another 30 min and try again. Gently tapping the chamber on the waterbath may help dislodge bubbles.
11. If the slide appears to be bubble-free, then dip your real sections into the chamber. Remember not to dip too deep, as this will waste expensive emulsion. The entire specimen must be covered, however. When in doubt, dip a blank slide and use that as a guide. Holding dipped slides up to the safe-light will expose them, so do not do it.
12. Wipe off the nonspecimen (nonfrosted) side of the slide, and let dry in a scintillation vial rack.
13. There are 100 individual squares in the rack; put the slide in dipped end down, specimen facing semiupward.
14. Upon filling a rack of 100, put the rack into a light-tight drawer to dry for 2 h.
15. Check the level of emulsion every 10th slide or so with a test slide.
16. After the slides are dipped, carefully pour the remaining emulsion out of the dipping chamber and back into the scintillation vial. Cap and wrap it in foil.

17. Put the foil-wrapped emulsion vial into a small box and wrap the box in three layers of regular foil. Label the foil "used," date and initial it, and place in the refrigerator.
18. After 2 h, put the dipped slides into a slide box. Be sure to keep the frosted sides at the same end so that you know where the specimen is when dipping.
19. Take 9 or 12 of the slides and box them separately, in two or three small cardboard slide boxes (three each). These miniboxes will be your test slides—you will develop these first and use them to estimate when the rest of your slides are ready to be developed. It is helpful to prepick test slides so you can dip them first (stubborn bubbles may go away after dipping a few slides; this way your test slides may get rid of those nefarious bubbles). Make sure you know where the test slides are in the vial rack—back row, perhaps.
20. Wrap the boxes in three layers of regular foil then wrap them in a layer of heavy-duty foil. Label them and put them in refrigerator.
21. In a few weeks, you can develop one of the small boxes (depending on probe used). If those slides look underexposed, then wait longer and develop your other test slides. If the test slides look alright, then develop all of the slides.

3.6.4. Developing Dipped Slides

1. You will need a tub filled with water and either three, six, or nine staining dishes, depending on how many slides you will be developing.
2. Using nine dishes allows you to develop three sets of slide carriers simultaneously.
3. Wash the dishes well.
4. Fill a large plastic tub with ice and water.
5. Set up and fill the dishes: D-19 developer in the leftmost dishes, ddH_2O in the middle dishes and fixer in the rightmost dishes. It is important that the dishes be set up so that you can tell which is which in the dark, and that you can find them in the dark. D-19 is only good for one use whereas fixer may be used up to four or five times. Do not attempt to save developer or fixer because they do go bad. (D-19 and fixative are prepared as per manufacturer's instructions).
6. Put a plastic tub in the sink and fill it with water; leave the water on after the tub is filled so that it overflows.
7. Determine approximate how many glass slide carriers or gray slide carriers you will need and place them where you can find them in the dark (always overestimate because you may not fill every carrier).
8. Get your dipped slides and unwrap them (in the dark).
9. Carefully load the slides into your carriers so surfaces of adjoining slides do not touch each other. Be careful not to scratch the emulsion. All the specimens should be directed to one side. You can use the safety light to determine which end it is.
10. Dip carriers into D-19 developer for 2 min (in the leftmost dishes).
11. Dip the carriers in dishes of dd H_2O for 20 s.
12. Dip the carriers in Fixer for 3 min.
13. Put the carrier in the tub of fresh/sink water for at least 10 min.
14. Go back and develop remainder of slides, until all are in the final tub.

15. Once the slides are in the tub of water, you may turn the lights back on. At this point, you should transfer the developed slides to carriers for staining and cover slipping. Keep the sections wet, do not allow them to dry out.

3.7. Nissl Staining of Tissue Sections

Staining sections enables one to define anatomy on slides. This is useful for defining anatomical boundaries and analyzing *in situ* data. You will be staining either unfixed tissue (adjacent sections) or *in situ*-hybridized (dipped and developed) slides. For adjacent slides, a deep, dark stain is desired. For *in situ* slides, you will want a light staining which does not interfere with visualization of the emulsion grains.

1. Parafilm and put cresyl violet stain (keep it in a flask) into the 37°C shaker/ incubator for 60 min.
2. Fill clean glass dishes with xylene and cover. The xylene will dissolve myelin in the sections. Xylene is toxic, so avoid breathing the vapor. Exercise caution as xylene will quickly penetrate gloves. Wear two layers of gloves with a vinyl glove on the outside and change the outer glove whenever it touches xylene. Change the inner gloves if the xylene has penetrated to them (when the inner gloves smell like xylene).
3. Put the following items into the hood where you will be cover slipping: a bluepad-covered board, some 22-mm-square cover slips, an extra dish of xylene, an aerosol bottle of air, a bottle of Permount, some paper towels, and some plastic squeeze-bulb pipetes.
4. When cresyl has been shaken for one hour, remove it from the shaker and filter it using #2 Whatman filter paper, a large ceramic funnel, a 500-mL filter flask, and a vacuum pump. You may use two filter papers instead of one to ensure thorough filtering.
5. Pour the filtered stain into a dish.
6. Have a dish of fresh dd H_2O prepared for rinse before ethanol washes. Make fresh graded ethanols.
7. Test by staining a slide first.
   a. Dip it in stain for 5 min (unfixed) or 2 min (developed).
   b. Dip it quickly in the water dish.
   c. Take it through the alcohol gradient, dipping it quickly in each dish. Look at the slide and determine how good the stain is. If it is too faint, you may have to stain your slides longer, If there is a precipitate on the slide, or if it looks bad, your stain may be bad. Do not proceed until you have confirmed the quality of your cresyl violet stain. Unfixed slides should be brought to room temperature and allowed to dry before loading into carriers.
8. Load the slides into carriers. If developed, the slides are currently soaking in water. If unfixed, the slides can be taken directly from the –80°C freezer; allow unfixed slides to reach room temperature before staining them.
9. Immerse slides in the cresyl violet for 2–5 min. Time varies widely, based on whether you are staining dipped slides (faint, 30 s) or whether you want dark

staining for adjacent sections (5 min). How old the cresyl is can also affect staining times.

10. Dip slides in ddH$_2$O and then in increasing concentrations of ethanol (50, 80, 95, and 100%). Length of dip in each varies, from quick to several seconds. The longer the slides are immersed, the more stain will leave the sections. If, after a dip in 100% EtOH, the slides are too dark, simply soak them longer. If they are too light, take the slides back down through the ethanol gradient, then ddH$_2$O, and let them stain a little longer. Then dehydrate/rinse them as before.

11. Put the dehydrated/stained slides into a dish of xylene for 5 min.

12. Move the slides into another dish of xylene for 5 min. Wear layers of gloves and change the outer layers when necessary.

13. When the slides have been in xylene for at least 10 min, you can begin cover slipping.

14. Move a dish of xylene-soaking slides into the hood.

15. Move one of the slide carriers into your extra dish—this will be your working dish.

16. In the hood, air-blast some cover slips and lay them out on paper towels.

17. Using a plastic squeeze-bulb pipet, put a bit of Permount down one edge of the cover slip.

18. Pull a slide out of the xylene and touch the section to a cover slip. The Permount should cover the section without bubbles.

19. Set the slide down on a board to dry (right side up). Make sure the slide is level, or the cover slip will slide off of the tissue while drying. If this happens, redo that slide. Unless the specimen is clearly visible under the cover slip (with no bubbles on it), you should redo it. Simply soak the cover slip off in the xylene. Lean the slide in the dish and try to cover slip it a little later. You will be able to soak off the cover slip for quite a while, so if you find slides that have dried poorly, you may soak them in xylene and recoverslip them.

20. Allow the cover slipped slides to dry until they no longer smell like xylene.

21. Put the dry slides into boxes.

4. Notes

1. Appropriate hybridization controls include both sense strand experiments and RNase pretreatment. At least one of these controls should be performed with each experiment.

2. Nonradioactive *in situ* hybridization can be performed using biotin- or digoxigenin-linked probes. Radioactive and nonradioactive techniques can also be combined to permit evaluation of coexpression of mRNAs of interest. These protocols are presented elsewhere *(2–4)*.

3. There are many factors affecting the type of probe selected for hybridization (e.g., oligonucleotide vs cRNA vs cDNA probes). Hybridization temperature will vary based on the nature of the probe used. The hybridization temperature presented in this protocol is one we use fairly routinely for riboprobe hybridizations. For a more detailed discussion of these issues, please *see* other references *(1,4)*.

4. Probe integrity can be verified by polyacrylamide gel electrophoresis. Also, full-length transcripts may be isolated by fractionation on a low-melting point agarose gel. Further details can be found in previous reports *(1,4)*.

5. Numerous methods for quantitation of *in situ* hybridization data have been proposed; a useful overview of this process is provided by Mize *(5)*.

References

1. Schafer, M. K. H., Herman, J. P., and Watson, S. J. (1993) In situ hybridization histochemistry. In *Imaging Drug Action in the Brain* (London, E. D., ed.), CRC, Ann Arbor, MI, pp. 337–378.

2. Marks, D. L., Wiemann, J. N., Burton, K. A., Lent, K. L., Clfiton, D. K., and Steiner, R. A. (1992) Simultaneous visualization of two cellular mRNA species in individual neurons by use of a new double in situ hybridization method. *Mol. Cell. Neurosci.* **3,** 395–405.

3. Braissant, O. and Wahli, W. (1998) A simplified in situ hybridization protocol using non-radioactively ed probes to detect abundant and rare mRNAs on tissue sections. *Biochemica* **1,** 10–15.

4. Watson, S., Patel, P., Burke, S., Herman, J., Schafer, M., and Kwak, S. (1988) In situ hybridization of mRNA in nervous tissue: A primer. *In Society for Neuroscience Short Course 1 Syllabus* (Sundermann, A., ed.), Society for Neuroscience, Washington, DC, pp. 4–29.

5. Mize, R. R. (1994) Quantitative image analysis for immunocytochemistry and in situ hybridization. *J. Neurosci. Methods* 219–237.

10

Quantitative Single-Cell RT-PCR for Opioid Receptors and Housekeeping Genes

Seth C. Silbert

1. Introduction

1.1. Overview

When the polymerase chain reaction (PCR) is applied to individual cells, variations in the efficiencies of cell harvest, reverse transcription (RT), and PCR confuse the interpretation of results. This chapter demonstrates three refinements of the standard RT-PCR strategy, which together provide explicit measurements of single-cell gene expression in terms of mRNA molecules per cell. (1) The entire cell is harvested and reverse transcribed. (2) Mutant sequences, included as internal controls, explicitly monitor the efficiency of RT and PCR in each reaction tube. (3) Multiple targets are independently amplified from each cell, including a constitutively expressed housekeeping gene, glyceraldehyde-3-phosphate dehydrogenase (GPD, GAPDH), confirming successful harvest and reverse transcription of each cell. Amplification of GPD, as well as two opioid receptor, and two peptide precursor sequences illustrates this approach. In the case of GPD, RT yields one amplifiable cDNA molecule for every 2–3 mRNA molecules. Sensory neurons maintain GPD mRNA in the nanomolar range, but with considerable variability (1.03 ± 0.61 nM). Competitive PCR can be applied to virtually any message sequence. In neurons expressing the sequence, message levels are explicitly quantified. In neurons not expressing the sequence, the absence of message is convincingly demonstrated. As few as 2–5 cDNA molecules are routinely detected. cDNA levels are quantified to within a factor of two, typically over a 100-fold range.

1.2. Background

RT followed by PCR can demonstrate gene expression at the single cell level *(1–5)*. With this technique, gene expression and electrophysiologic responses can be measured and compared in the same neuron (*see* **Fig. 1**). When PCR reactions are assembled, however, tube-to-tube variations of reaction efficiency and sensitivity often limit the interpretation of results. Threshold detection limits can vary from a few to thousands of cDNA molecules, whereas individual cells may regulate gene expression over a much narrower range. Though less frequently noted, variations in the proportion of each cell harvested and the efficiency of RT can similarly confound results. Complete cell harvest, followed by RT-PCRs with explicitly definable sensitivity and efficiency would generate amplification profiles that more convincingly reflect single cell gene expression patterns.

Nucleic acids can be quantitatively amplified using competitive PCR techniques developed by Becker-Andre and Hahlbrock and Gilliland et al. *(6–8)*. Samples of the desired target are combined and coamplified with known concentrations of a competitor sequence in each reaction tube. The competitor differs in length or contains an altered restriction site, but is otherwise identical to the wild type target sequence. Both sequences are amplified in the same tube using a single pair of primers. Aliquots of the sample are mixed with a dilution series of the competitor. When both sequences are amplified with equal efficiency, quantifying the target merely requires identifying the competitor concentration for which amplification generates equal amounts of both sequences. Tube-to-tube variations in reaction efficiency can alter the total amount of products generated, but their ratio remains unaffected and reflects that of their initial starting concentrations.

To summarize the amplification protocol: 1) Two sequences compete, under identical reaction conditions, for a single set of primers; and 2) the reaction set coamplifies aliquots of the tissue sample against a dilution series of the competitor. RNA and DNA competitors can be included to monitor both RT and PCRs. Together they make possible calculation of the number of mRNA molecules contained in a given nucleic acid sample. With these methods cDNA concentrations have been detected and quantified in preparations derived from as few as 2000 cells.

Standard competitive PCR cannot be applied to individual cells because it demands subdivision of the initial tissue sample. The experiments presented here solve the problems of single cell RT-PCR by augmenting the amplification reaction, thereby lowering threshold detection limits, and by including controls that quantify both RT and PC reactions. Where a given endogenous product fails to appear, these controls distinguish legitimate absent gene expression from three common experimental artifacts: the failures of cell har-
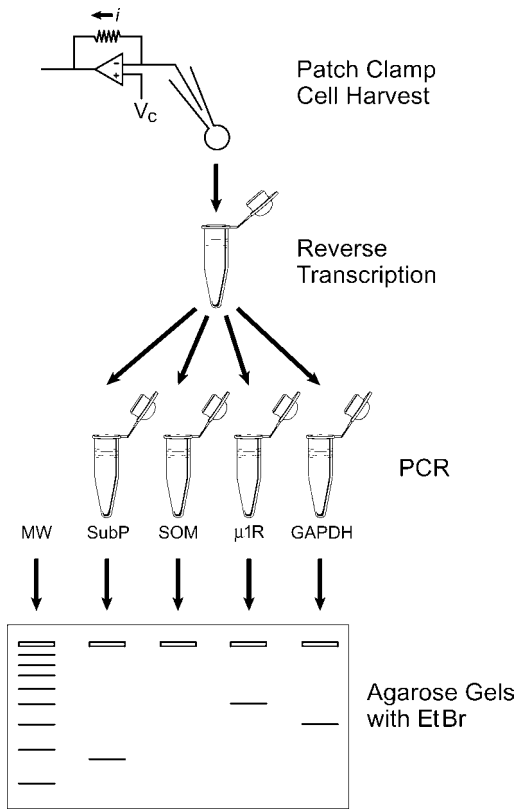
Fig. 1. The depicted standard protocol combines ion channel pharmacology with single-cell RT-PCR in the same cell. Typical steps include: 1) recording ion channel currents in the whole-cell patch clamp configuration; 2) aspirating the cytoplasm into the recording pipet, then expelling the pipet contents into a reaction tube; 3) reverse transcribing the mRNA using random hexamer or oligo dT primers; 4) PCR-amplifying specific sequences from aliquots of the reverse transcription reactions; and 5) agarose or polyacrylamide gel electrophoresis and analysis of the PCR product bands. Modifications which improve this technique include: 1) recording ion channel currents in the perforated-patch configuration; 2) using a second harvest pipet with dimensions optimized to draw the entire cell through the bath-air interface, then expelling the pipet contents into a reaction tube containing frozen primer mix and a mutant housekeeping gene (*GPD*) mRNA control; 3) performing a primer annealing reaction prior to reverse transcription; 4) including mutant cDNA controls corresponding to each sequence of interest in the PCRs, along with a calibration ladder to define the relation between initial concentrations of endogenous sequences and the ratio of wild-type to mutant PCR product bands; and 5) using the calibration ladder to quantify cDNA concentrations and reverse transcription efficiency in each tube.

vest, RT, and PCR. The results, expressed as mRNA molecules per cell, explicitly define both the resolution of each experiment and gene expression levels in each cell. In this chapter, single-cell expression of the constitutively expressed gene, GPD is measured and developed as an indicator of successful cell harvest. Experiments demonstrating that opioid responses in sensory neurons depend on selective expression of the mu opioid receptor gene rely heavily on these techniques *(9)*.

These experiments demonstrate two key refinements that make single-cell measurements possible. First, successive PCRs using nested primer pairs augment amplification, with threshold detection limits of 1–5 cDNA molecules. Second, a calibration curve relating the ratios of the templates before and after amplification is generated with each reaction set. Here, concentrations of the wild type sequence, spanning the anticipated range of cellular gene expression, vary against a fixed concentration of the competitor. As reaction efficiency varies from tube-to-tube, so does the intensity of the product bands representing the mutant (control) and wild-type sequences. This variation does not, however, affect the relative intensities of the two bands. This ratio depends only on the starting concentrations and relative transcription and amplification efficiencies for the two sequences. The-wild type target dilution series defines a curve relating the ratios of the product band intensities to those of the initial target concentrations. This internal calibration holds true for all the reaction tubes in a set and is generated anew with each reaction set.

2. Materials

1. Klentaq1, a recombinant *Thermus aquaticus* DNA polymerase *(10,11)*.
2. Superscript II RNase H- reverse transcriptase (Life Technologies, Inc.).
3. Garner 7052 capillary glass, baked 8 h at 200°C prior to fabrication of the recording and harvest pipets.
4. Electrophysiology equipment and instruments, treated with RNase AWAY (Molecular BioProducts).
5. Ribonucleic and deoxyribonucleic acids, including nucleotides, primers, as well as mRNA and DNA target sequences, prepared in 10 m*M* Tris-HCl, 0.1 m*M* ethylenediamine tetraacetic acid (EDTA), pH 8.0 (23°C), divided into limited-use (10 or fewer per tube) aliquots, and stored at –80°C.
6. 10× PCR buffer, stored at 4°C, as recommended by the supplier.
7. PCR solution: 28–58 m*M* Tris-HCl, pH 8.4–8.8 at 23°C, 16 m*M* $(NH_4)_2SO_4$, 150 µg/mL BSA, 10–15 m*M* KCl, 3–5 m*M* $MgCl_2$, 100 µ*M* tetramethyl ammonium chloride (TMAC), 6–8% dimethyl sulfoxide (DMSO), and 4 mU/µL Klentaq1.
8. Concentrated restriction and polymerase enzyme buffer solutions, stored at –20°C.
9. QIAGEN nucleotide purification kits for plasmid minipreps, extraction from agarose gels, and isolation of synthetic polyA+ mRNA.
10. Competent bacteria (e.g., DH5α) for plasmid transfection and miniprep amplification.

3. Methods

3.1. Overview

Figure 1 illustrates the general protocol that is followed. The photo sequence of **Fig. 2** illustrates the harvest procedure. **Figure 3** shows a resulting set of gels. The essential points of the protocol are the following:

1. Harvest the whole cell.
2. Add 4–10 K molecules of a mutant GPD mRNA having a 268-bp insert to each reaction tube as an internal control to quantify the concentration of wild-type GPD mRNA and estimate the efficiency of RT for each cell.
3. Prepare control RT reactions; they contain 4–10 k molecules of both the mutant and wild-type GPD mRNAs.
4. Amplify 10–50% of the RT product in a multiplex PCR.
5. 12–25 molecules of mutant μ-receptor cDNA (78-bp insert), 100–300 molecules of mutant ppTKβ (219-bp insert), 50–100 molecules of mutant ppSOM (88-bp insert), and 500–1000 molecules of mutant GPD cDNA (88-bp insert) are included in each of the PCR tubes for the first-round amplification.
6. Prepare a calibration ladder cut for each PCR run. The ladder consists of seven reaction tubes, each having a different amount of wild type cDNA but the same amount of mutant cDNA as added to the product of each RT.
7. Perform no more than 25 cycles of PCR. This requires that two sequential PCRs be performed using nested primers (those of the second reaction anneal to internal sites in the products of the first).

Figure 3 illustrates this approach applied to opioid receptor, peptide transmitter, and GPD message sequences in rat sensory neurons. The top panel depicts μ-receptor expression for these cells. To verify successful PCR amplification for all tubes, 12 molecules of the mutant μ-receptor sequence is included as an internal control and coamplified with the wild-type sequence in each reaction tube. The mutant contains an 88-bp insertion, generating the higher molecular weight μ-receptor band in each of the lanes. The mutant band appears in all lanes, confirming successful PCR, despite the variable presence of the corresponding wild-type band. The calibration curve to the left of the molecular weight markers enables ratios of the mutant and wild-type band intensities to be related to the ratio of their initial concentrations.

Failure of cell harvest or RT can also preclude amplification of wild-type μ-receptor sequence. To exclude these artifacts, transcripts of the constitutively expressed GPD gene are coamplified, displayed in the bottom panel of **Fig. 3**. As further described later, including an mRNA mutant of this gene in the RT reactions makes possible calculation of the number of GPD mRNA molecules captured with each harvested cell.
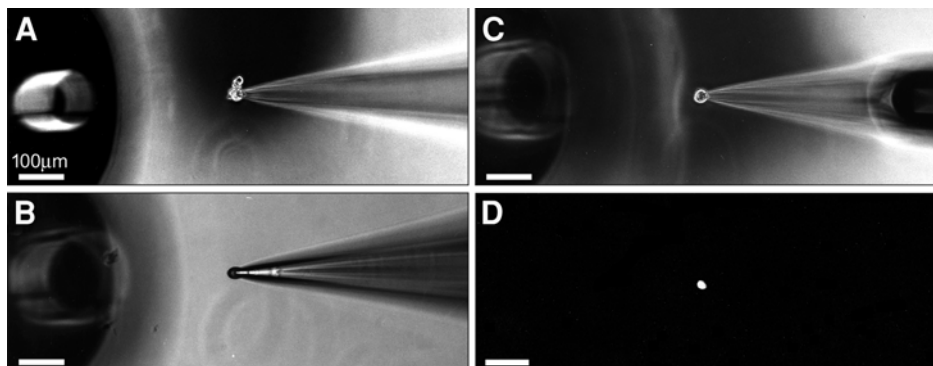
Fig. 2. Harvesting the entire cell through the bath–air interface. A diI-labeled neuron was plucked from the bottom of the culture dish using a pipet having a 7–10 μm tip inner diameter. (**A**) The pipet tip is just below the surface of the bath, prior to carrying the cell through the bath–air interface. The entire cell body remained attached to the pipet, including proximal portions of neurites and undesired extracellular debris. (**B**) The pipet tip is just above the surface of the bath, after drawing the cell throught the bath-air interface. The visible rounded profile of the cell at the pipet tip confirmed sucessful cell harvest. (**C**) The pipet and cell have been dipped into the bath again. This step is not normally included in the protocol. In this case, it demonstrates that the harvest procedure captured the entire cell body but removed neurites as well as potentially contaminating extracellular debris. (**D**) Pipet tip and cell are above the surface of the bath, as in (**B**), and photographed under flourescent illumination. The retained dye confirm the presence of harvested cell cytoplasm at the pipet tip.

3.2. Tissue Culture

Dissociated cell cultures of rat trigeminal sensory neurons were prepared as described in previous reports *(12,13)*. Cultures were incubated for 2–6 h at room temperature in serum-free L-15 media prior to harvest on the same day. Alternatively, cultures were incubated overnight at room temperature in L-15 containing 5% heat-inactivated fetal calf serum (FCS). Then cells were harvested on the following day.

3.3. Construction of Target Sequences

Wild-type and mutant clones of each desired target sequence were constructed using standard recombinant DNA techniques. They are included in all amplification reactions as internal controls, are coamplified with the endogenous sequences derived from harvested cells, and make quantification possible. Mutants were created by inserting small "stuffer" DNA fragments into a unique restriction site of the cDNA (*see* **Note 1**). Clones were prepared at care-
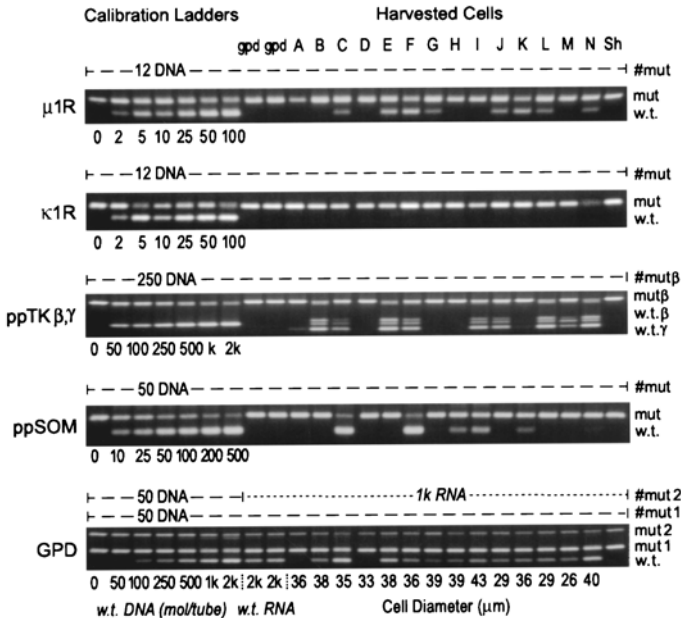
Fig. 3. Sensory neuron expression profiles. Fourteen sensory neurons from the trigeminal ganglia, corresponding to Lanes A-N, were harvested and sequences for the µ1-opioid receptor (µ1R), κ1-opioid receptor (κ1R), preprotachykinin β and γ (ppTKβ,γ; substance P precursors), preprosomatostatin (ppSOM), and glyceraldehyde-3-phosphate dehydrogenase (GPD) were RT-PCR amplified according to the improved technique. The seven lanes on the left of each gel represent a calibration series in which by various concentrations of each wild-type sequence competed in the PCR with fixed concentration of mutant sequences that were placed in each of the reaction tubes. The calibration series explicitly defines the relation between the initial concentration of wild type sequences and the ratio of wild type-to-mutant PCR products. For GPD amplification, both a cDNA control (Mut 1) and an mRNA control (Mut 2) were included in the amplification reaction so that both cDNA concentrations and corresponding mRNA concentrations could be measured for GPD in each reaction tube. The reverse transcription efficiency was then calculated and applied to the other sequences to convert cDNA to mRNA concentrations. Overall, the technique explicitly measures, for several desired sequences, the number of mRNA molecules contained in each of the cells.

fully measured concentrations for assembly of the control reactions. Essential steps for preparing the clones include:

1. Generate small stuffer fragments by digesting pBSSK- with the the restriction enzyme *Sau*3AI, which recognizes the four basepair sequence 5'-GATC-3' and produces numerous fragments between 50 and 260-bp (75, 78, 105, 219, 258-bp).

2. Agarose gel purify and extract the fragments.
3. Clone desired cDNA sequence into a standard expression plasmid (e.g., pBSSK-Stratagene Cloning Systems; pGEM-3Z, Promega Biotech).
4. Convert a unique restriction site in the cDNA clone into the *Bam*HI, *Bgl*II, or *Bcl*I recognition site. (Restriction of these sites by the corresponding enzyme creates compatible ends to the stuffer fragments.) The conversion can be accomplished by inserting a 10-bp linker sequence that contains, the desired recognition sequence and the sequence complemenatary to the overhanging ends generated by restriction with the original enzyme. Skip this step if the cDNA already contains a unique *Bam*HI, *Bgl*II, or *Bcl*I site.
5. Insert the stuffer fragments into the *Bam*HI, *Bgl*II, or *Bcl*I site.
6. Confirm the identity of the insertion by restriction analysis and/or sequencing the clones.
7. Miniprep amplify, excise, and gel-purify the desired cDNA sequences.
8. Spectrophotometrically measure the cDNA concentration of the stock solution, serially dilute in 10 mM Tris-HCl/0.1mM EDTA, pH 8.0 and store as limited-use aliquots (<5×) at –70°C.

Cloning strategies for each of the sequences used in our experiments are outlined here.

3.3.1. Glyceraldehyde-3-phosphate dehydrogenase (GPD) (**Fig. 4A,B**)

The GPD sequence from positions 5 to 1267 (relative to the transcription start site) *(14)* was amplified from rat sensory ganglia cDNA using the primers 5'-CTG CTC CTC CCT GTT CTA GAG ACA - 3' and 5' - TGC AGC GAA CTT TCT AGA TGG TAT T - 3' (Oligos Etc., Wilsonville, OR). The latter, negative strand primer, contains two mismatches, corresponding to A -> T and T -> G changes at positions 1252 and 1254, such that *Xba*I digestion would release a fragment corresponding to positions 19-1250 of the native sequence. For half of the PCR product, the linker sequence 5'-CATGAGATCT-3' was inserted into the *Rca*I site at position 586 to convert it to a *Bgl*II site. The two sequences were then cloned into the *Xba*I site of the phagemid pBluescript SK(-) (pBSSK-, Stratagene Cloning Sytems). Mutants were constructed by inserting 75-bp, 78-bp, and 258-bp *Sau*3AI-digested pBSSK- "stuffer" fragments (plasmid positions 1720–1794 and 1814–1891) into the *Bgl*II site of the modified clone. Ligation products were transformed into DH5α cells, then miniprep-amplified and isolated. Clones containing the native sequence, as well as 85-bp and 268-bp insertions were identified and analyzed. GPD cDNA was separated from the vector via XbaI digestion, followed by gel purification. After spectrophotometric quantification, sequences were serially diluted to the desired concentrations.
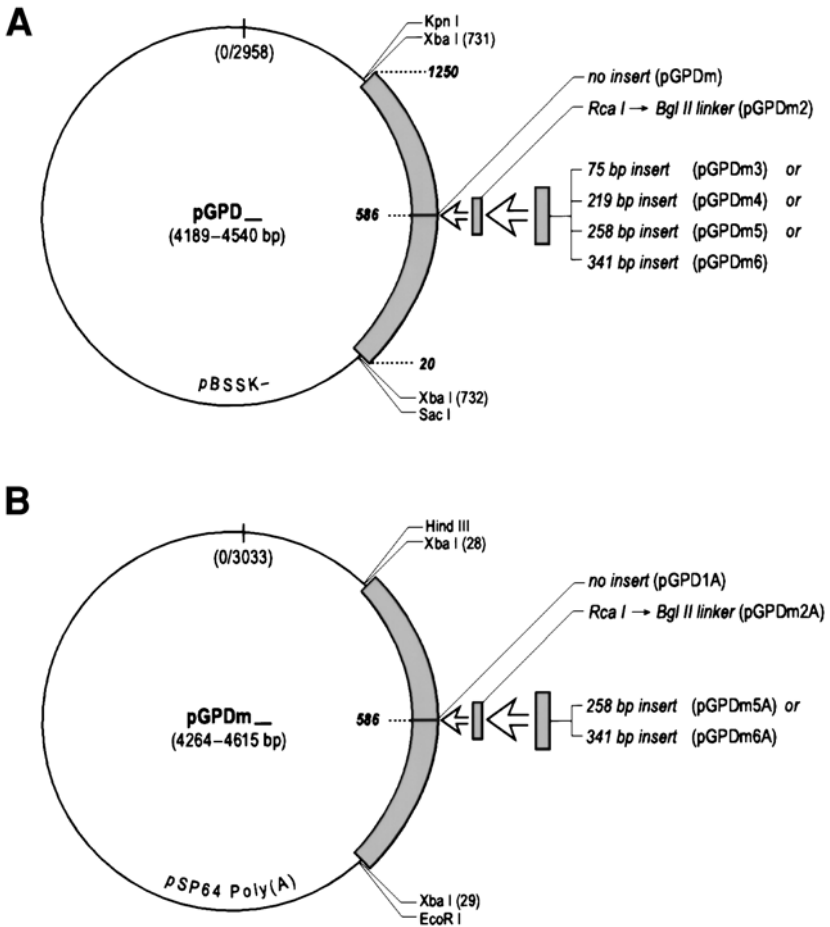
Fig. 4. Glyceraldehyde-3-phosphate dehydrogenase (GPD) cDNA plasmid constructs. GPD cDNA was amplified from rat sensory ganglia total RNA, using primers containing the native *Xba*I restriction site at position 19 and an artificial site at position 1250. A 10-bp *Rca*I to *Bgl*II linker was inserted into the GPD *Rca*I site at position 586 for half of the PCR product. (**A**) The cDNA sequence corresponding wild-type positions 20–1250 was cloned into the *Xba*I site of pBluescript SK(–) (pBSSK–, Strategene). Several *Sau*3AI-restricted pBSSK- fragments were inserted into the *Bgl*II site to generate insertion mutants containing 85–351 bp of inserted DNA. (**B**) Several of the resulting cDNA constructs were subcloned into the *Xba*I site of pSP64 Poly(A) (Promega) so that artificial GPD mRNA could be reverse transcribed.
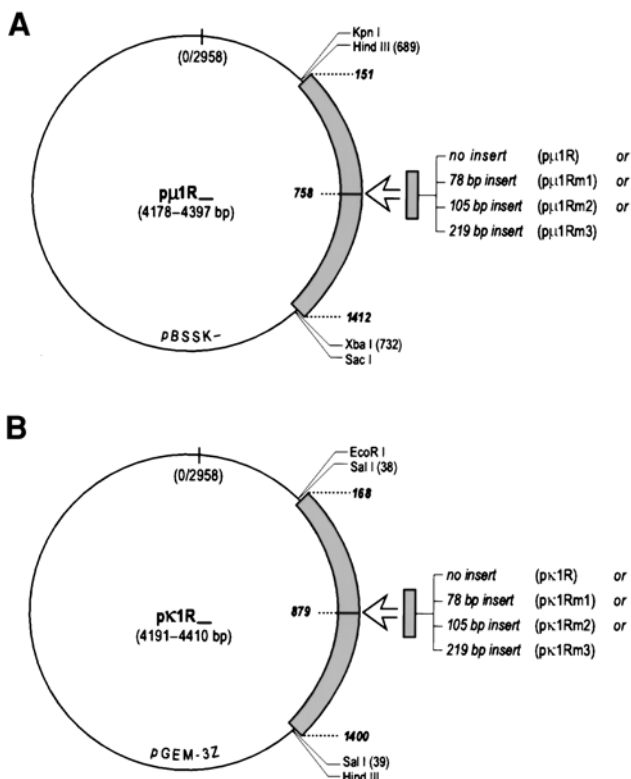
Fig. 5. Rat μ1 and κ1 opioid receptor (μ1R and κ1R) cDNA constructs. Clones representing the endogenous sequences were gifts of David K. Grandy *(14–17)*. Mutants were generated by inserting *Sau*3AI-restricted pBSSK- fragments into (**A**) the *Bam*HI site at μ1R position 758 and (**B**) the *Bgl*II site at κ1R position 879.

3.3.2. μ-1 and κ-1 Opioid Receptors (μ1, κ1-receptors) *(*see **Fig. 5A,B**)

David K. Grandy provided clones of the rat μ1- and κ1-opioid receptors *(15–18)*. Sequence positions 155–1411 of the μ1-receptor were inserted between the *Hind*III and *Xba*I sites of pBSSK-. Positions 173–1399 of the κ1-receptor were cloned into the *Sal*I site of pGEM-3Z (pGEM-Blue, Promega Biotech). The μ1 clone contains a unique *Bam*HI site at position 758 and the κ1 clone a *Bgl*II site at position 879. Inserting the 75-bp and 78-bp stuffer fragments into these unique sites create the desired mutants. Clones containing the 78-bp insertion, confirmed by restriction and sequence analysis, awere selected. Receptor cDNA was isolated by *Hind*III × *Xba*I digestion of μ1 clones and *Sal*I digestion of κ1 clones, gel purification, and serial dilution.
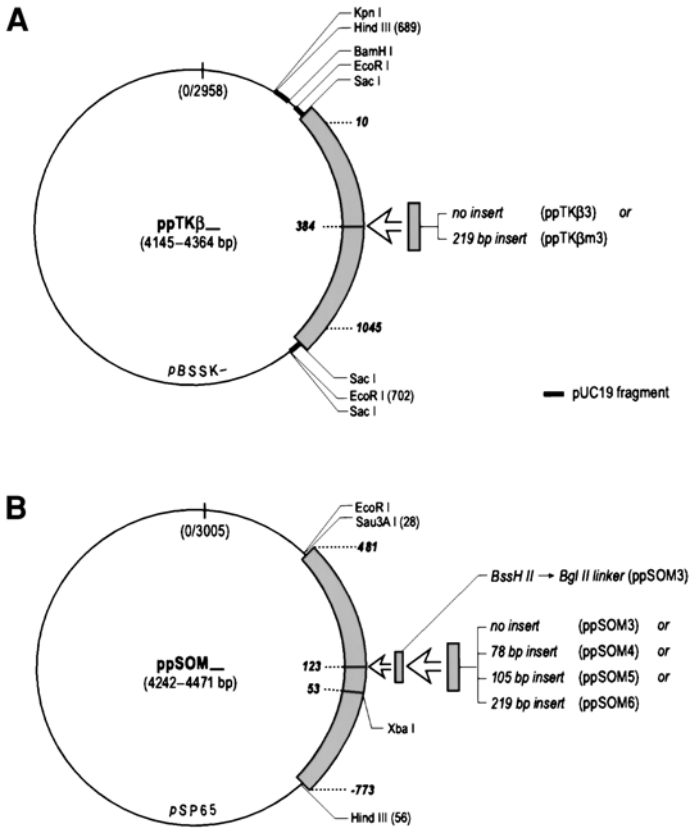
Fig. 6. Preprotachykinin β (ppTKβ, substance P precursor) and preprosomatostatin (ppSOM) cDNA constructs. (**A**) James E. Krause provided partial rat ppTKβ clones pSP27-4/4-7α and pSP31-1γ *(18,19)*. The full-length ppTKβ sequence, was reconstructed with the appropriate *Bam*HI-*Bgl*II fragments of these subclones and inserted into *Bam*HI-digested pBSSK-. *Sau*3AI-pBSSK- fragments were inserted into the *Bgl*II site at ppTKβ position 384. (**B**) Malcolm J. Low provided the rat ppSOM clones pSR-1 and pEJ-2 *(20)*. An 827-bp *Hind*III–*Xba*I fragment of pEJ-2 was cloned into pSR-1, generating a construct spanning nucleotides (–773) to (+481) of the gene. A 10-bp *Bss*HII to *Bgl*II linker sequence was inserted into the *Bss*HII restriction site at position 123 of ppSOM to convert it to a *Bgl*II site where pBSSK- fragments were inserted.

3.3.3. Preprotachykinin β (ppTKβ) and Preprosomatostatin (ppSOM) (see **Fig. 6A,B**)

James E. Krause provided the original rat ppTK clones pSP27-4/4-7α and pSP31-1γ, described in Krause et al. *(19)* and MacDonald et al. *(20)*. The full-length ppTKβ sequence, was reconstructed with the appropriate *Bam*HI-*Bgl*II

fragments of these subclones and inserted into *Bam*HI-digested pBSSK-. The clone was then digested with *Bgl*II, dephsophorylated, gel purified, and ligated with the 219-bp stuffer fragment. The identity and orientation of the insert was confirmed by analyzing *Bam*HI×*Sma*I digests of the plasmids. *Sac*I (*Sst*I) digestion, gel purification, and dilution produced isolated peptide precursor cDNA.

For preprosomatostatin (ppSOM), Malcolm J. Low provided the rat ppSOM clones pSR-1 *(21)* and pEJ-2. An 827-bp *Hind*III-*Xba*I fragment of pEJ-2, encoding genomic 5'-flanking regions and the first 53-bp of the ppSOM cDNA sequence, was cloned into pSR-1, generating a construct which spans nucleotides (–773) to (+481) of the gene, including the entire peptide coding sequence. The linker sequence 5'-CGCGAGATCT-3' (Oligos Etc.) was inserted into the *Bss*HII restriction site at position 123 of ppSOM to convert it to a *Bgl*II site. The resulting construct was digested with *Bgl*II, dephosphorylated, and ligated to 75- and 78-bp stuffer fragments. A clone containing the 78bp fragment was isolated and the insert orientation identified by *Sma*I × RcaI digestion of the plasmids. Peptide precursor cDNA was isolated by *Sac*I (*Sst*I) digestion, gel purification, and dilution.

3.4. In Vitro Transcription

GPD cDNA constructs representing the native sequence and a mutant with the additional 268-bp insertion have been subcloned into the *Xba*I site of pSP64 Poly(A) (Promega Biotech). PolyA+ mRNA was prepared from *Eco*RI-linearized templates and isolated using an oligo-dT based extraction kit (Oligotex Direct mRNA, QIAGEN, Inc.). After spectrophotometric quantification, mRNA was serially diluted and stored at –70°C as single-use aliquots until assembly of RT reactions.

3.5. Cell Harvest

The procedure captures the entire cell body (*see* **Fig. 2A–D**).

1. For sensory neurons, fire-polish pipets to an inner diameter of 6–7 µm for cells with a 40-µm diameter or less, and 8–10 µm for larger cells (pipet resistence = 100 kΩ).
2. Front-fill the initial 2–4 mm (<1 µL) of the pipet tip with harvest solution (135 m*M* KCl, 5 m*M* Tris-HCl, pH 8.2).
3. Bathe the cell to be harvested under a continuous flow of RNase-free Hanks solution and guide a pipet to its surface.
4. Syringe-apply suction to embeds 15–35% of the cell inside the pipet tip.
5. Under microscopic observation, carry the cell some intact through the air-liquid interface.
6. Expel the pipet contents by breaking the tip while applying positive pressure into the bottom of a thin-walled 200-µL PCR tube (Perkin Elmer), containing 10 µL of frozen primer mix.

Harvest pipets are too large for patch clamp recordings. To obtain recordings prior to harvest, perform perforated patch recordings *(22,23)* with a standard recording pipet. Then guide the harvest pipet to the cell with a separate manipulator to pull the cell away from the recording pipet. The perforated patch configuration avoids potential diffusion of the cellular components into the recording pipet. With practice, the entire harvest procedure adds only 5 min per cell to recording experiments (*see* **Note 2**).

3.6. Random Hexamer Annealing and RT

The RT primer mix contains 5 μ*M* random hexamers (*see* **Note 3**), 5 m*M* dithiothreitol (DTT), 0.5 U/μL RNasin, 250 ng/μL glycogen, 10^5 molecules of the GPD mRNA mutant, and DEPC-treated H_2O to a volume of 10 μL.

1. Freeze the cell-primer mix in a dry ice/EtOH bath, then thaw prior to the annealing reaction. This ensures membrane disruption and cell lysis.
2. Annealing proceeds with a 10-min incubation at 70°C, then a quick-chill on ice.
3. Add 1.8 μL 5× transcription buffer to each tube, mix, then heat to 42°C.
4. Prepare at 42°C a "master mix" that includes 10–20 U/μL Superscript II and divide it among the tubes in 8.2-μL aliquots.
5. Incubate the reactions for 60 min at 42°C, followed by 15 min at 75°C.
6. Tubes can then be stored up to several days at –20°C prior to PCR amplification.

Sham RT reactions lacking only the mutant mRNA were also assembled with each reaction set for use with tubes assembled to calibrate the PCR.

3.7. PCR Primer Selection

20–25-bp primers were selected, with a bias toward those with the greatest predicted melting temperatures (65–85°C) *(24)*. Two nested pairs of primers were chosen for each cDNA target. The second primer pair binds to sites on the target sequence that are internal to those bound by the first primer pair. Both pairs span at least one splice-site junction, as well as the site used to generate the insertion mutations (*see* **Note 4**). The μ1-receptor primers span exons 2 and 3 of the game *(25)*. The GPD primers span exons 5–8 *(26)*. All primers used in these experiments are listed.

μ1-opioid receptor
outer pair:
μ1R 215–238 (+): 5'- GCG ACT GCT CAG ACC CCT TAG CTC -3'
μ1R 1089–1112 (–): 5'- TCT GGA ATC GTG ATC AGC GCT TTG -3'
$T_a^{OPT} = 55.2$
inner pair:
μ1R 574–597 (+): 5'- GGA ACA TGG CCC TTC GGA ACC ATC -3'
μ1R 840–863 (–): 5'- TAC CAG GTT GGG TGG GAG AAC GTG -3'

T_a^{OPT} = 54.2
GPD
cloning pair:
GPD 5–28 (+): 5'- CTG CTC CTC CCT GTT CTA GAG ACA -3'
GPD 1243–1267 (–): 5'- TGC AGC GAA CTT TcT aGA TGG TAT T -3'
T_a^{OPT} = 54.2
outer pair:
GPD 335–358 (+): 5'- TGG TGC TGA GTA TGT CGT GGA GTC -3'
GPD 918–941 (–): 5'- AGA ATG GGA GTT GCT GTT GAA GTC -3'
T_a^{OPT} = 54.3
inner pair:
GPD 464–487 (+): 5'- GGG TGT GAA CCA CGA GAA ATA TGA -3'
GPD 681–704 (–): 5'- AGC ACC AGT GGA TGC AGG GAT GAT -3'
T_a^{OPT} = 52.8
κ1-opioid receptor
outer pair:
κ1R 835–858 (+): 5'- GAT AGT CCT TGG AGG CAC CAA AGT -3'
κ1R 1300–1323 (–): 5'- CTC TGG CGC TCC ATT CGC ATC TTA -3'
T_a^{OPT} = 52.4
inner pair:
κ1R 886–909 (+): 5'- CTC CTT GCA GTT TCC TGA TGA TGA -3'
κ1R 1076–1099 (–): 5'- TGC AAC CAC TAC CAG CAC CAG CTT -3'
T_a^{OPT} = 51.7
PpTKβ,γ
outer pair:
TKα,β,γ 193–212 (+): 5'- AAA TTA TTG GTC CGA CTG GT -3'
TKα,β,γ 487–506 (–): 5'- GGG TTT ATT TAC GCC TTC TT -3'
T_a^{OPT} = 47.8 (for ppTKβ)
inner pair(s):
TKα,β,γ 242–265 (+): 5'- CCG GAG CCC TTT GAG CAT CTT CTT -3'
TKβ,γ, 445–468 (–): 5'- CTT CTT TCA TAA GCC ACA GAA TTT -3'
TKα,β 316–338 (+): 5'- CAA ACG GGA TGC TGA TTC CTC AA -3'
TKγ   319–337 (+): 5'- ACG GGA TGC TGG GCA TGG T -3'
TKα,β 390–413 (–): 5'- TTC TTT CAT AAG CCA TTT TGT GAG -3'
T_a^{OPT} = 48.1, 46.0, 40.3 (primers 1 and 2, 2 and 3, and 2 and 4, respectively)
ppSOM
outer pair:
SOM 23–46 (+): 5'- TCG TCT CTG CTG CCT GCG GAC CTG -3'
SOM 64–87 (+): 5'- CCA CCG CGC TCA AGC TCG GCT GTC -3'
SOM 363–386 (–): 5'- TGG CTG GGT TCG AGT TGG CAG ACC -3'
T_a^{OPT} = 59.0 (both pairings)

inner pair:
SOM 100–123 (+): 5'- GAT GCT GTC CTG CCG TCT CCA GTG -3'
SOM 290–309 (–): 5'- GGC TCC AGG GCA TCG TTC TC -3'
$T_a^{OPT} = 57.2$

3.8. PCR Protocol

The protocol routinely detects as few as 1–5 target molecules. The primers bind sites of both stuffer fragment insertion and at least one splice junction. The amplification, therefore, distinguishes native transcript products from those of the mutant sequence and from possible contaminating genomic sequences. Sequencing PCR products generated from a heterogeneous cDNA stock further confirms the identity of the bands.

The nested reaction strategy, which employs two successive rounds of PCR amplification to generate visible ethidium-stained PCR products, enhances both the sensitivity and specificity of amplification. The first PCR round can be assembled as a "multiplex" reaction, provided that compatible primers have been designed, to amplify several nucleotide targets at once.

Example protocol:

1. 2–10 µL aliquots of each RT reaction are included tubes containing a reaction mixture that totals 20–50 µL for a 25-cycle first-round PCR.
2. Amplify 1-µL aliquots of the first PCR round in a second-round 17–24 cycle (17 cycles for GPD, 24 cycles for opioid receptors) PCR.

Reactions are cycled in a Perkin-Elmer 2400 thermal cycler. The first PCR amplification utilizes thermal intervals of 5 s at 98°C, 30 s at 54.4°C, and 2 min at 70°C, cycled 25 times. Typical parameters include 17–24 cycles with steps of 98°C for 5 s, 54°C for 30 s, and 70°C for 2 min. For the second amplification round, annealing temperature ranges from 48–56°C. Cycle numbers range from 17 for GPD to 24 for the µ opioid receptor. In both amplification rounds, the extension time is lengthened to 5 minutes for the first five cycles, and to 10 min for the final cycle. For the first amplification round, primers are included in PCR solution at 200 n*M*, nucleotides at 150 µ*M* (substituting dUTP for dTTP) (*see* **Note 5**). For the second, primer concentration is 500 n*M*, nucleotides are 250 µ*M*. The PCRs use a modified *Taq* polymerase developed by Wayne M. Barnes and designated Klentaq1 (KT1) *(10,11)* (*see* **Note 6**).

3.9. Competitive PCR Optimization

Reaction parameters were varied to identify wild-type:mutant pairs and amplification conditions for which equal numbers of the targets generates equimolar PCR products. In general, pH, Mg^{2+}, salt (K^+), TMAC, DMSO, nucleotide, and primer concentration influence the efficiency of PCR amplification. Tris-HCl concentration varies with pH because the optimization para-
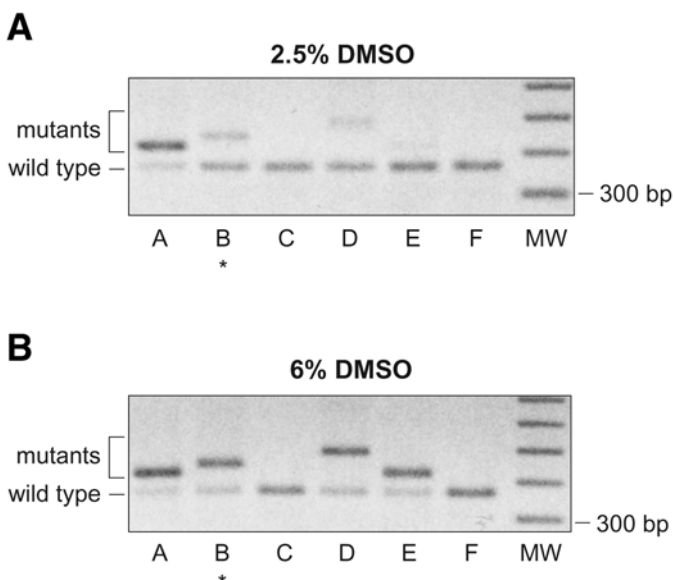
Fig. 7. Relative amplification efficiency depends upon DMSO concentration. To identify a mutant preprosomatostatin that is amplified with the same efficiency as the wild type, six candidate mutants (A–F) were paired with the wild type, at equal concentrations (1000 molecules each, per tube), and PCR amplified. The products were examined after amplification with 2.5% (**A**) or 6% DMSO (**B**). DMSO concentration profoundly affects PCR amplification efficiency. In cases A, D, and E, DMSO has the ability to reverse the relative amplification efficiency. Mutants A–F, respectively, represent insertions of 50, 88, 150, approx 150, 50, and 200 bp. Mutant B was selected as the competitor sequence for single cell amplifications because the relative amplification efficiency was least sensitive to DMSO concentration, but could still be intentionally reversed if desired. Cycle conditions: 94°C, 30 s; 58.4°C, 30 s; 72°C, 5 min (5 cycles); then 94°C, 30 s; 58.4°C, 30 s; 72°C, 90 s (30 cycles). Inverted image of EtBr-stained agarose gel.

digm involves adding 1 *M* Tris-HCl base to the standard 28 m*M* Tris-HCl, pH 8.4 (23°C) buffer. The identity of the sequence insertion and DMSO concentration have the greatest effect on relative amplification efficiencies, and these parameters were routinely varied to find conditions where wild-type and mutant were amplified with equal efficiency (*see* **Fig. 7**), (*see* **Note 7**).

3.10. Gel Electrophoresis and Analysis of PCR Products

Products of the second PCR amplification were combined with 6X gel-loading buffer, loaded onto a 1.0–1.3% agarose/Synergel (Diversified Biotech) gel,

and subjected to electrophoresis. The gel was stained with ethidium bromide and photographed under UV illumination. Photographs were digitized using a Hewlett-Packard ScanJet Plus scanner. Band intensities were quantified using ImageQuant v1.2 software (Molecular Dynamics). Calibration controls include seven tubes containing a fixed concentration of mutant sequences and variable concentrations of wild-type sequences, spanning the predicted range of cellular cDNA concentrations. For each wild-type:mutant pair, ratios of the PCR product band intensities are plotted against ratios of the corresponding initial target concentrations. Polynomial equations (of order 2–5) are fit to these plots and used to interpolate initial cellular wild-type mRNA concentrations for each of the target sequences. In the case of GPD, a second mRNA mutant was included in the reactions, enabling measurement of both GPD mRNA and cDNA for each cell. Results for GPD were used to estimate the efficiency of RT for each cell, which was then used to calculate mRNA concentrations for each of the target sequences.

3.11. Quantitative Measurements are Based on the Internal Controls

3.11.1. Quantifying the PCR

Mutant cDNAs in the PCR provide internal controls confirming successful amplification in each tube. The calibration ladder takes advantage of this internal control to make possible the measurement of initial cDNA concentrations of the corresponding wild-type sequences. The accuracy and reproducibility of the calibration ladder defines and limits the accuracy of single-cell measurements. To address this issue, the ladder was assembled multiple times to demonstrate that the calibration curves generated from it reproducibly distinguish twofold differences in the initial concentration of wild-type sequences.

For the experiments illustrated in **Fig. 8**, the ladder was assembled in triplicate in a single amplification reaction, then the products were separated by agarose gel electrophoresis (**A**). The reaction consisted of a series of tubes containing wild-type GPD cDNA ranging from zero to 2000 molecules per tube, in 2 to 2.5-fold increments. Each wild-type concentration was represented three times in the reaction. Each tube also contained 500 molecules of a mutant GPD cDNA, distinct from the wild-type sequence by the presence of 85-bp of inserted sequence. The mutant was amplified by the same primers and reaction conditions, and was therefore subject to the same tube-to-tube variations, as was the wild-type cDNA. This reaction set was then reassembled, amplified, and electrophoresed two additional times. For each gel, the ratio of intensities of the product bands was then plotted as a function of the initial concentrations of the target sequences (**B**).
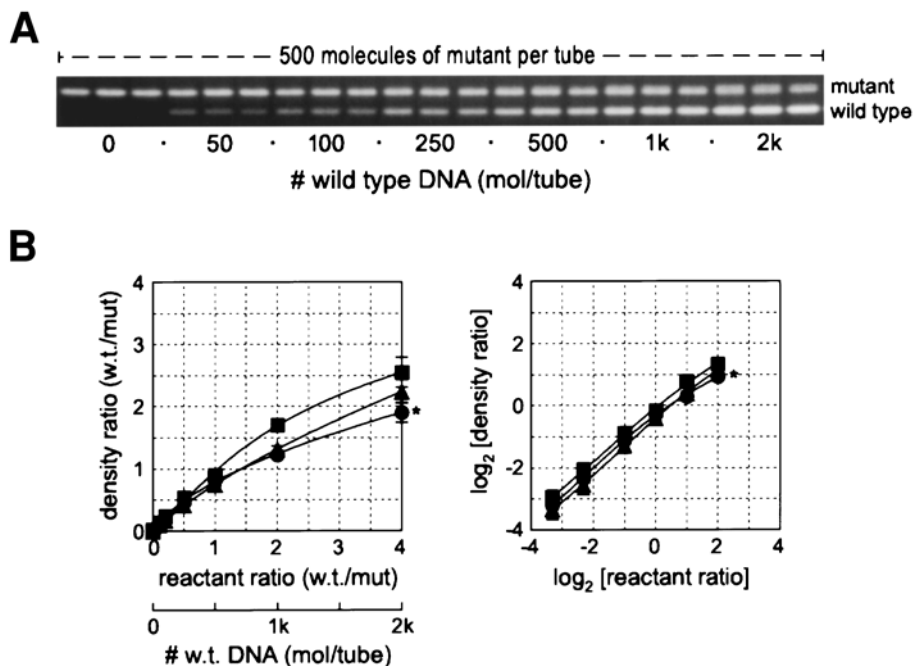
Fig. 8. Double band calibration series repeated in triplicate. (**A**) To assess the validity of using the calibration ladder to quantify cDNA concentrations, the series was assembled in triplicate in a single amplification reaction, then the products were separated by agarose gel electrophoresis. The reaction consisted of a series of tubes containing 0, 50, 100, 250, 500, 1000, or 2000 wild-type GPD cDNA, assembled in triplicate. Each tube also contained 500 molecules of a mutant GPD cDNA, distinct from the wild-type sequence by the presence of 85 bp of inserted sequence. The reaction set was then reassembled, amplified, and electrophoresed two additional times. (**B**) For each gel, the ratio of intensities of the product bands is plotted as a function of the initial concentrations of the target sequences, using both linear and logarithmic plots. Polynomial fits (of order 2–5) of the plotted points reveal smooth curves relating the ratio of band intensities to initial wild-type concentrations. Asterix and filled circles: data corresponding to the gel in (**A**). Discussed in **Subheading 3.11.1** and **Note 7**.

Polynomial fits (of order 2–5) of the plotted points reveal smooth curves relating the ratio of band intensities to initial wild type concentrations. For each gel, twofold differences in wild-type concentration are easily distinguishable throughout the range of wild-type concentrations. That is, the band intensity ratios for each concentration remain separated by at least one, if not two, standard deviation(s) from adjacent wild-type concentration steps. The curves do vary in value and shape from one reaction, or gel, to the next. Nevertheless, the

plots for a given dilution series are smooth and predictable, confirming that the concentration-band ratio curve can be accurately calibrated with the 7-tube concentration ladder included with each PCR. Plots on a linear scale additionally show moderate curvature, indicating that the ratio of band intensities saturates at high concentrations of the wild-type sequence. The effective range of accurate quantification is therefore limited to wild type concentrations that are less than ten times the concentration of the mutant competitor sequence (*see* **Note 8**).

3.11.2. Quantifying the RT Reaction

In principle, we can monitor the efficiency of each RT and PCR by including two competitor sequences in each tube: one as mRNA, the other as DNA. How do the product band intensity ratios relate to the initial concentrations of the target sequences when three compete with one another in the amplification reaction? **Figure 9** illustrates these relationships for the calibration of GPD amplification. Fixed concentrations of two GPD mutants compete with a dilution series of the wild-type sequence. As for **Fig. 8**, the ladder was assembled in triplicate in a single amplification reaction. In this case, Mutant 1 was the same GPD mutant used in the experiments described in **Subheading 3.11.1.** (*see* **Fig. 8**). It was present in the same concentration of 500 molecules per tube. Mutant 2 was a second GPD cDNA mutant that contains 268 bp of inserted sequence. It was also included at a concentration of 500 molecules per tube. After PCR, the products were separated by agarose gel electrophoresis (**Fig. 8A**). This reaction set was then reassembled, amplified, and electrophoresed two additional times. For each gel, the three possible pairings of product band intensities were plotted as a function of the initial target sequence concentration (B–D).

Polynomial fits (of order 2–5) of the plotted points again reveal smooth curves relating the ratio of band intensities to initial wild-type concentrations. Plots of both the Wild-Type:Mutant 1 and Wild-Type:Mutant 2 pairs are strikingly similar to the Wild-Type:Mutant plot of **Fig. 8**. The Wild-Type:Mutant 1 pairing of this figure is identical to the pairing of **Fig. 8**. The similarity of the plots for this pairing in these two figures argues that the presence of a third competitor sequence does not affect the competition, in terms of the product ratios, between a given pair of sequences. For these pairings, in each gel, two-fold differences in wild-type concentration produce easily distinguishable ratios of PCR products. Again, these plots saturate at high wild-type concentrations, limiting the quantifiable range to wild type concentrations that are less than ten times the concentration of the mutant competitor sequence.

The Mutant 1:Mutant 2 ratio, by contrast, remains virtually invariant, and near unity, over the range of wild-type concentrations tested. This plot demonstrates that the ratio of two PCR products again remains unaffected by the presence of a third competitor sequence, even though this third competitor reduces
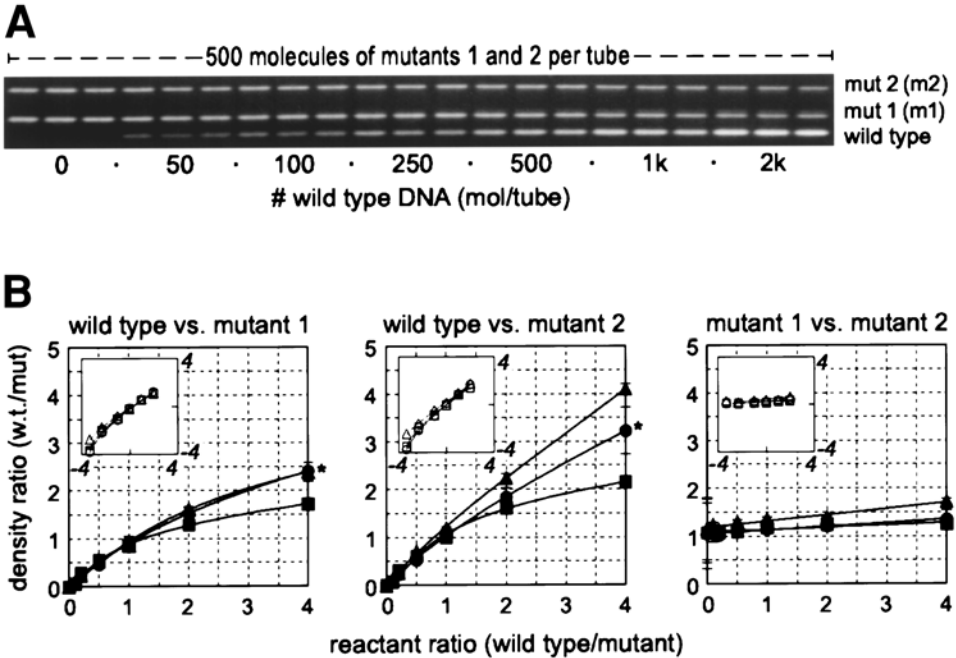
Fig. 9. Triple-band calibration series repeated in triplicate. Fixed concentrations of two GPD mutants compete with a dilution series of the wild type sequence. As for **Fig. 8**, the ladder was assembled in triplicate in a single amplification reaction, then the reaction was reassembled two times. Mutant 1 is the same GPD mutant used for the experiments of **Fig. 8**. It was present in the same concentration of 500 molecules per tube. Mutant 2 is a second GPD cDNA mutant that contains 268 bp of inserted sequence. It was also included at a concentration of 500 molecules per tube. (**A**) After PCR, the products were separated by agarose gel electrophoresis. (**B**) For each gel, the three possible pairings of product band intensities are plotted as a function of the initial target sequence concentration. Insets are plots of the data on symmetrical logarithmic axes (i.e., range –4 to 4 on both axes). Polynomial fits (of order 2–5) of the plotted points again reveal smooth curves relating the ratio of band intensities to initial wild type concentrations, strikingly similar to those for **Fig. 8**, arguing that the presence of a third competitor sequence does not affect the competition between a given pair of sequences. Asterix and filled circles: data corresponding to gel in (**A**). Discussed in **Subheading 3.11.2.** and **Note 7**.

the amount of PCR product generated from the other two sequences. In this case, the wild-type concentration varies from zero to four times the concentration of the other two sequences (*see* **Note 9**).

3.12. Sample Expression Profiles

3.12.1. GPD mRNA in Sensory Neurons

Figure 10 illustrates how the calibration ladder is used to quantify GPD cDNA and mRNA concentrations for individual harvested cells. Here, 500 molecules of Mutant 1 were included in each of the reaction tubes. In the calibration ladder, each tube also contained 500 molecules of Mutant 2 cDNA. The dilution series utilized the same wild-type GPD concentrations used in the two previous experiments. The reaction included a series of tubes, represented by Lanes A–J of the gel, containing half the products of reverse transcription from single harvested cells (**A**).

Prior to PCR there was no information indicating the amount of wild-type GPD cDNA (or the preceding mRNA) contained in each of Tubes A–J. However, plotting the ratio of Wild-Type:Mutant 1 band intensities against the initial Wild-Type concentration generates a smooth calibration curve. From the gel, Wild-Type:Mutant 1 ratios can be calculated for each of Lanes A–J, and the corresponding initial wild-type cDNA concentration can be obtained by interpolation along the calibration curve.

A similar strategy is used to calculate the initial mRNA concentrations from which the cDNA concentrations derive. In this case, Mutant 2 was the relevant competitor sequence. The corresponding plot of band intensity ratio against wild type concentration appears on the right side of **B**. Again, measuring the initial wild-type mRNA is a matter of calculating the ratio of Wild-Type:Mutant 2 band intensities and interpolating along the Wild-Type:Mutant 2 calibration curve. Note that Wild-Type mRNA concentrations are scaled fourfold upward, relative to the corresponding cDNA concentrations. This revision of the axis is required because the Mutant 2 cDNA in the cell harvest tubes derives from 2000 molecules of mRNA, compared to the 500 molecules of Mutant 2 cDNA used for the calibration ladder. In other words, these plots formally track how the ratio of wild-type to mutant PCR products varies as a function of the ratio of initial concentrations of the wild-type and mutant sequences. Because a fixed concentration of the mutant sequence was included in every tube, multiplying the initial ratio of target sequences by the initial concentration of mutant sequence (here, 2000 molecules of Mutant 2), yielded the corresponding initial Wild-Type concentration (*see* the calculation for Cell A in **C**).

Both cDNA and mRNA concentrations of GPD were calculated for each cell. Therefore, the efficiency of reverse transcribing GPD in each tube can be calculated by dividing the cDNA concentration by the corresponding mRNA concentration. By using these figures as an estimate of the overall RT efficiency in each tube, the concentrations of other cDNA sequences can be converted to the corresponding mRNA concentrations for each of the harvested cells.
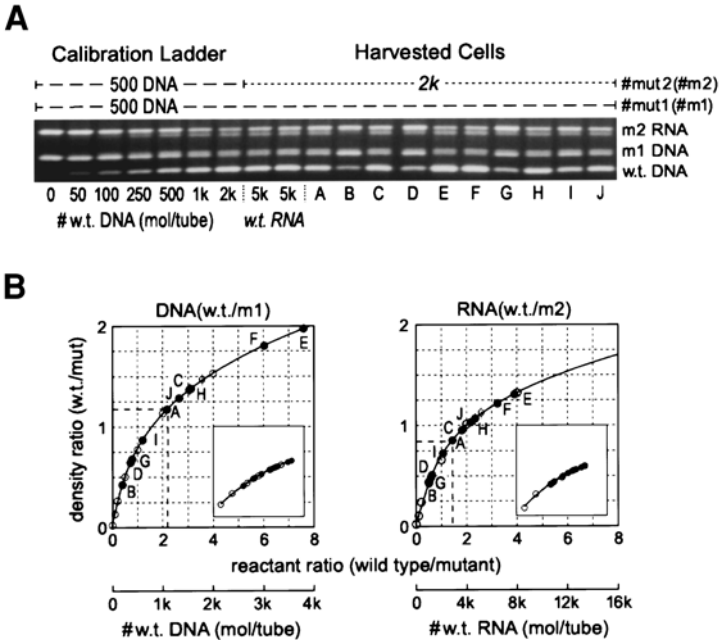
Fig. 10. Cell harvests and GPD amplification with DNA and RNA mutants. **(A)** Application of the RT-PCR technique to quantify GPD expression in single harvested neurons, labeled A–J. **(B)** Calibration curves, identical to those plotted in **Figs. 8** and **9**, are plotted using the ratios derived from the band intensities of the calibration series (open circles). From the gel, Wild-Type Mutant 1 ratios are calculated for each of Lanes A–J, and the corresponding initial wild-type cDNA concentrations are obtained by interpolation along the cDNA calibration curve (left plot). The corresponding wild type mRNA concentrations are obtained interpolating Wild-Type Mutant 2 ratios along the mRNA calibration curve (right plot). Insets are plots of the data on symmetrical logarithmic axes (i.e., range –4 to 4 on both axes). Note the fourfold adjustment of the mRNA abcissa, reflecting wild type mRNA competing with 2000 Mutant 2 mRNA, compared to WildType cDNA competing with only 500 Mutant 2 cDNA. (C) Calculations for Cell A GPD mRNA and RT efficiency are illustrated. Both cDNA and mRNA concentrations of GPD are calculated for each cell. Therefore, the efficiency of reverse transcribing GPD in each tube can be calculated by dividing the cDNA concentration by the corresponding mRNA concentration. By using these figures as an estimate of the overall RT efficiency in each tube, the concentrations of other cDNA sequences can be converted to the corresponding mRNA concentrations for each of the harvested cells. Discussed in **Subheading 3.12.2.** and **Note 7**.

3.12.2. Sensory Neuron Expression Profiles

The RT efficiency calculated from GPD amplifications can be used to convert the cDNA concentrations of several gene products to the corresponding cellular mRNA concentrations. **Table 1** illustrates this procedure applied to μ1-receptor and GPD amplifications pictured in **Fig. 3**. In the case of μ-receptor amplification, one fifth of each RT was used as the starting material. Absence of a wild-type sequence indicates that RT of a given cell generated fewer than 10 μ-receptor cDNA molecules (5× the lowest detectable cDNA concentration, two molecules per tube). For cells corresponding to Wild-Type positive lanes, RT yielded μ-receptor cDNA concentrations ranging from 20 molecules in Cells C, L, and N to 100 molecules in Cell F. RT efficiencies were calculated from the GPD amplifications and were used to convert measurements of μ-receptor cDNA to the corresponding concentration of receptor mRNA present in each cell.

For GPD, one-tenth of each RT was used as the starting material. PCR band intensities correspond to 40–1200 GPD cDNA molecules per tube, equivalent to 400 to 12k cDNA molecules per cell. For example, similar Wild-Type: Mutant 1 product ratios were generated both from 250 Wild-Type cDNA molecules in the calibration ladder and from Cell F (220 molecules, interpolating along the curve fit to the values generated by the calibration tubes). Thus, RT generated 2200 cDNA molecules from Cell F. Examining the Wild-Type: Mutant 2 product ratios, by contrast, reveals that the initial ratio of mRNAs for Cell F is most similar to that for the calibration tube containing 500 wild-type GPD molecules. The initial ratio of Wild Type:Mutant 2 molecules for this tube is 1. For Cell F, an initial Wild-Type:Mutant 2 mRNA ratio of 1.1 matches the observed ratio of the PCR product bands. Because the initial Mutant 2 mRNA concentration was 1000 molecules per tube, Cell F contributed 1100 mRNAs to the tube. Multiplying this value by 10 (because only one-tenth of the cell was amplified) yields 11,000—the total number of wild-type GPD mRNA molecules contained in Cell F. Dividing 2200 cDNAs by 11,000 mRNAs gives an RT efficiency of 0.2 for Cell F. Thus, in this tube, one cDNA was generated from every 5 mRNAs.

In this reaction set, one amplifiable cDNA was generated from every 3–7 GPD mRNA molecules (this was a low RT efficiency relative to the experiments of **Fig. 4**. This is a low RT efficiency). At the time of cell harvest, microscopic observation revealed questions about the health of the cell or the quality of the harvest in each of Cells A, D, and G. The poor to absent yield of wild-

Table 1
GPD and μ-Receptor Data for Cells Depicted in Fig. 3

Cell	Avg Diam (μm)	Vol ×10⁴ (μm³)	GPD				μ1-Opioid Receptor		
			cDNA (#/cell)	mRNA (#/cell)	[RNA] (pM)	RTEff (dna/rna)	cDNA (#/cell)	mRNA (#/cell)	[RNA] (pM)
20k rGPD	n/a	n/a	4224	19,241	n/a	0.220	1	6	n/a
20k rGPD	n/a	n/a	5078	24,410	n/a	0.208	0	−1	n/a
A	36.25	2.49	382	1292	86	0.296	−1	−2	−0.2
B	37.50	2.76	2732	14,428	868	0.189	1	8	0.5
C	35.00	2.24	11,724	88,967	6,581	0.132	21	158	11.7
D	32.50	1.80	363	1494	138	0.243	1	3	0.3
E	37.50	2.76	5671	28,403	1708	0.200	48	240	14.4
F	36.25	2.49	2238	11,320	754	0.198	98	495	33.0
G	38.75	3.05	850	2509	137	0.339	17	49	2.7
H	38.75	3.05	1300	7047	384	0.185	2	11	0.6
I	42.50	4.02	2854	14,340	592	0.199	1	7	0.3
J	28.75	1.24	1831	7427	991	0.246	30	120	16.0
K	36.25	2.49	2403	12,326	821	0.195	74	379	25.3
L	28.75	1.24	2702	11,690	1560	0.231	20	86	11.5
M	26.25	0.95	1918	7,263	1273	0.264	3	11	1.9
N	40.00	3.35	6963	48,063	2382	0.145	20	137	6.8
sham	n/a	n/a	86	244	n/a	0.351	2	5	n/a

type GPD PCR product confirmed these doubts. Therefore, the μ/R amplifications, as well as the κ/R, ppTK, and ppSOM amplifications, may have produced false negatives for Cells A and D, and an artificially low cDNA concentration for Cell G.

Successful harvest of sensory neurons consistently yields several thousand GPD mRNA molecules. Even at low RT efficiencies, GPD amplification easily confirms sucessful cell harvest. The sensitivity of the amplification protocol can be increased by amplifying a larger portion (up to 10 μL, or 50%) of the RT reaction. Provided μ-receptor and GPD mRNA are reverse transcribed with similar efficiency, absent μ-receptor cDNA in a successfully harvested cell indicates that the cell contained fewer than 10–30 μ-receptor mRNAs (*see* **Note 10**).

3.13. Signatures of Three Artifacts

Three failures, those of cell harvest, RT, and PCR constitute false negatives of RT-PCR at the single-cell level. The controls included in these experiments generate unique signatures that characterize each of these artifacts and distinguish them from examples where cells genuinely fail to transcribe a selected message sequence. They take advantage of expression of the housekeeping gene *GPD*. Its constitutive and abundant expression in numerous tissues (*see* **Note 11**) is repeated at the single-cell level, but over a wide concentration range, spanning 5–50 k molecules per cell. A failed cell harvest lacks endogenous GPD PCR product, as in **Fig. 3**, where Lanes A and D fail to generate a wild-type GPD PCR product band. RT failure prevents both top and bottom bands. PCR failure eliminates all bands. Conversely, the presence of all three bands confirms that harvest, RT, and PCR were successful in a given tube and ratios of the intensities of these three bands can be used to calculate the RT efficiency for each reaction tube. Combining measurements of RT efficiency and threshold detection limits defines a true negative as the failure to transcribe a given sequence above a specific number of mRNA molecules per cell.

Single-cell RT-PCR has suffered from the absence of controls that identify both false positives, and particularly, false negatives. These experiments present techniques to solve these problems, as well as quantify single-cell nucleic acid concentrations. They explicitly distinguish legitimate absent gene expression from the failures of cell harvest, RT, and PCR. The results, expressed as mRNA molecules per cell, explicitly define both the resolution of each experiment and gene expression levels in each cell. Amplification of GPD mRNA is explored and confirmed as an excellent test for successful cell harvest. Sensory neurons express a mean GPD mRNA concentration of 1.03 ± 0.61 n*M*.

4. Notes

1. Mutants are generated by insertion of small DNA fragments (50–300 bp) into a unique restriction site of the cloned endogenous cDNA sequence. These "stuffer fragments" are inserted for two reasons. First, mutant and endogenous PCR products differ in size and are, therefore, more easily distinguishable and quantifiable via standard agarose gel electrophoresis and ethidium staining than are wild-type mutant pairs that differ only by the presence or absence of a single restriction site. Second, mutant sequences with increased length are usually at least as difficult to amplify as the corresponding endogenous sequence. Thus, reaction conditions that successfully amplify the mutant should also amplify the native sequence. However, the many exceptions to this generalization favor the generation of several mutants and then optimization of reaction conditions to determine which of them amplify with similar efficiency as the wild-type sequence.
Sites located near an intron splice junction are chosen so that PCR amplification spans both mutation and splice junction locales. Compatible restriction site-stuffer fragment pairs contain "sticky ends" with complementary overhangs. For example, the frequent-cutting enzyme *Sau*3AI generates the same 5'-GATC overhang as do the enzymes *Bam*HI, *Bgl*II, and *Bcl*I. Standard cloning vectors, such as pBSSK- are a convenient source of stuffer fragments. Digestion of pBSSK- with Sau3AI generates numerous fragments between 50 and 300 bp (75, 78, 105, 219, and 258 bp). Mutants are generated by inserting the fragments into a unique *Bam*HI, *Bgl*II, or *Bcl*I site in the cDNA. When the gene lacks a *Sau*3AI-compatible site, one is created by inserting an appropriate linker into the endogenous sequence, as employed in the construction of GPD mutants.

2. Explicit harvest of the entire cell differs from previous reports which cite that fractions of cells are collected and amplified *(1–5)*. Carrying the cell soma through the interface removes debris (including undesired cells) that often coat and remain loosely attached to the desired cell, as illustrated in the sequence of photos in **Fig. 2**. Explicit observation of the harvest through the interface is strongly recommended, since harvest failure can account for examples of apparent poor gene expression (cf. **Fig. 3**, Cells A, D, and possibly G). Conversely, aspiration of the entire cell is discouraged because the accompanying variable amounts of bath solution can inhibit RT (*see* later), as well as contribute contaminating RNases or exogenous mRNA molecules.

3. In principle, random hexamer priming limits the number of amplifiable cDNA products because some of the transcribed fragments fail to span both PCR primer binding sites. Conversion to amplified cDNA can depend on how much sequence lies between the poly A tail and the location of the reverse (i.e., 3', antisense) primer. Thus, PCR primer choice and use of random hexamers vs oligo-dT primers can affect the apparent efficiency of measured RT and should be considered in using results from housekeeping gene amplification to estimate the transcription efficiency of other sequences. For the targets amplified in these experiments, there was no significant difference in RT efficiency between the two priming

methods. RT using random hexamer primers may generate a cDNA pool that is more representative of the mRNA source, because RT using oligo-dT primers is, in principle, more susceptible to failures caused by the secondary structure of specific mRNA targets. Whenever possible, we also choose PCR primers located at least a few hundred basepairs from either end of the full-length mRNA sequence.

4. We used the program OLIGO v5.0 (National Biosciences, Inc.) to select PCR primers. This program selects primer pairs with minimal intra- or intermolecular complementarity or PCR target false priming sites. TKα,β,γ 193-212 (+), TKα,β,γ 487-506 (–), and SOM 290-309 (–) were synthesized at the Washington University Protein Chemistry Laboratory. All other primer sequences were synthesized by Oligos Etc. (Wilsonville, OR). Labels indicate: 1) the targeted sequence; 2) the sequence positions of the corresponding positive strand, relative to the transcription start site; and 3) whether the primer corresponds to the positive or negative strand of the target sequence. Several preprotachykinin (substance P and neurokinin A precursor) primers catalyze amplification of two or more of the α,β, and γ splice variants *(19)*. In these cases, position numbers refer to the β sequence. T_a^{OPT} is the predicted optimal PCR annealing temperature calculated by OLIGO and is based on formulas outlined by Baldino et al. *(27)* and Rychlik et al. *(24)*.

5. The original experiments were designed to amplify DNA using dUTP as a substitute for dTTP and the reaction mixture was treated with the enzyme uracil DNA glycosylase (UDG) prior to the first amplification round. In theory, this practice eliminates the contamination of reactions with carryover products of previous reactions *(28)*. In practice, even a heat cycle of 95°C for 15 min fails to completely inactivate UDG. Because the remaining UDG degrades the products of PCR amplification in a temperature-sensitive manner, this enzyme was excluded from subsequent experiments. All reactions carry at least one sham tube lacking wild-type sequences. No evidence of PCR carryover contamination has been observed despite elimination of UDG from the experiments.

6. With the Klentaq1 enzyme preparation and buffer formula, KCl concentrations above 15 m*M* inhibit the amplification reaction. Because the RT buffer contains 75 m*M* KCl, first-round PCR volumes were adjusted so that the RT reaction products constituted less than 20% of the PCR volume. PCR volumes can be increased to 50 μL without significantly altering the amplification characteristics. Depending on the anticipated abundance of the cDNA target, each tube should receive 1–10 μL (5–50%) of an RT as the starting material for the first-round PCR.

7. DMSO concentration and the identity of the inserted stuffer fragment often profoundly influence the amplification efficiency of the mutant, relative to the native sequence. Whether a given stuffer fragment enhances or inhibits PCR amplification varies with the target sequence into which it is inserted, and more subtly, with the orientation of its insertion, as well as the primer pair used for amplification. Fortunately, a variety of mutants containing stuffer fragments of different

sequence and orientation can easily be tested against a range of DMSO concentrations (0–10%) to identify mutants and reaction conditions where both sequences amplify with equal efficiency.

Variation of DMSO concentration against a panel of mutants is an easy way to find a wild-type mutant pairing where two competing targets are amplified equivalently. For example, Lanes B, D, and E of **Fig. 7** illustrate that the relative efficiency of amplifying native and mutant ppSOM sequences is reversed when the DMSO concentration is changed from 2.5% to 6%. By including an equivalently amplified mutant as a calibration standard within each reaction set, endogenous target concentrations can be quantified against this standard, using product ratios arising from single sample amplifications.

The internal calibration ladder circumvents the requirement for a linear conversion of PCR product into digitized band intensities. The ladder explicitly defines the correlation of digitized product ratios with template concentrations for each reaction set. Template concentrations can also be routinely ascertained by eye to within a twofold error, easily distinguishing the presence or absence of a particular gene product in individual cells.

8. The calibration method can be further improved by applying autoradiographic techniques to the PCR. Cycle numbers could be reduced, thereby avoiding heteroduplex formation and reducing, perhaps even elimitating, the curvature of the calibration plots. Moreover, phosphorimaging equipment could be utilized to measure the radioactivity of the PCR products. This approach offers a greater range over which intensity measurements vary linearly with the concentration of the molecules contained within the band. Nonetheless, the protocols designed for the experiments presented here provide accurate, rapid, and inexpensive calibration over more than two orders of magnitude. They can be easily implemented and applied to a wide range of experiments requiring quantification of nucleic acid concentrations contained in tissue samples as small as a fraction of a cell.

Real time PCR offers an alternative, and now increasingly popular, method of quantitative PCR *(29)*. Advantages include ease of implementation and a wide quantitative range. However, this method provides less reliable detection of small numbers of cDNA molecules *(30)*, and would be at a serious disadvantage detecting mRNAs, such as receptor message sequences, that often remain scarce in individual neurons (a few to a few hundred per cell). The method described here also does not assume or require that wild type and competitor sequences are amplified with equal efficiency. Instead, a calibration ladder is created for every PCR. This technique has a more limited dynamic range compared to real time PCR, but offers more accurate quantification (easily within a factor of two).

9. Gel-to-gel variation of the shape of the calibration curve underscores the need for including the calibration ladder with each PCR. The calibration plot is smooth and predictable over more than three orders of magnitude of the initial wild-type concentration. Nonetheless, the plots show significant curvature as the wild-type concentration exceeds the mutant concentration by 5–10-fold. That is, the ratio of PCR products staturates for initial wild-type mutant concentration ratios above

10 or 20. This curvature indicates that the measured product ratios deviate significantly from those predicted for an ideal PCR. Ideally, the product ratio vs the ratio of initial target concentrations, plotted on either linear or logarithmic scales should be linear, with a slope of one. The following equations illustrate this prediction mathematically:

$$R_{out} = A_{out}/B_{out} = [A_{in}(E_A)^N] / [B_{in}(E_B)^N] \quad \text{when } E_A = E_B; R_{out} = A_{in}/B_{in} = R_{in}$$

$$\log R_{out} = \log R_{in} + (N)\log E_A/E_B \quad \text{when } E_A = E_B; \log R_{out} = \log R_{in}$$

Here, A and B correspond to wild-type and mutant sequences, respectively. A_{in} and B_{in} are the initial concentration of sequences A and B. A_{out} and B_{out} are the concentrations of the PCR products. R_{in} and R_{out} are the initial and product A/B concentration ratios, respectively. E_A and E_B are the PCR efficiencies for sequences A and B, respectively. N is the number of cycles of the PCR. The efficiency is defined as 2 for an ideal PCR, where each cycle doubles the amount of target sequence. The plots rely on two assumptions. 1) Each band represents a single sequence; and 2) The intensities of the photographed PCR bands (integrals of the band density across the area of the band) are proportional to the product concentration. When $E_B = E_B$, plots on both linear and log scales are linear with a slope of one and intercept at the origin.

Two conditions–saturation of the PCR and saturation of the gel photograph–can distort the shape of the plots. The first condition arises because PCR amplification is ultimately limited by the primer concentration. When the concentration of target sequences is high and the primer concentration has dwindled, additional PCR cycles fail to augment the concentration of PCR products. This can be seen in **(A)** of **Figs. 8–10**, where high concentrations of the wild-type sequence actually reduce the amount of mutant product generated, so that the total product concentration plateaus. Because this phenomenon affects both sequences equally (effectively by reducing N, the cycle number) plots on both linear and logarithmic scales remain linear. However, when primer concentrations dwindle, heteroduplexes form. That is, native and mutant sequences complex with each other during the PCR annealing step. On a gel, heteroduplexes typically migrate at a rate between those of the wild-type and native sequences, usually very close to that of the mutant sequence, as appears in **Fig. 10**. This phenomenon becomes most prominent at wild-type sequence concentrations that exceed the concentration of the mutant by several fold. The heteroduplex band is often difficult to separate from the mutant band. Therefore, both bands are usually incorporated into the measurement of the mutant band intensity. For wild-type A and mutant B, the measured R_{out} is less than the actual concentration ratio A_{out}/B_{out} when $A_{in} >> B_{in}$. In the extreme, all of B_{out} is bound as heteroduplex, effectively doubling the measured B_{out}. The linear scale R_{out} vs R_{in} plot shifts to follow the equation $R_{out} = [A_{in}(E_A)^N] / [B_{in}(E_B)^{N+1}]$, whereas the log scale plot shifts to $\log R_{out} = \log R_{in} + (N)\log E_A/E_B - \log E_B$. For $E_A = E_B = 2$, as A_{in} increases, the slope of the linear plot declines from one to one-half, whereas a base 2 logarithmic plot shifts

from tracing a straight line through the origin to a line through negative one. Both the linear and logarithmic plots in **(B)** of **Fig. 10** reveal curvature consistent with the appearance of the mutant-heteroduplex doublet that appears with higher concentrations of the wild-type sequence.

The second condition, saturation of the photograph of the gel, also occurs at high concentrations of the native sequence. At high concentrations of the wild-type sequence, the photograph fails to reveal increasing concentrations of the PCR product. In the extreme, the measured A_{out} plateaus above a certain band intensity. That is, the measurement of $[A_{in}(E_A)^N]$ no longer changes with increases in A_{in}. Therefore, R_{out} plateaus, causing both linear and log scale plots to plateau. This effect would not influence the value of B_{out}, so the mutant band should appear at the same intensity across all concentrations of A_{in}. Adjusting film exposure settings helps control this problem. When saturation of the photo is a problem, reducing exposure times reduces the curvature of the corresponding plots. Typically, photographs are taken at several exposure settings. Several of the images are digitized and the band intensity ratios are plotted. Images for which exposure times are maximized without increasing the curvature of the plots are selected for further analysis. Overall, the problem of photograph saturation limits the usable calibration range to between two and three orders of magnitude for the concentration of wild-type sequences.

A third issue, differential amplification efficiencies of the competitor sequences, also influences the intensity of the product bands but does not contribute to curvature in the calibration plots. The slope of the linear scale plot and the ordinate-intercept of the logarithmic scale plot reflect the relative amplification efficiences of the two sequences. Considering the problem of saturating the photograph, maximum calibration ranges can be achieved by selecting wild-type mutant pairs for which PCR amplifies both sequences equally, or slightly favors the mutant sequence.

10. Is GPD a good "housekeeping" gene at the level of individual cells? Sometimes transcription levels can be compared between cells by simply measuring the number of mRNA molecules of a particular gene in each cell. When the comparison groups contain cells that vary significantly in size, however, normalizing transcript content to cell volume is necessary so that concentrations can be compared. Alternatively, the content of a particular transcript can be normalized to the expression of a housekeeping gene. Ideally, the housekeeping gene is expressed as a consistent fraction of the total mRNA. As a first step to addressing the utility of GPD as a housekeeping gene, transcription of GPD mRNA was measured in a population of 49 cells. GPD content is plotted as a function of cell volume in **(A)** of **Fig. 11**. Frequency histograms of GPD mRNA concentration and reverse transcription efficiency are assembled in **(B)** and **(C)**, respectively. The plot in **A** clearly indicates that GPD mRNA content increases with increasing cell volume. Considerable variation is also apparent. Several points in the plot are displaced from the trend line. Similarly, GPD concentration shows an approximately normal distribution, with a mean of 1.03 n*M*; but the 0.61 n*M*
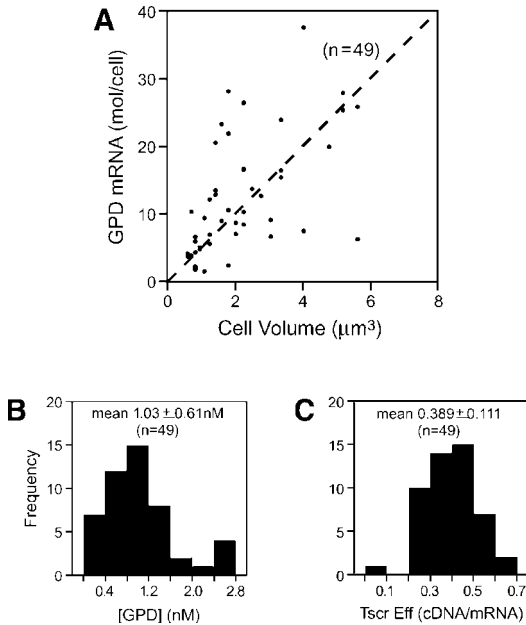
Fig. 11. GPD mRNA levels and RT efficiency for 49 sensory neurons. (**A**) The number of GPD mRNA molecules per cell were measured as described in the text and illustrated in **Fig. 10**. The scatter plot considers the relation between mRNA content and spherical volume, based on the average diameter oberved under the microscope at ×200 magnification. The dashed line represents a best linear fit of the data (constrained to intersect the origin). (**B**) Cellular GPD concentrations were obtained by dividing mRNA content by volume. The frequency histogram bins the data in 0.4 nM increments to assess the distribution of cellular concentration values. Concentration measurements for these 49 sensory neurons have a mean of 1.03 nM with a 0.61 nM standard deviation. (**C**) The histogram of corresponding RT efficiencies displays a mean of 0.389 with a 0.111 standard deviation, indicating that, on average, 1 GPD cDNA was generated for every 2.5 GPD mRNA molecules in these experiments.

standard deviation represents a significant fraction of this mean.

Some of this variation may represent variable quality of the cell harvests. Weighing against this interpretation: 1) the cells were harvested under explicit microscopic observation; 2) the time between attaching the harvest pipet to the cell, carrying it through the air-liqid interface, and expelling it onto the frozen primer mix was consistently kept to 1–2 min; and 3) anytime the harvest quality was questioned, the data was discarded. In sum, much of the variability of the GPD measurement may legitimately reflect biologic variation of GPD expression. Therefore, normalizing gene transcription to GPD levels could introduce additional noise into the data.

Volume may be the most suitable normalization parameter. Three common sources of experimental error, however, contribute to noise in this measure. 1) Cells are not perfect spheres; 2) simple measures of cell diameter remain imprecise; and 3) incomplete cell harvest reduces the actual volume analyzed. For 1 and 2, a twofold volume error requires measurement errors exceeding 25% in the estimate of cell radius (diameter; $1.26^3 = 2$). At ×200 each division of the microscope measuring graticule corresponds to 5 µm. Repeat measures, as well as multiple observer measurements, though, always are in agreement to within 0.5 div (10% error for 25 µm cell diameter—the vast majority of cells in our preparations have diameters between 20–45 µm). Incomplete harvests, such as, loss of the cell at the air-liquid interface, are easily excluded by directly observing cell recovery with the microscope.

Despite the variation of cellular GPD content and concentration, amplification of this housekeeping gene provides excellent confirmation of successful cell harvest. All cells for which the harvest quality was considered good (*n*=49 in these experiments, over 200 in other experiments) contain easily detectable concentrations of GPD mRNA.

Variation in RT efficiency can introduce experimental noise into the measurement of cDNA concentrations. RT efficiency typically ranges from 0.3–0.5 (mean 0.389 ± 0.111). Occasional reactions drop to 0.15–0.25, as illustrated by the **Fig. 3** and **Table 1** reaction set. Because RT efficiency can be measured explicitly, converting measurements of cDNA concentrations to the corresponding mRNA concentrations reduces experiment scatter.

11. GPD continues to be the most popular control or housekeeping gene used in studies comparing gene expression levels. In addition to the cell-to-cell variability of expression levels observed in this study, several recent reports emphasize that all commonly used endogenous controls display considerable variation in their expression levels *(31–33)*. Therefore, measurements of relative expression levels must be interpreted with extreme caution when based solely on normalizing data to the expression of endogenous control sequences.

Acknowledgment

References

1. Lambolez, B., Audinat, E., Bochet, P., Crepel, F., and Rossier, J. (1992) AMPA receptor subunits expressed by single Purkinje cells. *Neuron* **9,** 247–258.

2. Eberwine, J., Yeh, H., Miyashiro, K., Cao, Y., Nair, S., Finnell, R., et al. (1992) Analysis of gene expression in single live neurons. *Proc. Natl. Acad. Sci. USA* **89,** 3010–3014.

3. Smith, M. A. and O'Dowd, D. K. (1994) Cell-specific regulation of agrin RNA splicing in the chick ciliary ganglion. *Neuron* **12,** 795–804.

4. O'Dowd, D. K., Gee, J. R., and Smith, M. A. (1995) Sodium current density correlates with expression of specific alternatively spliced sodium channel mRNAs in single neurons. *J. Neurosci.* **15,** 4005–4012.

5. Sucher, N. J. and Deitcher, D. L. (1995) PCR and patch-clamp analysis of single neurons. *Neuron* **14,** 1095–1100.

6. Becker-Andre, M. and Hahlbrock, K. (1989) Absolute mRNA quantification using the polymerase chain reaction (PCR). A novel approach by a PCR aided transcript titration assay (PATTY). *Nucl. Acid. Res.* **17,** 9437–9446.

7. Gilliland, G., Perrin, S., Blanchard, K., and Bunn, H. F. (1990) Analysis of cytokine mRNA and DNA: detection and quantitation by competitive polymerase chain reaction. *Proc. Natl. Acad. Sci. USA* **87,** 2725–2729.

8. Gilliland, G., Perrin, S., and Bunn, H. F. (1990) Competitive PCR for quantitation of mRNA, in *PCR Protocols: A Guide to Methods and Applications* (Innis, M. A., Gelfand, D. H., Sninsky, J. J., and White, T. J., eds.), Academic,/Harcourt Brace Jovanovich, San Diego, CA, pp. 60–69.

9. Silbert, S. C., Beacham, D. W., and McCleskey, E. W. (2003) Quantitative single cell differences in μ-opioid receptor mRNA distinguish myelinated and unmyelinated nociceptors. *J. Neurosci.* **23,** 34–42.

10. Barnes, W. M. (1992) The fidelity of Taq polymerase catalyzing PCR is improved by an N-terminal deletion. *Gene* **112,** 29–35.

11. Barnes, W. M. (1994) PCR amplification of up to 35-kb DNA with high fidelity and high yield from λ bacteriophage templates. *Proc. Natl. Acad. Sci. USA* **91,** 2216–2220.

12. Taddese, A., Nah, S. Y., and McCleskey, E. W. (1995) Selective inhibition of small nociceptors. *Science* **270,** 1366–1369.

13. Eckert, S. P., Taddese, A., and McCleskey, E. W. (1997) Isolation and culture of rat sensory neurons having distinct sensory modality. *J. Neurosci. Meth.* **77,** 183–190.

14. Tso, J. Y., Sun, X. H., Kao, T. H., Reece, K. S. and Wu, R. (1985) Isolation and characterization of rat and human glyceraldehyde-3-phosphate dehydrogenase cDNAs: genomic complexity and molecular evolution of the gene. *Nucl. Acid Res.* **13,** 2485–2502.

15. Thompson, R. C., Mansour, A., Akil, H., and Watson, S. J. (1993) Cloning and pharmalogical characterization of a rat opioid receptor. *Neuron* **11,** 903–913.

16. Bunzow, J. R., Zhang, G., Bouvier, C., Saez, C., Ronnekleiv, O. K., Kell, M. J., et al. (1995) Characterization and distribution of a cloned rat μ-opioid receptor. *J. Neurochem.* **64,** 14–24.

17. Meng, F., Xie, G.-X., Thompson, R. C., Mansour, A., Goldstein, A., Watson, S. J., et al. (1993) Cloning and pharmacological characterization of a rat κ opioid receptor. *Proc. Natl. Acad. Sci. USA* **90,** 9954–9958.

18. Hjorth, S. A., Thirstrup, K., Grandy, D. K., and Schwartz, T. W. (1995) Analysis of selective binding epitopes for the kappa-opioid receptor antagonist nor-binaltorphimine. *Mol. Pharm.* **47,** 1089–1094.

19. Krause, J. E., Chirgwin, J. M., Carter, M. S., Xu, Z. S., and Hershey, A. D. (1987) Three rat preprotachykinin mRNAs encode the neuropeptides substance P and neurokinin A. *Proc. Natl. Acad. Sci. USA* **84,** 881–885.

20. MacDonald, M. R., McCourt, D. W., and Krause, J. E. (1988) Posttranslational procesing of α-, β-, and γ-preprotachykinins. Cell-free translation and early post-translational processing events. *J. Biol. Chem.* **263,** 15,176–15,183.

21. Montminy, M. R., Low, M. J., Tapia-Arancibia, L., Reichlin, S., Mandel, G., and Goodman, R. H. (1986) Cyclic AMP regulates somatostatin mRNA accumulation in primary diencephalic cultures and in transfected fibroblast cells. *J. Neurosci.* **6,** 1171–1176.

22. Kyrozis, A. and Reichling, D. B. (1995) Perforated-patch recording with gramici-din avoids artifactual changes in intracellular chloride concentration. *J. Neurosci. Meth.* **57,** 27–35.

23. Tajima, Y., Ono, K., and Akaike, A. N. (1996) Perforated patch-clamp recording in cardiac myocytes using cation-selective ionophore gramicidin. *Am. J. Physiol.* **271,** C524–C532.

24. Rychlik, W., Spencer, W. J., Rhoads, R. E. (1990) Optimization of the annealing temperature for DNA amplification in vitro. *Nucl. Acid. Res.* **18,** 6409–6412.

25. Pan, Y.-X., Xu, J., Bolan, E., Abbadie, C., Chang, A., Zuckerman, A., et al. (1999) Identification and characterization of three new alternatively spliced μ-opioid receptor isoforms. *Mol. Pharmacol.* **56,** 396–403.

26. Ercolani, L., Florence, B., Denaro, M., and Alexander, M. (1988) Isolation and complete sequence of a functional human glyceraldehyde-3-phosphate dehydro-genase gene. *J. Biol. Chem.* **263,** 15,335–15,341.

27. Baldino, F. J., Chesselet, M.-F., and Lewis, M. E. (1989) High-resolution *in situ* hybridization histochemistry. *Meth. Enzymol.* **168,** 761–777.

28. Longo, M. C., Beringer, M. S., and Hartley, J. L. (1990) Use of uracil DNA glycosylase to control carry-over contamination in polymerase chain reactions. *Gene* **93,** 125–128.

29. Heid, C. A., Stevens, J., Livak K. J., and Williams, P. M. (1996) Real time quan-titative PCR. *Genome Res.* **6,** 986–994.

30. Tkatch, T., Baranauskas, G., and Surmeier, D. J. (2000) Kv4.2 mRNA abundance and A-type K(+) current amplitude are linearly related in basal ganglia and basal forebrain neurons. *J. Neurosci.* **20,** 579–588

31. Matyas, J. R., Dingqiu, H., and Adams, M. E. (1999) A comparison of various "housekeeping" probes for northern analysis of normal and osteoarthritic articu-lar cartilage RNA. *Connect. Tiss. Res.* **40,** 163–172.

32. Suzuki, T., Higgins, P. J., and Crawford, D. R. (2000) Control selection for RNA quantitation. *Biotechniques* **29,** 332–337.

33. Stürzenbaum, S. R. and Kille, P. (2001) Control genes in quantitative molecular biological techniques: the variability of invariance. *Comp. Biochem. Physiol. Pt. B* **130,** 281–289.

11

Gene Arrays and Proteomics

A Primer

Lionel Moulédous and Howard B. Gutstein

1. Introduction

In recent years, molecular biology has increasingly focused on how cellular effectors are modulated by the environment and, in turn, modulate each other to control cellular functions. In the opioid field, we concern ourselves both with signaling mechanisms within cells and the functions of neural circuitry in mediating the behavioral effects of opioids. All of these mechanisms identified to date have proven to be extremely complex, suggesting that behavioral outcomes mediated by opioids are dependent on the interactions of multiple gene products. Opioid-mediated behavioral outcomes such as tolerance, dependence, and addiction may reflect problems in the regulation of complex biological and emotional functions. From this, it follows that slight alterations in the expression or function of individual genes that still fall within the "normal" range could lead to pathological effects or behaviors. Genetic polymorphisms cause changes in the coding and regulatory regions of genes. Thus, in addition to changes in levels of protein expression, encoded proteins may have slightly different functions or undergo differential regulation in cells.

Whereas scientists have been aware of these complex interactions for some time, most previous studies have evaluated specific target genes or proteins in isolation. The main reason for this approach has been that the technologies to examine multiple targets in parallel have not been available or lacked robustness. In recent years, multiple approaches to this problem have been

developed. In this chapter, we will focus on gene array or "gene chip" tech-
nologies for the parallel evaluation of genomic changes, and 2-dimensional gel
electrophoresis (2 DE)-based technologies for the evaluation of changes in pro-
tein expression and function.

2. Gene Arrays
2.1. Array Systems

There are two main types of gene array systems currently available: EST/
cDNA arrays and oligonucelotide arrays, also known as "gene chips" *(1)*. ESTs,
or expressed sequence tag arrays, involve the use of several hundred nucle-
otide sequences complementary to mRNAs endcoding cellular proteins *(2)*.
ESTs represent the portion of the genome expressed in cells, not regulatory or
other noncoding portions of the genome. The array is a glass slide spotted with
sense strand ESTs. This allows hybridization to the complementary
("antisense") cDNA strands produced by creating complementary DNA
(cDNA) strands from mRNA expressed in the sample being studied. The array
density is limited by the ability of the robotic system employed to accurately
spot ESTs and the analysis system to read and analyze the resultant data.

Oligonucleotide arrays involve the use of 10–20 base oligos spotted on a
glass base *(3)*. The best known of these arrays are the "gene chips" produced
by Affymetrix Corporation. The glass base is treated so it can bind single nucle-
otides. Stepwise on-chip synthesis of oligos is performed using modifications
of photolithographic techniques *(4)*. The shorter sequences used on gene chips
are more susceptible to hybridization mismatch, but as discussed later, can be
useful for the analysis of genetic polymorphisms.

2.2. Uses of Gene Arrays

Gene arrays can be used to address two main types of questions: differential
gene expression in different tissues or under different conditions, and analysis
of differences in genetic sequence of specific target genes. Evaluation of dif-
ferences in gene expression is accomplished by taking pools of mRNA from
samples of interest and transcribing them into cDNA with a fluorescent label
incorporated. Radioactive probes are less practical and far less commonly used
(2). Probes with different fluorescence characteristics are used to identify dif-
ferent samples. The cDNA pools are then applied to the chip and hybrids
allowed to form. The resultant hybrids are then scanned with a laser confocal
scanning microscope system that can detect and quantitate the fluorescent sig-
nal over the chip. In some cases, pairwise comparison of samples is done on a
single chip in an effort to minimize interchip and interspot variability. These
techniques have been successfully applied in neurobiology, for instance, in

identifying genes enriched in specific subregions of the amygdala *(5)* and comparing strain-specific gene expression in various regions of the mouse brain *(6)*.

Determining differences in specific gene sequences can be accomplished using a technique called sequencing by hybridization *(2,4)*. Oligonucleotide chips are designed to cover specific sequences in proteins of interest, for example, using 10 base oligo "windows" surrounding each nucleotide in the gene of interest. For each nucleotide, four spots will be placed, one with the correct base, and the other three with each of the other three bases substituted. If there is a mutation, hybridization to the "wrong" spot will be observed. This procedure is then repeated for each nucleotide in the sequence. In this way, single nucleotide polymorphisms (SNPs) can be determined for differing samples or populations. This technique is extremely relevant to the science of "pharmacogenomics," or the determination of individual variations in drug response *(4)*.

2.3. Issues in Evaluation of Array Data

The vast amount of data produced by array experiments has led to the development of increasingly sophisticated statistical techniques for data analysis *(7)*. New developments in matrix analysis and the development of clustering algorithms, covariate analysis, and pattern recognition have proven useful in identifying genes or clusters of genes that are differentially regulated under differing circumstances *(7–9)*. Technical issues such as normalization of data to common standards and the linearity and reproducibility of the hybridization signal also have been addressed in increasing detail. Background variation, variation in uniformity of spot intensity, and variation between arrays are other issues being addressed statistically *(2,4,7)*. There also appears to be a great deal of variation in hybridization of the same sequence in different arrays. Replication of hybridization experiments, although more expensive and requiring greater sample quantities, provides the best method of accounting for these individual variations, increasing statistical power, and providing increased confidence in the interpretation of results *(8,10)*.

2.4. Other Methods of Parallel Gene Analysis

1. Differential Display (DD-PCR). In this technique, complex ("degenerate") mixtures of PCR primers are used to amplify all mRNAs in a sample pool, and the amplified PCR products are displayed on agarose gels *(11)*. Although this technique is technically straightforward, a large amount of sequencing and cloning of sequences of interest is required, and nonspecific amplification artifacts are also a major confounding factor. PCR-based amplification is supposedly quantitative, but this is not always so.
2. Serial Analysis of Gene Expression (SAGE). SAGE involves the transcription of mRNA pools into cDNA *(12,13)*. The resultant cDNA is then subjected to a

restriction digest that produces 10 base "tags" from each mRNA. These tags are then linked together (concatenated) and placed into cloning vectors. Sequencing is performed, and the relative abundance of each fragment reflects its abundance in the initial mRNA pool. This technique, as the other alternatives presented, does not require preexisting knowledge of sequences of interest, thus enabling the discovery of novel genes. However, this technique is very labor intensive, requiring a vast amount of cloning, ligation, and sequencing reactions.

3. Subtractive Hybridization. Subtractive hybridization, or "subtractive cloning," permits the detection of upregulated mRNAs in a sample of interest *(14)*. An mRNA pool is generated from a sample of interest, and converted into a cDNA library. mRNA from a control sample is then added in excess, and the resultant hybrids removed by physical means. This process can be repeated several times to improve specificity. The remaining cDNAs are then characterized. This technique is biased toward genes that are dramatically upregulated, and is also quite labor intensive.

2.5. Comparison with Microarray Technologies

In comparison with the other techniques described above, microarrays have a much higher throughput and have much lower technical and experimental demands upon the scientist. At some institutions, gene arrays are run as core facilities, further reducing the experimental load. However, the investigator still must have enough knowledge of the technique and statistical methodology to intelligently interpret the data provided by the core. Array techniques also require that you know all of the sequences of interest, which does not enable the discovery of new genes. However, with the completion of genome projects and improvement in high-density array technologies, it should soon be possible to study all genes expressed in a genome using array technology, minimizing this disadvantage. The cost of array experiments, especially when using commercial systems, can be quite high. However, accessing core facilities can reduce this cost substantially.

3. 2-DE-Based Proteomic Approaches

As genomic sequences are completed, the nature of questions asked and studies proposed will change. Our focus will change to obtain a better understanding of the structure, function, interactions, and regulation of the resultant proteins. This is where the field of proteomics will take us. Proteomics, as we are defining it for this discussion, is the global analysis and comparison of cellular proteins *(15)*. Genomics and proteomics can be used to provide complementary information. Genomic approaches provide an accurate picture of transcriptional regulation inside the cell, whereas proteomics focuses on translational regulation (i.e., protein expression levels, as well as the characterization of posttranslational modifications). Genomic studies are technically

simpler, as the detection complexity for four bases is much less than for 20 amino acids and their associated post-translational modifications. Also, the detection sensitivity of genomic studies is greater because of the ability to use PCR to amplify transcripts of interest. However, proteomic studies target proteins, the actual working units of cells, thus providing a more accurate picture of the physiological state of the cell. Recent studies have shown that there can be poor correlation between changes in mRNA and protein expression in cells *(16,17)*, providing further justification for pursuing these more difficult and laborious studies.

The field of proteomics has expanded considerably during the last few years, and that term is used to cover a broad range of studies ranging from descriptive mapping of all cellular proteins to functional studies that determine specific changes induced by various pharmacological agents or disease states *(18–20)*. In addition, proteomic studies can be designed to investigate the changes in subcellular localization of proteins and to determine protein–protein interactions. Proteomics can also be applied to the study of signal transduction and long-term protein modifications induced by opioids on cell lines or nervous tissue.

This overview describes a general proteomic strategy that can be divided into four steps: extraction of proteins from cells of interest, separation of the extracted proteins, identification of the separated proteins, and informatic cataloging and analysis of the data obtained. This strategy provides a framework within which various techniques and emerging technologies can be evaluated. Although this review focuses mainly on a combination of techniques we have successfully employed, other techniques may be more suitable for the specific goals of each investigator.

3.1. Protein Extraction

Whatever the starting material, proteins must first be extracted from the tissue and solubilized. Detergents classically used for preparation of one-dimensional sodium dodecyle sulfate-polyacrylamide gel elecrophoresis (SDS-PAGE) electrophoresis samples often cannot be used because isoelectric focusing (IEF), the first step of 2-DE, which is commonly used to separate extracted proteins (see later), is not compatible with high salt concentrations. Alternative solubilization methods have been developed *(21)* that take advantage of the use of chaotropic agents (e.g., Urea 5-7 M, Thiourea 2 M) and nonionic or zwitterionic detergents such as sulfobetaine (CHAPS, SB 3-10, 2–5%). Samples previously prepared in a buffer containing high salt content (e.g., Tris-base to facilitate protein solubilization and minimize proteolysis) must be diluted before focusing. One strategy is to precipitate the proteins with trichloroacetic acid or acetone and resuspend them in an IEF compatible buffer *(22)*. In addition to salts, nucleic acids present in the sample also interfere with

IEF and can be removed by addition of protease-free endonuclease *(23)*. Commercially available carrier ampholyte cocktails (0.2–2%) can also be added to the sample buffer in order to facilitate the IEF process. Protease inhibitors should also be used during the extraction process to prevent protein degradation. Different separation techniques may have different requirements for solubilization conditions. Solubilization protocols also need to be adapted to subsequent separation ("arraying") techniques.

Satisfactory protein solubilization can be achieved with cultured cells by using chaotropic agents- and detergent-containing lysis buffer for 1 h at room temperature with occasional vortexing. When working with tissue, additional disruption methods such as mechanical homogenization or sonication may be needed.

Once the proteins are solubilized, it is necessary to reduce and alkylate the samples in order to avoid disulfide bridging between or within proteins. Dithiothreitol (DTT, 20–100 mM) or Tributylphosphine (TBP, 2–5 mM) are commonly used for reduction, whereas iodoacetamide (15 mM) or acrylamide (10 mM) are used for alkylation.

We mentioned previously that the goal of proteomics is the global analysis of cellular proteins. In order to be global, the analysis method should be able to separate the 15,000 to 30,000 proteins postulated to be expressed in a given cell *(24)*. No currently available separation technology possesses this degree of resolution *(20)*. Therefore, samples need to be simplified to improve protein detection *(25,26)*.

Subcellular fractionation methods (ultracentrifugation with or without density gradients, immunoisolation, flow cytometry) can be used to isolate and study cellular organelles *(27)*. However, these methods often require much more starting material than the methods outlined below. Another way to reduce the complexity of the sample is to extract proteins sequentially without targeting a specific cellular compartment *(28)*. Various commercial kits are available to sequentially extract proteins in increasingly stronger solubilization solutions (Sigma, St Louis, MO, and BioRad, Hercules, CA). Cytosolic hydrophilic proteins are first extracted in a buffer containing no detergent. Detergent-soluble proteins are then extracted in one or two steps in IEF compatible detergent-containing buffers. In addition to simplifying the sample, these methods enable enrichment in membrane proteins in detergent-containing fractions. Membrane proteins can be hard to solubilize using a one-step whole-cell extraction procedure.

3.2. Protein Separation

The goal of protein separation in proteomic studies is to permit the separation and subsequent identification of each protein expressed in the cell. Many different technologies have been proposed in an effort to achieve this goal, including

two-dimensional electrophoresis, capillary electrophoresis (CE), and high-pressure liquid chromatography (HPLC). No currently available technology has the resolution or sensitivity to detect all the proteins expressed in a given group of cells. However, 2-DE is considered the method of choice for global mapping studies because it has the greatest resolution power (up to 10,000 protein spots on the largest gels) of any currently available technique *(29)*.

3.2.1. 2-DE

In 2-DE, cellular proteins are separated first according to their isoelectric point (p*I*) by IEF, then according to their molecular weight using conventional SDS-PAGE. In the past, the reproducibility of the gels was a major concern. However, the availability of commercial precast immobilized pH gradient (IPG) strips for first dimension separation and SDS-PAGE gels has greatly reduced this variability. pH gradients for IPG strips are created by covalent incorporation of acrylamido buffers into polyacrylamide gels on the surface of the strip. Because they are preformed and covalently linked, IPGs are much more stable, linear, and reproducible than self-forming carrier ampholyte-based gradients previously used in tube gels. The 2-DE steps (strip rehydration, IEF run, strip equilibration and SDS-PAGE run) are now straightforward and performed using manufacturer's instructions.

In addition to greater reproducibility, the IPG technology has brought many other improvements in isoelectric separation. Various IPG strip lengths (7, 11, 13, 18, and 24 cm) covering narrow (from 1 to 4 pH units) gradients can be used in order to obtain better resolution. Liquid preparative IEF that prefractionates the proteins according to their pI can be very useful to obtain full benefits from narrow pH range strips *(30)*. In liquid preparative IEF, cellular proteins are separated by p*I* and trapped in 3 to 6 compartments delimited by immobiline-containing membranes using a device known as a multicompartment electrolyzer (MCE). There are two advantages to this method. First, as with any prefractionation technique, it enables one to concentrate a specific protein fraction and thus improve detection of low abundance proteins in the fractions. Second, it facilitates first dimension focusing on narrow pH gradient immobilized pH gradient (IPG) strips by eliminating proteins that are out of the pH range of the strip. These proteins would otherwise precipitate at the edges of the strip and impair focusing of proteins of interest inside the pH range of the strip. Preparative IEF combined with the use of narrow pH gradient IPG strips is particularly useful for the separation of basic proteins that have long proven to be difficult to focus *(25)*. However, precipitation of high molecular-weight proteins (above 120–150 kDa) in the IPG strip can still be an experimental issue. This can be partially circumvented by performing IEF in tube gels or in agarose and by applying low voltages during sample loading (*see* below) *(20)*.

IPG strips need to be rehydrated before use in a buffer similar to the one used to prepare the samples. Sample can be applied to the IPG strip during the rehydration step (in-gel rehydration). The application of low voltages during in-gel rehydration can facilitate the entry of high MW proteins. Another way to apply sample is sample cup loading *(22)*. In this technique, a small cup is used to apply the sample on the surface of the previously rehydrated strip just before IEF. In-gel rehydration for at least 8 h is the method of choice except for very alkaline IPGs (>9) that might require cup-loading at the anode. Focusing conditions required for steady-state IEF are dependent on both sample content (protein load, salts, impurities) and strip characteristics (length and pH range). Total volt-hours needed for focusing will increase from 10,000 to 100,000 with increasing protein load, salt content, and IPG strip length. Conditions can be adapted for each experiment using manufacturer's guidelines and empirical results.

After IEF, the protein-containing strips are equilibrated in SDS-containing solution to improve protein transfer to the second dimension gel. Strips are equilibrated for 2×15 min in 50 m*M* Tris-HCl, pH 6.8–7.0 solution containing 2–2.5% SDS, 3–6 *M* urea, and up to 30% w/v glycerol.

The equilibrated IPG strips are then loaded on top of the SDS-PAGE gel for separation in the second dimension. Similar to IPG strips, precast SDS-PAGE gels with a large range of separating capacities are available. The acrylamide content can range from 4 to 18% depending on the size of the proteins to be separated. As a first approach, gradient gels may be preferable as they provide good separation over a wide molecular weight range. Commercially prepared gradient gels are available, thus limiting the variability caused by individual gradient-casting techniques. Most precast gels tolerate high voltage conditions that enable short running time and thus minimize protein diffusion. Vertical gel systems are preferred as they permit higher throughput and more reproducible results.

3.2.2. Alternatives to 2-DE

When analyzing simple protein mixtures, conventional one-dimensional SDS-PAGE gels may provide adequate resolution, especially when the proteins to be separated have different molecular weights *(31)*. One-dimensional electrophoresis provides the advantages of better solubilization of hydrophobic proteins, less risk of precipitation of large proteins, and less loss of acidic or basic proteins. However, a stained band on the gel may contain several proteins, thus complicating both protein identification and quantification.

Liquid separation methods using capillary electrophoresis (CE), HPLC, or a combination of both methods can also be used to separate proteins or peptides *(32)*. The current trend in non-gel-based proteomics is to digest the proteins

first using trypsin, then separate the resulting peptides. This way, fragment peptides can be analyzed on-line by direct coupling of the column to the mass spectrometer. Most methods are based on the two-dimensional LC-LC or LC-CE separation of trypic fragments. For example, multidimensional protein identification technology (MudPIT) separates a complex peptide mixture on a microcapillary column by strong cation exchange followed by reverse phase chromatography. This method has been used to identify 1484 proteins from the *S. cerevisiae* proteome *(33)*. MudPIT does not permit relative protein quantification because the intact proteins are never identified. However, some non-gel-based methods permit quantification by labeling tryptic peptides before separation. The isotope coded affinity tag method (ICAT), which uses isotopic variants of a biotin-containing moiety to differentially label peptides, is the only method that is currently commercially available (Molecular Probes) *(34)*. The two samples to be compared are digested by trypsin and covalently labeled on cysteines using ICAT reagents. One sample is labeled with light reagent (containing no deuteriums) whereas the other is labeled with heavy reagent (containing eight deuteriums). Tagged peptides are affinity isolated on avidin columns and analyzed by on-line HPLC coupled to a mass spectrometer. The ratio of the ion intensities for an ICAT-labeled pair (heavy vs light) permits relative quantification of the parent proteins. This method has the disadvantage of being biased toward cysteine containing peptides. Other nonbiased methods, such as mass-coded abundance tagging (MCAT) which labels the C-terminal lysine present in every tryptic peptide, offer promising alternatives. Developments in peptide fragment separation are of interest because peptides tend to be more soluble and easier to separate than the parent proteins *(32)*. Whereas none of these alternative systems currently has the resolving power of 2-DE, they are valuable techniques for use in specific situation such as the analysis of less complex protein mixtures.

3.3. Protein Identification

3.3.1. Visualization of Separated Proteins

Three types of stains can be used to visualize proteins on 2-D gels. Silver staining is the most sensitive technique. It is able to detect sub-ng amounts of proteins. New staining protocols, available as kits from several manufacturers, are compatible with mass spectrometric analysis because they do not modify protein side chains *(35)*. However, a disadvantage of silver staining is that the spot intensity is not linearly related to protein amount. Therefore, other techniques should be considered when accurate relative quantification of changes in protein expression is required *(36)*. New fluorescent stains (SYPRO red, orange and ruby, Molecular Probes, Eugene, OR) offer an interesting alterna-

tive to silver stains as they have similar sensitivity to mass spectrometry-compatible silver stains (1 ng), but have a much larger linear dynamic range *(36)*. In situations when the detection of low abundance proteins is not an issue, such as with preparative electrophoresis, colloidal Coomassie brilliant blue stains are still the method of choice. They have detection limits of about 10 ng, and when maximum staining is achieved, they show linear dynamic range. Coomassie stains are fully compatible with mass spectrometric analysis *(35)*.

3.3.2. Imaging of Visualized Proteins

Two types of systems are available for gel imaging: flat bed scanners and charge-coupled device (CCD) cameras *(37)*. Scanners are available for both densitometric (Silver, Coomassie stains) and fluorescent (SYPRO stains) analysis. The importance of gel imaging in proteomics is often underestimated. Image quality is critical for subsequent quantitatve analysis. For protein differential display, the consistency of both gel staining and imaging procedures are of key importance for obtaining reliable results.

Several image analysis software packages are available, some of them coupled to a gel-imaging device. In order to analyze results from a proteomic study, imaging software should be able to perform the following basic tasks: detect the spots automatically but permit manual editing, quantify and normalize basic spot parameters (intensity, volume), and automatically match several gels to compare spot parameters between various treatment groups. Other options such as the ability to construct composite images by compiling data from replicate gels or to build a full pH range artificial gel from adjacent narrow pH gels can also be very useful. Beside these analytical capacities, it is also important to evaluate the data management capacities of the software: image annotation, data displayed as tables and graphics, statistical analyses (*see* **Subheading 3.4.**).

3.3.3. Protein Identification

Mass spectrometry (MS) is the tool of choice for the identification of proteins in proteomic studies *(19)*. It is more sensitive, easier to perform and permits a higher throughput than Edman sequencing. Western blotting is another way to identify proteins, but cannot be realistically applied to all the proteins present on a 2-D gel. Recent progress in both sources and detectors have made MS more and more sensitive (subfentomole level) and accurate *(38)*. Automation of mass spectrometers has also enabled high throughput.

In mass spectrometry, charged ions are produced from a sample, then are separated based on their mass-to-charge (m/z) ratios in a mass analyzer. Ions are then detected and a plot of ion abundance vs m/z (the mass spectrum) is generated. Two MS techniques are routinely used in proteomics:

MALDI-TOF (matrix-assisted laser desorption/ionization—time of flight) mass spectrometry and ESI MS/MS (tandem electro-spray ionization) mass spectrometry *(39)*.

MALDI MS is often used as a first approach *(20)*. In this technique, laser pulses desorb and ionize peptides crystallized in a UV-absorbing matrix. The ions formed are then accelerated by an electric field toward an ion detector. Compared with ESI MS, MALDI MS is more tolerant of impurities such as salts that might be present in the sample and, thus, requires less rigorous sample preparation *(39)*. MALDI spectra are also easier to interpret because the technique generates principally singly charged ions.

Protein identification by MALDI-TOF MS is based on a technique called peptide mass fingerprinting (PMF). The first step of the protein identification process is tryptic digestion of the protein spot of interest. The resulting peptides extracted from the spot are then analyzed by MALDI-TOF MS. Commercial systems are available to automatically excise spots from the gels, perform the tryptic digestion, clean the samples, and spot the samples on the MALDI plate. The masses of the tryptic digestion fragments obtained by MS are then compared to the theoretical digestion patterns of proteins in a database. Commercial and public domain search engines are available to search databases *(20,40)*. The matching of a sufficient number of experimentally obtained peptide masses to theoretically calculated masses permits identification.

In some cases, the peptides identified by MALDI MS do not cover a large enough part of the protein to permit confident identification. In this case, additional sequence information on these proteins can be obtained by using ESI-MS/MS (for details, *see* **ref. 39**).

3.4. Informatic Cataloging and Data Analysis

As with genomics, bioinformatics is an essential component of proteomics because the experiments generate massive amounts of information. An informatics system suitable for proteomics should allow data storage and retrieval for all stages of the process: gel images, image analysis results and statistics, raw mass spectra, analyzed mass spectra, and protein identification data. Ideally, the information should be stored in a relational database to facilitate data mining interfacing with other related databases (gene array results, web-based protein and posttranslational modifications databases). The database should permit high-level queries of the stored data and result sets. These queries may be hypothesis-driven (e.g., which proteins identified as kinases show significant changes in *p*I between treated and normal samples), or not (e.g., the clustering of all proteins from a sample according to the degree of change in expression between treated and normal groups).

Such powerful informatic data management systems are being developed by corporations and other consortia. For example, the widely used Melanie 3 software (Swiss Institute of Bioinformatics), initially designed for 2-D gel analysis, has evolved to assume some of these functions. The program is capable of linking 2-D gel images to data tables, MS spectra, and in-house or web-based protein and 2-D gel databases, and is commercially available. The use of this type of software in combination with publicly accessible protein and EST databases offers a reasonable starting point for undertaking these analyses. Continued advances in bioinformatics will improve the analysis and interpretation of data generated by proteomic experiments.

References

1. Ramsay, G. (1998) DNA chips: State-of-the-art. *Nature Biotechnol.* **16,** 40–44.
2. Watson, S. J. and Akil, H. (1999) Gene chips and arrays revealed: a primer on their power and their uses. *Biol. Psych.* **45,** 533–543.
3. Marshall, A. and Hodgson, J. (1998) DNA chips: An array of possibilities. *Nature Biotechnol.* **16,** 27–31.
4. Graves, D. J. (1999) Powerful tools for genetic analysis come of age. *Tibtech* **17,** 127–134.
5. Zirlinger, M., Kreiman, G., and Anderson, D. J. (2001) Amygdala-enriched genes identified by microarray technology are restricted to specific amygdaloid subnuclei. *Proc. Natl. Acad. Sci. USA* **98,** 5270–5275.
6. Sandberg, R., Yasuda, R., Pankratz, D., Carter, T., Del Rio, J., Wodicka, L., et al. (2000) Regional and stran-specific gene expression mapping in the adult mouse brain. *Proc. Natl. Acad. Sci. USA* **97,** 11,038–11,043.
7. Hess, K. R., Zhang, W., Baggerly, K. A., Stivers, D. N., and Coombes, K. R. (2001) Microarrays: handling the deluge of data and extracting reliable information. *Trends Biotechnol.* **19,** 463–468.
8. Wu, T. (2001) Analysing gene expression data from DNA microarrays to identify candidate genes. *J. Pathol.* **195,** 53–65.
9. Brazma, A. and Vilo, J. (2000) Gene expression data analysis. *FEBS Lett.* **480,** 17–24.
10. Lee, M., Kuo, F., Whitmore, G., and Sklar, J. (200) Importance of replication in microarray gene expression studies: Statistical methods and evidence from repetitive cDNA hybridizations. *Proc. Natl. Acad. Sci. USA* **97,** 9834–9839.
11. Livesey, F. and Hunt, S. (1996) Identifying changes in gene expression in the nervous system: mRNA differential display. *Trends Neurosci.* **19,** 84–88.
12. Velculescu, V. E., Zhang, L., Vogelstein, B., and Kinzler, K. W. (1995) Serial analysis of gene expression. *Science* **270,** 484–487.
13. Velculescu, V. E. (1999) Essay: Amersham Pharmacia Biotech & Science prize. Tantalizing transcriptomes—SAGE and its use in global gene expression analysis. *Science* **286,** 1491–1492.

14. Sagerstrom, C. G., Sun, B. I., and Sive, H. L. (1997). Subtractive cloning: past, present, and future. *Ann. Rev. Biochem.* **66,** 751–783.

15. Williams, K. L. and Hochstrasser, D. F. (1997) Introduction to the proteome. In *Proteome Research: New Frontiers in Functional Genomics* (Wilkins, M. R., Williams, K. L., Appel, R. D. and Hochstrasser, D. F., eds.), Springer, Berlin pp. 1–12.

16. Gygi, S. P., Rochon, Y., Franza, B. R., and Aebersold, R. (1999) Correlation between protein and mRNA abundance in yeast. *Mol. Cell Biol.* **19,** 1720–1730.

17. Anderson, L. and Seilhamer, J. (1997) A comparison of selected mRNA and protein abundances in human liver. *Electrophoresis* **18,** 533–537.

18. Chambers, G., Lawrie, L., Cash, P., and Murray, G. I. (2000) Proteomics: a new approach to the study of disease. *J. Pathol.* **192,** 280–288.

19. Godovac-Zimmermann, J. and Brown, L. R. (2001) Perspectives for mass spectrometry and functional proteomics. *Mass Spectrom. Rev.* **20,** 1–57.

20. Naaby-Hansen, S., Waterfield, M. D., and Cramer, R. (2001) Proteomics—post-genomic cartography to understand gene function. *Trends Pharmacol. Sci.* **22,** 376–384.

21. Herbert, B. (1999) Advances in protein solubilisation for two-dimensional electrophoresis. *Electrophoresis* **20,** 660–663.

22. Gorg, A., Obermaier, C., Boguth, G., Harder, A., Scheibe, B., Wildgruber, R., et al. (2000) The current state of two-dimensional electrophoresis with immobilized pH gradients. *Electrophoresis* **21,** 1037–1053.

23. Molloy, M. P., Herbert, B. R., Williams, K. L., and Gooley, A. A. (1999) Extraction of Escherichia coli proteins with organic solvents prior to two-dimensional electrophoresis. *Electrophoresis* **20,** 701–704.

24. Hastie, N. D. and Bishop, J. O. (1976) The expression of three abundance classes of messenger RNA in mouse tissues. *Cell* **9,** 761–774.

25. Herbert, B. R., Harry, J. L., Packer, N. H., Gooley, A. A., Pedersen, S. K., and Williams, K. L. (2001) What place for polyacrylamide in proteomics? *Trends Biotechnol.* **19,** S3–9.

26. Corthals, G. L., Wasinger, V. C., Hochstrasser, D. F., and Sanchez, J. C. (2000) The dynamic range of protein expression: a challenge for proteomic research. *Electrophoresis* **21,** 1104–1115.

27. Pasquali, C., Fialka, I. and Huber, L. A. (1999) Subcellular fractionation, electromigration analysis and mapping of organelles. *J. Chromatogr. B. Biomed. Sci. Appl.* **722,** 89–102.

28. Molloy, M. P., Herbert, B. R., Walsh, B. J., Tyler, M. I., Traini, M., Sanchez, J. C., et al. (1998) Extraction of membrane proteins by differential solubilization for separation using two-dimensional gel electrophoresis. *Electrophoresis* **19,** 837–844.

29. Klose, J. and Kobalz, U. (1995) Two-dimensional electrophoresis of proteins: an updated protocol and implications for a functional analysis of the genome. *Electrophoresis* **16,** 1034–1059.

30. Herbert, B. and Righetti, P. G. (2000) A turning point in proteome analysis: sample prefractionation via multicompartment electrolyzers with isoelectric membranes. *Electrophoresis* **21,** 3639–3648.

31. Husi, H., Ward, M. A., Choudhary, J. S., Blackstock, W. P., and Grant, S. G. (2000) Proteomic analysis of NMDA receptor-adhesion protein signaling complexes. *Natl. Neurosci.* **3,** 661–669.
32. Issaq, H. J. (2001) The role of separation science in proteomics research. *Electrophoresis* **22,** 3629–3638.
33. Washburn, M. P., Wolters, D., and Yates, J. R., 3rd. (2001) Large-scale analysis of the yeast proteome by multidimensional protein identification technology. *Nat. Biotechnol.* **19,** 242–247.
34. Moseley, M. A. (2001) Current trends in differential expression proteomics: isotopically coded tags. *Trends Biotechnol.* **19,** S10–16.
35. Lauber, W. M., Carroll, J. A., Dufield, D. R., Radabaugh, M. R., and Malone, J. P. (2001) Mass spectrometry compatibility of two-dimensional gel protein stains. *Electrophoresis* **22,** 906–918.
36. Yan, J. X., Harry, R. A., Spibey, C., and Dunn, M. J. (2000) Postelectrophoretic staining of proteins separated by two-dimensional gel electrophoresis using SYPRO dyes. *Electrophoresis* **21,** 3657–3665.
37. Miller, M. D., Jr., Acey, R. A., Lee, L. Y., and Edwards, A. J. (2001) Digital imaging considerations for gel electrophoresis analysis systems. *Electrophoresis* **22,** 791–800.
38. Chalmers, M. J. and Gaskell, S. J. (2000) Advances in mass spectrometry for proteome analysis. *Curr. Opin. Biotechnol.* **11,** 384–390.
39. Yates, J. R., 3rd. (1998) Mass spectrometry and the age of the proteome. *J. Mass. Spectrom.* **33,** 1–19.
40. Fenyo, D. (2000) Identifying the proteome: software tools. *Curr. Opin. Biotechnol.* **11,** 391–395.

12

Opioid Receptor Oligomerization

Detection and Functional Characterization
of Interacting Receptors

Ivone Gomes, Julija Filipovska, and Lakshmi A. Devi

1. Introduction

Opioid receptors are members of the G-protein coupled receptor (GPCR) family characterized by the presence of seven transmembrane domains. These receptors are classified as mu (μ), delta (δ), and kappa (κ). Activation of these receptors leads to uncoupling of the inhibitory G-proteins (G_i) followed by the activation of multiple signal transduction pathways including the inhibition of adenylyl cyclase, modulation of inwardly rectifying K^+ channels or voltage-dependent calcium channels and regulation of mitogen-activated protein (MAP) kinase activity *(1–4)*.

A number of studies using a variety of techniques have demonstrated that GPCRs can associate with each other *(5,6)*. This association can be homomeric (between products of the same gene) or heteromeric (between products of distinct genes). The latter can involve associations with closely related proteins (members belonging to the same subfamily) or distantly related proteins (members belonging to distinct subfamilies). In this chapter, we describe the various steps involved in the detection and characterization of interactions between opioid receptors. These involve biochemical detection via immunoprecipitation and Western blot analysis and in vivo detection using a biophysical technique such as bioluminescence resonance energy transfer (BRET). In addition, we discuss assays to characterize the pharmacological, signaling, and trafficking properties of these receptors that could be altered because of these interac-

tions. We also provide some suggestions about precautions to be taken and controls to be used in these experiments.

2. Materials

2.1. General Materials

1. 10-cm dishes (Becton Dickinson, San Jose, CA).
2. 30% acrylamide/*bis*-acrylamide solution (Sigma Chemical Company, MO).
3. [^{3}H]diprenorphine, [^{3}H]DAMGO, [^{3}H]deltorphin II (Perkin-Elmer Life Sciences, Inc., Boston, MA).
4. BCA assay reagent (Pierce, Rockford, IL).
5. Cyclic adenosine monophospate (cAMP) antisera (Biomedical Technologies, Inc., Stoughton, MA).
6. *c-myc* polyclonal antibody (Santa Cruz Biotechnology, CA).
7. Dulbecco's modified Eagle's medium (DMEM; Gibco/BRL, Rockville, MD).
8. Fetal bovine serum (FBS; Gibco/BRL).
9. GraphPad Prism 2.0 (GraphPad Software, San Diego, CA).
10. HA polyclonal antibody (Santa Cruz Biotechnology).
11. Human embryonic kidney (HEK-293) cells (American Type Culture Collection, Rockville, MD).
12. NIH image software (Version 1.62).
13. Penicillin-streptomycin (Gibco/BRL).
14. Ponceau S (Sigma Chemical Company).
15. Protease inhibitor cocktail (Sigma Chemical Company).
16. Protein A beads (Sigma Chemical Company, MO).
17. PROTRAN nitrocellulose membranes (Schleicher and Schuell, Keene, NH).
18. SuperSignal Chemiluminescent Substrate mix (Pierce, Rockford, IL).
19. Trypsin-ethylenediamine tetraacetic acid (EDTA) (Gibco/BRL).
20. Vectors for *RLuc* fusion, pR*Luc*-N1, -N2, and -N3, (Perkin-Elmer Life Sciences Inc.).
21. Whatman GF/B filters (Schleicher and Schuell).
22. X-ray films (Eastman Kodak Company, NY).
23. YFP fusion vector (pEYFP-N1; Clontech, Palo Alto, CA).

2.2. Cell Culture

HEK-293 cells were grown in 10-cm dishes in 10 mL growth medium (DMEM containing 10% FBS and 0.2 mL of penicillin-streptomycin solution). When cells were 70% confluent, the media was discarded and cells were treated with 1 mL of trypsin-EDTA for 1 min at 37°C. Cells were resuspended in 10 mL PBS and a single-cell suspension was made by trituration. For long-term storage, cells were centrifuged at 1000*g* for 3 min. The cell pellet was frozen in liquid nitrogen after the addition of 1 mL DMEM containing 20% FBS and 10% dimethyl sulfoxide (DMSO). Every 3 mo, one frozen vial was thawed,

centrifuged at 1000*g* for 3 min, supernatant discarded and the pellet suspended in 1 mL growth media, and added to 10-cm plates containing 9 mL growth media.

2.3. Transient Transfection

1. HeBS 2×: Dissolve 16.4 g NaCl, 11.9 g HEPES acid, 0.21 g Na_2HPO_4 in 1 L of water. Titrate exactly to 7.05 pH with 5 *M* NaOH and filter sterilize. Store in 10 mL aliquots at –20°C.
2. Calcium chloride (2.5*M*): Filter sterilize a 2.5 *M* stock solution. Store in 10 mL aliquots at –20°C.
3. cDNA solutions: Ethanol precipitate Flag-, *myc*- or HA-tagged plasmid cDNA to make it sterile and resuspend in sterile double distilled water at a concentration of 1 mg/mL. Store in aliquots at –20°C.
4. Glycerol (10%): Prepare a 10% solution in DMEM. Filter sterilize and store at room temperature.
5. PBS 1×: Dissolve 8 g NaCl, 0.2 g KCl, 1.44 g Na_2HPO_4, and 0.24 g KH_2PO_4 in 1 L of water. Adjust the pH with 1*N* HCl to 7.4. Filter sterilize and store at room temperature.

2.4. Cell Lysis

1. Buffer G: 50 m*M* Tris-Cl, pH 7.4, containing 300 m*M* NaCl, 1% Triton X-100, 10% glycerol, 1.5 m*M* $MgCl_2$, and 1 m*M* $CaCl_2$. Store at 4°C.
2. RIPA buffer: 50 m*M* Tris-Cl pH 8.0, containing 150 m*M* NaCl, 1% NP40, 0.5% sodium deoxycholate, 0.1% sodium dodecyl sulfate (SDS), and 1 m*M* $CaCl_2$. Store at 4°C.
3. NP40 buffer: 10 m*M* Tris-Cl, pH 8.0, containing 1% NP40, 150 m*M* NaCl, 1 m*M* EDTA, 10% glycerol, and 1 m*M* $CaCl_2$. Store at 4°C.
4. CHAPS buffer: 1% CHAPS in 50 m*M* Tris-Cl, pH 7.4. Store at 4°C.
5. Dodecyl maltoside buffer: 0.5% dodecyl maltoside in 50 m*M* Tris-Cl, pH 7.4. Store at 4°C.
6. Phenylmethylsulfonyl fluoride (PMSF): Store a 100 m*M* stock solution made in ethanol in aliquots at room temperature.
7. Iodoacetamide: Store a 1 *M* stock made in distilled water in aliquots at –20°C. Do not reuse same aliquot.

2.5. Immunoprecipitation

1. Antibody solution: Use 1 μg of stock anti-Flag M1, anti-*myc*, or anti-HA antibodies for each immunoprecipitation.
2. Sample buffer (2×): 120 m*M* Tris-Cl, pH 6.8, containing 4% SDS, 20% glycerol, and 0.002% bromophenol blue. Store in aliquots at –20°C till use.
3. Running gel: For a 30-mL solution, mix 13.9 mL distilled water, 8 mL of 30% acrylamide mix (use gloves), and 7.5 mL 1.5 *M* Tris-Cl, pH 8.8. Add 0.3 mL 10% SDS (wear gloves and a face mask while weighing the powder), 0.3 mL ammo-

nium persulfate and 0.018 mL TEMED. Prepare the gel on the same day in order to obtain a reproducible pattern of protein separation.

4. Stacking gel: For a 16 mL solution, mix 9 mL distilled water, 2.6 mL 30% acrylamide mix, 4 mL 1 M Tris, pH 6.8, 0.16 mL 10% SDS, 0.16 mL ammonium persulfate, and 0.016 mL TEMED. Allow to polymerize for 1 h at room temperature prior to use.
5. Electrophoresis buffer: Weigh 12 g Tris and 57.6 g glycine. Add 40 mL 10% SDS solution and make up the volume to 4 L with water. Keep at room temperature.
6. Transfer buffer: For 4 L weigh 12.12 g Tris and 57.68 g glycine. Add 800 mL methanol. Make up the volume with distilled water. Store at 4°C.

2.6. Western Blotting

1. TBS: 50 mM Tris-Cl, pH 7.4, containing 150 mM NaCl. Store at room temperature.
2. TTBS: TBS with 0.1% Tween-20. Prepared fresh.
3. Ml monoclonal (Flag) antibody: 8 μg/mL in TTBS containing 5% protease free bovine serum albumin and 0.01% sodium azide.
4. Anti-*myc* polyclonal antibody: 1 μg/mL in TTBS containing 5% protease free bovine serum albumin and 0.01% sodium azide.
5. Anti-HA polyclonal antibody: 1 μg/mL in TTBS containing 5% protease free bovine serum albumin and 0.01% sodium azide.
6. Anti-mouse immunoglobulin (IgG) conjugated to horseradish peroxidase (Vector Laboratories, CA): 1:5000 dilution in 5% nonfat dried milk in TTBS.
7. Anti-rabbit IgG conjugated to horseradish peroxidase (Vector Laboratories): 1:20,000 dilution in 5% nonfat dried milk in TTBS.

2.7. BRET Assay

1. Assay buffer: Prepare PBS as in **Subheading 2.3.** Add EDTA (sodium salt) to a final concentration of 1 mM.
2. Coelenterazine h (Molecular Probes, Eugene, OR): Prepare 1mM stock solutions in methanol. Store dessicated at –70°C.

2.8. Binding Assays

1. Assay buffer: 50 mM Tris-Cl, pH 7.4.
2. Radiolabeled ligands: Prepare stocks in 50 mM Tris-Cl, pH 7.4 such that final concentrations are from 1–10 nM for saturation assays and around the *Kd* for displacement assays.
3. Unlabeled ligand: Prepare stocks in 50 mM Tris-Cl pH 7.4 such that final concentrations are 1 μM for saturation binding and 0.01 nM–10 μM for displacement assays.

2.9. GTPγS Assay

1. Assay buffer: 50 mM Tris-Cl, pH 7.4, containing 5 mM MgCl$_2$ 100 mM NaCl and 0.2 mM EGTA.
2. Guanosine 5'-diphosphate (GDP): Freshly prepare a 50 μM stock in assay buffer.
3. [^{35}S]GTPγS: Thaw a stock vial in a hood. Store at –70°C in aliquots such that one is used per assay. When required for assay, thaw quickly and dilute in ice-cold assay buffer.
4. Unlabeled GTPγS: Prepare a 10 mM stock in water. Store at –70°C in aliquots such that only one aliquot is used per assay.

2.10. cAMP Assay

1. Assay buffer: 50 mM sodium acetate buffer, pH 6.2. Store at 4°C.
2. Forskolin: 100 μM stocks in 50 mM Tris-Cl, pH 7.4. Store in aliquots at –20°C. Use each aliquot only once.
3. Polyethylene Glycol: 17.5% PEG 8000 in 50 mM sodium phosphate buffer , pH 7.5. Store at 4°C.
4. ^{125}I cAMP: Add 10 mL of assay buffer to the original vial. Use a 1:10 dilution. Store at 4°C.
5. Anti-cAMP antibody: Resuspend in 10 mL assay buffer. Use a 1:25 dilution. Store at 4°C.
6. cAMP: Prepare stocks in the assay buffer such that final concentrations range from 3 μM–3 mM. Store at 4°C.
7. Trichloroacetic acid (TCA): 5% trichloroacetic acid in water. Store at 4°C and use ice-cold.
8. Potassium carbonate: 2.5 M solution in water. Keep at room temperature.

3. Methods

3.1. Principle for Biochemical Characterization of Receptor Associations

In order to demonstrate physical interactions between receptors, cells are cotransfected with the Flag-tagged and the *myc*-tagged versions of the two receptor cDNAs to be examined. After cell lysis *myc*-tagged receptors are immunoprecipitated using anti-*myc* antisera. The immunoprecipitates are then subjected to sodium dodecyl sulfate-polyacrylamide gel electrophoresis (SDS-PAGE) under nonreducing conditions and Western blots are treated with antisera to the other tag. In order to avoid crossreactivity, antisera from two different species are used. A signal is detected in the blots only if there is an association between the *myc*- and Flag-tagged opioid receptors *(7–9)*. This technique can also be used to detect interactions between epitope-tagged opioid

IP: anti-HA
WB : anti-Flag
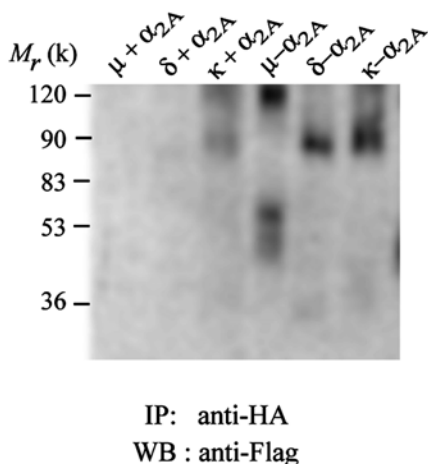
Fig. 1. Detection of opioid adrenergic interactions by immunoprecipitation and Western blot analysis. HEK-293 cells were cotransfected with differentially epitope tagged μ-α_{2A}, δ-α_{2A}, and κ-α_{2A} receptors and subjected to immunoprecipitation with anti-HA antibodies and Western blot with anti-Flag antibody. Controls (μ+α_{2A}, δ+α_{2A}, and κ+α_{2A}) comprise of a mixture of cells individually expressing each receptor type and subjected to the same immunoprecipitation and Western blot analysis.

receptors and other epitope tagged GPCRs like the α_{2A} adrenergic receptor (*see* **Fig. 1**).

3.1.1. Transient Cell Transfection Using Calcium Phosphate Precipitation

In this method, a calcium phosphate-DNA precipitate is formed by slowly mixing HEPES-buffered saline (2× HeBS) with a solution containing calcium chloride and the DNA of interest. This precipitate adheres to the surface of the cells to be transfected and is visible under the phase contrast microscope as a fine sandy precipitate. Glycerol shock increases the amount of DNA absorbed by the cells. The protocol that we use for cotransfection of cells with Flag- and *myc*-tagged opioid receptors is as follows:

1. Grow HEK-293 cells in DMEM containing 10% FBS and 0.2 mL penicillin-streptomycin in a 10 cm dish till 60–70% confluent.
2. The day before the transfection split cells from a confluent plate in a 1:5 ratio and plate into 10 cm dishes. Care must be taken to ensure that there are no cell clumps and that the cells are well separated from each other.
3. On the day of the transfection feed cells with 9 mL DMEM pH 7.1–7.2, 2 h prior to the addition of DNA precipitate.
4. Place 500 µL of 2× HeBS solution in a 15-mL sterile centrifuge tube.

5. In another tube, mix 50 μL of 2.5 *M* calcium chloride with 5–25 μg of Flag-tagged receptor cDNA and 5–25 μg of *myc*-tagged receptor cDNA, and add sterile distilled water to a final volume of 500 μL.
6. Vortex the HeBS solution and add the DNA/CaCl$_2$ solution dropwise with the help of a Pasteur pipet.
7. Continue vortexing for another 5 s.
8. Allow the precipitate to form for 20 min at room temperature.
9. Distribute the precipitate evenly (dropwise) over the cells in the 10-cm dish and gently rock the plate to mix the precipitate with the medium.
10. Incubate the cells at 37°C for 4 h and then remove the media.
11. Add 2 mL 10% sterile glycerol (in media) to the cells.
12. Incubate for 3 min at room temperature
13. Add 5 mL 1× PBS to the plate, mix, and remove the solution.
14. Wash the cells twice more with 5 mL 1× PBS.
15. Add complete media (containing FBS) and grow them for 48–72 h.
16. In addition to HEK-293 cells, Chinese hamster ovary (CHO) and COS cells can also be used for transient transfections using this protocol. However, in the case of both CHO and COS cells, it is essential to shock these cells with glycerol after transfection in order to improve the transfection efficiency.

3.1.2. Lysis of Cells

A number of different buffers can be used to lyse the transfected cells. There are two important considerations in the choice of lysis buffer, one is the efficient solubilization of the transfected receptor without affecting receptor associations and the other is its recognition by the antibody to be used in immunoprecipitation. Therefore, the conditions used for cell lysis should be as gentle as possible so as to retain antibody recognition and avoid solubilization of background proteins. However, it should be harsh enough to ensure quantitative release of the tagged receptors being investigated. Variables that can drastically affect the solubilization of proteins are salt concentration, pH and type of detergent used.

We have used different types of lysis buffer in order to examine opioid receptor interactions (*see* **Subheading 2.4.**). The following protocol was used to lyse the cells:

1. 48–72 h after transfection, wash the cells, in a 10-cm dish, twice carefully at room temperature with 5 mL 1× PBS.
2. Place the 10-cm dish on ice and add 1.5 mL of prechilled lysis buffer containing protease inhibitors, 1 m*M* PMSF and 10 m*M* iodoacetamide to each plate.
3. Scrape off the cells and collect them in an Eppendorf tube.
4. Incubate for 1 h at 4°C in a rocking shaker.
5. Centrifuge in a microfuge at 16,000*g* for 20 min at 4°C.
6. Transfer supernatant to a fresh Eppendorf tube.
7. Take an aliquot for protein estimation using BCA assay reagent according to the protocol described by the manufacturer.

3.1.3. Immunoprecipitation of Tagged Receptors

During immunoprecipitation, *myc*-tagged receptors are isolated from the mixture of proteins present in the detergent solubilized cell lysate by means of a specific polyclonal antibody directed against the receptor tag. The antibody in the immunocomplex is then allowed to adsorb to Protein A beads. The unbound proteins are then removed by washing the beads with lysis buffer leaving the purified antibody-receptor complex bound to the beads. The immunoprecipitated material bound to the protein A beads is then subjected to further analysis by SDS-PAGE and Western blot (*see* **Notes 1–4** for precautions and controls to be used). We use the following protocol for the immunoprecipitation of epitope tagged opioid receptors.

1. Take 150 µg of protein in an Eppendorf tube and add 5 µL of c-*myc* polyclonal antibody, 12 µL protease inhibitor cocktail and make the volume to 1.2 mL with lysis buffer.
2. Incubate overnight on a rocker at 4°C.
3. Equilibrate protein A beads in lysis buffer and add 150 µL to each tube.
4. Incubate for 2 h at 4°C on a rocker.
5. Centrifuge at 16,000*g* for 1 min at 4°C.
6. Wash the beads three times with 500 µL of lysis buffer containing protease inhibitors.
7. After the last wash, remove the lysis buffer completely with the help of an insulin syringe.
8. Add 70 µL 2× sample buffer to the pellet and incubate for 15 min at 60°C.
9. Spin down the samples and run 10–15 µL on 8% SDS-PAGE gels till the dye front just runs off the gel.
10. Transfer the separated proteins to PROTRAN nitrocellulose membranes.

3.1.4. Western Blot Analysis

This technique, when used in combination with immunoprecipitation, is a powerful tool that can be used for the detection of low levels of antigen and to study the specific interactions between antigens. Proteins separated by gel electrophoresis and transferred to nitrocellulose membranes are blocked to eliminate nonspecific interactions with the membrane. The location of specific antigens is then determined using a primary antibody followed by a secondary antibody conjugated to horseradish peroxidase. If a monoclonal antibody is used for immunoprecipitation, then a polyclonal antibody should be used for Western blotting and vice versa in order to avoid crossreactivity (*see* **Note 5**). The protocol for detection of opioid receptor heterodimers by immunoblotting in our laboratory is as follows:

1. After transfer of proteins to nitrocellulose membranes, rinse the membranes briefly in TBS.

2. Stain membranes for 1 min in Ponceau S to visualize the bands.
3. Wash membranes with 4 × 20 mL TTBS till the stain disappears.
4. Incubate the membranes overnight at 4°C with 25 mL of 5% nonfat dried milk in TTBS.
5. Rinse the membranes in TTBS.
6. Incubate with 25 mL (8 µg/mL) anti-Flag monoclonal antibody for 2 h at room temperature in a shaker.
7. Wash the membranes 6 × (5 min each wash) with 20–25 mL TTBS.
8. Incubate with 25 mL anti-mouse IgG conjugated to horseradish peroxidase for 1–2 h at room temperature on a shaker.
9. Wash the membranes 6 ×(5 min each wash) with 20–25 mL TTBS.
10. In order to visualize the signal, incubate membranes for 5 min with 8 mL SuperSignal Chemiluminescent Substrate mixed as per manufacturer's instructions.
11. Detect signal by exposure of the membrane to X-ray films for different time periods.

3.2. Bioluminescence Resonance Energy Transfer

Biochemical and pharmacological studies have been crucial in establishing the concept of receptor heterodimerization and its importance for the function of opioid receptors *(7–10)*. However, these approaches have certain limitations and need to be complemented with those that allow monitoring of protein–protein interactions in live cells. In order to study the molecular mechanisms involved in opioid receptor interactions and their effect in live cells, we have also employed a biophysical method that allows examination of the proximity of interacting receptors under physiological conditions in live cells.

BRET is a proximity-based assay in which the energy generated by a luminescent donor, *Renilla luciferase* (*RLuc*), upon the catalysis of its substrate, coelenterazine h, is transferred to a fluorescent acceptor, *Yellow fluorescent protein* (YFP), or *enhanced green fluorescent protein* (EGFP) *(11)*. The energy transfer can occur only if the donor and the acceptor are in close proximity (less than 100 Å), thus allowing the examination of close interactions between the donor and acceptor tagged opioid receptors (*see* **Notes 6** and **7**).

The principle of the BRET assay is schematically represented in **Fig. 2**. One receptor is tagged with *RLuc* to generate the donor and another with YFP or EGFP to generate the acceptor molecules (*see* **Fig. 3**). When the substrate, coelenterazine h, is added to the cells co-expressing these receptors, it is oxidized by the *RLuc* and emits light at 470 nm. If *RLuc* and YFP tagged opioid receptors are more than 100 Å apart, the light emission collected from such cells exhibits a single peak at 470 nm (*see* **Fig. 2**, black curve). However, if *RLuc* and YFP tagged opioid receptors are in close proximity, this light can cause excita-
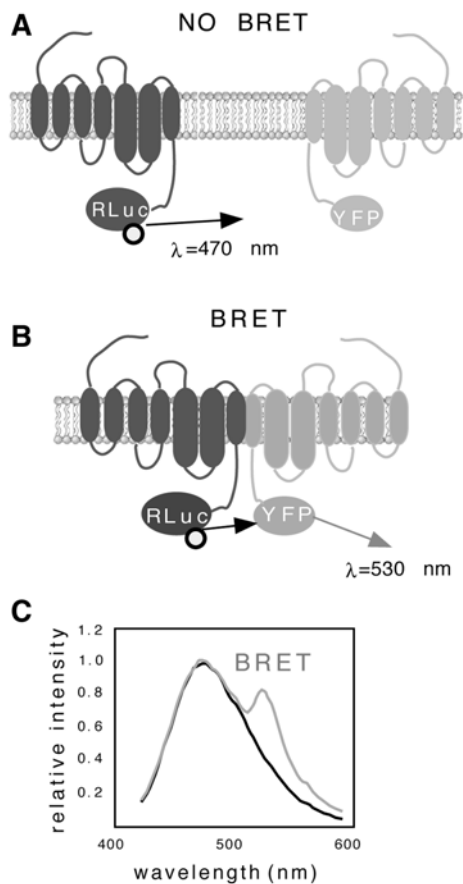
Fig. 2. Principle of bioluminescence resonance energy transfer assay. Upper panels: schematic representation of opioid receptors with seven transmembrane domains fused to Renilla luciferase (*RLuc*) and yellow fluorescent protein (YFP). (**A**)When they are far apart the light from the luminescent donor *RLuc* cannot excite the fluorescent acceptor YFP. (**B**) If two differentially tagged receptors interact and are brought close together, the acceptor is excited and emits light at 530 nm. (**C**) Typical spectra obtained in the absence (black) and in the presence (gray) of receptor-receptor interactions with a peak at 470 nm (black) and peaks at 470 and 530 nm (gray).

tion of YFP and thus the light emission collected from such cells exhibit two peaks, 470 nm and 530 nm (*see* **Fig. 2**, gray curve). The YFP emission peak is a result of the transfer of bioluminescence energy from the luciferase to YFP and is often referred to as "BRET signal." Its intensity depends on the proximity of
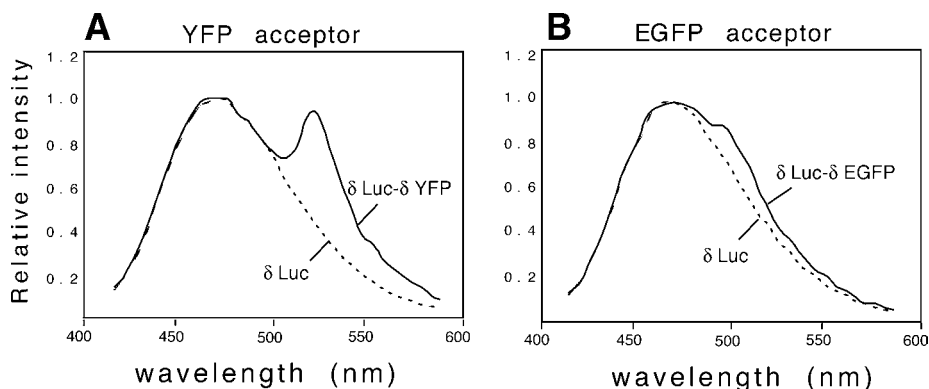
Fig. 3. Intensity and resolution of the BRET assay depends on the type of acceptor. Black curve: light emission spectrum with cells expressing δ opioid receptors fused to *Renilla luciferase* (δLuc) and (**A**) yellow fluorescent protein (δYFP) (**B**) or enhanced green fluorescent protein (δEGFP). The dotted curve represents the spectrum obtained with cells expressing *δLuc* alone.

the Rluc and YFP tagged receptors as well as the relative level and ratio of the hetero-(*RLuc*/YFP) vs homo-(*RLuc*/*RLuc* or YFP/YFP) dimeric receptors. This technique can also be used to monitor the effects of receptor expression levels and agonist treatment on BRET signal (*see* **Figs. 4** and **5**)

3.2.1. Construction of Opioid Receptors Fused to RLuc and Mutant GFPs

In order to minimize the possibility that *RLuc* or YFP interferes with the normal functioning of the opioid receptors, only the stop codon is mutated (by introducing a restriction site) and subcloned in frame with the donor or acceptor molecule in the p*Rluc* or pYFP vectors. The resulting receptors express *RLuc* or YFP at the C-terminus (*see* **Note 8**). We find that this does not substantially alter the ligand binding properties of the receptors.

3.2.2. Transfection Using Calcium Phosphate Precipitation

Transfect HEK-293 cells with pRLuc and pYFP vectors (0.25–1 µg recombinant plasmid) as described in **Subheading 3.1.1.** Use cells for BRET assay 36 h after transfection (*see* **Notes 9–15**).

3.2.3. BRET Assay

The following protocol is used routinely in our laboratory for the BRET assay.

1. Add 10 mL PBS with 1 m*M* EDTA to the transfected cells and incubate for 2–5 min at room temperature.
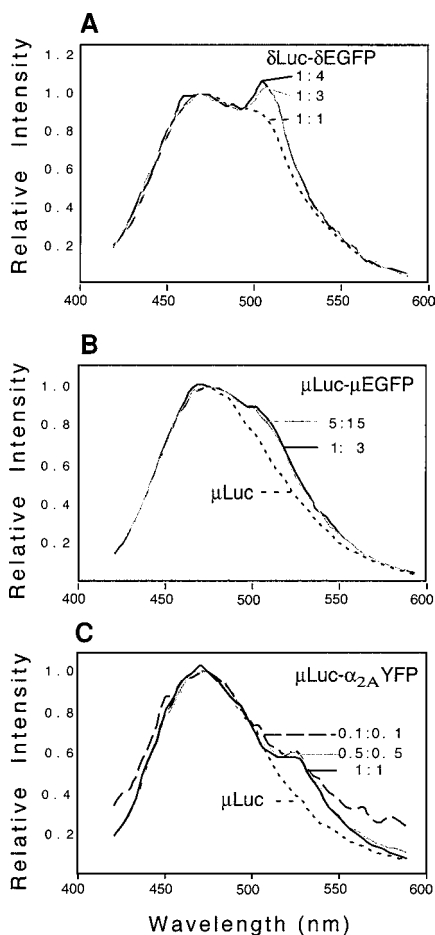
Fig. 4. Determination of optimal conditions for specific BRET signal. Homotypic association of (**A**) δ and (**B**) μ opioid receptors monitored by BRET in live cells. (**A**) The level of BRET signal with varying ratios of donor and acceptor fusion proteins; dotted (1:1) gray (1:3) and black (1:4). (**B**) The level of BRET signal while varying the total amount μLuc + μEGFP DNA while keeping the ratio constant (1:3); black (4 μg) and gray (20 μg). The dotted curve represents the spectrum obtained with cells expressing *μLuc* alone. (**C**) Heterotypic association of μ and α_{2A} adrenergic receptors monitored by BRET does not significantly vary in a wide range of receptor expression. Numbers correspond to μg of each DNA used for transfection.

2. Collect the cells with a pipette, transfer into 15 mL Falcon tubes and centrifuge for 5 min at 1000*g*.
3. Wash the cells twice with PBS and repeat the centrifugation steps.
4. Resuspend cells in 4–6 mL PBS with 1 mM EDTA to approx $1–2 \times 10^6$ cells/mL.
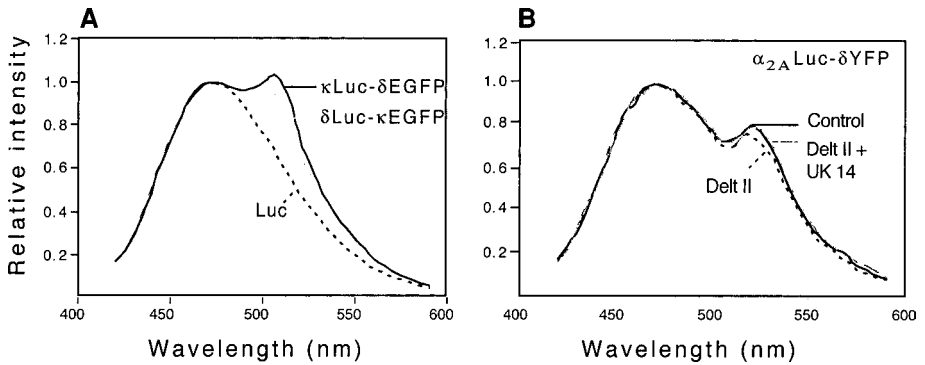
Fig 5. Heterotypic interaction of GPCRs monitored by BRET. (**A**) BRET signal (the peak at 509 nm) is detected when δ*Luc* is used as a donor and κEGFP as an acceptor (gray curve) as well as when κ*Luc* is the donor and δEGFP the acceptor (black curve). The dotted curve represents the spectrum obtained with cells expressing δ*Luc* alone. (**B**) BRET signal is also observed when $\alpha_{2A}Luc$ and δYFP are tested (solid black curve). This heterotypic interaction between δ and α_{2A} adrenergic receptor is not modulated by δ and α_{2A} specific ligands Deltorphin II (Delt II) and UK14 (dotted and gray curve), respectively.

5. Place 2 mL cell suspension in the fluorometer cuvette.
6. Add coelenterazine h to a 5 μ*M* final concentration and vigorously mix the cells.
7. Begin monitoring light emission from 420 to 590 nm at 5-nm intervals for 0.5 s immediately after the addition of coelenterazine h. It is important to have the excitation slit of the spectrometer in the closed position. Alternatively, instead of monitoring light emission for the entire spectrum, monitor the peak emissions at 470 and 530 nm (if YFP is used as an acceptor) or at 509 nm (if EGFP is used as an acceptor). In this case, a spectrophotometer (BRET counter) with appropriate filters can be used to measure light emissions.

3.2.4. Data Presentation

The intensity of the emitted light varies from experiment to experiment as a result of different transfection efficiencies, number of cells used as well as the time of start of the oxidation reaction upon addition of coelenterazine h and onset of light collection. However, the proportion of YFP tagged receptors that emit at 530 nm depends only on the relative proximity of the R*Luc* and YFP tagged receptors. Thus, light emission at the maximal intensity at 470 nm is taken as 1. When the light emission is monitored from 470 nm to 530 nm, the BRET signal is represented as the difference between the area under the emission spectrum of the cotransfected cells (gray in **Fig. 2**) and that of the R*Luc* tagged opioid receptor transfected alone (black in **Fig. 2**). When the light emis-

sion is monitored only at 470 and 530 nm, the BRET signal is represented as a BRET ratio: the ratio of the emission at 530 to the emission at 470 nm obtained when R*Luc*-tagged and YFP-tagged receptors are coexpressed, standardized to the ratio when R*Luc*-tagged receptor is expressed alone [(E_{530}/E_{470})R*Luc*.YFP/(E_{530}/E_{470})R*Luc*] *(11)*.

3.3. Pharmacological Characterization of Receptor Heterodimers

The effect of receptor–receptor interactions on the pharmacological profile of receptors can be examined through the use of radioligand binding assays. These assays can be carried out in cell suspensions, cells attached in 24-well plates and membrane preparations (*see* **Notes 16–19**). Two types of binding studies can be carried out: saturation binding analysis and displacement assays.

In the case of saturation binding analysis, cells or membranes are incubated with different concentrations of a radiolabeled ligand specific for the receptor being investigated; this gives us the total amount of radiolabeled ligand bound. Nonspecific binding is determined in the presence of high concentrations of unlabeled ligand (1–10 μ*M*), which displaces the radiolabeled ligand bound specifically to the receptor. The difference between total and nonspecific binding gives us the amount of radioligand specifically bound to the receptor. A plot of radiolabeled ligand concentration versus specific bound counts expressed as fmoles bound/ mg protein gives as a saturation curve from which we can determine the *Kd* and the *Bmax* using the program GraphPad Prism 2.0.

For displacement studies, cells or membranes are incubated with a single concentration of radiolabeled ligand in the absence or presence of different concentrations of unlabeled ligand. The data is plotted as unlabeled ligand concentration vs fmoles bound/mg protein to give displacement curves, where half-maximal inhibitory concentrations (IC_{50} values) and inhibition constants (*Ki*) can be determined using GraphPad Prism 2.0. A comparison is then made of the *Kd* or *Ki* values of membranes expressing two interacting receptors with those of membranes expressing individual receptors.

Saturation and displacement binding are equilibrium assays and therefore, time of incubation with radiolabeled ligand is important. When carrying out assays at 37°C, 1–2 h of incubation is sufficient for most ligands. For ligands that take a longer time period to reach equilibrium, it is recommended that the assays be carried out at 4°C overnight.

3.3.1. Membrane Preparation

1. Grow cells coexpressing the two receptors of interest or expressing each individual receptor in 10-cm plates.
2. When 60–70% confluent, wash cells twice with PBS.
3. Collect cells with the help of a rubber policeman in 5 m*M* Tris-Cl, pH 7.4.

4. Let the cells incubate in this low hypotonic solution for 30 min at room temperature (this causes swelling of the cells).
5. Disrupt cells by sonication for 30 s followed by centrifugation at 1000*g* for 10 min.
6. Suspend the pellet in 5 m*M* Tris-Cl, pH 7.4, and repeat **step 5**.
7. Discard the pellet (that contains nuclei and other organelles) and combine the supernatants obtained in **steps 5** and **6**.
8. Centrifuge the combined supernatants at 50,000*g* for 10 min.
9. Wash the pellet three times with 50 m*M* Tris-Cl, pH 7.4.
10. Determine protein concentration and resuspend pellet at a concentration of 1 mg/mL. Store at –80°C till use.

3.3.2. Ligand Binding Studies on Membranes

1. To determine nonspecific binding in a final assay volume of 1 mL, first add 700 μL 50 m*M* Tris-Cl, pH 7.4 to the tubes, followed by addition of 100 μL of unlabeled ligand and then 100 μL of the radiolabeled ligand (0.1–10 n*M*).
2. To determine total binding in a final assay volume of 1 mL, first add 800 μL of 50 m*M* Tris-Cl, pH 7.4 to the tubes followed by addition of 100 μL of the radiolabeled ligand (0.1–10 n*M*).
3. When investigating the effect of ligands to another receptor on the saturation kinetics of the receptor of interest, the assay should be carried out in the absence and presence of a single concentration (100 μL) of the ligand for the other receptor.
4. Initiate the reaction by adding 50–100 μg membranes in 100 μL of 50 m*M* Tris-Cl, pH 7.4, prepared as described in **Subheading 3.3.1.**
5. Incubate for 1–2 h at 37°C.
6. Place tubes on ice and filter through a Brandel filtration system using Whatman GF/B filters.
7. Wash the filters 3 × 3 mL with ice-cold 50 m*M* Tris-Cl, pH 7.4.
8. Place the filters in scintillation vials and leave overnight in scintillation fluid.
9. Count in a beta counter and plot the data in GraphPad Prism to obtain the *Kd* and Bmax.
10. For analysis of ligand binding on whole cells in suspension, collect cells coexpressing two receptors or individually expressing each receptor and resuspend in 50 m*M* Tris-Cl, pH 7.4. Estimate the cell number and set the binding assay with 5×10^5 cells/tube essentially as described above in **steps 1–9**.

3.3.3. Displacement Curves for Cells and Membranes

1. Carry out the assay in 1 mL final volume in 50 m*M* Tris-Cl, pH 7.4.
2. Add 100 μL of the ligand for the second receptor (0–10 μ*M*) to 100 μL of the radiolabeled ligand (concentration around the *Kd*) for the receptor of interest.
3. Determine nonspecific binding by adding 100 μL of unlabeled ligand (approx 1 μ*M*) directed against the receptor of interest to a parallel set of tubes.
4. Initiate the reaction by adding the cell suspension (5×10^5 cells/tube) or by addition of 50–100 μg membranes prepared as described in **Subheading 3.3.1.**

5. Incubate for 1–2 h at 37°C.
6. At the end of the incubation period place tubes on ice.
7. Filter the tubes through a Brandel filtration system using Whatman GF/B filters.
8. Wash the filters 3 × 3 mL with ice-cold 50 m*M* Tris-Cl, pH 7.4.
9. Place the filters in scintillation vials and leave overnight in scintillation fluid.
10. Count in a beta counter and plot the data in GraphPad Prism to obtain the *Ki* and IC$_{50}$ values.

3.3.4. Ligand Binding Studies for Attached Cells

1. Plate 2×10^5 cells coexpressing the two interacting receptors or each receptor alone into each well of a 24-well plate coated with poly-L-lysine and allow the cells to attach (which usually takes 4–16 h depending on cell type).
2. Rinse wells gently twice with 500 μL of 50 m*M* Tris-Cl, pH 7.4.
3. To determine nonspecific binding in a final assay volume of 300 μL, first add 100 μL of 50 m*M* Tris-Cl, pH 7.4 to the wells followed by addition of 100 μL of unlabeled ligand and then 100 μL of the radiolabeled ligand (0.1–10 n*M*).
4. To determine total binding in a final assay volume of 300 μL, first add 200 μL of 50 m*M* Tris-Cl, pH 7.4 to the wells followed by addition of 100 μL of the radio-labeled ligand (0.1–10 n*M*).
5. When investigating the effect of ligands to another receptor on the saturation kinetics of the receptor of interest, the assay should be carried out in the absence and presence of a single concentration (100 μL) of the ligand for the other receptor.
6. Incubate for 1–2 h at 37°C.
7. At the end of the incubation period, place plates on ice and wash wells gently thrice with 500 μL of ice-cold 50 m*M* Tris-Cl, pH 7.4 (take care not to aspirate the cells).
8. Add 100 μL of 1*N* NaOH to each of the wells in order to lyse the cells and leave overnight at room temperature.
9. Add 100 μL of 1*N* HCl to each of the wells to neutralize the NaOH.
10. Collect into scintillation vials, add scintillation fluid, and count in a beta counter.
11. Plot the data with the help of GraphPad Prism and use it to determine the *Kd* and *Bmax*.

3.4. Characterization of the Signaling Properties of Receptor Heterodimers

In the case of opioid receptors, we have examined signaling at three levels: agonist stimulation of GTPγS binding, decrease in forskolin stimulated cAMP levels, and activation of the MAP kinase pathway *(7–10,12)*.

Binding of agonist to the receptor causes a conformational change leading to the dissociation of the associated trimeric G-proteins into the α_i and $\beta\gamma$ subunits. The α_i subunit exchanges associated GDP for GTP. It then induces secondary signaling events such as the inhibition of adenylyl cyclase, which ultimately leads to changes in cAMP levels. Additional signaling cascades such as MAP kinase are also activated by the dissociated $\beta\gamma$ subunits.

Agonist effects at the level of G proteins can be monitored directly by measuring the levels of $[^{35}S]GTP\gamma S$ (a nonhydrolysable analog of GTP) bound in response to the agonist (*see* **Note 20**). The dose-dependent effects of agonists on cAMP levels are measured by radioimmunoassay using radioiodinated cAMP or by binding assays using protein kinase A (*see* **Note 21**). The activation of the MAP kinase pathway is measured by determining phosphorylated MAPK by Western blot using E10 monoclonal antibody that detects the phosphorylated forms of ERK (p42 and p44) (*see* **Note 22**). In the next Subheadings, we describe the protocols routinely used in these assays.

3.4.1. Membrane Preparation for GTPγ S Assay

1. Prepared membranes from different brain regions or from spinal cords by homogenization in ice-cold 50 m*M* Tris-Cl, pH 7.4, containing 1 m*M* EDTA and 10% sucrose (prepared fresh) using a Teflon tissue grinder (15–20 stokes).
2. Centrifuge homogenates at 17,000*g* for 20 min.
3. Discard the supernatants and resuspend the pellet in ice-cold 50 m*M* Tris-Cl, pH 7.4, containing 1 m*M* EDTA.
4. Keep on ice for 30 min.
5. Centrifuge at 35,000*g* for 20 min.
6. Resuspend pellets in minimum volume of ice-cold 50 m*M* Tris-Cl, pH 7.4. Pass through an insulin syringe to ensure homogeneous suspension.
7. Keep an aliquot for protein estimation.
8. Aliquot the membrane suspension (500 µg/ aliquot), freeze quickly and store at –70°C till use.

3.4.2. Agonist Stimulation of [³⁵S]GTPγS Binding

The following protocol is used routinely in our laboratory to determine opioid induced stimulation of $[^{35}S]GTP\gamma S$ binding:

1. Incubate 10 µg of membranes in 50 m*M* Tris-Cl, pH 7.5, containing 5 m*M* MgCl$_2$, 100 m*M* NaCl, 0.2 m*M* EGTA, 100 µ*M* GDP, 0.1 n*M* $[^{35}S]GTP\gamma S$ and 0–10 µ*M* of receptor agonist in the absence or presence of 10 n*M* of the ligand for the second receptor in a final volume of 1 mL.
2. Determine total binding in the absence of GDP, agonist for the first receptor, agonist or antagonist for the second receptor and cold GTPγS.
3. Determine basal binding in the presence of GDP and absence of agonist for the first receptor, agonist or antagonist for the second receptor and cold GTPγS.
4. Determine non-specific binding by adding 10 µ*M* GTPγS to a parallel set of tubes as in **step 3**.
5. Incubate for 1 h at 30°C.
6. Filter the samples through Brandel cell harvester using Whatman GF/B filters.
7. Wash the filters 3 × 3 mL with ice-cold 50 m*M* Tris-Cl, pH 7.4.
8. Determine bound radioactivity by scintillation counting.
9. Express agonist stimulation of GTPγS binding as a percentage of basal values.

10. Use the GraphPad Prism software to determine EC_{50} values.
11. For a reproducible assay, it is important to thaw the membrane aliquot, dilute it in ice-cold assay buffer and pass through an insulin syringe to ensure that a homogeneous suspension without aggregates is added to the assay tubes. The amount of $MgCl_2$, NaCl and GDP present in the assay buffer can influence the binding of $[^{35}S]GTP\gamma S$ and optimum amounts have to be established in pilot experiments. The temperature and time of incubation will have to be optimized depending on the type of receptor being investigated.

3.4.3. Determination of cAMP Levels

The protocol described below detects the intracellular levels of cyclic AMP by using a radioimmunoassay.

1. Plate $1–2 \times 10^5$ cells co-expressing differentially tagged opioid receptors or expressing each receptor alone onto a 24-well plate.
2. On the next day, pretreat the cells for 1 h with 10 μM forskolin.
3. Treat cells for 20 min with increasing doses of agonist for the first receptor in the absence or presence of a single dose of the ligand (agonist or antagonist) for the second receptor.
4. Terminate the reaction by placing the plate on ice, remove media by suction, and add 250 μL of 5% trichloroacetic acid.
5. Incubate for 10–30 min on ice.
6. Transfer 200 μL of TCA extract into an eppendorf tube and add 800 μL 50 mM sodium acetate buffer, pH 6.2 and 12 μL of 2.5 M potassium carbonate. Mix well and determine the level of cAMP by radioimmunoassay (RIA).
7. For the cAMP RIA, take 10–50 μL of neutralized cell extract, a dilution of cAMP antiserum (1:25) that gives approx 30% binding of ^{125}I-cAMP, approx 5000 cpm of ^{125}I-cAMP and incubate in 50 mM sodium acetate buffer, pH 6.2, in a final volume of 300 μL. For the standard curve, add 10 μL of cAMP standards (3–3000 μM) instead of sample.
8. After overnight incubation at 4°C, terminate the RIA by the addition of 50 μL of calf serum and 1 mL of 17.5% polyethylene glycol 8000 in 50 mM sodium phosphate buffer, pH 7.5.
9. Incubate for 20 min at 4°C and collect the antigen-antibody complex by centrifugation at 3000g for 15 min.
10. Determine the radioactivity in the precipitate using a gamma counter.
11. The cAMP RIA assay should be carried out in glass tubes. It is very important to neutralize the TCA extract being used for the RIA because it would otherwise prevent antibody binding. The time of incubation with PEG 8000 and centrifugation should be the same (this improves reproducibility). Care should also be taken to aspirate the PEG completely without disturbing the pellet.

3.4.4. Determination of the Levels of Phosphorylated MAP Kinase

In this assay, it is important to starve the cells in growth media lacking FBS in order to reduce basal levels of phosphorylated MAP kinase. Another precaution to be taken is that ligands added for the induction of phosphorylated MAP kinase have to be at 37°C. Otherwise, basal levels are high and mask the changes induced by the receptor agonist. The protocol used for the detection of agonist induced changes in phosphorylated MAP kinase is as follows.

1. Plate $1–2 \times 10^5$ cells coexpressing differentially tagged receptors or expressing each receptor alone onto a 24-well plate.
2. After the cells have attached, remove the media and add fresh media without FBS.
3. Incubate the cells in growth media without FBS for 24 h (in order to decrease endogeneous signal).
4. Incubate the cells with different concentrations of agonist for the first receptor in the absence or presence of a single concentration of the ligand (agonist or antagonist) for the second receptor for 1–5 min at 37°C.
5. Terminate the reaction by quickly removing the media and adding 100 μL of 2% SDS in 50 m*M* Tris-Cl, pH 6.8.
6. Sonicate for 3 sec (no frothing).
7. Determine the amount of protein.
8. Take 10–30 μg of protein and add sample buffer containing β-mercaptoethanol.
9. Run on 10% SDS-PAGE gels and carry out Western blotting as described in **Subheading 3.1.4.**

3.4.5. Effect of Heterodimerization on Receptor Trafficking

One of the possible consequences of receptor heterodimerization is that it alters the receptor trafficking properties (*see* **Notes 23–25**). We have shown that opioid receptors exhibit differential trafficking properties *(7,8,10,12–14)*. For example, δ and μ receptors undergo agonist-mediated internalization, whereas κ do not. However, δ opioid receptors, when coexpressed with κ receptors, undergo decreased internalization upon agonist treatment. Similarly, we have shown that in cells coexpressing β2-adrenergic and κ opioid receptors, there is a retention of β receptors at the cell surface following treatment with β2-adrenergic receptor agonists, as compared to cells expressing only β2 receptors. We use the following protocol to examine the trafficking properties of opioid receptor heterodimers:

1. Plate $1–2 \times 10^5$ cells coexpressing differentially tagged receptors or expressing individual receptors onto a 24-well plate.

2. Allow the cells to attach for 24 h.
3. Remove the medium and incubate the cells with different concentrations of the agonist for one of the receptors in the absence or presence of the ligand for the second receptor for 60 min at 37°C.
4. Place the plates on ice and treat the cells with 4% paraformaldehyde.
5. Wash the wells thrice with 500 μL of PBS.
6. Treat the cells with a primary antibody (1 μg/mL in PBS containing 50% FBS) directed against the receptor epitope tag. Probe a parallel set of wells with antibody against the second receptor epitope tag for 1–2 h at 4°C.
7. Wash the wells thrice with 500 μL of 10% FBS in PBS.
8. Incubate the cells with HRP labeled second antibody (1:1000 in PBS containing 10% FBS) for 1 h at room temperature.
9. Wash the wells three times with 500 μL of 10% FBS in PBS.
10. Incubate for 10 min with 1 μg/mL substrate, ABTS in 0.1 M citrate-phosphate buffer, pH 4, containing 4 μL/mL of H_2O_2.
11. Measure absorbance at 410 nm.
12. For data calculation, cells not treated with the ligands (agonists or antagonists) for both receptors are taken as control and expressed as 100%.
13. The ligands have to be prepared in media or in a buffer that does not prevent receptor internalization. The ABTS substrate (without H_2O_2) should be prepared at the time of incubation with second antibody and kept in dark. H_2O_2 should be added to the ABTS substrate after **step 9**. If colour does not develop after 10 min, because the number of receptors at the cell surface is low, continue the incubation up to 30 min.

4. Notes

1. One of the important criteria to ensure that the results from immunoprecipitation studies are due to direct interaction of receptors is the use of appropriate controls. A major concern with the use of immunoprecipitation in the identification of receptor heterodimers is the possibility of artifactual receptor aggregation during solubilization/immunoprecitipation conditions owing to the inherent hydrophobic nature of GPCRs. To rule out this possibility, a variety of solubilization conditions including different combination of detergents have been used *(8)*. In addition, controls in which cells expressing individual receptors are mixed prior to solubilization and subjected to the same solubilization and immunoprecipitation conditions as the cells coexpressing both receptors, should be used. Under these conditions, if the dimers are observed only in cells coexpressing both receptors and not in the mixed cells, this would suggest that the heterodimers are not the result of artifactual aggregation. In **Fig. 1**, we observe an interaction between μ or δ with α_{2A} adrenergic receptors only in cells co-expressing both receptors and not in the mixture of cells individually expressing each receptor type. However, a signal is observed in mixed cells of κ and α_{2A} interactions and we are in the process of investigating whether this represents strong artifactual hydrophobic interactions or a real association between the two receptors by BRET.

2. Artifactual receptor aggregation can also occur owing to the release of disulfide bonds upon solubilization of membranes. In order to protect proteins from artifactual covalent associations capping agents such as iodoacetamide are used *(7–9)*. Some receptors such as the kappa opioid receptor exist as SDS stable dimers irrespective of the presence or absence of crosslinkers *(8)*. This suggests the involvement of covalent bonds in receptor dimerization. This can be tested by treatment with reducing agents such as dithiothreitol (DTT) followed by use of capping agents. Iodoacetamide is used in the solubilization buffer as well as in the immunoprecipitation buffer.

3. Harsh solubilization procedures can disrupt receptor associations. A variety of crosslinking reagents have been used to address this concern *(7)*. The presence of dimeric forms of the receptor in the presence of crosslinking reagents, irrespective of their functional properties, would then suggest that the crosslinkers stabilize the interactions and that they do not induce receptor dimerization.

4. Many extraction procedures cause the release of proteases in the lysis buffer. Because this can become a problem during immunoprecipitation, care should be taken to minimize its effects. This is done by first keeping the samples in ice because temperature has a profound effect on the rate of protein degradation by most proteases. Another precaution that can be taken is the supplementation of lysis buffer with protease inhibitors. We routinely use a protease inhibitor cocktail (Sigma Chemical Co, MO, cat No.P-8340) in our cell lysis and immunoprecipitation protocols. To prevent the masking of the signal owing to the presence of nonspecific proteins during immunoprecipitation, it is advisable to preclear the cell lysate with normal serum (e.g., rabbit serum if using rabbit polyclonal antibody for immunoprecipitation) followed by binding to protein A beads. This removes all proteins that bind nonspecifically to the antibody or to the beads.

5. A number of procedures can be used to minimize the presence of a diffuse background or nonspecific bands in the Western blots. These include the use of a different blocking buffer, reducing the time of incubation with primary/secondary antibody, using harsher conditions for washing membranes after antibody incubation (e.g., 50 mM Tris-Cl, pH 7.5, containing 150 mM NaCl, 1% NP40, 0.5% deoxycholate and 0.1% SDS), adding detergent to the primary/secondary antibody preparation up to a concentration of 1%, reducing the time of incubation with substrate, or using a less sensitive substrate.

6. BRET assay can provide valuable information about the proximity and likelihood of interactions between different proteins in the context of live cells. Therefore, this assay excludes the possible effects of different detergents and membrane preparations on protein–protein interactions. However, certain concerns should be addressed because it relies on transient transfections and the ectopic expression of proteins from strong viral promoters.

7. A number of fluorescent acceptors can be used for the BRET assay. A combination of *RLuc* as donor and YFP as acceptor permits a good separation for the light emitted by the donor (470 nm) and the acceptor (530 nm). As seen in **Fig. 3A**, this leads to an increase in the signal-to-noise ratio and consequently to the abil-

ity of detecting BRET signal. In contrast, EGFP (Enhanced Green Fluorescent Protein) emits light maximally at 509 nm. This largely overlaps with the emission of the donor and therefore only very strong or close interactions can be detected because of a low signal-to-noise ratio (compare **Fig. 3A** and **3B**). An even better separation of emission peaks can be obtained with *RLuc* as donor and a mutated GFP version, GFP^2 (BioSignal Packard Cat. No. 6310200), as acceptor by using Deep Blue coelenterazine (BioSignal Packard Cat. No. 6310100C) as substrate. The emission maximum of GFP^2 is 505 nm and that of Deep Blue coelenterazine is 390 nm. However, the intensity of luminescence of Deep Blue coelenterazine is a few fold lower relative to that of coelenterazine h (data not shown). Thus, when using Deep Blue coelenterazine and GFP^2, high levels of expression of R*luc* in the cells or an extremely high number of cells ($>2\times10^6$/ assay) are required in order to obtain consistent results.

8. The donor *RLuc* and acceptor YFP or GFP are generally fused to the C-terminus of opioid receptors to minimize the problems associated with the membrane expression of the fusion proteins. In any case, the subcellular localization of *RLuc*- and YFP-tagged receptors should be determined by fluorescence microscopy and/or immunostaining. The ligand binding characteristics of the receptors should be tested whenever a receptor is tagged with any version of *RLuc* or GFP variant. For this, a radioactive ligand binding experiment should be carried out in a suspension of cells (*see* **Subheading 3.3.2.**) and untagged and tagged receptors should be compared. In addition, the fraction of surface and intracellular opioid receptors can also be determined by radioactive ligand binding (methods described in **Subheading 3.3.2.**) through the use of hydrophobic and hydrophilic radioligands.

9. To ensure optimal interactions between tagged opioid receptor molecules and consequently BRET signal, the fusion constructs are transfected into cells such as HEK-293 that do not express endogenous opioid receptors that would compete for interaction with the tagged receptors. In addition, these cells express high levels of trimeric G proteins, which are important for proper coupling of the opioid receptors to the signaling machinery of the cells.

10. A transfection method that maximizes the coexpression of the two *RLuc* and YFP tagged opioid receptors should be used. We generally use the calcium phosphate transfection method. The level of expression of the tagged opioid receptors is important for detection of BRET signal and also for the specificity of the interaction. A balance between the high levels of expression required for detection of BRET signal and the relatively low levels of expression observed under physiological conditions should be sought. This is achieved by using different amounts and ratios of *RLuc*- and YFP-tagged receptors. In order to determine the specificity of the interactions between different opioid receptors fused to *RLuc* and YFP, a competition assay with untagged opioid receptors and other unrelated proteins is used. The use of unrelated proteins that do not interact with opioid receptors under the same transfection conditions ideally serves as a negative control. Because such an experiment would involve simultaneous transfection of three

different expression vectors, the relative levels of expression of the proteins is difficult to control. The simplest controls universally used are the *RLuc* or YFP vectors (without the recombinant protein) in combination with YFP or *RLuc* tagged opioid receptors, respectively.

11. One important issue that is always being considered when examining protein-protein interactions in transiently transfected cells is the level of expression of the proteins of interest. Very often the level of protein expression that generates the best signal-to-noise ratio for the BRET assay does not match its "physiological level" of expression. In order to optimize the signal to noise (BRET to Luciferase) ratio as well as the specificity of interactions, a variety of transfection protocols that allow for optimal expression of fusion proteins should be considered. The level of expression should be estimated by independent methods (ligand binding assay described in **Subheading 3.3.2.**). Ideally, cells stably expressing a 1:1 ratio of *RLuc*- and YFP-tagged receptors should be used.

12. To maximize BRET signal, i.e., donor-acceptor associations as compared to donor–donor and acceptor-acceptor combinations, we have varied the levels of *RLuc* to GFP/YFP fusion proteins. As demonstrated in **Fig. 4A** in the case of δ–δ interactions, increasing the level of acceptor δ-EGFP gives stronger BRET signal (*see* **Fig. 4A**). The increase was significant when a 1:3 instead of a 1:1 donor to acceptor ratio was tested (compare dotted and gray curves in **Fig. 4A**). This could be due to the increased probability of donor-acceptor rather than acceptor-acceptor association when increasing the concentration of one of the components. Further increase of the acceptor molecule does not significantly increase the BRET signal (compare gray and black curves in **Fig. 4A**). It is possible that further increase in acceptor expression leads to increased acceptor-acceptor associations (that do not contribute to BRET signal).

13. It is also possible that increasing the protein expression leads to nonspecific interactions driven by mass action. To examine if the total level of protein expressed affects the BRET signal, we varied the level of receptor expression while keeping a constant ratio of donor to acceptor (*see* **Fig. 4B** and **4C**). Our results with the μ opioid receptor show that under these conditions the BRET signal does not vary even with a five-fold increase in the level of μ receptor expression (200–1000 fmols/mg of protein as determined by radioligand binding). In **Fig. 4B**, a 1:3 donor to acceptor ratio is presented. Similar results were obtained with a 1:1 ratio (data not shown). The same result is true in the case of opioid receptor interaction with other seven transmembrane proteins. As demonstrated in **Fig. 4C**, a 10-fold increase in the level of expression of μ and α_{2A} adrenergic receptor does not significantly affect the relative intensity of YFP emission or BRET signal (compare dashed, gray and black curves in **Fig. 4C**). The level of receptor expression varied from 50–500 and 500–5000 fmol/mg of protein for the μ opioid and α_{2A} adrenergic receptors, respectively, (determined by radioactive diprenorphine and yohimbine binding).

14. Another important consideration, especially when examining receptor heterodimerization, is the differences in the relative level of expression of each

of the fusion proteins. We have addressed this by using both combinations of donor/acceptor pairs. For example, both κ-*RLuc* and δ-EGFP as well as δ-*RLuc* and κ-EGFP yield a significant BRET signal (*see* **Fig. 5A**).

15. Since BRET can be performed in live cells, it appears to be an ideal assay for examining the effect of ligands on the receptor association. Two independent studies have found ligand induced changes in BRET signal *(11,15)*. We have recently examined the effect of a single or combination of ligands in opioid-adrenergic interactions. We find that either deltorphin II alone or in combination with UK14 does not significantly affect the BRET signal from cells co-expressing δ-$α_{2A}$ receptors (*see* **Fig. 5B**). These cells exhibit high level of constitutive association as determined by BRET. This is consistent with the results from immunoprecipitation studies (*see* **Fig. 1**) with the two receptors. BRET and similar assays that take advantage of the use of recombinant receptors and live cells would most certainly be the methods of choice in such studies and will hopefully prove to be as useful as they are convenient and simple.

16. When examining the effects of receptor–receptor associations on the binding properties of individual receptors, results from assays carried out in cells coexpressing both receptors should be compared to those of cells expressing individual receptors.

17. Binding assays can be performed in whole cells either in cell suspension or in attached cells. Assays are easier to carry out in cell suspensions because no especial precautions have to be taken. However, if the cells being used usually grow attached, assays done with suspensions of these cells may not reflect physiological parameters. In this case, the assays should be conducted in attached cells, however, in the latter case, precautions have to be taken to ensure that cells are not lost during the wash steps used to remove unbound ligand. These precautions involve the coating of the plates with poly-L-lysine to achieve a better attachment of the cells to the plate and gentle addition and removal of solutions.

18. Receptor cDNAs can be transfected into cells such as to obtain transient and stable transfections. Transient transfections provide a method of obtaining an overexpression of high numbers of receptors in a relatively short period of time. Usually, cells express maximum number of receptors by 72 h after transfection. After that time, the number declines drastically. Therefore, experiments to be conducted with transient transfections have only a very short window of time under which they can be carried out. Additionally, we cannot be sure that all the transfected cells express the same number of receptors. These problems are not there in cells obtained from stable transfections where each cell expresses the same number of receptors which remains constant with time. However, the procedures involved in the generation of stable transfectants is very time consuming.

19. Last, pharmacological studies can also be carried out in cells endogenously expressing the receptors of interest. This is of great advantage because these cells possess all the signaling machinery required and probably reflect the in vivo behavior of the receptor being investigated. When receptors are expressed in heterologous cells, we can never be sure that they reflect the in vivo behavior because these cells may not possess all the signaling machinery required.

20. The first step involved in opioid receptor signaling occurs at the level of G proteins and can be monitored directly by measuring the levels of [^{35}S]GTPγS bound in response to the agonist. This assay can be carried out with membranes obtained from different tissues obtained from wild-type and knock-out animals. The effect of agonist stimulation of [^{35}S]GTPγS binding by one receptor in the presence or absence of the agonist or antagonist for the other receptor can be determined and compared with knock-out animals lacking the second receptor. This assay can also be carried out in heterologous as wells as endogenous cell lines or membranes. Heterologous cell lines (i.e., transfected with the receptor) express a higher level of receptor and therefore, exhibit a robust signal. However, endogenous cell lines reflect a more physiological signal because they express the receptors naturally and at more physiologic levels. However, a problem that is frequently encountered in performing these assays in cell lines or membranes is the reproducibility and low levels of signal obtained. We have recently observed that pre-treatment of cells with low concentrations of detergent gives us highly reproducible [^{35}S]GTPγS binding curves.

21. Receptor activation can have effects on the intracellular levels of cAMP either by causing its increase or decrease. If receptor activation leads to a decrease in cAMP levels, it is better to use either forskolin or prostaglandin E1 to stimulate basal levels so that an observable decline in cAMP levels can be detected. In addition, IBMX, a phosphodiesterase inhibitor, can also be included in the assay. However, if receptor activation leads to a stimulation of cAMP levels, these agents can be omitted from the assay. The levels of intracellular cyclic AMP can be measured either by radioimmunoassay or by binding to protein A. The RIA for detection of cAMP is very sensitive. However, this technique is expensive and involves the use of radioiodinated cAMP. Measurement of cAMP levels by binding to protein A is a much cheaper technique with the disadvantage of being much less sensitive than the RIA. Another assay involves directly measuring the levels of adenylyl cyclase, the enzyme responsible for the synthesis of cAMP. However, the latter technique is quite cumbersome because it involves the isolation of the enzyme using DOWEX columns.

22. An assay that can be used to detect effect of agonists not only on receptor signaling, but also on receptor desensitization and resensitization involves the detection of phosphorylated levels of MAP kinase (ERK1/2). The assay is quick and very sensitive and unlike the [^{35}S]GTPγS binding or the cAMP RIA does not involve the use of radiolabeled ligands.

23. One of the techniques that can be used to monitor receptor traficking is enzyme-linked immunosorbent assay (ELISA). This is a relatively quick and cheap technique. However, the technique is semiquantitative and requires the availability of antibodies either directed towards the receptor tags or against the endogenous receptor. The technique only monitors levels of surface receptor and does not provide any additional information as regards to their intracellular localization.

24. Another technique that can be used to detect receptor trafficking is fluorescence activated cell sorting analysis (FACS analysis). This technique is very similar to ELISA except that the secondary antibody used is coupled to a fluorescent dye

instead of horseradish peroxidase. The technique is more quantitative than ELISA, however, it is more expensive and requires the involvement of expert help for FACS analysis.

25. Immunofluorescence is another technique that can be used to monitor receptor trafficking. It has a distinct advantage over ELISA and FACS analysis in that in can provide us with additional information about the internalized receptors, especially when examined under confocal microscopy. It can also provide us with semiquantitative data about receptor colocalization, subcellular location and association with specific proteins. However, it requires the staining of a large number of cells in order to obtain statistically significant data.

References

1. Herz, A. (1993) *Opioids*, vol. 1, Springer-Verlag, Berlin, Germany.
2. Jordan, B. A. and Devi, L. A. (1998) Molecular mechanisms of opioid receptor signal transduction. *Br. J. Anaesth.* **81,** 12–19.
3. Li, L.Y. and Chang, K. J. (1996) The stimulatory effects of opioids on mitogen activated protein kinase in Chinese hamster ovary cells transfected to express mu-opioid receptors. *Mol. Pharmacol.* **50,** 599–602.
4. Sarne, Y., Fields, A., Keren, O., and Gafni, M. (1996) Stimulatory effects of opioids on transmitter release and possible cellular mechanisms: overview and original results. *Neurochem. Res.* **21,** 1353–1361.
5. Gomes, I., Jordan, B. A., Rios, C., Trapaidze, N., and Devi, L. A. (2001) G-protein coupled receptor dimerization: implications in modulating receptor function. *J. Mol. Med.* **79,** 226–242.
6. Rios, C. D., Jordan, B. A., Gomes, I., and Devi L. A. (2001) G-protein-coupled receptor dimerization: modulation of receptor function. *Pharmacol. Ther.* **92,** 71–87.
7. Cvejic, S. and Devi, L. A. (1997). Dimerization of the delta opioid receptor: implication for a role in receptor internalization. *J. Biol .Chem.* **272,** 26,959–26,964.
8. Jordan,B. A. and Devi, L. A. (1999) G-protein-coupled receptor hetero-dimerization modulates receptor function. *Nature* **399,** 697–700.
9. Gomes, I., Jordan, B.A., Gupta, A., Trapaidze, N., Nagy, V., and Devi L. A. (2000) Heterodimerization of mu and delta opioid receptors: A role in opiate synergy. *J. Neurosci.* **20,** RC110, 1–5.
10. Jordan, B. A., Trapaidze, N., Gomes, I., Nivarthi, R., and Devi, L. A. (2001) Oligomerization of opioid receptors with beta 2-adrenergic receptors: a role in trafficking and mitogen-activated protein kinase activation. *Proc. Natl. Acad. Sci. USA* **98,** 343–348.
11. Angers, S., Salahpour, A., and Bouvier, M. (2001) Biochemical and biophysical demonstration of GPCR oligomerization in mammalian cells. *Life Sci.* **68,** 2243–2250.
12. Trapaidze, N., Gomes, I., Cvejic, S., Bansinath, M., and Devi, L. A. (2000) Opioid receptor endocytosis and activation of MAP kinase pathway. *Mol. Brain Res.* **76,** 220–228.

13. Trapaidze, N., Gomes, I., Bansinath, M., and Devi, L. A. (2000) Recycling and resensitization of delta opioid receptors. *DNA Cell Biol*. **19,** 195–204.
14. Gomes, I., Trapaidze, N., Turndorf, H., Devi, L. A., and Bansinath, M. (2000) Acute ethanol treatment modulates delta opioid receptors in N18TG2 cells. *Anesthesiology* **92,** 1789–1798.
15. Kroeger, K. M., Hanyaloglu, A. C., Seeber, R. M., Miles, L. E., and Eidne, K. A. (2001) Constitutive and agonist-dependent homo-oligomerization of the thyrotropin-releasing hormone receptor. Detection in living cells using bioluminescence resonance energy transfer. *J. Biol. Chem.* **276,** 12,736–12,743.

13

Recombinant Opioid Receptors

Structure–Function Relationship

**Julija Filipovska, Ivone Gomes, Wei Xu, Chongguang Chen,
Lee-Yuan Liu-Chen, and Lakshmi A. Devi**

1. Introduction

Opioid receptors are members of the superfamily of the seven transmembrane G protein-coupled receptors (GPCRs). They were initially recognized as three distinct entities in the late 1970s and early 1980s on the basis of pharmacological studies that demonstrated differential distribution and binding of endogenous and synthetic ligands *(1,2)*. However, their molecular characterization was only possible after the cloning of the three distinct cDNAs for δ, μ, and κ opioid receptors in the early 1990s *(3–7)*. The predicted amino acid sequence for the different opioid receptors led to the identification of several structural characteristics that are shared among members of the GPCR receptor superfamily. They contain an extracellular N-terminus, seven hydrophobic transmembrane domains (TM1-7), connected by relatively short intracellular and extracellular loops, and a short intracellular C-terminal tail. Comparison of their deduced protein sequences revealed that opioid receptors are about 60% identical, with the greatest identity found in the transmembrane domains (73–76%) and intracellular loops (86–100%) *(3)*. Despite these similarities, δ, μ, and κ opioid receptors bind specific ligands with different affinities. Furthermore, ligand binding induces conformational changes of the receptors leading to the activation of the G_i/G_o proteins and consequently very specific cellular responses. Each of the steps of opioid receptor function: ligand binding, conformational changes, and coupling to trimeric G proteins can represent an important point of regulation of the receptor function. Thus, availability of cDNAs for opioid receptors com-

bined with different techniques that allow molecular manipulation of their sequences and subsequent structural and pharmacological analyses can greatly contribute to the understanding of their function and regulation. In this chapter, we describe some of the techniques that have been successfully used to examine the structure–function relationship for opioid receptors. In general, the approach involves substitution of domains, sets of specific sequences or individual amino acid residues by mutagenesis of the cloned cDNA. The mutant receptor is then subcloned into expression vectors and the functional properties are analyzed for ligand affinity, accessibility of certain amino acid side chains to water-soluble agents, subcellular distribution, signaling, and so on (*see* **Note 1**). The approaches described here have also been used to study the structure–function relationship of many other GPCRs *(8)*.

2. Materials

1. pCDNA3 expression vector (Invitrogen, Carlsbad, CA).
2. 2X HeBS buffer: 0.3 M NaCl, 50 mM HEPES acid, and 5 mM Na_2HPO_4 pH 7.05.
3. 50 mM Tris-Cl, pH 7.5.
4. Buffer A: 140 mM NaCl, 5.4 mM KCl, 1 mM ethylenediamine tetraacetic acid (EDTA), 25 mM HEPES, and 0.006% bovine serum albumin (BSA).
5. DH5α bacterial cells.
6. HEK-239, COS-7, CHO cells (American Type Culture Collection, Rockville, MD).
7. Methanethiosulfonate (MTS) derivatives: MTS ethylammonium (MTSEA), MTS ethyltrimethylammonium (MTSET) and MTS ethylsulfonate (MTSES), (Toronto Research Chemicals Inc., Ontario, Canada).
8. Oligonucleotide primers (custom made).
9. Polymerase, calf intestinal phosphatase (New England Biolabs, Beverly, MA).
10. QIAEX II gel extraction kit (Qiagen, Valencia, CA).
11. Radioactive ligands: [^{3}H]diprenorphine, [^{3}H]DAMGO, [^{3}H]DPDPE, [^{3}H] U69593 or [^{3}H] Naloxone (Perkin-Elmer Life Sciences, Inc, Boston, MA).
12. Restriction enzymes, Taq polymerase, T4 DNA Ligase, Klenow Enzyme, T4 DNA.
13. Whatman GF/B glass fiber filters (Schleicher and Schuell, Keene, NH).

3. Methods

3.1. Chimeric Opioid Receptors

Despite the high degree of identity between the different opioid receptors, they exhibit significant differences in terms of specificity, affinity, and efficacy of ligand binding and subsequent signaling. To address the molecular basis for such differences, many laboratories have used chimeric receptors where a portion of the sequence of one receptor type is substituted with the equivalent region from another type of opioid receptor *(9)*. These experiments helped to delineate the regions responsible for opioid receptor binding selectivity.

For example, in the case of the μ receptor, region conferring ligand-binding selectivity appears to depend on the type of chimeric receptors used and the ligands examined *(10,11)*. Using μ/κ chimeras, TMs 6 and 7 and the third extracellular (e3) loop of the μ receptor were found to be important for binding of selective agonists *(12,13)*. In contrast, when μ/δ chimeras were used, TMs 1–3 and the first extracellular (e1) loop of the μ opioid receptor conferred binding selectivity for sulfentanyl *(11)*. The determinant for DAMGO selectivity by the μ receptor was found to be located in the e1 loop, based on the analysis of DAMGO binding to a series of chimeric μ/δ opioid receptors *(10,14,15)*. The e1 loop was also partly involved in selectivity for other peptide ligands but not for nonpeptide ligands *(10)*. Major determinants for binding of morphine and codeine are within TMs 5–7 as determined by binding to μ/δ chimeras *(14)*. By examining [^{3}H]β-FNA binding to four chimeric μ/κ receptors, regions of TM 6, e3 loop, and TM 7 of the μ receptor were found to be essential for β-FNA covalent binding *(16)*.

In the case of the δ receptor, κ/δ or μ/δ chimeric receptors were used to determine the major determinant for binding of δ selective ligands (DPDPE, naltrindole, BNTX, and NTB); this was found to reside in TMs 5–7 *(14,17)*. Regions of TM 6, e3 loop, and TM 7 of the δ receptor were found to be crucial for the receptor-type selectivity *(18,19)* particularly Trp6.58(284), Val7.31(296), and Val7.32(297) *(14)*. Using μ/δ chimeras, the segment containing the TM2, e1 loop, and TM 3 of the δ receptor was shown to be important for selective irreversible binding of SUPERFIT *(20)*.

Finally, in the case of the κ receptor using μ/κ chimeric receptors, Xue et al. *(21)* and Wong et al. *(22)* demonstrated that the e2 loop was essential for the high affinity binding of dynorphin peptides (*see* **Table 1**). In addition, TMs 6 and 7 and the e3 loop were found to be critical for the binding of the selective antagonist nor-binaltorphimine (nor-BNI) (*see* **Table 1***)*. This was also reported by Hjorth et al. **(23)** and Meng et al. **(17)**.

3.1.1. Constructing Chimeric Receptors by Swapping cDNA Sequences

Because of the high degree of sequence homology between the opioid receptor subtypes some unique restriction sites are also conserved and positioned in a convenient way to enable swapping of sequences that encode an equivalent region of two opioid receptors. When no such restriction sites are available, one can generate restriction sites at specific sites by mutagenesis without changing the amino acid sequences. This approach was successfully used by Meng et al., to generate chimeras of rat δ/κ, μ/δ, and μ/κ receptors *(17,24)*. The schematic outline of their approach is presented in **Fig. 1A**. Two conserved restriction sites X and Y (Afl3 and Bgl2 in the case of δ/κ chimera)

Table 1
Ki **Values (in n***M***) of** κ **Compounds for Rat** μ **and** κ **Opioid Receptors and Chimeric** μ/κ **Receptors Expressed in COS-1 Cells**

Ligands	wildtypes		chimeras					
	RKOR	RMOR	I	II	III	IV	XI	XII
Dynorphin A	0.15±0.11	8.2±0.1	7.1±3.9	0.17±0.04	53±12	0.43±0.14	ND	ND
α-Neo-endorphin	0.42±0.05	22±6	15±5	0.13±0.22	68±15	0.44±0.05	ND	ND
Dynorphin B	1.8±0.4	47±13	19±2	0.64±0.26	>10000	7.4±1.2	ND	ND
U50,488	4.8±1.4	>10000	14±3	>10000	>10000	>10000	>10000	99±27
U69,593	7.3±2.1	>10000	8.5±1.5	>10000	>10000	>10000	ND	ND
Nor-BNI	0.21±0.03	24±11	0.31±0.15	24±0.6	24±5	0.45±0.13	0.15±0.06	28.3±4.7

Six chimeric receptors were constructed from the rat μ and κ opioid receptors: chimeras I (aa κ1-184/μ194-268/263-380) and II (aa μ1-193/κ185-262/μ269-398), chimeras III (aa κ1-141/μ151-398) and IV (aa μ1-150/κ142-380), and chimera XI (aa μ1-268/κ263-380) and XII (aa κ1-262/κ269-398). Each chimeric or wt receptor was transiently expressed in COS-1 cells. Competitive inhibition of [³H]diprenorphine binding to each receptor by the ligands was conducted on membrane preparations. These results indicate that 1) the second extracellular loop and the adjoining C-terminal portion of the TM4 helix was essential for the high affinity binding of dynorphin A, α-neo-endorphin and dynorphin B to the κ receptor; 2) the third extracellular loop and the sixth and TM6 & 7 helices played an important role in determining the selectivity of nor-BNI for the κ over the μ receptor; 3) U50,488H and U69,593 appeared to require the whole κ receptor except the second extracellular loop to attain high-affinity binding. Data are shown as mean ± SEM of three independent determinations in duplicate. ND: not determined. (Adapted from Xue et al. *[21]* with permission).

are present in the cDNA for both receptors OR1 and OR2. The X site lies in the middle of TM3 and the Y site at the end of extracellular loop 2 (e2) of each receptor.

Outline of a protocol to generate chimeras of two opioid receptors, OR1/OR2:

1. Digest plasmids containing OR1 and OR2 cDNA with enzymes X and Y.
2. Separate the digested fragments in agarose gel.
3. Purify fragments A, A1, B, and B1 from the gel using QIAEX II gel extraction kit according to manufacturer's instructions (Qiagen, Cat. No. 20021).
4. For ligation, mix approx 50 ng fragment A, approx 150 ng fragment B1, 1.5 μL 10X ligation buffer, 1 μL T4 DNA ligase, and H$_2$O in a final volume of 15 μL and incubate overnight at 16°C.
5. Use approx 5 μL of ligation reaction to transform into competent DH5α *Escherichia coli* cells (these cells can be used with most vectors).
6. Screen few colonies by restriction digestion analysis and confirm the presence of chimeric sequences by DNA sequencing.
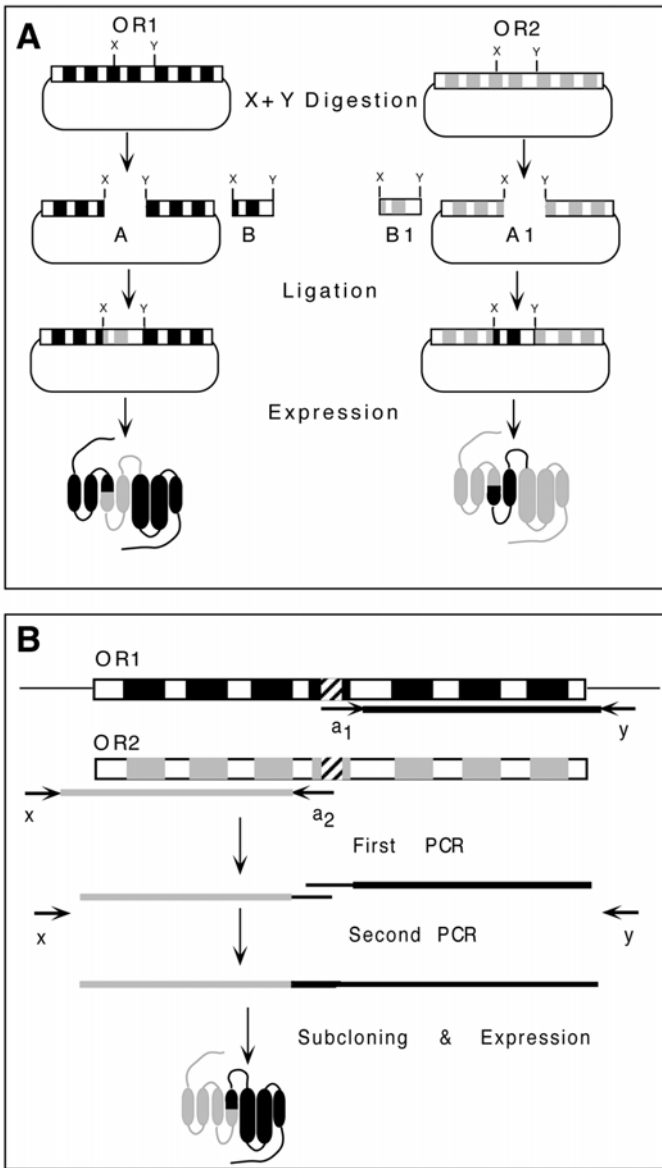
Fig. 1. Schematic representation for the creation of receptor chimeras. Swapping of domains between opioid receptors 1 and 2 (OR1 and OR2) by restriction digestion **(A)** and by overlapping PCR **(B)**. X and Y are unique restriction sites. Primers a1 and a2 have complementary 5' ends that anneal to a conserved region in both ORs (hatched). The regions of cDNA encoding for the transmembrane regions are represented in black for OR1 and gray for OR2.

3.1.2. Constructing Chimeric Receptors by Polymerase Chain Reaction (PCR)-Based Methods

Most often no restriction sites are positioned conveniently to allow the desired exchange of corresponding domains. Thus, alternative methods should be considered. In fact, because of the high degree of homology between the opioid receptors, a variation of the PCR-based approach, outlined in **Fig. 1B** can be employed. This method has been used successfully by several groups *(15,12,21)*. PCR primers a1 and a2 are chosen to be complementary to a homologous region in the receptors of interest such that they overlap in most of their 5' portion (hatched in **Fig. 1B**). The 3' portion of these primers is complementary to the receptor specific sequence (black or gray in **Fig. 1B**) (*see* **Note 2**). Primers x and y are complementary to the vector sequence in which the receptor cDNAs are subcloned and contain unique restriction sites. After the first round of PCR in which wild-type (wt) cDNA of each of the two receptors is used as a template, two products are generated whose sequences overlap within the region of primers a1 and a2. They are then used together as a template for PCR using only primers x and y. The final PCR product contains the chimeric cDNA sequence of OR1 and OR2. It can be digested with restriction enzymes x and y and subcloned into the same expression vector as the wt opioid receptor.

1. First PCR: mix 10 μL 10X PCR buffer, 100 pmol of each oligonucleotide primer (a1 & y or a2 & x), 2 m*M* each dNTP, 100 ng DNA template, and H_2O to a final volume of 100 μL.
2. Perform the reaction for 30 cycles: denaturation at 94°C for 30 s, annealing at 50°C for 30 s (or depending on the melting temperature of the primers) and extension at 72°C for 1 min (*see* **Notes 3** and **4**).
3. Resolve the PCR products by agarose gel electrophoresis.
4. Cut out the gel regions containing the PCR products of interest, dilute the agarose with water, and melt at 99°C for 5–10 min.
5. Second PCR: The reaction mixture is similar to the first PCR except that 1 μL aliquot from the two melted gels slices containing the PCR products from the first round are used as template and oligonucleotides x and y are used as primers.
6. Perform the second PCR as follows: For the first 10 cycles, denaturation at 94°C for 30 s, annealing at 30°C for 30 s, extension at 72°C for 1 min. This is followed by standard 30 cycles (*see* **step 2**).
7. Resolve the PCR product by agarose gel electrophoresis.
8. Purify the PCR product of appropriate size from the gel using QIAEX II gel extraction kit and subclone into the expression vector of choice.
9. Confirm sequence by DNA sequencing (*see* **Note 5**).

3.1.3. Analysis of Chimeric Receptors

3.1.3.1. TRANSFECTION OF CELL LINES USING THE CALCIUM PHOSPHATE PRECIPITATION METHOD

Transfect expression vectors containing cDNA encoding the chimeric or wt opioid receptors into the cell line of choice (HEK-239 or Cos-7) essentially as described here.

1. Plate cells into 10-cm^2 dishes so that they are <50% confluent in 24 h.
2. Replace medium 2–4 h prior to transfection.
3. In an Eppendorf tube (A) mix 1 to 10 µg of each recombinant plasmid, 50 µL of 2.5 M CaCl$_2$, and add H$_2$O to a final volume of 500 µL.
4. In a 15-mL Falcon tube (B) add 500 µL of 2X HeBS buffer.
5. Add dropwise the contents of tube A to tube B while vortexing.
6. Let the precipitate stand for 20 min at room temperature.
7. Add the precipitate to the cells dropwise.
8. Incubate cells at 37°C for 16–18 h.
9. Aspirate the medium and replace it with fresh medium.

In the majority of cases sufficient levels of expression are achieved within 24–48 h after transfection (*see* **Notes 6** and **7**). However, it is advisable to monitor the cells for maximal receptor expression levels at different time-points after transfection using immunoblotting or a radioactive ligand-binding assay (*see* **Notes 8–10**).

3.1.3.2. DETERMINING LIGAND BINDING PROPERTIES OF MUTANT OPIOID RECEPTORS

Ligand-binding properties are examined using [^{3}H] labeled ligands (e.g., diprenorphine, DAMGO, deltorphin II, DPDPE, U69593, naloxone). The procedure is essentially as follows:

1. Detach cells from the plates by adding 10 mL of PBS/1 m*M* EDTA and incubate 2–5 min at room temperature.
2. Collect the cells and transfer into 15-mL Falcon tubes.
3. Pellet cells by centrifugation.
4. Wash the cell pellet two times with 50 m*M* Tris-Cl, pH 7.4.
5. Resuspend cells to approx 0.5×10^6 cells/100 µL.
6. Aliquot 100 µL of 0.2, 2, 6, 12, 16, and 20 n*M* radioactive ligand in triplicates.
7. Make another set of aliquots like above that also contain 1 µ*M* unlabeled ligand.
8. Add 100 µL of cell suspension and incubate for 1 h at 37°C.
9. Separate bound and unbound radiolabeled ligand by filtration using a cell harvester.

10. Wash the filters three times with ice-cold 50 m*M* Tris-HCl, pH 7.4.
11. Add scintillating liquid to the filters and determine bound radioactivity using a β counter.
12. Analyze binding data (disintegration per minute as a function of radioactive ligand concentration) using the program GraphPad Prism. Compare *Kd* and B_{max} to those of wt receptors determined in the same experiment.

The receptor ligand-binding properties can also be determined in membrane preparations using a protocol similar to the one outlined earlier except that instead of cells, aliquots of membrane preparations containing 10–500 μg of proteins should be used. The amount of proteins added depends on the receptor expression level. If performing studies with a single concentration of the radioactive ligand, it is important to avoid ligand depletion. For this purpose, the receptor expression level should be in the range that would bind <10% of the radioactive ligand when it is used at a concentration around its *Kd* value. Protocol for membrane preparation is described in the preceding chapter (Gomes et al., **Subheading 3.3.1.2.**).

Other functional characteristics of the chimeric receptors such as activation and signaling can also be examined by determining GTPγS binding, intracellular cAMP levels, MAP kinase activation, and using the protocols described earlier (Gomes et al., **Subheading 3.4.2.–3.4.4.**).

3.2. Site-Directed Mutagenesis of Opioid Receptors

Site-directed mutagenesis has also been used to determine residues important for their ligand-binding and signaling properties. Here, we summarize some studies that significantly contributed to the understanding of the ligand-binding properties of opioid receptors.

The analysis of residues involved with the irreversible binding of β-FNA in μ receptors was examined by site-directed mutagenesis of Lys5.39(233). This mutation led to a significant loss of specific [³H]β-FNA binding indicating an involvement of Lys5.39(233) in the binding of this irreversible antagonist (*see* **Fig. 2**). Li et al. *(18)* used a similar technique to demonstrate that Asp3.32(147) formed an ionic bond with the protonated nitrogen of morphine and naltrexone. Finally, a κ receptor mutant in which Glu6.58 (297), Ser7.33 (310), Tyr7.35(312), and Tyr7.36(313) were changed to the corresponding residues in the μ receptor (*Lys*, *Val*, *Trp*, and *His*, respectively) was found to bind DAMGO with high affinity and efficiently mediated the inhibitory effects of DAMGO on intracellular cAMP accumulation *(25)*.

In the case of δ receptors point mutations of *Arg291Glu* and *Arg292Glu* in the e3 loop were found to abolish DSLET binding while not affecting bremazocine, etorphine, or naltrindole binding *(15)*. δ/μ 291-300 chimeras were used to demonstrate an increased affinity for δ selective ligands when
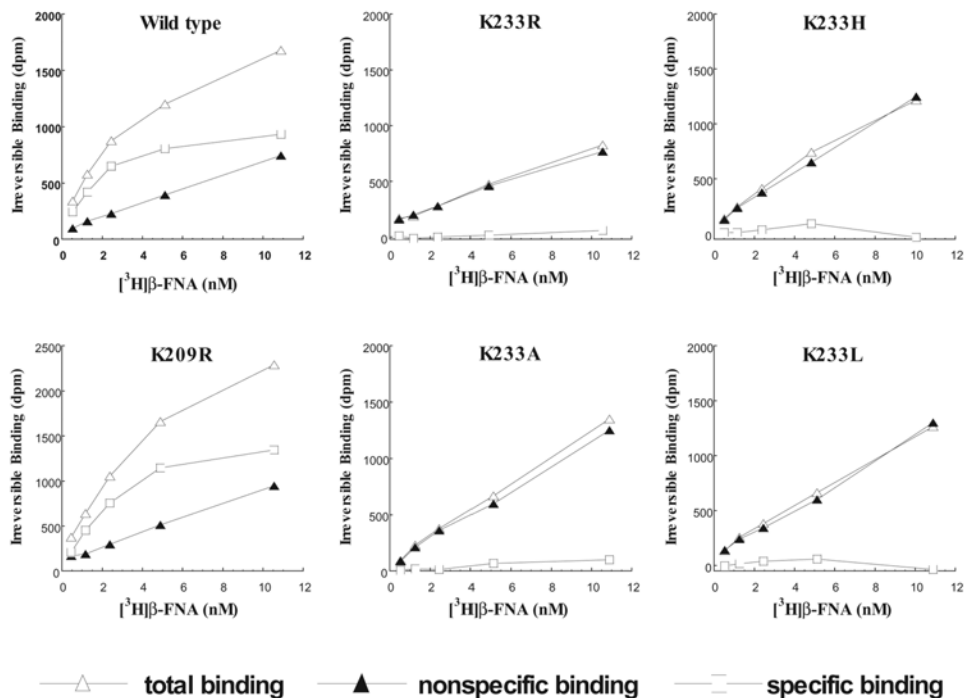
Fig. 2. Determination of the amino acid residue involved in covalent binding of [³H]β-FNA to the rat μ opioid receptor. The amino acid residue involved in the covalent incorporation of β-FNA was determined by site-directed mutagenesis of Lys5.39(233) to *Arg*, *His*, *Ala*, or *Leu*. Wild-type and mutant μ opioid receptors were transiently transfected into COS-1 cells and covalent and reversible binding of [³H]β-FNA to the receptors was determined on membrane preparations with receptor concentration of 40 60 fmole/ml/tube for each. Mutation of Lys233 to *Ala*, *Arg*, *His*, and *Leu* completely eliminated covalent binding of [³H]β-FNA although these mutants bound β-FNA with high affinity. In contrast, K209R (shown as an example), S214A, C217A, S222A C235S, C235A mutations (not shown) did not affect covalent binding of [³H]β-FNA. These results indicate that [³H]β-FNA binds covalently to Lys5.39(233). This figure represents one of three experiments performed for each receptor with similar results. Variations between experiments were less than 10%. (Adapted from Chen et al. *[26]* with permission.)

Trp300 (μ residue) of the chimera was reverted to leucine (δ residue); further site-directed mutagenesis experiments suggested that the presence of a *Trp* at this position (position 300) probably blocked the access of δ selective ligands to their docking site *(27)*.

Site-directed mutagenesis has also been used to examine sites involved in nor-BNI binding in κ receptors. Following up on the results from chimeric κ/μ receptor studies, Hjorth et al. *(23)* demonstrated that exchange of a single residue, Glu6.58(297), for lysine (corresponding residue in μ receptor) significantly reduced the binding affinity for nor-BNI without affecting the binding of non-selective compounds (-)-naloxone and diprenorphine. They concluded that the selective binding of nor-BNI to κ receptors is determined by nonconserved residues located in extracellular loop 3 and transmembrane VII and that Glu297, located just outside transmembrane segment VI, plays a major role in the κ-selective binding characteristics of nor-BNI.

Finally, substitutions of multiple amino acids have been used to address opioid vs nonopioid binding pockets. By mutating four amino acids [VQV6.51-6.53(279-281)IHI in TM 6 and T7.39I in TM7] in the orphanin FQ receptor to those of opioid receptors, a mutant receptor was generated. This receptor recognized dynorphin peptides with high affinity and yet bound orphanin FQ with high affinity *(28)*. An additional mutation of A5.39(216)K in the TM 5 [along with VQV6.51-6.53(279-281)IHI and T7.39I in TM7] generated a mutant orphanin FQ receptor that bound the alkaloid opioid antagonists naltrindole, naltriben, naltrexone, and nor-BNI with high affinity *(29)*. This suggests that the orphanin FQ receptor has developed features that specifically exclude the opioids and that these features are distinct from those required for the high affinity binding of its own endogenous ligand *(29)*.

3.2.1. Introducing Point Mutations by PCR-Based Methods

Specific amino acids of the opioid receptors can be mutated using a number of commercially available mutagenesis systems. One of those, Altered Sites(tm) in vitro mutagenesis system (Promega) has been successfully used in studying regulation of δ receptor function *(30)*. These mutagenesis systems come with detailed step by step protocols recommended by the manufacturer, thus, they will not be described here. A generic PCR-based protocol that can be modified to generate a specific mutant is described below. This method, schematically outlined in **Fig. 3A**, is somewhat similar to that described for generating chimeric receptors (*see* **Subheading 3.1.2.**), except that primers m1 and m2 containing the desired mutations are used. The sequence to be mutated should be positioned closer to the 5' end of the primer to allow for efficient annealing of the 3' end of the primer to the template. The two-step PCR protocol is essentially the same as the one described in **Subheading 3.1.2.**
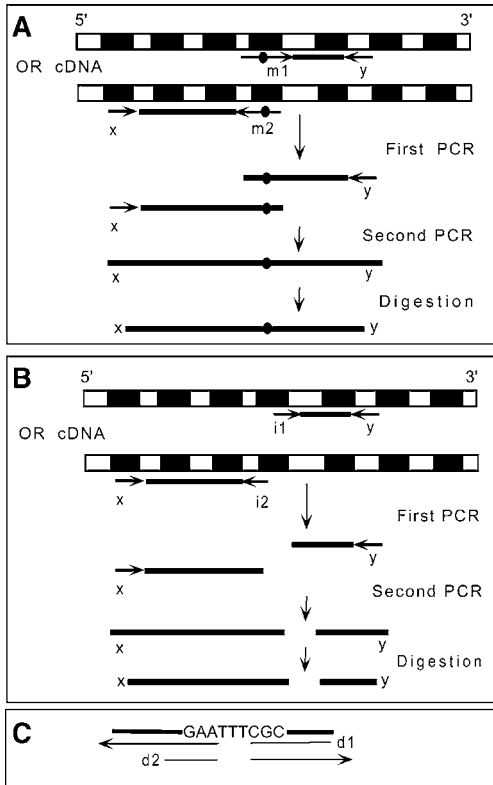
Fig. 3. Schematic representation of PCR-based protocols for nucleotide mutations (**A**), insertions (**B**) and deletions (**C**). OR cDNA: Schematic representation of the cDNA of the opioid receptor in which mutations are to be introduced. In (**C**), only the detail of the sequence of the overlapping primers is shown. The overall two-step PCR protocol is the same as in (**A**) and (**B**). Details of the procedure are discussed in the text.

3.2.2. Introducing Small Insertions and Deletions by PCR-Based Methods

These methods are schematically outlined in **Fig. 3B** and **C**. They include two rounds of PCR amplification and subcloning. When inserting nucleotides they are added to the 5' end of two overlapping primers i1 and i2 (**Fig. 3B**).

To generate receptors with specific deletions, primers should be constructed as described in **Fig. 3C**, where the sequence of the overlapping primers d1 and d2 contain only nucleotides surrounding the nucleotides to be deleted. For efficient annealing during the first step PCR, at least 15 nucleotides on the 3' end of primer complementary to the wt sequence should be used. If, for some reason, this is not possible, the annealing temperature in the first step PCR should

be lowered. Following the generation of plasmids with either insertions or deletions, they should be confirmed by sequencing. Analysis of the functional aspects of the mutated opioid receptors is carried out essentially as described in **Subheading 3.1.3.**

3.3. Probing Opioid Receptor Structure and Function by Substituted-Cysteine Accessibility Method (SCAM)

The substituted-cysteine accessibility method (SCAM) has been used to identify residues that form the surface of the ligand binding-site crevice in a number of G-protein coupled receptors including opioid receptors *(31)*. In this approach, residues in the membrane-spanning segments are mutated to cysteine, one at a time, and the mutant receptors are expressed in heterologous cells. This approach is based on the assumption that the substituted cysteine lies in an orientation similar to that of the wt residue. If ligand binding to a cysteine-substitution mutant is near-normal, it is assumed that the structure of the mutant receptor, especially around the binding site, is similar to that of the wt. In the membrane-spanning segments, the sulfhydryl of a cysteine facing into the binding-site crevice would react much faster with charged, polar, sulfhydryl-specific reagents than with sulfhydryls facing into the interior of the protein or lipid bilayer. These reagents include derivatives of methanethiosulfonate (MTS) such as those with positively charges, i.e., MTS ethylammonium (MTSEA) and MTS ethyltrimethylammonium (MTSET) or those with negative charges, i.e., MTS ethylsulfonate (MTSES) *(31)*. They have maximum dimensions of approx 10 Å by 6 Å and can form disulfides with the sulfhydryl group of the cysteine. Generally, two criteria are used to determine if an engineered cysteine is involved in the surface of the binding-site crevice: 1) the interaction of the receptor with the MTS reagent irreversibly alters ligand binding; 2) the interaction of receptor with a ligand inhibits the reaction of specific cysteines with the MTS reagent. The effect of MTS on a cysteine at a specific position in the mutant receptor is compared to that of the wt receptor.

Before one can apply SCAM to probe receptor structures, it is necessary to determine whether the wt receptor, is sensitive to MTS reagents (*see* **Note 11**). In the case of μ, δ, and κ opioid receptors, pretreatment with MTSEA dose-dependently inhibited binding of the nonselective opioid antagonist [^{3}H]diprenorphine; the order of MTSEA sensitivity was κ>μ>>δ. (–)Naloxone, but not (+)naloxone, prevented the MTSEA effect, indicating that the reaction occurs within or in the vicinity of the binding pocket. The cysteine residues in the binding pocket that conferred the sensitivity were then determined by site-directed mutagenesis. Each cysteine residue in the TMs of the three receptors was mutated singly and the effects of MTSEA treatment were examined. C7.38(321)S, C7.38(303)S, and C7.38(315)S mutations rendered μ, δ, and κ opioid receptors less sensitive to the effect of MTSEA, respectively *(32)*.

Using the C7.38S MTSEA-insensitive constructs as the templates, Xu et al. *(33)* employed SCAM to probe the structure of TM6 of the opioid receptors. Twenty-two consecutive residues in TM6 (excluding C6.47) of each receptor were mutated to cysteine, one at a time. Most mutants retained binding affinities for [^{3}H]diprenorphine, similar to that of the template receptors. Treatment with MTSEA significantly inhibited [^{3}H]diprenorphine binding to 11 of 22 mutants of the μ receptor, 9 of 22 mutants of the δ receptor, and 10 of 22 mutants of the κ receptor. Naloxone or diprenorphine protected all sensitive mutants, except the A6.42(287)C μ mutant. Thus, residues of the μ receptor that are on the water-accessible surface of the binding-site crevices are: V6.40(285), F6.44(289), W6.48(293), I6.51(296), Y6.54(299), V6.55(300), I6.56(301), I6.57(302), K6.58(303), and A6.59(304; residues of δ receptor are F6.44(270), I6.51(277), F6.54(280), V6.55(281), I6.56(282), V6.57(283), W6.58(284), T6.59(285), and L6.60(286); and residues of κ receptor are F6.44(283), W6.48(287), I6.51(290), F6.54(293), I6.55(294), L6.56(295), V6.57(296), E6.58(297), A6.59(298), and L6.60(299). The accessibility patterns of residues in the TM6 of the μ, δ, and κ opioid receptors are consistent with the notion that the TM 6 in each case is in α-helical conformation with a narrow stripe of accessibility on the cytoplasmic side of 6.54 and a wider area of accessibility on the extracellular side of 6.54. This is likely due to a proline kink at 6.50 that bends the helix in toward the binding pocket and enables considerable motion in this region. The conservation of the accessibility pattern on the cytoplasmic side of 6.54 suggests that this region may be important for receptor activation. This accessibility pattern is similar to that of the D2 dopamine receptor, the only other GPCR in which TM6 has been mapped by SCAM *(34)*. In addition, these results are also consistent with the high-resolution X-ray diffraction results with rhodopsin showing that the TM6 has an α-helical structure with a strong proline kink *(35)*. The similar accessibility patterns of the TM6 of opioids and the remotely related dopamine D2 receptor suggest that this region of GPCRs belonging to the rhodopsin subfamily has a conserved secondary structure and packaging into the TM bundle and may therefore have a similar tertiary structure.

3.3.1. Generation of Cysteine Substituted Mutants, Reaction with MTS Reagents and Effect on Ligand Binding

The protocol used for investigation of the effects of ligand binding in MTS treated receptors is given below.

1. Generate the cysteine substituted mutants using methods described in **Subheading 3.2.**
2. Transfect cells with the DNA carrying the mutant receptors as described in **Subheading 3.1.3.1., step 1**.

3. Collect cells 24–48 h after transfection, wash them and resuspended to approx 5×10^5 cells/100 μL in buffer A (*see* **Note 12**).
4. Incubate 100 μL aliquots of cell suspension with freshly prepared MTS reagent (typically 0.1, 0.25, 1, and 2.5 m*M*) in a final volume of 0.5 mL at room temperature for 3 min (*see* **Notes 13–15**).
5. Stop the reaction with 0.5 mL of 0.8% BSA solution.
6. Pellet cells and wash once with buffer A.
7. Centrifuge again and resuspend the pellets with 1 mL buffer A.
8. Use 200 μL aliquots for ^{3}H radioactive ligand binding (**Subheading 3.1.3., step 2**).

Compare binding curves for the "template" and *Cys*-substituted mutant and calculate inhibition of ligand binding by MTS reagents as 1-[(specific binding after the MTS reagent)/(specific binding without the reagent)] *(31,33)*.

3.3.2. Inhibition of MTS Reaction by Ligand

The protocol used to investigate the inhibition of MTS reaction by ligand bound receptor is described.

1. Transfect cells with the DNA carrying the mutant receptors as described in **Subheading 3.1.3., step (1)**.
2. Collect cells 24–48 h after transfection, as described in **Subheading 3.3.2.**
3. Resuspend cells in 1 mL of buffer A.
4. Incubate 0.5 mL aliquots in the absence and presence of saturating concentration of ligand for 1 h or until binding reaches equilibrium.
5. Treat both group of cells with a concentration of MTS reagent that is sufficient to achieve maximal inhibition of binding to the receptor (determined as in **Subheading 3.3.1.**).
6. Pellet cells by centrifugation.
7. Wash 3 times and resuspend to approx 5×10^5 cells/100 μL with buffer A.
8. Assay with [^{3}H]-labeled ligand binding as described in **Subheading 3.1.3., step (2)**. Compare binding curves from cells incubated without and with saturated amounts of unlabeled ligand (*see* **step 4**) and calculate protection as 1– [(inhibition in the presence of cold ligand)/(inhibition in the absence)] *(31,33)*.

4. Notes

1. Chimeric receptors allow determination of the roles of certain regions of the receptors in binding selectivity and receptor functions, whereas site-directed mutagenesis studies permit elucidation of the importance of a particular residue in receptor binding/functions. SCAM, on the other hand, yields detailed experimental information on residues lining the surface of the binding-site crevice, orientation of the side chain of each residue within the TMs, as well as the secondary structure of the TMs.
2. To avoid any problems with generating chimeric receptor cDNAs, DNA fragments should always be gel-purified and their relative amounts carefully compared. The most critical step for generating any kind of mutant receptor by

PCR-based method is selection of the primers. The primers used for the introduction of mutation should have 10–15 nucleotides complementary to the wt sequence on their 3' end. In general it is advisable to have G or C residues at the very end of any primer to stabilize the interaction with the template. The complementary regions of receptors a1 and a2 should be no shorter than 15 basepairs to obtain efficient second step overlapping PCR.

3. If the templates contain high percent of GC base pairs, amplification using standard PCR conditions may prove difficult. In such cases adding 2–10% of formamide or DMSO may be useful. Different concentrations of these compounds should be tested since every reaction has very specific requirements.

4. The optimal annealing temperature may also vary for different primer/template combinations. We have suggested conditions that are efficient with most combinations as long as the primers are at least 18 nucleotides long and with approx 50% GC content. If possible, a silent mutation of the cDNA can be introduced if it results in the generation of a restriction site that would help identify clones containing the intended mutation.

5. Whenever long stretches of sequence are generated by PCR, the entire region should be sequenced to ensure that unintended mutations are not introduced.

6. The efficiency of transfection is crucial in obtaining sufficient amount of receptors expressed for analysis. Therefore, different techniques are used and the level of expression is determined to ensure that the mutant receptors are expressed in levels that are comparable to the wt receptors.

7. Two important requirements for use of chimeric receptors in defining ligand-binding domains are that the chimera has reasonable expression levels and the chimera retains the conformation of the binding pockets of the parent receptors, at least to some extent. For this, one needs to determine Kd or Ki and B_{max} values of binding of nonselective ligands for the chimeras. If the affinities are drastically changed, the chimera cannot be used. When the receptor conformation is retained, an increase in binding activity indicates the importance of the primary structure modification, but a reduction in activity may be due to changes in primary, secondary, or tertiary structures. With the chimera approach, it is impossible to exclude potential local conformational changes in the binding pocket, or alterations of direct interactions between the receptor and the ligand.

8. Whole (intact) cell binding with hydrophilic ligand will provide information about the level of receptors expressed on the cell surface. Some mutant receptors may not mature and be trapped in the endoplasmic reticulum. These receptors could be detected in intact cells through the use of lypophilic ligands.

9. For consistent results with the ligand binding assay, only highest quality ligands should be used. Nonspecific binding should be 10% or less of total binding. Ligands should be checked for purity periodically by HPLC or other appropriate methods. [³H], rather than ¹²⁵I, labeled ligands are preferable since the smallest hydrogen group is less likely to interfere with the binding of the ligand.

10. For the mutagenesis approach, the role of a particular residue in ligand binding is inferred from, for most studies, the detrimental effects of its substitution. Alterations in ligand binding after mutation can be due to changes in direct ligand-

receptor interaction, global conformational changes in the receptor and/or local conformation changes in or around the binding pocket. When a mutation affects ligand binding, it requires further probing to differentiate these possibilities.

11. An essential prerequisite for SCAM analysis is that an MTS reagent-insensitive construct can be generated. If mutations of water-accessible cysteine residues greatly affect expression or binding properties of the receptor, it will be impossible to generate an appropriate MTS reagent-insensitive mutant and the receptor cannot be analyzed by SCAM. When substitution of a residue with cysteine substantially reduces binding affinity and/or expression level, it becomes difficult, or even impossible, to determine its accessibility in the binding-site crevice. Whether this residue is exposed in the binding-site crevice can only be inferred from neighboring residues. Lack of effect by MTS reagent treatment on ligand binding to a substituted cysteine mutant can be a result of several different possibilities. It can indicate a lack of reaction owing to the inaccessibility of the cysteine in the binding-site crevice. Alternatively, the cysteine residue may be exposed in the binding-site crevice, but is prevented from reacting with the MTS reagent by steric hindrance or unfavorable charge in the microenvironment surrounding the residue. In addition, because ligand binding is often used as the measure of MTS effect, it is possible that the MTS reagent reacts with a cysteine residue without inhibiting binding.

12. When using different MTS reagents, an alternative buffer can also be tested: Kreb's buffer (130 mM NaCl, 4.8 mM KCl, 1.2 mM KH$_2$PO$_4$, 1.3 mM CaCl$_2$, 1.2 mM MgSO$_4$, 10 mM glucose, and 25 mM HEPES, pH 7.4).

13. Some methanethiosulfonates are hygroscopic and hydrolyze in water over a period of time, particularly in the presence of nucleophiles. They should be stored in a dessicator at –20°C and warmed up to room temperature before opening the vial. For optimum results, solutions should be made up immediately prior to use even though solutions in distilled water appear to be stable for hours at 4°C.

14. Reactions with MTS reagents and effects on ligand binding should be conducted on intact cells in a physiological buffer. In doing so, one can avoid complications associated with MTS reagents reacting with intracellular cysteines, which may affect receptor binding. In intact cell preparations, MTS reagents added extracellularly react with water-accessible cysteine residues, most likely within the binding-site crevice formed by the TMs and/or within the extracellular domains.

15. Because some MTS reagents (for example, MTSEA) are able to cross plasma membranes, albeit at slow rates, a short incubation time (2–5 min) should be used to minimize penetration of the reagents and hence their interactions with intracellular cysteines.

Acknowledgment

References

1. Jordan, B. and Devi, L. A. (1998) Molecular mechanisms of opioid receptor signal transduction. *Br. J. Anaesth.* **81(1),** 12–19.
2. Wei, L. N. and Loh, H. H. (2002) Regulation of opioid receptor expression. *Curr. Opin. Pharmacol.* **1,** 69–75.
3. Chen, Y., Mestek, A., Liu, J., and Yu, L. (1993) Molecular cloning of a rat kappa opioid receptor reveals sequence similarities to the mu and delta opioid receptors. *Biochem. J.* **295,** 625–628.
4. Chen, Y., Mestek, A., Liu, J., Hurley, J. A., and Yu, L. (1993) Molecular cloning and functional expression of a mu-opioid receptor from rat brain. *Mol. Pharmacol.* **44,** 8–12.
5. Evans, C. J., Keith, D. E., Jr., Morrison, H., Magendzo, K., and Edwards, R. H. (1992) Cloning of a delta opioid receptor by functional expression. *Science* **258,** 1952–1955.
6. Kieffer, B. L., Befort, K., Gaveriaux-Ruff, C., and Hirth, C. G. (1992) The delta-opioid receptor: isolation of a cDNA by expression cloning and pharmacological characterization. *Proc. Natl. Acad. Sci. USA* **89,** 12,048–12,052.
7. Xie, G. X., Miyajima, A., and Goldstein, A. (1992) Expression cloning of cDNA encoding a seven-helix receptor from human placenta with affinity for opioid ligands. *Proc. Natl. Acad. Sci. USA* **89,** 4124–4128.
8. Wess, J., ed. (1999) *Structure-Function Analysis of G Protein-Coupled Receptors. Receptor Biochemistry and Methodology*. (Sibley, D. and Strader, C., eds.), Wiley, London.
9. Law, P. Y., Wong, Y. H., and Loh, H. H. (1999) Mutational analysis of the structure and function of opioid receptors. *Biopolymers* **51,** 440–455.
10. Onogi, T., Minami, M., Katao, Y., Nakagawa, T., Aoki, Y., Toya, T., et al. (1995) DAMGO, a mu-opioid receptor selective agonist, distinguishes between mu- and delta-opioid receptors around their first extracellular loops. *FEBS Lett.* **357,** 93–97.
11. Zhu, J., Xue, J. C., Law, P. Y., Claude, P. A., Luo, L. Y., Yin, J., Chen, C., et al. (1996) The region in the mu opioid receptor conferring selectivity for sufentanil over the delta receptor is different from that over the kappa receptor. *FEBS Lett.* **384,** 198–202.
12. Xue, J. C., Chen, C., Zhu, J., Kunapuli, S. P., de Riel, J. K., Yu, L., et al. (1995) The third extracellular loop of the mu opioid receptor is important for agonist selectivity. *J. Biol. Chem.* **270,** 12,977–12,979.
13. Minami, M., Onogi, T., Nakagawa, T., Katao, Y., Aoki, Y., Katsumata, S., et al. (1995) DAMGO, a mu-opioid receptor selective ligand, distinguishes between mu- and kappa-opioid receptors at a different region from that for the distinction between mu- and delta-opioid receptors. *FEBS Lett.* **364,** 23–27.
14. Fukuda, K., Kato, S., and Mori, K. (1995) Location of regions of the opioid receptor involved in selective agonist binding. *J. Biol. Chem.* **270,** 6702–6709.

15. Wang, W. W., Shahrestanifar, M., Jin, J., and Howells, R. D. (1995) Studies on mu and delta opioid receptor selectivity utilizing chimeric and site-mutagenized receptors. *Proc. Natl. Acad. Sci. USA* **92,** 12,436–12,440.

16. Chen, C., Xue, J. C., Zhu, J., Chen, Y. W., Kunapuli, S., Kim de Riel, J., et al. (1995) Characterization of irreversible binding of beta-funaltrexamine to the cloned rat mu opioid receptor. *J. Biol. Chem.* **270,** 17,866–17,870.

17. Meng, F., Hoversten, M. T., Thompson, R. C., Taylor, L., Watson, S. J., and Akil, H. (1995) A chimeric study of the molecular basis of affinity and selectivity of the kappa and the delta opioid receptors. Potential role of extracellular domains. *J. Biol. Chem.* **270,** 12,730–12,736.

18. Li, J. G., Chen, C., Yin, J., Rice, K., Zhang, Y., Matecka, D., et al. (1999) ASP147 in the third transmembrane helix of the rat mu opioid receptor forms ion-pairing with morphine and naltrexone. *Life Sci.* **65,** 175–185.

19. Valiquette, M., Vu, H. K., Yue, S. Y., Wahlestedt, C., and Walker, P. (1996) Involvement of Trp-284, Val-296, and Val-297 of the human delta-opioid receptor in binding of delta-selective ligands. *J. Biol. Chem.* **271,** 18,789–18,796.

20. Zhu, J., Yin, J., Law, P. Y., Claude, P. A., Rice, K. C., Evans, C. J., et al. (1996) Irreversible binding of cis-(+)-3-methylfentanyl isothiocyanate to the delta opioid receptor and determination of its binding domain. *J. Biol. Chem.* **271,** 1430–1434.

21. Xue, J. C., Chen, C., Zhu, J., Kunapuli, S., DeRiel, J. K., Yu, L., et al. (1994) Differential binding domains of peptide and non-peptide ligands in the cloned rat kappa opioid receptor. *J. Biol. Chem.* **269,** 30,195–30,199.

22. Wang, J. B., Johnson, P. S., Wu, J. M., Wang, W. F., and Uhl, G. R. (1994) Human kappa opiate receptor second extracellular loop elevates dynorphin's affinity for human mu/kappa chimeras. *J. Biol. Chem.* **269,** 25,966–25,969.

23. Hjorth, S. A., Thirstrup, K., Grandy, D. K., and Schwartz, T. W. (1995) Analysis of selective binding epitopes for the kappa-opioid receptor antagonist nor-binaltorphimine. *Mol. Pharmacol.* **47,** 1089–1094.

24. Watson, B., Meng, F., and Akil, H. (1996) A chimeric analysis of the opioid receptor domains critical for the binding selectivity of mu opioid ligands. *Neurobiol. Dis.* **3,** 87–96.

25. Seki, T., Minami, M., Nakagawa, T., Ienaga, Y., Morisada, A., and Satoh, M. (1998) DAMGO recognizes four residues in the third extracellular loop to discriminate between mu- and kappa-opioid receptors. *Eur. J. Pharmacol.* **350,** 301–310.

26. Chen, C., Yin, J., Riel, J. K., DesJarlais, R. L., Raveglia, L. F., Zhu, J., et al. (1996) Determination of the amino acid residue involved in [3H]beta-funaltrexamine covalent binding in the cloned rat mu-opioid receptor. *J. Biol. Chem.* **271,** 21,422–21,429.

27. Pepin, M. C., Yue, S. Y., Roberts, E., Wahlestedt, C., and Walker, P. (1997) Novel "restoration of function" mutagenesis strategy to identify amino acids of the delta-opioid receptor involved in ligand binding. *J. Biol. Chem.* **272,** 9260–9267.

28. Meng, F., Taylor, L. P., Hoversten, M. T., Ueda, Y., Ardati, A., Reinscheid, R. K., et al. (1996) Moving from the orphanin FQ receptor to an opioid receptor using four point mutations. *J Biol Chem* **27,** 32,016–32,020.

29. Meng, F., Ueda, Y., Hoversten, M. T., Taylor, L. P., Reinscheid, R. K., Monsma, F. J., et al. (1998) Creating a functional opioid alkaloid binding site in the orphanin FQ receptor through site-directed mutagenesis. *Mol. Pharmacol.* **53,** 772–777.
30. Law, P. Y., Kouhen, O. M., Solberg, J., Wang, W., Erickson, L. J., and Loh, H. H. (2000) Deltorphin II-induced rapid desensitization of delta-opioid receptor requires both phosphorylation and internalization of the receptor. *J. Biol. Chem.* **275,** 32,057–32,065.
31. Javitch, J. A. (1999) The substituted-cysteine accessibility method, in *Structure-Function Analysis of G Protein-Coupled Receptors* (Wess, J., ed.), Wiley, London.
32. Xu, W., Chen, C., Huang, P., Li, J., de Riel, J. K., Javitch, J. A., et al. (2000) The conserved cysteine 7.38 residue is differentially accessible in the binding-site crevices of the mu, delta, and kappa opioid receptors. *Biochemistry* **39,** 13,904–13,915.
33. Xu, W., Li, J., Chen, C., Huang, P., Weinstein, H., Javitch, J. A., et al. (2001) Comparison of the amino acid residues in the sixth transmembrane domains accessible in the binding-site crevices of mu, delta, and kappa opioid receptors. *Biochemistry* **40,** 8018–8029.
34. Javitch, J. A., Ballesteros, J. A., Weinstein, H., and Chen, J. (1998) A cluster of aromatic residues in the sixth membrane-spanning segment of the dopamine D2 receptor is accessible in the binding-site crevice. *Biochemistry* **37,** 998–1006.
35. Palczewski, K., Kumasaka, T., Hori, T., Behnke, C. A., Motoshima, H., Fox, B. A., et al. (2000) Crystal structure of rhodopsin: a G protein-coupled receptor. *Science* **289,** 739–745.

14

Receptor Knock-Out and Gene Targeting

Generation of Knock-Out Mice

Ichiro Sora, Kazutaka Ikeda, and Yuji Mishina

1. Introduction

Until recently, opioid receptors were studied only by a pharmacological approach because agonists and antagonists were the only tools available *(1)*. Interpretation of the experimental data was complicated because of the poor selectivity of opioid compounds. The precise contribution of each receptor to the effects of opioid drugs remained to be elucidated.

Gene knock-out technology, to generate a mouse with a null mutation in each opioid receptor, is one of the most important advances in studying the function of opioid receptors in vivo. Gene knock-out technology makes it possible to analyze the function of each opioid receptor with no influence of other receptor systems *(2–8)*. This chapter demonstrates the manipulation of embryonic stem (ES) cell following a previous chapter for isolation of genomic clones and another series for construction of targeting vectors. We also describe generation of chimeric mice from ES cells and analyze phenotypes for the knock-out mice involved. Because of the complexity of the techniques involved in targeting to cells, we suggest that readers examine another volume in this series *Gene Knock-out Protocols (9)*, and a further textbook *(10)* for more extensive coverage and fuller details.

2. Materials
2.1. Equipment

1. Tissue culture incubator and hood with ultraviolet (UV) light.
2. Inverted microscope.
3. Fluorometer (Pharmacia-Hoefer, DyNA count 200).

4. Electroporation apparatus (Bio-Rad Gene pulsar, #165-2105).
5. Electroporation cuvettes (Bio-Rad, #165-2088).
6. Mouse ear puncher and ear metal tags (International Market Supplies).

2.2. Tissue Culture Reagents

1. Embryonic stem (ES) cells.
2. Feeder cells (mitotically inactivated fibroblast cells).
3. Leukemia inhibitory factor (LIF, Gibco, #13275-019).
4. β-mercaptoethanol (Sigma, #M-7522).
5. Lyophilized mitomycin C (MMC, Sigma M-0503, 2 mg/bottle).
6. Phosphate-buffered saline (PBS, Gibco, #14190-250).
7. Fetal bovine serum (FBS) (*see* **Note 1**).
8. Dulbecco's modified Eagle's medium (DMEM, Gibco, #10556-016).
9. Trypsin-ethylenediaminetetraacetate (EDTA, Gibco, #25200-056).
10. STO medium (500 mL): mix in 5 mL of 100X Penicillin-streptomycin, 5 mL of 100X glutamine-200 mM, 35 mL of FCS, and 455 mL of DMEM.
11. ES medium (500 mL): mix in 5 mL of 100X penicillin-streptomycin, 5 mL of 100X L-glutamine-200 mM, 5 mL of 100X β-mercaptoethanol, 75 mL of FBS, 500,000 U of LIF, and 410 mL of DMEM.
12. ES cell lysis buffer: 10 mM Tris-HCl, pH 8.0, 10 mM sodium chloride, 10 mM EDTA, 0.5% Sarcosyl, and 1 mg/mL proteinase K.
13. Restriction enzyme cocktail (per plate): 300 μL of 10X enzyme buffer, 300 μL of 10 mM spermidine, 150 μLof 10 U/μL restriction enzyme, and 2.25 mL of water.
14. G418 sulfate (Geneticin, Gibco, #11811-031).
15. Gancyclovir (Cyovene, Syntex).

3. Methods
3.1. Manipulation of ES Cells

Pluripotency of ES cells can be maintained by culturing them on feeder cell layers with the addition of LIF (*see* **Fig. 1**). A gene targeting construct is introduced, using electroporation, into the genome of ES cells via homologous recombination. Positive-negative selection is used to enrich targeting events. Stringent culture conditions are required to maintain the pluripotency of ES cells. Prolonged periods of culture or exposure of exhausted medium affects the ability of ES cells to contribute to the mouse germline.

3.1.1. Preparation of Fibroblast Feeder Cells from Stocks

Primary embryonic fibroblast (EMFI) cells or STO fibroblast cell lines are most commonly used as feeder layers in maintaining pluripotency of ES cells. It is best to use the same type of feeder cells as those on which the ES cells was originally established. Feeder cells must be resistant to selective reagents for screening of targeting events (e.g., G418). The following protocols are for the STO fibroblast cell line.
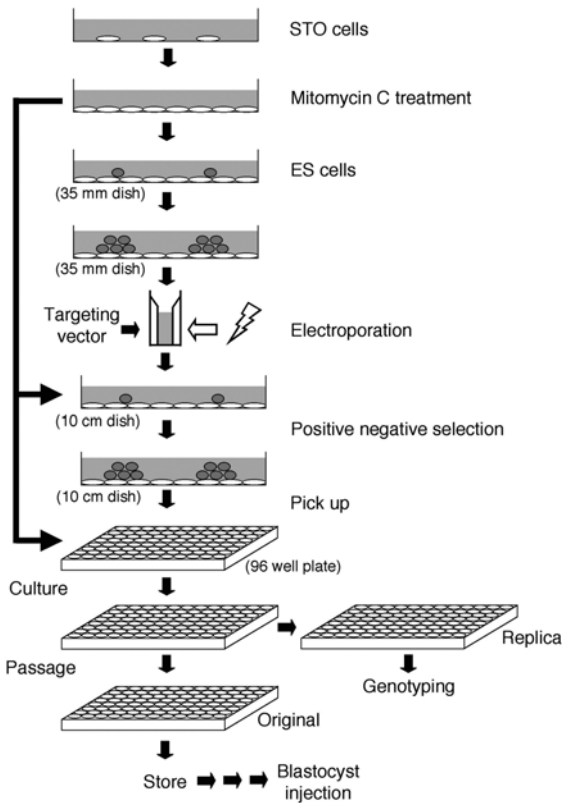
Fig. 1. Schematic illustration of procedure for screening of recombinant ES cells. ES cells are cultured on the feeder cells prepared from STO cells. The targeting vector is introduced in the ES cells by electroporation. The ES cell colonies resistant against positive-negative selection are picked up and cultured on the 96-well plates. Replicas of the 96-well plates are screened for analysis of genotype; the originals are frozen to await the results. After genotyping, correctly targeted clones are expanded to make frozen vials for blastocyst injection.

1. Put 0.1% gelatin in culture dishes and stand at room temperature at least for 1 h (gelatinized dish).
2. Remove frozen STO cell vials from the liquid nitrogen tank (5×10^6 cells) and transfer to 37°C water bath to thaw (1–2 min). Sterilize the outside of the vials with 70% ethanol.
3. Transfer the cell suspension to a sterile 15-mL tube by a transfer pipet.
4. Add 5 mL of STO medium, and centrifuge at 270g for 5 min. During centrifuging, remove the gelatin solution from the dishes.
5. Aspirate off the supernatant, resuspend the cell pellet in 2 mL of STO medium, and plate out the cells on a gelatinized 35-mm dish.

6. Change the medium every 3 d until STO cell become confluent.
7. Transfer to gelatinized dishes with dilution of 8 or 10 (one 35-mm dish to three 6-cm dishes, and so on).
8. When the passage number reaches 30, begin again from new frozen stock.

3.1.2. Preparation of Mitomycin C (MMC) Treated Fibroblast Feeder Layers

1. Add 4 mL of PBS to the bottle of lyophilized MMC to dissolve it. The final concentration is 0.5 mg/mL. Store at 4°C. Wear gloves for your protection from MMC toxicity.
2. Add 1/50 vol of 0.5 mg/mL freshly prepared MMC to STO medium (STO-MMC medium).
3. Aspirate medium from the dishes that have STO cells and add STO-MMC medium, then incubate for 2 h at 37°C (6 mL for 10-cm dish, 2 mL for 6-cm dish).
4. Trypsinize cells for 5 min at 37°C and make up 35 mL suspension with STO medium.
5. Take 10 μL and count the cell number with a hemacyto meter.
6. Centrifuge at 270g for 5 min and aspirate off the supernatant.
7. Add a sufficient amount of STO medium to the pellet to make 3.5×10^5 cells/mL suspension.
8. Distribute the suspension to gelatinized dishes. These will be ready for use within 6 h.

3.1.3. Thawing of ES Cells

In general, cells should be frozen slowly and thawed quickly. ES cells can be frozen in a freezing medium containing DMSO as a cryoprotectant. It is important to thaw the cells rapidly and remove the DMSO-containing medium as soon as possible.

1. Remove vials from liquid nitrogen tank and transfer to 37°C water bath to thaw (1–2 min).
2. Sterilize the outside of the vials with 70% ethanol.
3. Transfer the cell suspension to a sterile 15-mL tube using a transfer pipet.
4. Add 5 mL of ES medium and centrifuge at 270g for 5 min.
5. Aspirate off the supernatant and resuspend the cell pellet in 2 mL of ES medium.
6. Plate out the cells on a 35-mm dish having feeder cells.

3.1.4. Passage of ES Cells

1. Check ES cells under a microscope. If ES cells are 70–80% confluent, it is time for passage.
2. Refeed them and wait 2 h.
3. Remove medium and wash twice with PBS.
4. Add trypsin and incubate for 10 min at 37°C. (0.5 mL for 6 cm, 1 mL for 10-cm dish)
5. Add equal volume of ES medium to stop the reaction, and pipet up and down

10–15 times to make single cells.

6. Remove STO medium from feeder dishes and add appropriate volume of ES medium. (4 mL for 6 cm, 12 mL for 10-cm dish).
7. Add appropriate volume of ES cell suspension (*see* **Note 2**).

3.1.5. Freezing of ES Cells

1. Trypsinize cells and make up 10 mL suspension with ES medium.
2. Take 10 μL and dilute 10-fold with ES medium, then count the cell number with a hematocyto meter.
3. Centrifuge at 270*g* for 5 min and aspirate off the supernatant.
4. Add sufficient amount of ES medium to the pellet to make 1×10^7 cells/mL.
5. Add an equal amount of 2 × freezing medium dropwise to make final cell density 5×10^6. (2 × freezing medium; 60% DMEM, 20% FBS, 20% DMSO, mix in this order and prepare freshly.)
6. Distribute into sterile freezing vials (0.5 mL or 1 mL/vial) and place in Nalgen freezing container.
7. Store the container at –80°C overnight, then transfer to the liquid nitrogen tank.

3.1.6. Electroporation of DNA into ES

A linearized targeting vector is mixed with a suspension of ES cells in an apparatus that delivers electrical current (*see* **Fig. 1**). After electroporation, ES cells are plated onto *Neo*-resistant feeders with G418 for positive selection and with Gancyclovir for negative selection. The appropriate concentration of G418 for different ES cell lines must be determined by performing kill curves (usually somewhere between 150–350 μg/mL).

1. Trypsinize ES cells to make PBS suspension at 1.1×10^7 cells/mL.
2. Put 25 μL of linearized targeting vector DNA solution to a 0.4-cm cuvet.
3. Transfer 925 μL of cell suspension to the cuvet.
4. Set up the electroporation apparatus (e.g., 0.23 kV, 500 μF for Bio-Rad Gene pulsar).
5. Start the electroporation apparatus and monitor time constant (*see* **Note 3**).
6. Leave the cuvet at room temperature for 3 min, then transfer the cells in the cuvet tube to make up 30 mL with ES medium (without selection drugs).
7. Distribute the cell suspension in six 10-cm dishes of MMC-treated feeder cells (5-mL dish). Add 7 mL of ES medium (without selection drugs) to each dish to make a total medium volume of 12 mL.
8. From the next day, refeed each day with ES medium containing G418 (150–350 μg/mL) and Gancyclovir (2 m*M*).
9. Pick up colonies 10–14 d later.

3.1.7. Screening Colonies with Homologous Targeting Events

On the 10–14th d after electroporation, ES cell clones should reach picking size. Typically, 100–300 ES clones need to be analyzed to identify a handful of targeted events.

3.1.7.1. Pick-Up of ES Cell Colonies with Homologous Recombination

1. Prepare 96-well feeder plates.
2. Refeed 10-cm dish 2 h before picking up colonies.
3. Wash one of the dishes with PBS once and add 10 mL of PBS. Leave the others in the incubator until their turn. If necessary, count the number of colonies.
4. Distribute Trypsin (50 μL/well) to fresh 96-well plates (not to feeders).
5. Pick up the 96 colonies (*see* **Note 4**), then incubate the 96-well plate at 37°C for 10 min. It takes 1 h to pick up 96 colonies, but trypsin will not work on ES cells if it is kept at room temperature.
6. During incubation, remove STO medium from 96-well plates with feeders and add 100 μL/well of ES medium.
7. After incubation, add 50 μL/well of ES medium to Trypsin and pipet up and down to make a single-cell suspension. Transfer the suspension to the 96-well feeders (*see* **Note 5**). Move on to the next dish (*see* **step 2**).
8. Refeed each day (*see* **Note 6**).

3.1.7.2. Freeze-Down of ES Cell Colonies and Screening the Positive ES Clones

1. Prepare two sets of gelatinized 96-well plates.
2. Check each well in the plate with picked-up ES cells for confluence.
3. Refeed the 96-well plates 2 h before freezing down.
4. Remove ES medium and wash twice with PBS, then add 50 μL/well of Trypsin.
5. Incubate the 96-well plates at 37°C for 10 min. During incubation, remove gelatin from two sets of gelatinized plates and add 150 μL/well of ES medium.
6. Add 150 μL/well of ES medium to the Trypsinized plate. Add ES medium to all of the wells without changing tips.
7. Set multichannel pipette at 50 μL and mix the medium in the well by pipeting up and down 10 times to make single cells. Then transfer 50 μL of suspension to two of the gelatinized plates (*see* **Note 7**).
8. Add 100 μL/well of 2 × freezing medium to the original plate, and mix by pipeting up and down a couple of times.
9. Seal the original plate with Parafilm. Freeze at –80°C (*see* **Note 8**).
10. Put replica plates in a CO_2 incubator, and refeed everyday until 90–100% confluence is reached (3–4 d).
11. When cells on the replica plates have become confluent, wash the plates twice with PBS and add 50 μL of ES cell lysis buffer per well containing freshly added proteinase K.
12. Put 96-well plates into Tupperware with water and paper towel for humidity, and incubate at 55°C overnight. Make sure the lid is completely secured.
13. The next day, prepare a mix of sodium chloride and ethanol in a solution reservoir. (Per plate: 10 mL of ethanol + 150 μL of 5 *M* sodium chloride.) Add 100 μL/well of salt/ethanol mixture and stand at room temperature for 20–30 min. DNA will precipitate and stick to the bottom.

14. Invert the plate to discard the solution and place on a paper towel to drain. Add 150 μL/well of 70% ethanol to rinse. Discard the solution and place on a paper towel to drain. Repeat this step at least six times. After final rinse, dry the pellet completely at room temperature.
15. Add 30 μL/well of restriction enzyme cocktail. Incubate the plates at 37°C (or proper temperature for the enzymes) overnight.
16. Follow the regular Southern blotting protocol for screening the positive ES clones with homologous recombination (*see* **Note 9**).

3.2. Generating, Analyzing, and Maintaining Knock-Out Mice

ES cells are introduced into developing embryos to generate chimeras, either by blastocyst injection or by aggregation with morula-stage preimplantation embryos (*see* **Fig. 2**). These techniques are described in detail elsewhere *(10)*. We describe here the blastocyst injection technique that is most commonly used. Blastocysts injected with ES cells are implanted into the uterine of pseudopregnant recipient foster mothers. Chimeras are generally test bred to ascertain the contribution of the ES cells to the germline. Once germline chimeras are identified, the next step will be to obtain homozygous mice for phenotype analysis. Elsewhere, we describe phenotype analysis of opioid receptor knockout mice including our own *(1–8,11–13)*.

3.2.1. Blastocyst Injection

Blastocysts are very early-stage embryos that can be collected from the uterus of d 3.5 pregnant females. The C57BL/6 inbred strain is often used. The standard procedure is to inject 10–20 ES cells into the blastocoel cavity of the blastocysts. After injection, culture the embryos for a short period (2–3 h) to allow reexpansion of the blastocoel cavity, and then transfer to the uterine horns of the pseudopregnant outbred mice. The CD-1 outbred strain is often used as recipient, because these mice sustain pregnancies well and provide good parental care.

3.2.2. Chimeric Production and Coat Color Strategy

The resulting mouse pup has tissues and organs consisting of a mosaic mixture of cells derived from the original 129 ES cells and the C57BL/6 host blastocysts. The pups are called chimeras because they contain cells from two independent sources. The coat color of chimeric pups is a mosaic of black from the C57 and Agouti from 129 strain. Appearance of the Agouti coat color is a useful early marker of a successful mutation.

Once chimeras are generated, they are bred to the C57BL/6 strain because germline transmission of the ES cell genome can be identified from the coat color of their pups. Half of the Agouti pups should be heterozygous mutants. Heterozygous mating can then be set up to generate wild-type, heterozygous, and homozygous gene-targeted mice.
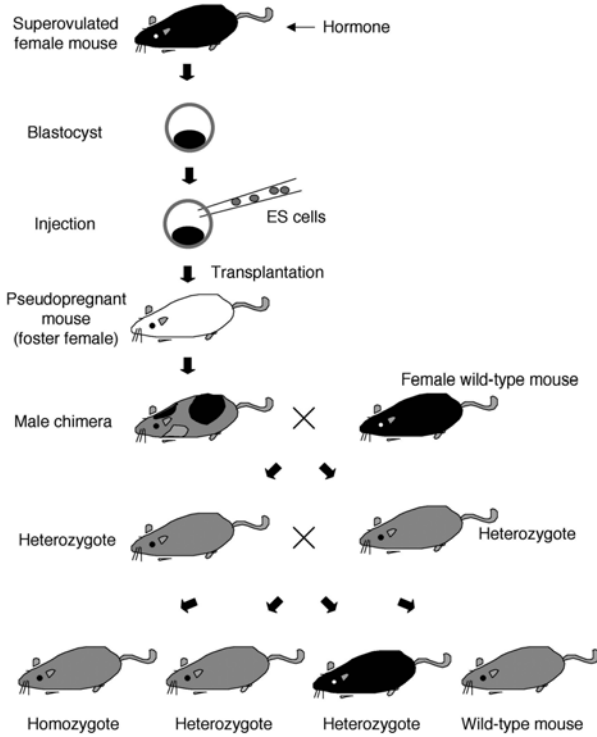
Fig. 2. Schematic illustration of procedure for generation of chimeric mice and derivation of the mouse mutant line. The targeted ES cells are injected into the blastocyst harvested from a superovulated female, then implanted in the uterus of pseudopregnant females. The resulting chimeric male mice are mated with wild-type females to confirm germline transmission. Heterozygous mice born from the wild-type female are mated to produce homozygous mice for phenotypic analyses.

3.2.3. Breeding Scheme

Mice are commonly bred in pairs, in trios (one male with two females), or in harems (one male with more than two females). Weekly rotation of a male mouse through cages containing pairs of females may be used to optimize the yield of offspring from a single male. Mice are weaned at approx 3 wk of age, and should be removed from the breeding cage before the birth of a subsequent litter. Breeding records should be kept to identify those animals to be used as replacement breeders, to maintain pedigree details, and to ensure that unproductive animals can be identified. The mouse database can be kept using any PC spreadsheet software (*see* example in **Table 1**). The breeding nucleus of a congenic strain must be maintained by full-sib mating (brother × sister) whereas outbred strains must be maintained so as to minimize inbreeding.

3.2.4. Analysis of Phenotypes

Phenotypes to be tested for opioid receptor knock-out mice include behaviors such as the analgesia test and reward test. A series of preliminary observations of general health, home cage behavior, sensory abilities, and motor functions is first conducted before analysis of altered responses to opioids, ethanol, and psychostimulant drugs of abuse. If an animal has a major health problem or a gross motor defect, then it will be unable to perform many behavioral tasks for reasons not necessarily specific to the mutation. SHIRPA is a systematic, objective protocol for phenotype analysis that can provide general phenotype assessment *(14)* (http://www.mgu.har.mrc.ac.uk/mutabase/shirpa_summary.html,). The SHIRPA protocol involves three stages, of which the first two give a detailed general phenotype assessment, and the tertiary stage provides a specialized screen tailored primarily to neurological deficits (*see* **Table 2**). The genetic background of knock-out mice influences the phenotype observed to some extent. The issue of genetic background is important, especially in the analysis of complex behavioral phenotypes. Specific protocols for individual behavioral tasks can be found in the original publications, and in several recent reviews *(13,15)*.

Significant numbers of opioid-receptor knock-out mice have now been made. Analyses of μ-opioid receptor (MOR) clearly show that MOR is necessary to mediate morphine action on both pain and reward pathways *(2,3,13)*. MOR knock-out mice show reduced analgesia after administration of morphine, a MOR agonist, but also after administration of δ-opioid receptor agonists *(2,3,11,12)*. κ-opioid receptor (KOR) knock-out mice show no analgesia after administration of KOR agonists, whereas analgesic effects of morphine are intact *(7)*. Conditioning with morphine induced place preference in KOR knock-out mice *(7)*. However, morphine did not induce place preference and self-administration in MOR knock-out mice *(2,13)*.

4. Notes

1. The quality of the FBS is very important for the maintenance of ES cells. Different batches from different suppliers (Hyclone, GIBCO) should be tested for their support growth of pluripotent ES cells. Suitable FBS batches should be purchased in large quantities.
2. One-third or one-quarter of the suspension can be transferred to the same size of fresh dish. Dilution should be no greater than fourfold.
3. Usually 6.5–7.0 ms. If there are extra cells, set up cuvet without DNA to check condition.
4. Set P20 Pipetteman at 2 μL. Under stereomicroscope, circle feeders that surround an ES colony to detach from dish. Suck up the colony and transfer to 96-well plate trypsin. Change tip and move on to the next colony. To avoid confusion, a newly opened tip box should be used.
5. Each well should have 200 μL of suspension. A multichannel pipet is most helpful. Tips must be changed for each row.

Table 1
Example of Mouse Database

Tag#	Location	Color	ID #	Male parent	Female parent	Tagged Date	DOB	Sex	Genotype	Used	Date	Outcome	Date
60	RS	A	MK1-3-1	MK25	MK21	2/7/01	12/21/00	F	+/–	Breeder	3/2/01	Analgesia	9/12/01
61	LN	A	MK1-3-2	MK25	MK21	2/7/01	12/21/00	F	–/–			Died	3/10/01
62	R	B	MK1-3-3	MK25	MK21	2/7/01	12/21/00	M	+/–	CPP	5/16/01	Euthanasia	5/16/01

Tag#: Metal ear tag ID number. Location: location of ear tag, L-left, R-right, S-slash, N-notch. Color: coat color, A-agouti, B-black. ID #: ID number based on male parent. Male parent: ear tag ID number. Female parent: ear tag ID number. DOB: date of birth.

Table 2
Overview of SHIRPA Protocol Stages

Primary Screen for Behavioral Observation Profile
  1. Behavior recorded in the viewing jar:
        Body position, spontaneous activity, respiration rate, tremor.
  2. Behavior recorded in the arena:
        Transfer arousal, locomotor activity, palpebral closure, piloerection,
        startle response, gait, pelvic elevation, tail elevation, touch escape,
        positional passivity.
  3. Behavior recorded on or above the arena:
        Trunk curl, limb grasping, visual placing, grip strength, body tone,
        pinna reflex, corneal reflex, toe pinch, wire manoeuvre.
  4. Behavior recorded during supine restraint:
        Skin color, heart rate, limb tone, abdominal tone, lacrimation, saliva-
        tion, provoked biting, righting reflex, contact righting reflex, negative
        geotaxis, fear, irritability, aggression, vocalization, body temperature.

Secondary Screen
  1. Locomotor activity.
  2. Food and water intake.
  3. Balance and coordination.
  4. Analgesia.
  5. Histology.
  6. Biochemistry.

Tertiary Screen
  1. Anxiety.
  2. Learning and memory.
  3. Prepulse inhibition.
  4. Electroencephalography.
  5. Nerve conduction.
  6. Magnetic resonance imaging.

  6. Most wells will become confluent within 4 d. When they are 80% confluent,
     prepare two sets of gelatinized 96-well plates.
  7. These plates are replicas (50 μL × 2 of suspension will be removed, leaving 100
     μL in the original well). Tips must be changed for each row. To avoid confusion,
     a newly opened tip box should be used.
  8. Put the plates in a plastic bag, then put these in a used Styrofoam box.
     Southern screen uses a restriction enzyme that cuts once outside one region of
     homology and a second time within (or at the other side of) the construct, in
     combination with a single-copy probe outside the region of homology.

References

1. Kieffer, B. L. (1999) Opioids: first lessons from knockout mice. *Trends Pharmacol. Sci.* **20,** 19–26.
2. Matthes, H. W., Maldonado, R., Simonin, F., Valverde, O., Slowe, S., Kitchen, I., et al. (1996) Loss of morphine-induced analgesia, reward effect and withdrawal symptoms in mice lacking the mu-opioid-receptor gene. *Nature* **383,** 819–823.
3. Sora, I., Takahashi, N., Funada, M., Ujike, H., Revay, R. S., Donovan, D. M., et al. (1997) Opiate receptor knockout mice define mu receptor roles in endogenous nociceptive responses and morphine-induced analgesia. *Proc. Natl. Acad. Sci. USA* **94,** 1544–1549.
4. Tian, M., Broxmeyer, H. E., Fan, Y., Lai, Z., Zhang, S., Aronica, S., et al. (1997) Altered hematopoiesis, behavior, and sexual function in mu opioid receptor-deficient mice. *J. Exp. Med.* **185,** 1517–1522.
5. Loh, H. H., Liu, H. C., Cavalli, A., Yang, W., Chen, Y. F., and Wei, L. N. (1998) mu Opioid receptor knockout in mice: effects on ligand-induced analgesia and morphine lethality. *Brain Res. Mol. Brain Res.* **54,** 321–326.
6. Filliol, D., Ghozland, S., Chluba, J., Martin, M., Matthes, H.W., Simonin, F., et al. (2000) Mice deficient for delta- and mu-opioid receptors exhibit opposing alterations of emotional responses. *Nat. Genet.* **25,** 195–200.
7. Simonin, F., Valverde, O., Smadja, C., Slowe, S., Kitchen, I., Dierich, A., et al. (1998) Disruption of the kappa-opioid receptor gene in mice enhances sensitivity to chemical visceral pain, impairs pharmacological actions of the selective kappa-agonist U-50,488H and attenuates morphine withdrawal. *Embo. J.* **17,** 886–897.
8. Schuller, A. G., King, M. A., Zhang, J., Bolan, E., Pan, Y. X., Morgan, D. J., et al. (1999) Retention of heroin and morphine-6 beta-glucuronide analgesia in a new line of mice lacking exon 1 of MOR-1. *Nat. Neurosci.* **2,** 151–156.
9. Tymms, M. J. and Ismail, I., eds. (2001) *Gene Knockout Protocols*. Methods in Molecular Biology, vol. 158, Humana, Totowa, NJ.
10. Joyner, A. L., ed. (2000) *Gene Targeting - A Practical Approach* (Second Edition), Oxford University Press, New York.
11. Fuchs, P. N., Roza, C., Sora, I., Uhl, G., and Raja, S. N. (1999) Characterization of mechanical withdrawal responses and effects of mu-, delta- and kappa-opioid agonists in normal and mu-opioid receptor knockout mice. *Brain Res.* **821,** 480–486.
12. Sora, I., Funada, M., and Uhl, G. R. (1997) The mu-opioid receptor is necessary for [D-Pen2,D-Pen5]enkephalin- induced analgesia. *Eur. J. Pharmacol.* **324,** R1–R2.
13. Sora, I., Elmer, G., Funada, M., Pieper, J., Li, X.-F., Hall, S., et al. (2001) Mu opiate receptor gene dose effects on different morphine actions: evidence for differential in vivo mu receptor reserve. *Neuropsychopharmacology* **25,** 41–54.
14. Rogers, D. C., Fisher, E. M., Brown, S. D., Peters, J., Hunter, A. J., and Martin, J. E. (1997) Behavioral and functional analysis of mouse phenotype: SHIRPA, a proposed protocol for comprehensive phenotype assessment. *Mamm. Genome* **8,** 711–713.
15. Crawley, J. N. (2000) *What's Wrong With My Mouse?: Behavioral Phenotyping of Transgenic and Knockout Mice*. Wiley-Liss, New York.

15

Pharmacological Interventions at the Spinal Cord

Intrathecal Injections

Daphné A. Robinson and Min Zhuo

1. Introduction

Both sensory inputs and motor outputs of the brain occur via the spinal cord. Spinalization, via a simple surgical cut, has allowed the elucidation of some of the intrinsic spinal circuitry underlying spinal reflexes. To understand the modulation of spinal processing by local spinal innervations and descending fibers from supraspinal structures to the spinal cord, a pharmacological approach is often more useful than a surgical one. The development of intrathecal injections *(1)* has permitted the introduction of specific agonists or antagonists locally into the spinal cord. In particular, the spinal action of opioids was thus proven *(2)*.

In the clinics, the use of intrathecal injections has decreased the side effects of painkillers, such as morphine, and of anesthetics. Intrathecal injections allow a decrease in the doses used and prevent the spread of the drug to many essential organs.

In animals, intrathecal injections are usually performed via an implanted catheter, although injections in mice are performed by an acute lumbar puncture *(3)*. The later technique is technically more demanding and requires much more practice before it can be performed in an experiment. It can also be used in rats, when a single injection is sufficient *(4)*. Both methods are described here.

2. Materials

1. PE 10 (polyethylene) tubing (ID: 0.22 mm, OD: 0.61 mm).
2. Halothane, a halothane vaporizer, a nose mask, and a halothane waste filter (beware of liver toxicity, use with appropriate equipment, including a T/C Air filter to collect halothane waste) (*see* **Note 1**).

3. A 50-μL Hamilton syringe.
4. Dental cement.
5. Surgical equipment: retractors, scalpel, suture and suturing needle, and forceps.
6. Stereotax and heating pad.
7. Small stainless steel tube for injector (OD: about 0.2 mm, to fit in PE 10).
8. 30-gage needle.

3. Methods

3.1. Intrathecal Catheterization

For repeated administration of drugs, chronic catheterization of the animal is necessary (*see* **Fig. 1**). This also has the advantage of eliminating possible interactions with anesthetic residuals. The procedure is described here in the rat, but can be adapted to bigger animals such as cats.

3.1.1. Catheter Preparation

Use PE-10 tubing to tie a loose knot without pinching the tubing and create a small circle about 5 mm in diameter. Apply dental cement to cover the knot, thus creating a bead that will hold the catheter into place. On one side of the bead, cut the catheter at a length of 8.5 cm to reach the lumbar enlargement in 300–350 g Sprague–Dawley rats (*see* **Note 2**). On the other side of the bead, keep 4–6 cm of the catheter to allow easy access to the catheter. Sterilized the catheter with alcohol and fill it with sterile saline.

3.1.2. Surgery

Anesthetize the rat preferably with 2% halothane and place it in a stereotax with the head tilted down to gain easy access to the back of the neck (*see* **Note 3**). Shave the back of the neck and make an anterocaudal incision starting at the interaural level and extending about 2 cm caudally. Cut the superficial neck muscles at the midline, but separate the deeper muscles naturally. Install retractors to allow access to the atlanto-occipital membrane. This is the membrane that links the back of the skull to the first vertebrae. Use a needle or the tip of a fine scalpel blade to delicately pierce this membrane. The atlanto-occipital membrane is composed of several layers. Once all the layers, including the dura, are cut, clear cerebrospinal fluid will flow out of the incision.

3.1.3. Catheter Insertion

At that point, the rat can be removed from the stereotax. The head needs to be tilted down at a 90° angle to allow the catheter to enter the spine from the smallest angle possible. Maintain the spine as straight as possible, when necessary, by gently tugging on the tail to decrease the possibility of injury to the cord.
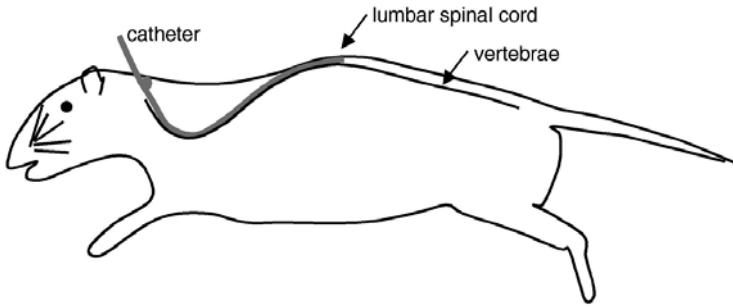
Fig. 1. Illustration of a rat with an implanted catheter. Note the location of the catheter tip in the lumbar spinal cord with respect to the total length of the vertebral column.

Push the catheter slowly along the dorsal side of the cord, while rotating the tubing between thumb and forefinger. Any increase in resistance probably indicates that the tip of the catheter has encountered an obstacle; it could be pushing against the bone or entering the spinal canal. In such a case, retraction of the catheter will usually solve the problem. Similarly, any twitching of the body probably indicates compression of a spinal root. It can be corrected by a small retraction of the catheter. Insert 8.5 cm of the catheter until the bead of dental cement rests upon the altanto-occipital membrane. This prevents the catheter from migrating posteriorly. Sew up the skin, leaving just 4–5 cm of the catheter externally (*see* **Note 4**). The external tip of the catheter can then be heated shut.

The choice of halothane or a similar anesthetic minimizes operative stress. During the procedure, the anesthetic level can be carefully monitored and kept at the minimum necessary to abolish nociceptive responses. Furthermore, the animal will wake up within 5 min after the operation. Therefore, the postoperative recovery period can be reduced to a few hours.

Any animal exhibiting any motor impairment should be immediately euthanized. Motor impairment can develop after surgery; therefore the animals need to be monitored regularly. Care must also be taken to monitor any sign of infection. If this occurs, application of an antibiotic ointment can prevent further infection (*see* **Note 5**).

3.1.4. Drug Injection

If the postoperative period is 5–7 d, it is necessary to first flush the catheter with saline to test whether scar tissue has obstructed the catheter tip. Drug injection can be performed a couple of hours later.

Construct the injector by connecting a steel tip (external diameter about 0.2 mm) to the end of a length of PE-10 tubing attached to a 50-μL Hamilton

syringe. It is easier to calibrate the tubing prior to injection; 10 μL will occupy a fixed length of tubing. Drugs should always be freshly prepared on the day of experiment and dissolved in saline. The injection volume is 10 μL (*see* **Note 6**). Aspirate into the injector 10 μL of saline, followed by a small bubble of air and 10 μL of the drug of interest. Flush the catheter with 10 μL of saline after drug injection.

For injection, the animal only needs to be lightly restrained until the injector is inserted into the catheter. Monitor the injection by observing the air bubble moving behind the solution. The effect of the drug should be seen 10 min after injection (*see* **Note 7**).

3.2. Acute Lumbar Puncture

Perform lumbar punctures with the steel tip of a 30-gage needle connected to PE-10 tubing attached to the tip of a Hamilton syringe. To avoid possible stress during the injection, anesthetize the animal with halothane (2%). Insert the needle between the lumbar vertebrae L5 and L6 (*see* **Note 8**) at a 20° angle. The needle can be passed between the spinous and transverse process of the vertebrae. Then reduce the angle to about 10° and insert the needle by about 0.5 cm. A tail flick marks the piercing of the dura. At that point, the tip of the needle should be in the subarachnoid space.

Monitor the injection by observing the moving air behind the solution. In rats, the volume of injection is 10 μL and 5 μL in mice. Drugs should be always prepared freshly on the day of experiments and dissolved in saline. After the injection, the animals will take 2–3 min to recover.

4. Notes

1. Isofluorane can be used as a less toxic alternative to halothane.
2. The catheter length varies depending on the size of the rat and the spinal level targeted. For instance, in 400–425 g rats, an 8.5-cm catheter will reach lumbosacral afferents, whereas in 350–400 g rats, it will reach the lumbar enlargement.
3. A stereotax is not entirely necessary, but it is particularly useful when one is learning the procedure.
4. No more than 4–5 cm of the catheter should be kept externally, to prevent it from being destroyed by the rat postoperatively or from getting caught in the cage.
5. It is rare that infections would occur in rats. However, if infections do occur, or if the catheter must be kept in place for a long time, sterile techniques must be applied for all surgeries. In particular, the instruments must be thoroughly disinfected and anything that might have come in contact with the skin should not touch the exposed muscles or membranes.
6. The volume injected is usually 10 μL in rats and 5 μL in mice. The maximal volume should not be more than 10% of the total CSF volume, which is unfortunately hard to estimate. The volume of the saline flush must remove the drug from the catheter.

7. The interpretation of the results needs to take into account several factors *(5)*.

   a. Indirect effects: As in any pharmacological experiment, any indirect effect of the drug, owing to pH, for instance, must be minimized. Furthermore, the lipophilicity of the drug appears to affect its effectiveness, as reflected in the time course.
   b. Locus of action: Any effect seen can be owing to a direct effect on spinal neurons or on the nerve roots. Depending on the spread of the drug in the cerebrospinal fluid, an effect seen after intrathecal injection could be owing to a supraspinal action. The antero caudal spread is obviously proportional to the volume injected. An injection of eight 10 µL of blue dye (Evans blue or bromophenol blue) will spread about 2.5–3.5 cm from the tip in each direction. The exact spread of the drug used will depend.

   Scar tissue will form at the tip of the catheter and eventually along its whole length. This can alter the diffusion of the drug and should be taken into account when comparing injections over several days.

   Apart from controlling the volume of the injection, control experiments can also be done to clarify the site of action of the drug. Injection at various spinal levels should produce different effects, corresponding to the variations in receptor distribution. Injection at the cervical level, using a shorter catheter, should produce greater effects if drugs act through supraspinal structures. However, less or no effect may be induced if drugs primarily act on neurons in the lumbar spinal cord *(6)*. The definitive identification of the spread of the drug can be made using a radioactively tagged drug.

   It is also important to point out that drugs may produce effects by acting on spinal interneurons and/or motor neurons. For example, the inhibition of behavioral responses to noxious stimuli may not necessarily be directly interpreted as reflecting the inhibition of nociceptive transmission in the spinal cord. It is important to assure the effects of drugs by using other approaches such as in vivo electrophysiological recordings of spinal dorsal horn neurons and in vitro synaptic electrophysiology in spinal cord slices *(7, 8)*.

8. At the intersection between L5 and L6, the cord consists mostly of the cauda equina. This spinal level is chosen to minimize potential damage to the cord while being as close as possible to it.

References

1. Yaksh, T. L. and Rudy, T. A. (1976) Chronic catheterization of the spinal subarachnoid space. *Physiol. Behav.* **17,** 1031–1036.
2. Yaksh, T. L. and Rudy, T. A. (1976) Analgesia mediated by a direct spinal action of narcotics. *Science* **192,** 1357–1358.
3. Hylden, J. L. and Wilcox, G. L. (1980) Intrathecal morphine in mice: a new technique. *Eur. J. Pharmacol.* **67,** 313–316.
4. Mestre, C., Pelissier, T., Fialip J., Wilcox G., and Eschalier, A. (1994) A method to perform direct transcutaneous intrathecal injection in rats. *J. Pharm. Toxicol. Meth.* **32,** 197–200.

5. Hammond, D. L. (1988) Intrathecal administration: methodological consider-
   ations. *Progr. Br. Res.* **77,** 313–320.
6. Chiang, C. Y. and Zhuo, M. (1989) Evidence for the involvement of descending
   cholinergic pathway in systemic morphine analgesia. *Brain Res.* **478,** 293–300.
7. Li, P., Wilding, T. J, Kim, S. J., Calejesan, A. A., Huettner, J. E., and Zhuo, M.
   (1999) Kainate receptor-mediated sensory synaptic transmission in mammalian
   spinal cord. *Nature* **397,** 161–164.
8. Li, P. and Zhuo, M. (2001). Cholinergic, noradrenergic and serotonergic inhibi-
   tion of fast synaptic transmission in spinal lumbar dorsal horn of rat. *Brain Res.
   Bull.* **54,** 639–647.

16

Opioid Tolerance in Adult and Neonatal Rats

Zhizhong Z. Pan

1. Introduction

One of the main actions of natural and synthetic opioids is powerful analgesia. For many decades, opioid-based drugs, such as morphine, remain to be the most effective analgesics and are widely used in current clinical management of various pain conditions. They are particularly required to chronically treat severe and persistent pain in patients suffering from chronic diseases, such as cancer. Repeated use of opioid drugs, however, induces the development of opioid tolerance that reduces their analgesic potency so that increasing doses are required to maintain the desired level of analgesia. As opioids also have undesirable and even dangerous side effects at higher doses, such as respiratory depression, opioid tolerance is, therefore, a major problem in clinical management of pain.

In order to circumvent opioid tolerance and improve opioid treatment of chronic pain, intensive clinical and animal studies have been undertaken for decades to investigate the neurobiological mechanisms underlying the development of opioid tolerance. We now know that opioid tolerance results from complex adaptive or compensatory responses to chronic exposure to opioid drugs in both opioid receptors and other neurotransmission systems of the central nervous system (CNS) *(1,2)*. These adaptive responses counteract opioid actions at the receptor, cellular, and system levels, resulting in reduced opioid-mediated analgesic effects. Our knowledge of the adaptive responses after chronic opioid exposure has been remarkably advanced in recent years. Multiple adaptive

changes at molecular and cellular levels have been identified and related to the development of opioid tolerance. Most important changes include desensitization of opioid receptors, upregulation of the cyclic AMP (cAMP) signal transduction pathway and activation of numeral protein kinases *(2,3)*. The mechanism for opioid receptor desensitization, common for the family of G- protein-coupled receptors, has been well characterized in terms of its contribution to opioid tolerance. Activation of opioid receptors by the continuous presence of opioid agonists promotes receptor phosphorylation through G protein coupled receptor kinases. Receptor phosphorylation and subsequent binding to β-arrestin lead to receptor uncoupling from G proteins and receptor sequestration, diminishing opioid receptor-mediated actions and contributing to opioid tolerance *(2,4–7)*. An upregulated cAMP system enhances GABA synaptic transmission *(8–10)*, changes ion channel activity *(11,12)*, and alters gene expression through protein kinase A *(13,14)*. However, the roles of these cAMP-mediated effects in the induction of opioid tolerance are still unknown. Finally, chronic opioids also activate many protein kinases including kinase C and mitogen-activated protein kinases (MAPKs) to possibly change gene expression in a long term *(3,15,16)*. Although the involvement of these protein kinases in opioid tolerance has been well characterized, the mechanisms underlying their contribution to opioid tolerance remain unclear.

Currently, a major challenging goal for studies of opioid tolerance is to understand the detailed molecular and cellular mechanisms of opioid tolerance and then develop new pharmacological strategies to overcome tolerance problems. However, we do not know at present how most of these identified changes lead to the reduced analgesic effect of opioids. The adaptive changes identified in studies on isolated cells in vitro still cannot explain the magnitude of opioid tolerance found in intact systems. Important adaptations also occur at the local neuronal networks mediating opioid analgesia through altered receptor expression, ion channel activity, and synaptic transmission. Our knowledge is particularly lacking regarding network adaptations and how they contribute to opioid tolerance. Network adaptations are manifested in interactions between different opioid receptor subtypes and between opioid and other receptor systems as well as in synaptic transmission between functionally distinct types of neurons. Finally, recent molecular studies using genetic tools have been particularly successful in identifying the role of specific proteins in the signal transduction pathway for opioid receptors in the development of opioid tolerance *(5,17,18)*. Overall, all these mechanistic studies are required to use animal models of opioid tolerance. An animal model of opioid tolerance is and will remain to be a fundamental and necessary tool for studies on opioid tolerance at the molecular, cellular, and system levels. It also serves as a represen-

tative model system to study the general plasticity of signal transduction pathways and neural networks in the brain.

As in other research fields, the most commonly used animals for opioid tolerance models are rodents. A rat model has been most widely used in opioid tolerance studies due to our most extensive knowledge of the animal through previous studies. Opioid studies with molecular and genetic tools generally use mice. That makes a mouse model of opioid tolerance increasingly popular. The method to induce opioid tolerance is similar in these two species.

Another interesting issue is the ontogeny of opioid tolerance in neonates. Opioid drugs are increasingly used in human neonates and infants for various pain conditions and tolerance is also a main problem in these young patients receiving chronic opioid treatments at increasing doses *(19)*. Furthermore, neonatal rats are often used in opioid studies that involve visualization of live, unstained neurons, because young rats have technical advantages over adult rats in offering clearer images of neurons in preparations in vitro *(20)*. Therefore, both clinically and experimentally, there is a need to use an opioid tolerance model of neonatal rats, in addition to adult models. Nevertheless, few studies have been directed at the development of opioid tolerance in neonates. Moreover, although it is generally accepted that opioid tolerance develops in neonatal rat, there has been a discrepancy that at what age chronic opioids induce analgesic tolerance *(19,21–25)*. Thus, when neonatal animals of various ages are used, it is important to demonstrate the existence of opioid tolerance with a specific procedure of chronic opioid treatment. This chapter describes step-by-step methods to induce morphine tolerance in adult and neonatal rats.

2. Materials

1. Rats, Sprague–Dawley, or Wistar strain at various ages depending on needs (generally from newborn to 300 g).
2. Animal cone bags (Stoelting Co., IL).
3. Halothane, an anesthetic.
4. Surgical tools and a hair clipper.
5. Morphine pellets, containing 75 mg morphine each (light sensitive, stored at room temperature).
6. Placebo pellets.
7. Morphine sulfate, made with saline solution, 1 mg/mL–10 mg/mL (light sensitive, stored at 4°C, stable for weeks).
8. Alzet osmotic minipumps (Alza Corp., CA).
9. Wound clips.
10. A heating pad (37°C).
11. An analgesia Instrument (Stoelting Co)

3. Methods

There are generally two methods commonly used to induce morphine tolerance: implantation of morphine pellets or osmotic minipumps and injections of morphine solution (*see* **Note 1**), described in details later. Both methods can be applied to adult or neonatal rats, although some procedures are slightly different and extra care is needed for neonatal rats.

3.1. Implantation of Morphine Pellets

Subcutaneous implantation of morphine pellets is the most commonly used method in current studies with adult rats. It has been well established and generally accepted as a reliable way to induce morphine tolerance in adult rats. However, it is more difficult to perform the implantation in neonatal rats owing to their small sizes. Implantation of minipumps has been successfully used in postnatal d 6 rats *(25)*.

3.1.1. Animals

Male rats (*see* **Note 2**) were randomly divided into two groups. The morphine group received implantation of morphine pellets and rats in the control group were implanted with placebo pellets as control with the same procedure and schedule.

3.1.2. Anesthesia

In a fume hood, an adult rat was placed in a cone bag with its nose sticking out through the front opening of the bag and the back of the bag was closed by hand. This restraint is not necessary for neonatal rats. Instead, a neonatal rat was placed on a heating pad (37°C) because of its inability to thermoregulate by itself. The rat was then anesthetized via inhalation of halothane. Adequate anesthesia was indicated by the lack of response to paw pinch. The anesthesia level was constantly monitored throughout the implantation procedure to ensure adequate anesthesia and to avoid overdose. The advantage of this anesthesia method is its quickness. The rat can recover later from the anesthesia in just minutes.

3.1.3. Surgery and Implantation

After the hair was shaved, the skin over one side of the caudal dorsum was swabbed with 70% ethanol and an incision of approx 1 cm was made with a surgical blade. The subcutaneous space was then separated through the incision for implantation of pellets or minipumps. For the morphine group, one morphine pellet was implanted in a rat on d 1. On d 4, two more morphine pellets were implanted in the other side of the dorsum in the same rat. Same implantation schedules were followed to implant placebo pellets in rats from the control

group. Osmotic minipumps loaded with either morphine or saline solution can be implanted with the same procedure, but implantation of one minipump for 3–5 d is usually adequate to induce morphine tolerance. After each implantation, the incision was closed with wound clips. The rat was then allowed to recover from anesthesia before being returned to an animal care facility. The health conditions of these implanted rats were carefully monitored daily. Animals that show clear signs of pain, infection, diseases, or other health problems should be excluded from studies.

3.2. Injections of Morphine Solution

This method also induces consistent analgesic tolerance to morphine in both adult and neonatal rats if proper morphine dosage and injection regimen are adopted. Because of implantation difficulties on neonatal rats less than 1-wk old, this injection method is often used to induce morphine tolerance in neonatal rats.

3.2.1. Animals and Anesthesia

The anesthesia procedures are the same as those in the implantation method described in (**Subheadings 3.1.1.** and **3.1.2.**). Rats were randomly divided into the morphine group and the control group to receive morphine injections or saline injections, respectively. A rat was briefly anesthetized before injection.

3.2.2. Injection Regimen

A rat received twice daily injections of morphine or saline for 6 d, one approx at 9 AM and the second injection at around 6 PM on each day. Morphine solution (1 mg/mL–10 mg/mL, 0.1–0.3 mL) was injected either subcutaneously (sc) or intrapertoneally (ip) (*see* **Note 3**). The dose of morphine was 10 mg/kg on the first day and increased by 5 mg/kg each day to reach a maximum dose of 30 mg/kg on day 5 (*see* **Note 4**). Analgesia tests were taken on d 7 on rats in both morphine- and saline-treated groups.

3.3. Analgesia Tests

The analgesic effect of morphine in control and morphine-treated rats (implantation or injection) can be measured by commonly used analgesia tests such as the tail-flick (TF) test or the paw withdrawal (PW) test.

3.3.1. Test Procedures

The pain threshold of a rat was measured with an analgesia instrument (Stoelting Co.). This instrument can be used for both TF and PW tests. A rat to be tested was placed in the glass chamber with glass bottom and was allowed to move around within the chamber for about 20 min. This step habituates the

animal to the test environment to avoid consequent stress-induced analgesia. Furthermore, the animal can move freely during the entire process of testing, eliminating the interfering stress-induced analgesia resulting from handling and restraining of the rat *(26)* (*see* **Note 5**). To test pain threshold, a laser heat source was pointed to the bottom of the tail (TF test) or paw (PW test). A rat flicks its tail or withdrawal its paw from the heat source when it feels pain. The time between the start of the heat stimulus and the moment of the rat response was automatically recorded as pain threshold, or latencies.

3.3.2. Baseline Latencies

For each rat, a number of trials were performed until steady latencies were obtained. Then 4–6 latencies were taken as baseline latencies (usually 3–4 s for TF tests). The following steps were followed to avoid tissue damage and to get consistent results.

1. Trials were at least 2 min apart.
2. Two to three fixed tail locations or different paws of a rat were used alternatively in a single test.
3. A cutoff time was set (between 10–12 s for TF tests) so that the heat stimulus was shut off at the cutoff time even without the rat's response.

3.3.3. Morphine Latencies and Dose-Response Curves

After baseline latency measurements, a rat was given a series of four or five morphine injections (sc or ip) at increasing doses with a logarithmic scale. Latencies were measured 30 min after the first injection and each subsequent injections that immediately followed. Thus, injections were performed sequentially with increasing doses. Morphine doses were chosen so that at the maximum dose, the latency did not increase or the cutoff time was reached. Morphine latencies were then converted to a percentage maximum possible effect (%MPE) according to the equation: %MPE = [(morphine latency–baseline latency)/(cutoff time - baseline latency)] × 100. A cumulative dose-response curve was then constructed by plotting the %MPE against the morphine doses.

3.4. Data Analysis and Assessment of Morphine Tolerance

Baseline latencies and morphine latencies were obtained both before (d 0) and after (d 7) (*see* **Note 6**) the chronic treatment in both morphine and control groups. ED_{50} values and 95% confidence intervals for each curve were calculated (Prism 2, Graphpad, Inc.) and compared to assess the development of morphine tolerance. A statistically significant rightward shift of the ED_{50} values after the treatment in the morphine group, but not in the control group, suggests the occurrence of morphine tolerance.
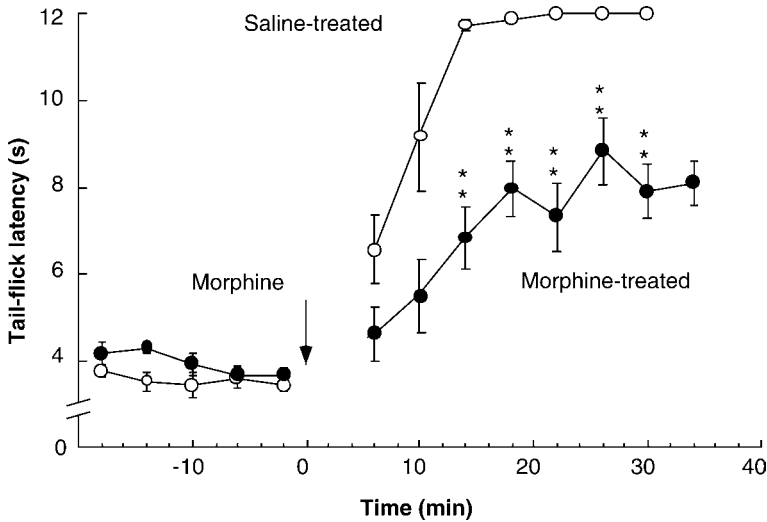
Fig. 1. Tolerance induced by chronic morphine in neonatal rats. Tail-flick laten-cies (mean + SEM) were recorded from saline- or morphine-treated rats ($n = 8$ in each group) before and after a test dose of morphine (10 mg/kg, ip) injected at time 0. ** $p < 0.01$, an ANOVA for repeated measures and the Tukey/Kramer procedure of *post hoc* analysis.

Fig. 1 shows an example of morphine tolerance in neonatal (9-d old) rats. Young male rats were treated with saline or morphine by daily injections according to the doses and injection regimen described above (**Subheading 3.2.2.**). On day 7, a test dose of morphine (10 mg/kg, ip) produced signifi-cantly less analgesic effect in the morphine-treated group than in the saline-treated group. This result demonstrates the existence of morphine tolerance in neonatal rats.

4. Notes

1. Both implantation and injection methods can induce reliable morphine tolerance in rats and mice. The implantation method is often preferred, especially for adult rats or mice because much less animal handling is needed during treatment. It reduces the workload and more importantly, decreases the potential effect of repeated handling on the development of morphine tolerance. Another advantage is that it permits studies on the time-course of tolerance development on a daily basis with a test dose of morphine. A potential pitfall of this method is inconsis-tent release of morphine from implanted pellets, causing possible temporary with-drawal. An osmotic minipump can eliminate this problem by releasing its content constantly through a period of several days. The daily injection method is some-what closer to common clinical settings at which patients receive increasing doses

of opioids periodically, or to the case of drug addicts for studies on opioid addiction. That is why chronic treatment with an increasing dose regimen is generally adopted. Repeated daily injections and handling, however, cause animal stress and could potentially interfere with the development of opioid tolerance.

2. Previous studies have demonstrated that sensitivity to the analgesic effect of morphine, to the effects of different opioid receptor agonists and susceptibility to the development of opioid tolerance can be significantly different in different gender of both animals and humans *(27–29)*. Therefore, whenever possible, it is recommended to use single gender to avoid the complication.

3. A common problem in injections is leaking of drug solution after withdrawal of the needle, particularly in neonatal rats. Because of the small volume injected, the result could be significant. Small injection volumes, slow process of injection, and needle withdrawal can usually prevent the problem. Slight side-way movement of the needle tip within the subcutaneous space also helps.

4. There are conflicting reports on the age of neonatal rats at which opioid tolerance occurs. An important fact one should be aware of is that μ-opioid receptors proliferate significantly during the first 2 wk after birth in rats *(22,30)*. Accordingly, analgesic effect of morphine increases during that period *(30)*. Thus, using too-low doses in neonatal rats could run the risk of undetected opioid tolerance that is masked by the increasing analgesic effect of morphine within that period.

5. It is known that restraining animals causes stress-induced analgesia *(26,31)*. The extent of this effect could vary among restraints from time to time. Apparently, stress-induced analgesia affects pain threshold measured during analgesic tests for the assessment of morphine tolerance. It is, therefore, the most appropriate to take analgesia tests on unrestraint, freely moving animals.

6. It is well documented that during opioid withdrawal, pain sensitivity increases, a phenomenon defined as opioid withdrawal-induced hyperalgesia. Opioid withdrawal can be triggered by abrupt opioid abstinence. Therefore, it is important to perform analgesia tests at an appropriate time after chronic opioid treatment. In order to avoid both problems of opioid residues from a previous dose and opioid withdrawal, analgesia tests are most commonly taken near the time when the next morphine dose would otherwise be applied by schedule.

Acknowledgment

References

1. Nestler, E. J. (1996) Under siege: The brain on opiates. *Neuron* **16,** 897–900.
2. Williams, J. T., Christie, M. J., and Manzoni, O. (2001) Cellular and synaptic adaptations mediating opioid dependence. *Physiol. Rev.* **81,** 299–343.

3. Liu, J. G. and Anand, K. J. (2001) Protein kinases modulate the cellular adaptations associated with opioid tolerance and dependence. *Brain Res. Brain Res. Rev.* **38,** 1–19.

4. Ozaita, A., Escriba, P. V., Ventayol, P., Murga, C., Mayor, F. Jr., and Garcia-Sevilla, J. A. (1998) Regulation of G protein-coupled receptor kinase 2 in brains of opiate-treated rats and human opiate addicts. *J. Neurochem.* **70,** 1249–1257.

5. Bohn, L. M., Gainetdinov, R. R., Lin, F. T., Lefkowitz, R. J., and Caron, M. G. (2000) Mu-opioid receptor desensitization by beta-arrestin-2 determines morphine tolerance but not dependence. *Nature* **408,** 720–723.

6. Bohn, L. M., Lefkowitz, R. J., Gainetdinov, R. R., Peppel, K., Caron, M. G., and Lin, F. T. (1999) Enhanced morphine analgesia in mice lacking beta-arrestin 2. *Science* **286,** 2495–2498.

7. Hurle, M. A. (2001) Changes in the expression of G protein-coupled receptor kinases and beta-arrestin 2 in rat brain during opioid tolerance and supersensitivity. *J. Neurochem.* **77,** 486–492.

8. Ingram, S. L., Vaughan, C. W., Bagley, E. E., Connor, M., and Christie, M. J. (1998) Enhanced opioid efficacy in opioid dependence is caused by an altered signal transduction pathway. *J. Neurosci.* **18,** 10,269–10,276.

9. Bonci, A. and Williams, J. T. (1997) Increased probability of GABA release during withdrawal from morphine. *J. Neurosci.* **17,** 796–803.

10. Jolas, T., Nestler, E. J., and Aghajanian, G. K. (2000) Chronic morphine increases GABA tone on serotonergic neurons of the dorsal raphe nucleus: association with an up-regulation of the cyclic AMP pathway. *Neurosci.* **95,** 433–443.

11. Chieng, B. and Christie, M. D. (1996) Local opioid withdrawal in rat single periaqueductal gray neurons in vitro. *J. Neurosci.* **16,** 7128–7136.

12. Kogan, J. H., Nestler, E. J., and Aghajanian, G. K. (1992) Elevated basal firing rates and enhanced responses to 8-Br-cAMP in locus coeruleus neurons in brain slices from opiate-dependent rats. *Eur. J. Pharmacol.* **211,** 47–53.

13. Koob, G. F. Sanna, P. P., and Bloom, F. E. (1998) Neuroscience of addiction. *Neuron* **21,** 467–476.

14. Nestler, E. J. and Aghajanian, G. K. (1997) Molecular and cellular basis of addiction. *Science* **278,** 58–63.

15. Ortiz, J., Harris, H. W., Guitart, X., Terwilliger, R. Z., Haycock, J. W., and Nestler, E. J. (1995) Extracellular signal-regulated protein kinases (ERKs) and ERK kinase (MEK) in brain: regional distribution and regulation by chronic morphine. *J. Neurosci.* **15,** 1285–1297.

16. Schulz, S. and Hollt, V. (1998) Opioid withdrawal activates MAP kinase in locus coeruleus neurons in morphine-dependent rats in vivo. *Eur. J. Neurosci.* **10,** 1196–1201.

17. Zeitz, K. P., Malmberg, A. B., Gilbert, H., and Basbaum, A. I. (2001) Reduced development of tolerance to the analgesic effects of morphine and clonidine in PKC gamma mutant mice. *Pain* **94,** 245–253.

18. Ueda, H., Inoue, M., Takeshima, H., and Iwasawa, Y. (2000) Enhanced spinal nociceptin receptor expression develops morphine tolerance and dependence. *J. Neurosci.* **20,** 7640–7647.

19. Suresh, S. and Anand, K. J. (2001) Opioid tolerance in neonates: a state-of-the-art review. *Paediatr. Anaesth.* **11,** 511–521.
20. Pan, Z., Tershner, S., and Fields, H. (1997) Cellular mechanism for anti-analgesic action of agonists of the κ-opioid receptor. *Nature* **389,** 382–385.
21. Windh, R. T., Little, P. J., and Kuhn, C. M. (1995) The ontogeny of mu opiate tolerance and dependence in the rat: antinociceptive and biochemical studies. *J. Pharmacol. Exp. Ther.* **273,** 1361–1374.
22. Van Praag, H. and Frenk, H. (1991) Evidence for opiate tolerance in newborn rats. *Brain Res. Dev. Brain Res.* **60,** 99–102.
23. Barr, G. A. and Wang, S. (1992) Tolerance and withdrawal to chronic morphine treatment in the week-old rat pup. *Eur. J. Pharmacol.* **215,** 35–42.
24. Fanselow, M. S. and Cramer, C. P. (1988) The ontogeny of opiate tolerance and withdrawal in infant rats. *Pharmacol. Biochem. Behav.* **31,** 431–438.
25. Thornton, S. R. and Smith, F. L. (1997) Characterization of neonatal rat fentanyl tolerance and dependence. *J. Pharmacol. Exp. Ther.* **281,** 514–521.
26. Mogil, J. F.-G., Grisel, J., Reinscheid, R., Civelli, O., Belknap, J., and Grandy, D. (1996) Orphanin FQ is a functional anti-opioid peptide. *Neurosci.* **75,** 333–337.
27. South, S. M., Wright, A. W., Lau, M., Mather, L. E., and Smith, M. T. (2001) Sex-related differences in antinociception and tolerance development following chronic intravenous infusion of morphine in the rat: modulatory role of testosterone via morphine clearance. *J. Pharmacol. Exp. Ther.* **297,** 446–457.
28. Tershner, S. A., Mitchell, J. M., and Fields, H. L. (2000) Brainstem pain modulating circuitry is sexually dimorphic with respect to mu and kappa opioid receptor function. *Pain* **85,** 153–159.
29. Gear, R. W., Miaskowski, C., Gordon, N. C., Paul, S. M., Heller, P. H., and Levine, J. D. (1996) Kappa-opioids produce significantly greater analgesia in women than in men. *Nat. Med.* **2,** 1248–1250.
30. Zhang, A. and Pasternak, G. (1981) Ontogeny of opioid pharmacology and receptors: high and low affinity site differences. *Eur. J. Pharmacol.* **73,** 29–40.
31. Vaccarino, A. L., Olson, G. A., Olson, R. D., and Kastin, A. J. (1999) Endogenous opiates: 1998. *Peptides* **20,** 1527–1574.

17

Animal Models of Neuropathic Pain

William J. Martin, Laike St. A. Stewart, and Jason W. Tarpley

1. Introduction

Despite its prevalence, nerve injury-related (neuropathic) pain in humans is not well understood and, as such, remains difficult to manage *(1–3)*. A variety of clinical conditions can lead to neuropathic pain, which contributes to our lack of understanding of this phenomenon. Although there is substantial etiological heterogeneity among neuropathic pain conditions, commonalities exist. For example, most patients present with combinations of spontaneous and stimulus-evoked pain, the latter of which is characterized by a hypersensitivity to previously innocuous tactile or thermal stimuli (allodynia). To improve our understanding of neuropathic pain, the challenge for basic scientists has been twofold: 1) to develop animal models of persistent pain that more closely mimic clinical pain in humans; and 2) to ensure high reproducibility, within and between animals, across different investigators and laboratories.

The models of nerve injury developed in rodents over the past 15 yr have helped elucidate the putative mechanisms that contribute to persistent neuropathic pain in humans. Though these models differ by the locus and type of injury, most of them involve traumatic injury to peripheral nerves which lead to behavioral hypersensitivity similar to that observed clinically. For example, partial ligation (PSL) *(4)* or constriction of the sciatic nerve (CCI) *(5)*, ligation of the L5/L6 spinal nerves (SNL) *(6)*, or the transection of two nerves while sparing a third (spared nerve injury model, SNI) *(7)* all increase sensitivity to nonpainful (allodynia) and painful (hyperalgesia) stimuli. The behavioral manifestations of these different injuries, however, vary in magnitude, time-course

and, to some extent, by modality (e.g., mechanical, thermal). Moreover, because the surgical procedures and behavioral evaluation that accompany these models are more complex than those involving inflammation and/or acute nociception, variability between different investigators/laboratories can be high, which may confound efforts to identify underlying mechanisms and/or novel therapeutic agents. The purpose of this chapter is to describe the surgical procedures for two models of neuropathic pain, as well as the procedures for determining behavioral hypersensitivity.

2. Materials

1. Rats, 150–280 g at time of surgery (*see* **Note 1**).
2. Rodent anesthesia system with Isoflurane vaporizor.
3. Electric clippers.
4. 70% alcohol , 10% povidone-iodine solution.
5. Sterile drape fenestrated (Henry Schein Melville, NY).
6. Scalpel and surgical blades # 10.
7. Micro Dissecting Scissors #RS-5990 (Roboz Surgical, Rockville, MD).
8. 3" McPherson Vanna microscissors (Roboz).
9. 4" Micro Dissecting Scissors with probe points (Miltex 18-784).
10. 4 1/2" tissue forceps (Roboz Surgical RS-8160).
11. 5 1/2" straight crile forceps (Henry Schein HS- 100-5322).
12. 5 1/2" straight metzenbaum scissors (F.S.T. 14018-13).
13. 3 1/2" Hartman mosquito forceps (Roboz Surgical RS-7101).
14. Microrongeur with extra-fine tips (SNL only: Fine Science Tools Foster City, CA).
15. Sterile cotton-tipped applicators.
16. #5 forceps 11 cm × 2 (Fine Science Tools Foster City, CA).
17. Glass hook-ca. 2 mm diameter (made in-house).
18. Stainless-steel wound clips (SurgiMate skin stapler 35R-25-3002, DeRoyal Industries, Inc. Powell, TN).
19. 6-0 Silk suture, 3-0 Polydiaxone (Ethicon, Somerville, NJ).
20. Needle holder (Fine Science Tools Foster City, CA).
21. 0.9% sterile saline (Phoenix Scientific, St. Joseph, MO) 2" × 2" 4-ply cotton gauze (Johnson and Johnson).
22. Recirculating heating pad system (Gaymar T/Pad Temperature Therapy System).
23. Bead sterilizer (Germinator Rockville, MD).
24. von Frey Monofilament kit (Stoelting, Wood Dale, IL).
25. Wire mesh or plastic (with holes) platform.
26. Polycarbonate boxes (8 cm × 8 cm).
27. Acetone.

3. Methods

3.1. The Spared Nerve Injury Model (ref. 7): Axotomy and Ligation of the Tibial and Common Peroneal Nerves, Leaving the Sural Nerve Intact

1. Anesthetize animals with 3–4% isoflurane in an induction chamber (*see* **Note 2**).
2. Remove animal and shave the left lateral hind limb to the level of the wing of the ilium, dorsally, and to the level of the sacrum, caudally, and the tarsus ventrally. Clean area with 70% alcohol swabs and liberally apply 10% povidone-iodine scrub to left lateral thigh and distal hind limb.
3. Maintain animal at 2–3% isoflurane via a nose cone on heated surgical platform. Place animal in right lateral recumbency and the limb through the opening in the sterile drape.
4. Palpate the head of the femur and the stifle as landmarks. Incise the skin on the lateral thigh, approx 1/2″ caudal and ventral to the head of the femur with a # 10 blade. Skin incision should only be 1–1 1/2″ in length. Incise to the level of the distal one-third of the femur.
5. Make a section directly through the biceps femoris and vastus lateralis muscles. Use the microdissecting scissor with probe points to separate the muscle belly in the direction of the initial skin incision. When approaching the nerves, care should be taken when dissecting the muscle belly, as the common peroneal nerve is in close proximity to the overlying muscle.
6. Careful blunt dissection results in exposure of the sciatic nerve and its three terminal branches (sural, common peroneal, and tibial nerves) at the mid- to lower-thigh level. Carefully identify and isolate the common peroneal nerve which courses on top of a branch of the popliteal artery, cranially and ventrally toward the stifle. Elevate the nerve using the curved microdissecting forceps (or glass hook) and double ligate the nerve with (6-0) silk suture (*see* **Note 3**).
7. Transect between the ligatures, removing a section 2–3 mm in length. Caudal to the stifle, and dorsal to the gastrocnemius muscle, the tibial nerve can be visualized by elevating the fat and connective tissue overlaying it. With the Crile forceps, gently elevate the fat pad dorsally to visualize the tibial nerve and associated structures (*see* **Fig. 1**).
8. With the curved forceps, gently isolate the tibial nerve, which is the largest of the three and courses beneath the popliteal artery (a branch of the femoral artery), from surrounding connective tissue. Avoid manipulation of the sural nerve, which courses directly behind the tibial nerve in a caudal-ventral direction. Elevate the tibial nerve and introduce two silk ligatures. Be aware of, and avoid ligating, the popliteal artery which travels perpendicular to the tibial nerve, at the level of the proximal ligature. Double ligate the tibial nerve and remove a section of 1–2 mm, if possible. Note that if the tibial nerve is exposed very distal from the trifurcation, then the gastrocnemius nerves will branch from the tibial nerve.
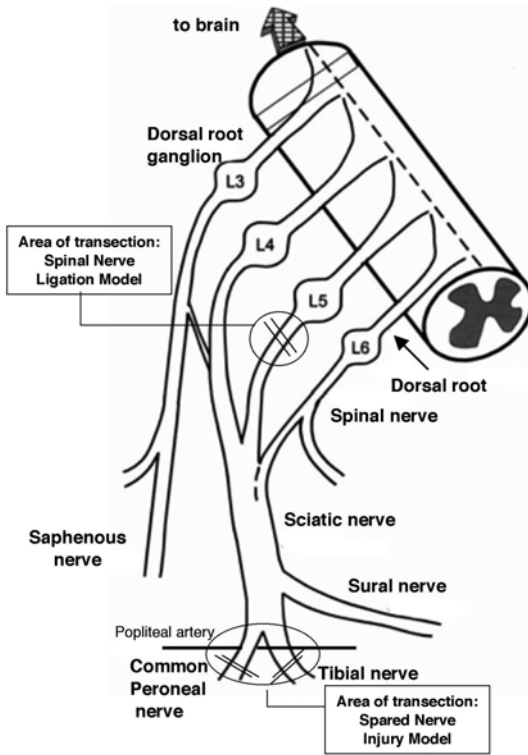
Fig. 1. Schematic representation of the sciatic and saphenous nerves. Illustrated is the target area for the SNI and SNL models. (*n* = 5/group.) (Modified from **ref. 7** with permission by the IASP, Seattle, WA.)

9. Close muscle and fascia with 3-0 Polydiaxone (PDS) to avoid dead space and subsequent serous fluid accumulation at the site of injury. Close the skin incision with stainless steel wound clips. Recover animals in their respective cages, which should be placed on heating pads. Observe animals periodically throughout the day for adequate recovery, ambulation, and signs of autotomy. Wound clips should be removed within 7–10 d postoperatively (*see* **Note 4**).

3.2. Ligation and Transection of the L5 Spinal Nerve: A Modification of the Model by Kim and Chung, 1992 (ref. 6)

1. Rats should be in the range of 150–220 g at the time of surgery (*see* **Note 5**).
2. Anesthetize animals with 3–4% isoflurane in an induction chamber. Remove animal and shave the sacral region of the back. Clean area with 70% alcohol swabs and liberally apply 10% povidone-iodine scrub.
3. Maintain animal at 2–3% isoflurane via a nose cone on heated surgical platform. With a #10 scalpel blade, make a sagittal incision in the skin about 3-cm long

along the dorsum of the back. The midpoint of the incision should be placed at the level of the iliac crests (with a 1.5-cm incision rostral and caudal to the crests).

4. Palpate the vertebral column to locate the spinous processes. Directly left and lateral to the row of spinous processes, make an incision through the erector muscles of the spine. This incision should be 2-cm long and to the depth of the transverse processes below. Retract skin and muscle (*see* **Note 6**).

5. With the wooden handle of a sterile cotton swab, bluntly dissect the muscles and tendons to expose the transverse process directly across the iliac crest. Use the cotton-tipped end of the applicator to clear the area of blood/debris. Visualize the tip of the iliac crest and the transverse process (L6) that is directly medial to it (*see* **Note 7**).

6. Remove the lateral half of the L6 transverse process with the rongeurs, being careful not to damage either nerve lying beneath it. This will expose one or both of the nerves beneath (L4, L5).

7. Gently lower a small glass hook into the cavity and isolate the L5 spinal nerve. L5 is located medial to L4. Avoid manipulation with L4. Excessive manipulation of L4 can result in paralysis. With 6-0 silk, ligate the L5 nerve twice leaving 2–3 mm between the ligatures. Transect the nerve between the ligatures with microscissors.

8. Carefully return the two nerve ends to their *in situ* position and remove the retraction. Flush the surgical area with 0.9% normal sterile saline and remove excess saline with sterile gauze. Close the incision using 3-0 PDS for muscle and fascia and surgical clips for the skin.

9. Recover animals in their respective cages until fully ambulatory. Cages should be placed on heating pads. Observe animals periodically throughout the day for adequate recovery, ambulation, and signs of autotomy. Wound clips should be removed within 7–10 d postoperatively (*see* **Note 4**).

3.3. Behavioral Determination of Hypersensitivity (see *Fig. 2*)

3.3.1. Static Mechanical Allodynia (see *Fig. 3*)

Mechanical allodynia is measured by testing the force required to elicit a paw withdrawal reflex to an innocuous stimulus using calibrated von Frey filaments, using the up-down paradigm, as previously described *(8)*. Animals will be placed in a test chamber on a wire mesh screen and a series of calibrated nylon monofilaments (von Frey) will be applied to the plantar surface (medial/lateral) for 6 s or until the hind paw is withdrawn briskly.

Place animals in individual polycarbonate boxes on a raised platform, and allow to acclimate for 30–60min. Two test sessions should be carried out before surgery (baseline measurements). To determine the 50% response threshold, apply von Frey filaments in an ascending fashion (over a range of intensities from 0.4 to 28.8 g; handle marking 3.61, 3.84, 4.08, 4.31, 4.56, 4.74, 4.93, 5.18, 5.46) for 6 s or until a withdrawal response occurs. Test in the same area on each hind paw (*see* **Note 8**).
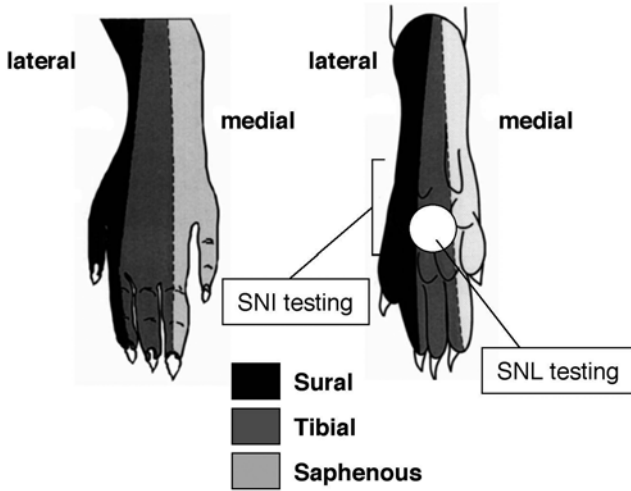
Fig. 2. Diagram of the zones of innervation of the hind paw by the sciatic and saphenous nerves. The areas for testing of allodynia for the SNI and SNL models are shown. (Modified from **ref. 7** with permission by the IASP, Seattle, WA.)

Begin with the mid-range filament. After eliciting a positive response, test an incrementally weaker stimulus. If there is no response to a stimulus, then present an incrementally stronger stimulus. A positive response is recorded as "X" and a negative response as "0." After the initial threshold crossing, repeat this procedure for four stimulus presentations per animal per test session. Calculate mechanical sensitivity by interpolating the 50% response threshold using the following formula *(8)*:

$$50\% \text{ g threshold} = (10^{[Xf + k\delta]})/10{,}000$$

where Xf = value (in log units) of the final von Frey filament used; k = tabular value [*see (8)* for value based on response pattern]; and δ = mean difference (in log units) between stimuli. If there are no responses to any filament and/or the paw is lifted by the application of the highest force filament, then the threshold for that filament is assigned.

3.3.2. Dynamic Mechanical Allodynia *(*see **Fig. 4A***)*

Dynamic allodynia is tested after static allodynia by using a camel-hair brush to gently stroke the plantar surface of the injured and then noninjured hindpaw. Brush at a rate of 1 stroke/s for 15 s or until a withdrawal response occurs. Record time of withdrawal.
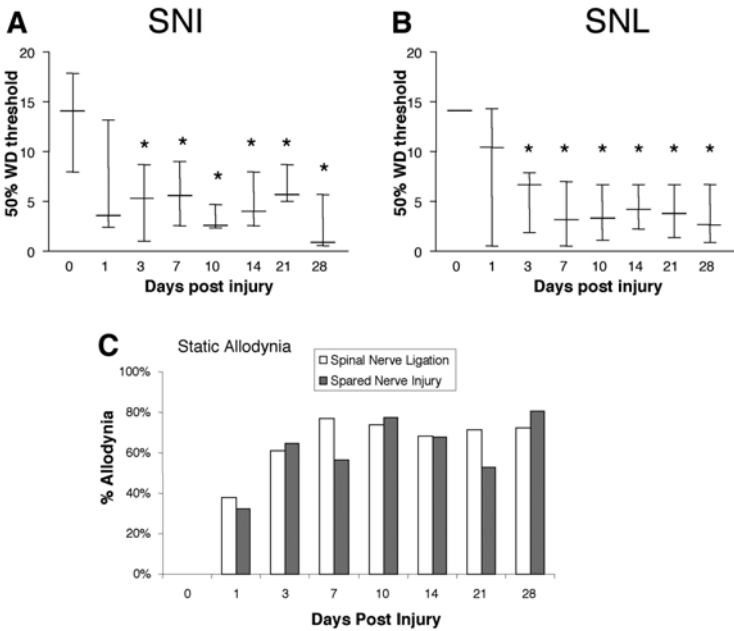
Fig. 3. Static mechanical allodynia in SNI (**A**) and SNL (**B**). The median (± the minimum and maximum values) withdrawal threshold is represented by the horizontal line. The onset and duration of allodynia as well as the (**C**) the percentage of animals exhibiting allodynia is comparable in both models. *$p < 0.05$, Friedman's test followed by Dunn's Multiple Comparison Test.

3.3.3. Cold Allodynia (see **Fig. 4B**)

Ideally, cold allodynia should be tested after mechanical allodynia or on a different day. Without touching the skin, apply a drop of acetone to the lateral one-third of the noninjured and then injured hindpaw using a blunt-ended 20-gage needle on a 3-cm^3 syringe. After each application, observe the animal for a period of 30 s to determine the time the paw remains elevated following a withdrawal response. Both the number of flinches and the total time the paw was kept elevated following withdrawal are recorded during the 30 s period. Repeat the procedure for five trials with a minimum recovery period of 10–15 min between each trial.

4. Notes

1. All experiments were approved by the Merck Research Laboratories-Rahway Institutional Animal Care and Use Committee. All of the work described here was carried out in male Sprague Dawley rats obtained from Charles River Labo-
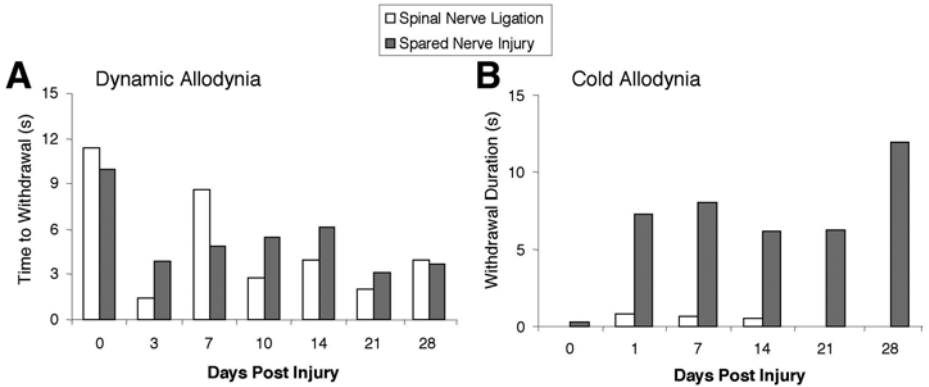
Fig. 4. Dynamic mechanical (**A**) and allodynia (**B**) in SNI and SNL models. The onset and duration of dynamic allodynia is comparable in both models, but the incidence of cold allodynia is low in the SNL model and robust and long-lasting in the SNI model.

ratories (Raleigh, NC) raised on a standard Harlan Teklad diet (7012 LM-485). Results from other strains of rats or rats with a different dietary composition may vary from what is reported here. For optimal development of allodynia in the SNL model, the rats should weigh no more than 200 g and ideally should weigh < 170 g. For SNI, we have used rats in the range of 225–280 g. For anesthetic, we prefer isoflurane over injectable anesthetics because it offers superior control over the depth of anesthesia, the recovery time is shorter and animals more readily resume species typical behavior.

2. Prior to the first incision, care should be taken to ensure that a sufficient level of anesthesia has been obtained by testing ocular or paw withdrawal reflex behavior. Aseptic technique should be used throughout all procedures, including the use of sterile gloves, mask, and the maintenance of a sterile field. All instruments and surgical preparation equipment should be sterilized prior to use and bead sterilized between surgeries. This should obviate the need for antibiotics, but 30,000 U of penicillin G (Crystiben, Fort Dodge, IA) and (Microcillin, Pacific Animal Health, Irwindale, CA) can be administered (sc) postoperatively.

3. Care should be taken when isolating, elevating, and transecting the tibial nerve, to avoid ligating blood vessels in the area. Elevating fat and connective tissue overlying the nerve at the distal one-third of the femur provides more reliable access and decreases the incidence of accidental trauma to the sural nerve. Manipulation and certainly ligation of the nerves will cause spasms in the hindlimb, which should not be associated with pain sensation, if the animal is adequately anesthetized.

4. Postoperatively, rats may be given an injection of sterile 0.9% saline (10 mL/kg, sc) as fluid therapy. For studies in which behavioral sensitivity will be assessed

within 3 d after surgery, no postoperative analgesics are administered. If a greater recovery period exists between surgery and nociceptive threshold testing, then an NSAID (flunixin meglumine, 1.1 mg/kg) may be administered without any adverse accompanying effects. Observe animals periodically for signs of distress including weight loss, chromodacryorrhea (porphyrin staining around the nose and eyes), and autotomy. For the SNI model, some paresis may be present immediately following the surgery which should resolve within 1 d. The incidence of autotomy, though quite low, is unpredictable and usually occurs within 1–3 d of surgery. In our experience, autotomy is more likely with the SNI than the SNL model. Cold allodynia testing may also induce autotomy in a previously unaffected animal if performed within 1–3 d of surgery. There should be no hindlimb paralysis after either surgical procedure. Pair housing seems to improve recovery, as the animals resumed more species typical play behavior and grooming/feeding habits sooner than single housed counterparts. This also decreased anxiety during handling/weighing/testing by the investigator.

5. The L5/L6 spinal nerve ligation model is the more commonly used and accepted model. However, in our experience, mechanical allodynia following L5 ligation/transection develops over the same time-course and is comparable in magnitude to that produced by L5/L6. Moreover, the exposure and isolation of L6 significantly increases the invasiveness of the procedure such that "sham" animals will also develop allodynia. By contrast, sham L5 ligation/transection did not induce reliable allodynia. This result was similar to the lack of effects of sham surgery in the SNI model.

6. Although the SNI procedure can be performed without the use of a retractor (in fact, this may be preferred to minimize tissue trauma), the SNL procedure requires effective retraction of skin and muscle. We have not found any commercially available retractors as effective as the four-point tension system that we fashion out of rubber bands and sterilized paperclips which form the retractor hooks. Because the rubber bands degrade when autoclaved, we clean them with isopropyl alcohol pads.

7. It is necessary to visualize L4 and L5 together to ensure anatomical accuracy. In rare cases, L3 may be located medially and can be misinterpreted as L4. Therefore, if there is considerable space between the two isolated nerves, then L3 and L4 may have been isolated. Investigate medial to both nerves to see if other nerves are present. If there is one, it is L5. It is best to remove as little bone as possible when exposing the L4 and L5 spinal nerves. Aggressive removal of bone will cause severe bleeding which may be detrimental to the animal. Sometimes only L4 can be visualized, (in heavier animals) thus requiring the surgeon to gently hook L5 which is covered by the remaining processes and out of the surgeon's visual field.

8. For these studies, behavior testing commenced 1 d after the surgical procedure; however, in practice, reliable allodynia does not develop until 3 d postoperatively. The data presented here are for five rats per group. To illustrate variability of these surgical procedures, no animals were excluded from analysis. For pharmacology studies, however, a 50% drop in mechanical threshold is required for subsequent inclusion in studies. For SNI model, the "hot spot" will be approx 1 cm

proximal to the edge of the heel, and to the lateral one-third of the hindpaw (the area innervated by the intact sural nerve); whereas for the SNL model, the area of greatest sensitivity tends to be midplantar, but may occasionally be lateral to this area as well (*see* **Fig. 2**).

Acknowledgment

References

1. Basbaum, A. I. and Woolf, C. J. (1999) Pain. *Curr. Biol.* **9,** R429–431.
2. Koltzenburg, M. and Scadding, J. (2001) Neuropathic pain. *Curr. Opin. Neurol.* **14,** 641–647.
3. Mannion, R. J. and Woolf, C. J. (2000) Pain mechanisms and management: a central perspective. *Clin. J. Pain* **16,** S144–156.
4. Seltzer, Z., Dubner, R., and Shir, Y. (1990) A novel behavioral model of neuropathic pain disorders produced in rats by partial sciatic nerve injury. *Pain* **43,** 205–218.
5. Bennett, G. J. and Xie, Y. K. (1988) A peripheral mononeuropathy in rat that produces disorders of pain sensation like those seen in man. *Pain* **33,** 87–107.
6. Kim, S. H. and Chung, J. M. (1992) An experimental model for peripheral neuropathy produced by segmental spinal nerve ligation in the rat. *Pain* **50,** 355–363.
7. Decosterd, I. and Woolf, C. J. (2000) Spared nerve injury: an animal model of persistent peripheral neuropathic pain. *Pain* **87,** 149–158.
8. Chaplan, S. R., Bach, F. W., Pogrel, J. W., Chung, J. M., and Yaksh, T. L. (1994) Quantitative assessment of tactile allodynia in the rat paw. *J. Neurosci. Meth.* **53,** 55–63.

18

Place Conditioning to Study Drug Reward and Aversion

William A. Carlezon, Jr.

1. Introduction

Place conditioning is a classical conditioning paradigm in which animals (typically rats or mice) learn to associate the effects of a drug (or other discrete treatment) with a particular environment. Although it is often referred to as the "Conditioned Place Preference (CPP)" paradigm, this designation fails to capture the flexibility of the assay: it identifies both conditioned place preferences and conditioned place aversions, and thus it can be used to study both rewarding drug effects and aversive drug effects. There are several comprehensive place conditioning reviews in which methodology is described, results are summarized, and the theoretical underpinnings of the behavior are discussed *(1–3)*. The purpose of this chapter is to describe methodology that, at least in rats, minimizes training time and maximizes the sensitivity of the assay to reward, diminished reward (anhedonia), and aversion. As such, place conditioning can be used as a relatively high-throughput assay to study addiction *(4–7)* and other neuropsychiatric disorders involving brain reward systems, including depression *(8,9)*.

A fundamental aspect of place conditioning is that it involves the development of *stimulus–stimulus* associations, typically between a drug and an environment. As opposed to paradigms that involve operant conditioning—and thus require the development of *stimulus–response* associations—the place conditioning paradigm involves Pavlovian conditioning *(2)* because drug administration is always under the control of the experimenter rather than the behavior of the animal. Typically, on one occasion a discrete drug treatment (e.g., an injection of morphine, or of an opiate antagonist in an opiate-dependent animal) is

administered as the animal is restricted to one distinct environment, and on another occasion a nondrug treatment (e.g., an injection of vehicle) is administered as the animal is restricted to a second distinct environment. The number of conditioning ("pairing") sessions between drug (and nondrug) and environment varies according to the group performing the studies, and ranges anywhere from one to more than a half-dozen each. Finally, on the test day, the animal is allowed free access to both environments (typically in a drug-free state), and the amount of time spent in the drug and nondrug environments is quantified. Animals have a tendency to approach and remain in contact with environments in which they have experienced rewarding drug effects, and they have a tendency to avoid environments in which they have experienced aversive drug effects.

The flexibility of the place conditioning assay is maximized when the animals can distinguish between the two conditioning environments, but do not have an *a priori* preference for (or aversion to) either environment. *A priori* preferences can often be detected by prescreening sessions in which the animals have access to the entire place conditioning apparatus. When the apparatus is "unbiased," it is possible to detect place preferences or place aversions while having minimal concerns that the data are confounded by phenomena such as ceiling effects, regression to the mean, or novelty-seeking that may occur when there is a strong initial preference for one of the environments. For example, after we installed lights in the ceiling of our place conditioning apparatus to balance an initial preference for an environment with dark walls, we were able to discover that drug-induced upregulation of the transcription factor CREB (cAMP response element binding protein) in the nucleus accumbens (NAc) is associated with aversive, drug withdrawal-like states *(5,8)*. Furthermore, if dose-effect functions are established for the drug under study, it can be determined if various manipulations (e.g., lesions, alterations in gene expression) affect sensitivity to the rewarding or aversive effects of a drug. For example, we discovered that CREB in the NAc is associated with dysphoria at low doses of drug, and reduced drug reward (anhedonia) at higher doses of drug *(5,9)*. We have also used place conditioning to examine the genes and to map the anatomical substrates involved in sensitivity to the rewarding and aversive effects of morphine *(4,7)*. The key element in all of these studies was that the apparatus was unbiased, such that an average animal did not tend to spend significantly more (or less) time in either of the environments before conditioning sessions commenced.

Below is a description of how we initially characterized our place conditioning apparatus, and the basic protocols that we use for our place conditioning studies. Because we often conduct our place conditioning studies in conjunction with viral-mediated gene transfer studies—in which gene expres-

sion is altered transiently for 4–5 d—we developed a "compressed" conditioning protocol that requires only 3–5 d total, making this assay particularly useful for situations in which time constraints make other rodent models of reward (intravenous self-administration, intracranial self-stimulation) impractical or impossible.

2. Materials

1. "Unbiased" place conditioning apparatus: different wall cues (e.g., white/black, horizontal stripes/vertical stripes), different floor textures (e.g., rods, mesh, solid), and adjustable ceiling lights (e.g., bright/dark).
2. Drugs (e.g., morphine; morphine-sustained release pellets; naloxone).
3. Syringes and needles.
4. Isopropyl alcohol wipes.

3. Methods

Our place conditioning apparatus has three types of distinguishing features: wall color (white, black), floor texture (rods, screen), and most importantly, light intensity (dim to bright) (*see* **Fig. 1**). To initially characterize our rat place conditioning apparatus, we used extra animals that, in some cases, had been in other types of behavioral studies. However, none had experience in the place conditioning apparatus. We found in 30 min screening sessions that, in general, animals prefer the environment (compartment) with the black walls more than the compartment with the white walls, and the screen floor more than the rod floor. We exploited the modular capabilities of our apparatus by placing the screen floor in the white compartment and the rod floor in the black compartment. In our experience, this combination still favored the black compartment, so we increased the intensity of the lights in the black compartments and decreased the intensity in the white compartments. The lights are always most intense in the middle compartment to discourage the animals from spending large amounts of time in this area, because it is never associated with either drug or nondrug conditions. The middle compartment is smaller than the side compartments, and it serves only as the starting point for test sessions and as a connector between the two large side compartments. We continued to adjust the lighting until there were no systematic preferences for either of the large side compartments, as indicated by similar overall averages for the time spent in the white compartment and black compartment across a group of animals (e.g., > 20 rats). We have avoided further adjustments to the lighting or floors after we established these conditions.

3.1. Place Conditioning Procedure

1. Place the apparatus in a quiet room. Minimize personnel entry into the room during place conditioning sessions because disruptions may alter the behavior of
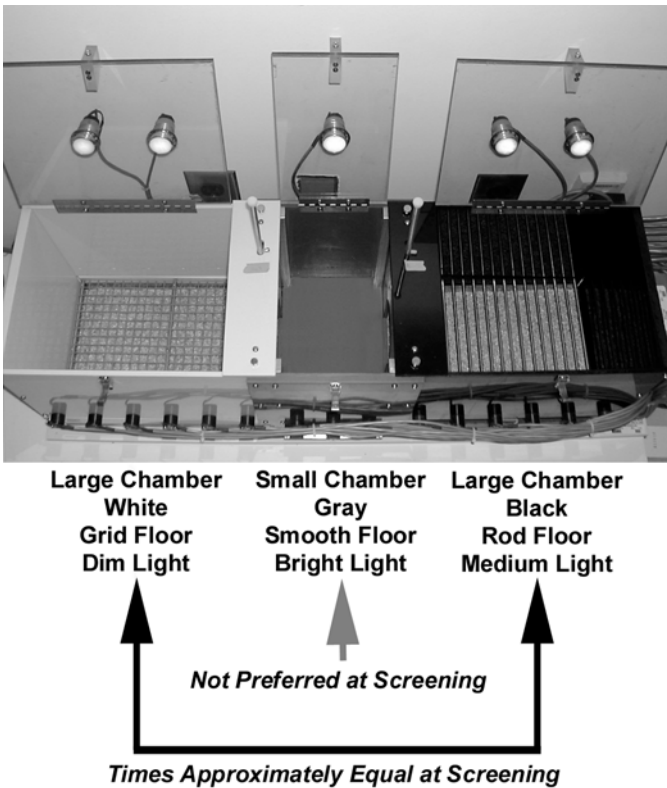
Fig. 1. Customized "unbiased" place conditioning apparatus.

the animals. All portions of the place conditioning procedure should be conducted during the light portion of the activity cycle with the lights off in the test room. These conditions maximize exploratory behavior in the apparatus.

2. Before each screening session, ensure that all chambers in the apparatus are accessible (i.e., doors open) and clean. To minimize olfactory cues associated with other animals, clean the entire apparatus with isopropyl alcohol wipes before testing each individual animal (*see* **Note 1**). Leave the tops open until ready for testing to allow the alcohol to evaporate and to otherwise minimize trapping odors within the apparatus.

3. *Screening (d 0)*. Close the tops of the side compartments. Gently place a naive animal into the center compartment of each apparatus, and close the top. Turn the lights off in the test room.

4. Screen the animals (rats) for 30 min. Remove the rats from the apparatus immediately after the testing session ends.

5. Counterbalance the animals such that each of the four possible conditions is represented within each experimental group (*see* **Note 2**).

6. If surgical procedures are required for the studies, they should be performed after screening (*see* **Note 3**), and adequate time should be allowed for the animals to recover (*see* **Note 4**).

7. *Conditioning (Day 1)*. Begin "compressed" conditioning paradigm (two sessions per day, *see* **Note 5**). Close the doors in the dividers that separate the compartments of the apparatus. In the morning, administer saline (1 mL/kg) and place each animal in the "nondrug" assigned compartment. Turn the lights off in the test room, and condition the rats for 1 h. After the conditioning session, return the animals to their home cages and the vivarium. Clean the entire apparatus with isopropyl alcohol wipes, and leave the tops open to minimize trapped odors. In the afternoon (at least 3 h later), administer the drug under study (e.g., morphine) and place each animal in the "drug" assigned compartment. Turn the lights off in the test room, and condition the rats for 1 h. After the conditioning session, return the animals to their home cages and the vivarium. It is particularly important to remove the animals from the apparatus immediately at the end of the drug conditioning sessions, to avoid associating the offset of the drug (which might be aversive) with the drug-paired compartment. Clean the entire apparatus with isopropyl alcohol wipes, and leave the tops open to minimize trapped odors.

8. *Conditioning (Day 2)*. If necessary, repeat the procedures used on d 1 exactly (*see* **Note 6**). Do not alternate the order of nondrug and drug pairings (*see* **Note 7**).

9. *Test*. Test the animals under the conditions used for screening (*see* **steps 2–4**, above) between the time periods used previously for the morning and afternoon conditioning sessions.

10. Immediately after testing, collect brain tissue for histological or molecular analyses (*see* **Note 8**).

11. Perform statistical analyses. To maximize statistical power, we typically use analyses of variance (ANOVA) with repeated measures: we compare the net differences in time spent in the drug side (i.e., time spent in drug side minus time spent in saline side, in sec) *before* and *after* treatment. Significant effects are further analyzed with Fisher's *post hoc* tests.

4. Notes

1. We thoroughly clean the apparatus between each conditioning session to minimize possible between-animal confounds associated with olfactory stimuli. We clean the walls, tops, and floors with isopropyl alcohol wipes, and we replace the absorbent material (wood chips) in the waste trays located below the floors to ensure that the apparatus is totally clean for each individual animal.

2. Individual animals often show nominal preferences for one of the large side compartments. We counterbalance the compartment assignments such that some animals will receive drug in their preferred environment and some will receive it in their nonpreferred environment. We also counterbalance each treatment group such that approximately the same number of animals receive drug associated with the white compartment as in the black compartment. Accordingly, there are four possible types of drug-environment pairings: the drug paired with the white/pre-

    ferred environment; drug with the white/nonpreferred environment; drug with the black/preferred environment; and drug with the black/nonpreferred environment. Ideally, each possibility should be represented equally within each group in the study.

3. Occasionally, animals show strong preferences for one of the environments. We screen the animals before conducting any labor-intensive or expensive procedures (e.g., intracranial surgery for viral-mediated gene transfer) so that we can eliminate those with large *a priori* preferences for a particular environment before proceeding further.

4. We normally conduct surgical procedures on d 0, following screening. The recovery period depends upon the type of surgical procedure conducted. Following intracranial (e.g., viral-mediated gene transfer) surgery, we allow 2 d recovery, such that conditioning sessions begin on d 3. For subcutaneous implantation of sustained-release morphine pellets, we allow three days exposure to a constant morphine titer in the blood, such that conditioning sessions begin on d 4.

5. On each day, the animals receive two conditioning sessions: nondrug (i.e., vehicle) in the morning and drug in the afternoon. This "compressed" conditioning paradigm may generate dose-effect functions for each drug that are different than those reported in papers in which more extended conditioning protocols are used.

6. In our experience, reliable place preferences require two nondrug (e.g., vehicle) and two drug (e.g., morphine) conditioning sessions. However, we and others *(10)* have found that precipitated opiate withdrawal establishes reliable place aversions after only one nondrug and one drug (e.g., naloxone in opiate-dependent rats) conditioning session.

7. In the "compressed" protocol, it is important that the nondrug pairings always precede drug pairings. If the animals receive drug in the morning conditioning session, it is possible that they could associate symptoms of dysphoria (e.g., acute drug withdrawal) with the nondrug environment during the afternoon session.

8. In some cases, it will only be possible to perform either a histological analysis or a molecular analysis (i.e., if immunoblotting studies will be conducted, it is necessary to collect tissue from the area of the microinjection). In cases where a surgical manipulation (e.g., lesion, gene transfer) was used, we generally favor procedures that will allow detailed examination of the targeted brain regions because animals in which the manipulation was not targeted to the appropriate region should be eliminated from statistical analyses.

Acknowledgment

References

1. Carr, G. D., Fibiger, H. C., and Phillips, A. G. (1989) Conditioned place preference as a measure of drug reward, in *The Neuropharmacological Basis of Reward*, (Liebman, J. M. and Cooper, S .J., eds.) Clarendon, Oxford, U.K., pp. 264–319.

2. Wise, R. A. (1989) The brain and reward, in *The Neuropharmacological Basis of Reward* (Liebman, J. M. and Cooper, S. J., eds.) Clarendon, Oxford, U.K., pp. 377–424.

3. Tzschentke, T. M. (1998) Measuring reward with the place preference paradigm: a comprehensive review of drug effects, recent progress, and new issues. *Progr. Neurobiol.* **56,** 613–672.

4. Carlezon, W. A. Jr., Boundy, V. A., Haile, C.N., Lane, S. B., Kalb, R. G., Neve, R. L., and Nestler, E. J. (1997) Sensitization to morphine induced by viral-mediated gene transfer. *Science* **277,** 812–814.

5. Carlezon, W. A. Jr., Thome, J., Olson, V., Lane-Ladd, S. B., Brodkin, E. S., Hiroi, N., et al. (1998) Regulation of Cocaine Reward by CREB. *Science* **282,** 2272–2275.

6. Kelz, M. B., Chen, J. S., Carlezon, W. A. Jr., Whisler, K., Gilden, L., Steffen, C., et al. (1999) Expression of the transcription factor ΔFosB in the brain controls sensitivity to cocaine. *Nature* **401,** 272–276.

7. Carlezon, W. A., Jr., Haile, C. N., Coopersmith, R., Hayashi, Y., Malinow, R., Neve, R. L., and Nestler, E. J. (2000) Distinct sites of opiate reward and aversion within the midbrain identified by a herpes simplex virus vector expressing GluR1. *J. Neurosci.* **20,** RC62.

8. Pliakas, A.M., Carlson, R., Neve, R. L., Konradi, C., Nestler, E. J., and Carlezon, W. A. Jr. (2001) Altered responsiveness to cocaine and increased immobility in the forced swim test associated with elevated cAMP response element binding protein expression in nucleus accumbens. *J. Neurosci.* **21,** 7397–7403.

9. Andersen, S. L., Arvanitogiannis, A., Pliakas, A. M., LeBlanc, C., and Carlezon, W. A. Jr. (2002) Altered responsiveness to cocaine in rats exposed to methylphenidate during early development. *Nature Neurosci.* **5,** 13–14.

10. Gracy, K. N., Dankiewicz, L. A., and Koob, G. F. (2000) Opiate withdrawal-induced Fos immunoreactivity in the rat extended amygdala parallels the development of condtioned place aversion. *Neuropsychopharmacol.* **24,** 152–160.

19

Opiate Self-Administration

Zheng-Xiong Xi and Elliot A. Stein

1. Introduction

Opiates are powerful analgesics commonly used clinically to relieve pain. However, their repeated administration can lead to the development of drug dependence. During this transition from casual use to abuse, individuals initially respond to opioids as positively rewarding. Tolerance and then physical dependence develop over time, with withdrawal symptoms seen upon drug cessation. Drug craving, induced either by conditioned cues, stressors, or administration of the drug itself, often lead to compulsive drug-seeking behavior, which, in turn, may lead to drug taking and relapse. Three major animal models have been widely used to investigate the behavioral properties and neurobiological mechanisms of drug addiction, i.e., self-administration (SA), conditioned place preference (CPP), and intracranial self-stimulation (ICSS). Generally, operant SA procedures are used to model reward (reinforcement) and relapse (reinstatement) (*see* **Note 1**). CPP is a relatively simple Pavlovian reinforcement procedure that can be used to evaluate the effects of environmental cues on both the positive rewarding and negative or aversive reinforcing properties of opiates (*see* **Chapter 18**). Finally, ICSS is commonly used to map specific brain reward systems or circuits and their potential modification during the stages of drug dependence. The particular research question, of course, determines the choice of the methodology employed.

The SA model has been extensively used to address a wide range of research questions, including:

1. Modeling patterns of human drug taking behavior.
2. Assessing the abuse liability of specific compounds.

3. Identifying the neural circuits and neurochemical mechanisms underlying drug reward and motivation through the local or central administration of specific receptor agonists or antagonists, and/or neurotoxin or electrical lesions of specific brain regions.
4. Characterizing the effects of pharmacological manipulations on SA behavior (and drug reinforcement).
5. Investigating the interaction of environmental cues with drug-taking behavior (conditioned reinforcement).
6. Modeling "relapse" (reinstatement). Drug SA is thought to most closely parallel human drug-taking behavior and has been thought to be able to represent both the motivational aspects of drug seeking and taking as well as the reinforcing properties of the drug after administration.

In addition to these wide-ranging implications, another principal advantage of the SA paradigm is its high sensitivity to low drug doses and high predictive validity and reliability. In contrast, its main disadvantages are technical, including the need for survival surgery, relatively sophisticated testing apparatus and special training skills and experimental procedures [see *(1,2)* for reviews]. This chapter details the methodology of intravenous and intracranial drug SA procedures in rats and then discusses several commonly used operant behavioral schedules used in intravenous SA experiments.

2. Materials
2.1. Animals

For a number of reasons including size, cost, extensive existing knowledge of basic neurobiology, and neuropharmacology of the species, the rat is the most common animal species used in drug SA experiments. Other species less frequently used include mice and nonhuman primates.

2.2. Apparatus

Because many investigators choose to custom fabricate their own SA equipment, most major pieces can be purchased from one of several commercial sources. For the purposes of informing the reader and for practical expediency, equipment will be illustrated from one or two commercial manufacturers, unless otherwise unavailable.

2.2.1. Operant Chamber

SA chambers, approx 26 × 32 × 25 cm (height × width × depth) can be purchased from a number of commercial vendors such as Med-Associates (ENV-008; Med Associates Inc., E. Fairfield, VT) (*see* **Fig. 1**). This chamber is equipped with two levers (5 cm width) on the right-hand wall, situated 11 cm apart, and 7 cm above the steel grid floor (*see* **Note 2**). The size of the chamber
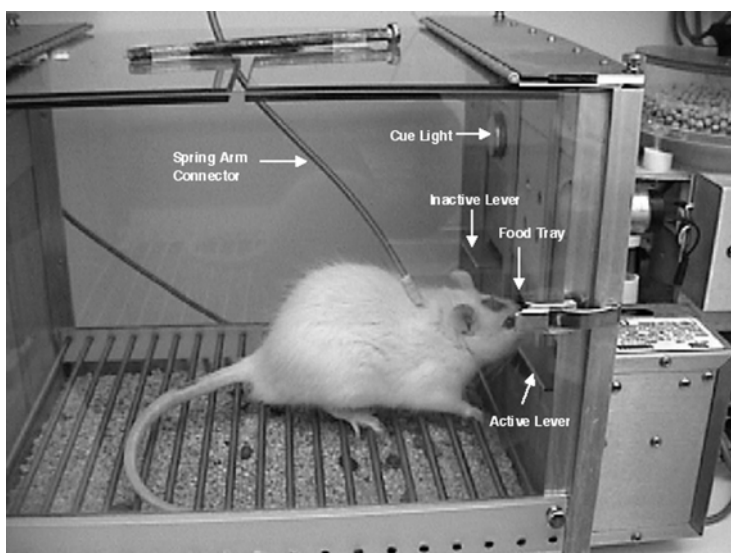
Fig. 1. Self-administration (SA) chamber. It can be used for iv and intracranial SA experiments and food reinforcement.

should be small enough to maximize the probability of the rat "accidentally" hitting the lever, but not too small to prevent normal grooming and exploratory behavior. Chamber construction should also be optimized to facilitate cleaning of the walls and floor between sessions so that odor markings do not influence the behavior of other animals.

2.2.2. Computer with Software

Responses on both levers are recorded by a PC-based program (Med-PC; Med-Associates), and can be analyzed by the accompanied software. The time and duration of the pump is also software controlled.

2.2.3. Syringe Pump Apparatus

Simple pneumatic syringe pumps for intravenous (iv) SA experiments can be purchased from Razel (Stamford, CT) or IITC Life Science (Chicago, IL). An electrolytic microinfusion transducer (EMIT) drug-delivery system *(3)* is generally used for intracranial drug SA experiments when the volume of delivery is in the nanoliter range, although other micro volume delivery strategies have been developed *(4,5)* for intracranial SA experiments.

2.2.4. Spring Arm Connector Assembly

This assembly is necessary to prevent the rat from chewing through the polyethylene intravenous catheter and ancillary anchoring devices and can be purchased from Plastics One, Inc., Roanoke, CA (#C313CS).

2.2.5. Jugular Catheters

Jugular catheters can be easily made (see below) or purchased from MRE (Braintree, MA).

2.3. General Materials

1. Guide and injection cannulas: 22- and 28-gage (C313G, C323ICT, Plastics One, Inc., Roanoke, VA).
2. Obdurator: 28-gage (C313DC, Plastics One, Inc.).
3. Silicon rubber tubing (Silastic®): 0.025 inner diameter, 0.047 outer diameter (#62999-101, VWR).
4. Cranioplastic powder and liquid (300CPP and 300CP, Plastics One, Inc.).
5. Marlex® mesh (0112660, Davol).
6. Mersilene mesh (Ethicon).
7. Stainless steel obdurator: 33-gage, 14-mm (Small Parts Inc., Miami Lakes, FL).

2.4. Specific Chemicals and Reagents

1. Artificial CSF vehicle: 120 mM NaCl, 4.8 mM KCl, 1.2 mM KH_2PO_4, 1.2 mM $MgSO_4$, 25 mM $NaHCO_3$, 2.5 mM $CaCl_2$, and 10 mM D-glucose, pH 7.4.
2. Heroin, morphine, saline, heparin, anesthetics (ketamine/xylazine), antibiotics (procaine penicillin G).

3. Methods

3.1. Intravenous (iv) Drug Self-Administration

3.1.1. Fabrication of Jugular Catheters (see **Fig. 2**)

1. Bend a 28-gage guide cannulae 90°, being careful not to crimp it such that fluid flow through the cannulae would be impeded.
2. Cut a 13-cm piece of silicon rubber tubing and slide it over the bent end of the guide cannulae and secure with Super glue® (methylmethacrylate adhesive). Allow it to dry overnight.
3. Place the fastened cannula and Silastic® tubing into a silicon sprayed catheter mold.
4. Mix cranioplastic powder with cranioplastic liquid until a viscous yet fluid consistency is reached. Drip the cranioplastic cement into the mold surrounding the catheter, making sure no air bubbles are in the cement matrix.
5. When the mold is filled, apply a 2.5 × 2.5 cm square of Marlex® mesh to the base of the catheter to be held in place by the dried cranioplastic cement. Allow the catheter to sit in the mold overnight to fully dry.
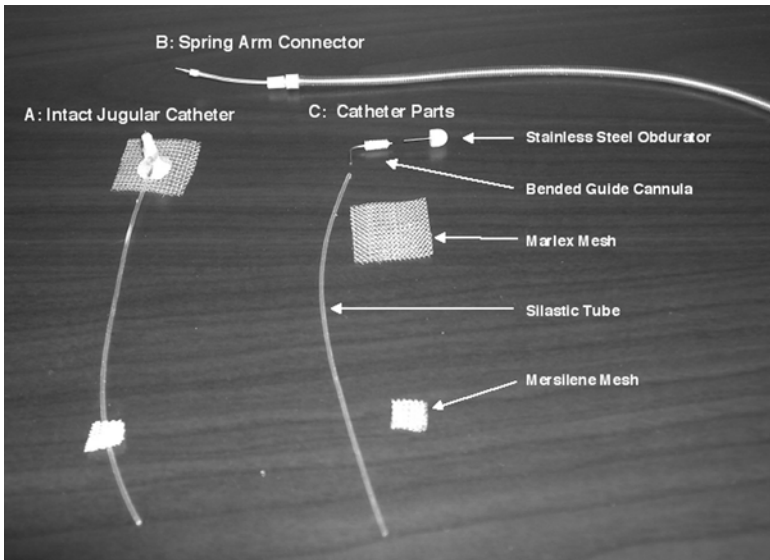
Fig. 2. Examples of an intact jugular catheter and a spring arm connector (left) and the major parts of the jugular catheter.

6. Remove the catheter from the mold and fit with a piece of 1 cm × 1 cm Mersilene mesh placed 3 cm from the end of the Silastic tubing away from the catheter.
7. Insert stainless steel obdurator into the guide cannulae to prevent air and debris from entering.

3.1.2. Surgery for Jugular Catheter Implantation

1. Use male Sprague–Dawley or Wistar rats, aged 50–80 d, initially weighing 200–300 g. Although they may be group housed under standard laboratory conditions before surgery, they are generally housed in single cages after surgery and during subsequent experimental manipulations. As rats are nocturnal animals and are most active during the dark phase of their day, it is often desirable to house rats on a reverse day–night schedule so that they will be most active when experiments are to be performed during the experimenter's usual business day. Give food and water *ad libidum*, except where otherwise noted in the course of SA training.
2. Anesthetize rats by IP administration of 50 mg/kg ketamine and 10 mg/kg xylazine.
3. Insert a guide cannula, attached to Silastic® tubing and Marlex® mesh via dental cement, subcutaneously (sc) between the shoulder blades and exit the skin via a dermal biopsy hole (3 mm). Thread the other end of the tubing under the skin, insert 3 cm into the right jugular vein, and then suture securely to the underlying muscle tissue.
4. Suture the catheter to the vein and anchor to the surrounding tissue at three points. Suture the anchoring (guide cannula) end to the musculature and secure in place

with the 2.5 × 2.5 cm pierce of Marlex® mesh over the base of the cannula end to the underlying tissue. Some groups prefer to also add a drop of Superglue® to the catheter/vein juncture and the catheter/tissue suture location for additional strength.

5. Close the ventral and dorsal incisions with sterile nylon sutures.

6. After surgery, inject 0.5-mL of heparinized saline (50 U/mL) to replace body fluids lost during surgery. Procaine penicillin G (100,000 IU) can also be given deep IM for prophylaxis. Return the rat to its home cage with free access to food and water after recovery from anesthesia.

7. Supplemental surgeries: Because the majority of SA studies are associated with a manipulation of regionally specific brain function, a guide cannulae for drug microinjection or microdialysis, or an electrode for electrochemical or electro-physiological recordings are often implanted into one or more specific brain re-gions, including the ventral tegmental area (VTA), dorsal striatum, nucleus accumbens (NAcc), prefrontal cortex (PFC), or amygdala. *(6,7)*.

3.1.3. Drug Self-Administration Training Procedures

1. Following 5–7 d of recovery from surgery, place rats into a SA chamber. Uncap the end of the guide cannulae and insert a 28-gage sterile needle connected to PE50 tubing into the jugular catheter through the anchoring guide cannulae. The PE50 tube is prefilled with a 0.9% saline solution vehicle of the SA drug. The PE tubing is contained in a spring arm connector assembly for protection. Secure the lower spring end to the threaded anchoring guide cannulae. Generally, give rats sufficient time to accommodate to the novel environment and stress of handling prior to experimental manipulations

2. Connect the spring arm assembly to a fluid swivel attachment above the chamber (Instech MCLA counterbalance level arm, on a 375/20 swivel). PE50 tubing then connects the swivel to a pneumatic syringe infusion pump. Pumps generally are available with single- or multiple-speed capabilities. If single-speed pumps are chosen (they are considerably cheaper than multispeed models), ensure that the motor speed is appropriate for the injection volume and time and syringe size anticipated. In general (see later), volumes of 100–150 μL and injection times of 5–15 s are used. Depending on the duration of the experiment (anywhere from 1 h to multiple days), syringe sizes may need to vary from 1 mL to 30 mL.

3. Program the computer to administer drug or saline at a rate of approx 100 μL over 10 s when the rat presses the active lever. Some investigators only use an active pedal in the chamber, others prefer to use two pedals. Responding on the second is pro-grammed to have no behavioral consequence and are simply counted and used to demonstrate specificity of the learned SA behavior. Specificity is generally demon-strated by responding on the active lever increasing and then stabilizing over days (see later), while responding on the inactive lever rapidly falls towards zero.

4. Train the rat to lever press for heroin (0.06 mg/kg/infusion) on a fixed ratio 1 (FR1) schedule of reinforcement, i.e., each press of the active lever will result in one drug infusion. In order to maintain discreet stimulus-reward learning, since drug administration leads to an extended drug perception period, drug infusions

are generally followed by a "time out" period where responding on the active lever is counted but no longer delivers a drug infusion. This period can be anywhere from 10 s to many minutes. Finally, depending on the experimental question, a secondary reinforcer (e.g., a light above the pedal or chamber or a tone) may be programmed to turn on coincident with the drug injection.

5. After each heroin SA training session, the jugular catheter guide cannulae should be recapped to prevent obstruction by debris before rats are returned to their home cages.

3.1.4. Acquisition, Maintenance, Extinction, and Reinstatement of Opiate SA

SA experiments may be thought to consist of four phases: initiation, maintenance, extinction, and reinstatement.

1. Acquisition: Priming injections of heroin may be given by the experimenter at the beginning of the initial training session until the animal learns to respond on the correct (active) lever. Mildly food-depriving animals the night prior to SA training (give only three 45-mg Noyes, Lancaster, NH) often facilitates the acquisition of drug SA by increasing exploratory behavior and general motivational state (*see* **Note 3**). Ware should always be available *ad lib*, even during food deprivation.

2. Maintenance: Stable SA behavior is generally defined as ± 10% variance on the active lever for at least 3 d (*see* **Note 4**), although specific experiments may define stable behavior differently. Experiments that call for animals during the maintenance phase of drug SA may be initiated once a stable level of responding is established. These experiments are usually used to evaluate the effects of a treatment such as GABAergic agents on drug reward or reinforcement *(6,8)*.

3. Extinction: Following the maintenance phase of an experiment, rats can undergo a period of extinction where responding on the active lever results in the infusion of saline instead of heroin. A typical extinction pattern of responding is shown in **Fig. 3** and is generally characterized by initial high response bursts followed by dramatic response slowing and cessation. After several days of such extinction, response rates go almost to zero. Opiate withdrawal responses (e.g., diarrhea, "wet dog" shakes, ptosis) are often observed during extinction and the effects of various behavioral or pharmacological treatments on extinction or withdrawal responses may be evaluated during this time period.

4. Reinstatement: After days, weeks, or even months of extinction and drug abstinence, animals may undergo a reinstatement (relapse) procedure. Three types of priming stimuli are most commonly used to trigger reinstatement. They include drug priming (e.g., an iv heroin challenge), stress (e.g., electrical foot shock stimulation) or environment-related cue stimulation (e.g., a light or sound that was previously paired with each heroin SA during the acquisition and maintenance phase) *(9)*. Following each environmental or drug challenge, a high rate of lever pressing is observed, although these responses do not have to cause any
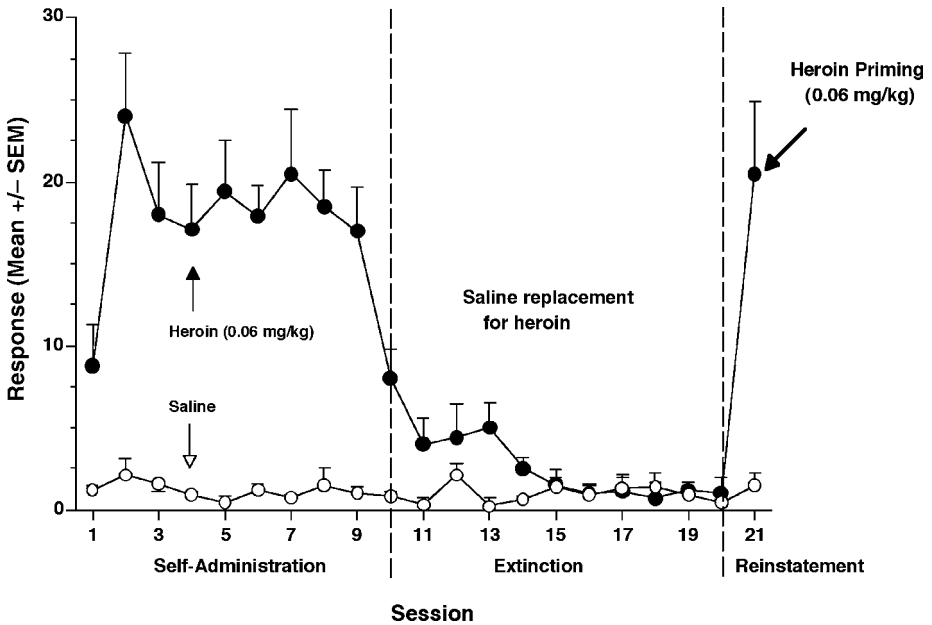
Fig. 3. Group data from a typical SA experiment. Each training trial lasted for 4 h or until the subject self-administered 10–20 infusions of heroin with a regular inter-injection interval. An arbitrary acquisition criterion required that subjects' active lever presses varied by ±10% or less over the course of three consecutive maintenance days before they were moved to the extinction phase of the experiment. During mainte-nance, subjects administered an average of 1–1.5 mg/kg heroin during the 4-h ses-sion. Once subjects met the maintenance criterion, extinction procedures were instituted. During extinction, subjects again experienced 4-h daily training sessions, however, saline was substituted for heroin in response to active lever presses. Thus, active lever presses now resulted in no drug delivery. Subjects remained in the extinction phase until responding on the active lever fell to <10% of the level during maintenance. After extinction, subjects were tested for their propensity to reinstate responding on the active lever after a systemic injection of heroin (0.06 mg/kg). All subjects were tested twice during successive test days separated by additional extinc-tion trials, in which subjects were required to again meet the extinction criterion before the second test trial. During reinstatement testing, active lever presses resulted only in delivery of intravenous saline and not heroin.

further drug infusions (*see* **Fig. 3**). The effects of various pharmacological or behavioral treatments on drug-seeking reinstatement can now be evaluated *(7,10)*.

3.2. Intracranial Drug Self-Administration

3.2.1. Rationale

The above iv SA experiments are reasonably straightforward and allow great flexibility of experimental design. However, the identification of distinct brain

loci responsible for drug reward may be problematic following systemic drug delivery. Further, various manipulations during iv SA may effect properties of the drug that may be unrelated to reinforcement, therefore, resulting in potentially erroneous conclusions. Intracranial SA offers an alternative procedure to investigate the neurobiology of drug reinforcement by providing direct SA of drug into discrete brain regions, such as the NAcc, VTA, or mPFC *(11–13)*.

3.2.2. Surgery

Under ketamine and xylazine anesthesia, implant stereotaxically a unilateral 22-gage guide cannulae into one hemisphere and aim 1 mm above the center of the cortical or subcortical structure of interest. For the NAcc, an area of intense experimental interest in drug abuse *(14)*, the coordinates are 1.7 mm anterior to bregma, 2.0 mm lateral to the midline suture, and 5.9 mm below the dura *(15)*. The incisor bar must be elevated to 5-mm above the intraaural line, and the cannulae inserted at an angle toward the midline at 10° from the vertical. Secure the guide cannula to the skull with stainless steel screws and acrylic dental cement. Finally, insert a 28-gage obdurator and extend 0.5 mm beyond the tip of the guide cannulae.

3.2.3. Apparatus

The same operant chambers used for intravenous SA experiments may also be used for intracranial SA. In this case, an electrolytic microinfusion transducer (EMIT) drug-delivery system *(3)* is generally used for infusing the test drug. Briefly, place two platinum electrodes in an infusate-filled cylinder (28 mm in length × 6 mm in diameter) equipped with a 28-gage injection cannulae. Connect the electrodes via a spring-protected cable (Plastics One) and a swivel (Model 205, Mercotac, Inc., Carlsbad, CA) to a constant current generator (MNC, Inc., Shreveport, LA), which is set to deliver 6 µA of quiescent current and 200 µA of infusion current between the electrodes. Depression of the active infusion lever activates the constant current generator for 5 s, which will lead to the rapid generation of H_2 gas in the gas tight cylinder and, in turn, force 100 nL of the infusate through the injection cannulae.

3.2.4. Procedures

Before each test session, the reservoir of each EMIT unit must be filled with an appropriate drug or artificial CSF vehicle. Insert the injector cannulae through the guide cannula and screw it into place. Place animals in the operant chamber. Each depression of the active lever results in illumination of a cue light and delivery of 100 nL drug or vehicle solution over a 5-s period followed by a time-out period of 60 s. Depression of the inactive control lever has no programmed consequence at any time. No shaping techniques such as priming injection of drugs should be used to facilitate the acquisition of lever responding. Record the number of infusions and responses on the active and inactive levers.

3.3. Operant Food Responding

3.3.1. Rationale

This procedure is often used as a natural reward control to determine whether a pharmacological or behavioral treatment selectively effects drug reinforcement and/or relapse vs a nonspecific alteration in motor responding or general motivational state.

3.3.2. Procedures

Prior to training, animals must be food restricted to about 80% of their free-feeding body weight. This is generally obtained by restricting the number of food pellets given (usually 3–4/d) and water is always available *ad lib*. Because the new weight must be maintained for the duration of the experiment, animals should be weighed daily. Similar to drug SA procedures (*see* **Fig. 3**), train subjects to respond on an active lever to obtain food pellets, with training beginning immediately after food restriction reduces body weight (2–3 d). Initially, train rats to lever press on an FR1 schedule for reinforcement for a single (45 mg) food pellet. On subsequent days, the schedule can be increased to an FR3 or FR5. Once each rat has displayed stable responding on the FR-5 schedule, extinction procedures can be instituted such that lever presses no longer result in food delivery. On each schedule, subjects are required to display stable operant behavior (<10% variation across 3 d), before being moved to the next schedule. As in drug SA, extinction trials can be initiated if desired followed by the ability of noncontingent food delivery to reinstate lever responding. This food reinstatement experiment may be conducted after a procedure that parallels drug reinstatement as closely as possible. An intermittent schedule of reinforcement may also be instituted to help ensure robust reinstatement responding.

3.4. Reinforcement Schedules

Various schedules of reinforcement have been used in intravenous SA experiments, each intended to generate different behavioral patterns that are used to model various aspects of drug reinforcement, including FR, second-order, choice procedures, discrete trials, and progressive ratio (PR) schedules. The vast majority of SA experiments in rats have employed FR schedules, while the more complex schedules have been reserved for nonhuman primate studies (*see* **refs. *1,2,16*,** for reviews), although recently, second-order and PR schedules have been successfully introduced in rat SA experiments *(17,18)*.

3.4.1. FR Schedules

Once regular lever pressing has been established on a continuous reinforcement schedule (CRF), whereby the rat self-administers 15–20 injections of 0.06

mg/kg of heroin in a 4-h session with regular interinjection intervals of 10–15 min, gradually increase the ratio requirement, i.e., the number of lever presses required for an infusion of drug. Rats can be moved to an FR2, FR3, FR4, up to RF10 schedule within a few weeks of testing.

The main advantage of FR schedules is that rats learn the task more readily (especially on FR1) than under any other schedule, thereby making it especially effective as a tool to initially screen a drug for abuse potential. The weakness of FR schedules, however, is that a change in SA behavior on a FR1 schedule may be difficult to interpret at certain experimental conditions (*see* **Note 5**).

3.4.2. Second-Order Schedules

Second-order schedules differ from FR schedules with respect to the unit dose-response function. In a second-order schedule, a drug reinforcer (such as heroin or morphine) is presented according to a schedule in which a more or less extended sequence of responses is reinforced intermittently. Briefly, following acquisition of heroin SA under a CRF schedule, second-order training begins under a FR schedule of the type FRx(FRy:S), where y is the number of responses after which a 1-s light conditioned stimulus (CS) will be presented and x is the number of light CS presentations after which the drug is infused. After several days of training, change the second-order schedule to a fixed interval (FI) schedule of the type FIx(FRy:S), with x being the number of minutes after which the first completed CS requirement, as designed by FRy:S, would result in an infusion of iv heroin. For example, FI60 min (FR30:S), indicates that after every 30 responses, the CS (1-s light) is presented (this is often called the component or unit schedule), and following the 30th response after completion of a fixed interval (FI) of 60 min, heroin is delivered *(17,19)*.

In contrast to simple fixed-interval schedules, response rates on second-order schedules have been shown to increase with increasing drug doses, although further dose increases lead to decreases in response rates. This sigmoidal or inverted-U-shaped dose-response function is quite sensitive to pharmacological manipulations. For example, dopamine receptor antagonists have been shown to shift an inverted-U-shaped unit dose-response function completely to the right in monkeys, suggesting that dopamine receptor antagonists attenuate the effects of self-administered cocaine *(20)*. One of the principal advantages of second-order schedules is that they reliably maintain high rates of responding in a variety of species and require extensive sequences of behavior before any drug administration, which provides alternative endpoints that might be influenced by the drug (e.g., learning). Thus, potentially disruptive nonspecific acute drug and treatment effects on locomotor behavior that might impact on response rates can be minimized. These schedules, however, are technically more difficult to use than FR schedules and require longer training periods before stable responding is obtained.

3.4.3. PR Schedules

After demonstrating stable patterns of responding on an FR1 schedule for several days, rats may be trained to respond on a PR schedule. Via computer software, a sequence of increased responses can be required for each successive drug delivery. This increase in lever presses may be set with an arbitrary arithmetic increment, or set at twice the value of the previous one (i.e., 1, 2, 4, 8, 16, and so on). As the ratio progressively increases, a certain point will be reached wherein the animals will no longer respond on the lever (break point), reflecting the maximum effort that an animal will expend in order to receive a single drug infusion. Higher break point values are taken to indicate a higher reinforcement value of the drug and thus likely higher human abuse liability. Increasing the unit dose of the self-administered drug generally increases the break point on a PR schedule. Such PR schedules have been used to evaluate the reinforcing efficacy of various drugs *(18)*. In addition, pharmacological manipulations such as dopamine receptor antagonists or GABA receptor agonists have been shown to decrease the break point during cocaine SA behavior *(18,21)*.

3.5. Data Analysis

Drug SA behavioral data may be analyzed either with standard spreadsheet and statistical software packages (generally using a one-way or two-way ANOVA, and *post hoc* comparisons between individual treatment groups) or with proprietary software packages (e.g., from Med Associates, Inc.).

4. Notes

1. Definitions of reinforcement and reward: Reinforcement may be defined operationally as a sequence of any events that increases the probability of a response. This definition may also be used to signify a definition for reward, and the two words are often used interchangeably. However, reward often connotes some additional emotional value such as pleasure.
2. It should be noted that not all investigators use pedals as the manipulandum of choice. Others have used nose poking *(22)*, whereas still others use no manipulandum, but rather have employed a straight runway tract with running speed as the operant behavioral response *(23)*.
3. It is possible that after 3–5 d of priming and food restriction, some animals still will not learn the operant task. These subjects should be removed from the group and no longer used in the study. The most common cause of failure are iv catheter blockade, sick or distressed animal, equipment failures leading to inability to discriminate between active and inactive levers (>20% responding on the inactive lever), blockade of an intracranial guide cannulae for experimental drug microinjections or incorrect cannulae placement.

4. If rats continue to demonstrate an irregular SA pattern after several days of training or an extinction-like pattern becomes evident during normal SA training, the most common reason is partial obstruction of the catheter. Thus, catheters should be tested intermittently throughout the study by iv injection of 0.1 mL of the short-acting barbiturate anesthetic Brevital® sodium (1% methohexital) that, if the catheter is patent, will rapidly and reversibly induce loss of muscle tone. To help minimize catheter failures, 0.1 mL heparinized saline (10 IU/mL) prior to and at the completion of each SA session should be used to completely flush the catheter.

5. Data interpretation for FR schedules: Within a range of doses that maintain stable responding, rats increase their SA rate as the unit dose is decreased, apparently compensating for decreases in the unit dose *(24)*. Conversely, animals reduce their SA rate as the unit dose increases. Thus, pharmacological modulations that increase the SA rate on a FR schedule resembles a decrease in the unit dose, causing a shift of the dose-response curve to the right and suggesting a partial reduction of drug reinforcement by the manipulation *(1,2)*. However, other interpretations are also possible. For example, Tsibulsky and Norman (1999) have shown that response rate in cocaine-trained animals may be controlled by some sort of a "satiety threshold." Experimental treatments may act to decrease or increase this threshold. In the latter case, response rates will be increased. This increase in lever pressing may not necessarily indicate a reduction in reinforcement by experimental treatment. It should be noted that there is only limited evidence supporting the existence of such a "satiety threshold."

References

1. Mello, N. K. and Negus, S. S. (1996) Preclinical evaluation of pharmacotherapies for treatment of cocaine and opioid abuse using drug self-administration procedures. *Neuropsychopharmacology* **14,** 375–424.
2. Gardner, E. L. (2000) What we have learned about addiction from animal models of drug self-administration. *Am. J. Addict.* **9,** 285–313.
3. Criswell, H. L. (1977) A simple chronic microinjection system for use with chemitrodes. *Pharmacol. Biochem. Behav.* **6,** 237–238.
4. Stein, E. A. and Rodd, D. (1980) A new pump for intracerebral injection of drugs. *Pharmacol. Biochem. Behav.* **12,** 815–817.
5. Olds, M. E. and Williams, K. N. (1980) Self-administration of D-Ala2-Met-enkephalinamide at hypothalamic self-stimulation sites. *Brain Res.* **194,** 155–170.
6. Xi, Z. X. and Stein, E. A. (2000) Increased mesolimbic GABA concentration blocks heroin self-administration in the rat. *J. Pharmacol. Exp. Ther.* **294,** 613–619.
7. McFarland, K. and Kalivas, P. W. (2001) The circuitry mediating cocaine-induced reinstatement of drug-seeking behavior. *J. Neurosci.* **21,** 8655–8663.
8. Xi, Z. X. and Stein, E. A. (1999) Baclofen inhibits heroin self-administration and mesolimbic dopamine release. *J. Pharmacol. Exp. Ther.* **290,** 1369–1374.
9. Shaham, Y., Erb, S., and Stewart, J. (2000) Stress-induced relapse to heroin and cocaine seeking in rats: a review. *Brain Res. Rev.* **33,** 13–33.
10. Cornish, J. L., Duffy, P., and Kalivas, P. W. (1999) A role for nucleus accumbens glutamate transmission in the relapse to cocaine-seeking behavior. *Neuroscience* **93,** 1359–1367.

11. Bozarth, M. A. and Wise, R. A. (1981) Intracranial self-administration of morphine into the ventral tegmental area in rats. *Life Sci.* **28,** 551–555.
12. Goeders, N. E. and Smith, J. E. (1983) Cortical dopaminergic involvement in cocaine reinforcement. *Science* **221,** 773–775.
13. Goeders, N. E. and Smith, J. E. (1987) Intracranial self-administration methodologies. *Neurosci. Biobehav. Rev.* **11,** 319–329.
14. Carlezon, Jr., W. A. and Wise, R. A. (1996) Rewarding actions of phencyclidine and related drugs in nucleus accumbens shell and frontal cortex. *J. Neurosci.* **16,** 3112–3122.
15. Paxinos, G., and Watson, C. (1998) *The Rat Brain in Stereotaxic Coordinates*, 4th ed. Academic, San Diego.
16. Iversen, S. D. and Iversen, L. L. (1981) *Behavioral Pharmacology*, 2nd ed. Oxford University Press, New York.
17. Alderson, H. L., Robbins, T. W., and Everitt, B. J. (2000) Heroin self-administration under a second-order schedule of reinforcement: acquisition and maintenance of heroin-seeking behavior in rats. *Psychopharmacology* **153,** 120–133.
18. Richardson, N. R. and Roberts, D. C. S. (1996) Progreesive ratio schedules in drug self-administration studies in rats: a method to evaluate reinforcing efficacy. *J. Neurosci. Meth.* **66,** 1–11.
19. Everitt, B. J. and Robbins, T. W. (2000) Second-order schedules of drug reinforcement in rats and monkeys: Measurement of reinforcing efficacy and drug-seeking behavior. *Psychopharmacology* **153,** 17–30.
20. Howell, L. L. and Byrd, L. D. (1991) Characterization of the effects of cocaine and GBR 12909, a dopamine uptake inhibitor, on behavior in the squirrel monkey. *J. Pharmacol. Exp. Ther.* **258,** 178–185.
21. Arnold, J. M. and Roberts, D. C. S. (1997) A critique of fixed and progressive ratio schedules used to examine the neural substrates of drug reinforcement. *Pharmacol. Biochem. Behav.* **57,** 441–447.
22. Panlilio, L. V., Weiss, S. J., and Schindler, C. W. (2000) Effects of compounding drug-related stimuli: escalation of heroin self-administration. *J. Exp. Anal. Behav.* **73,** 211–224.
23. Ettenberg, A. and Geist, T. D. (1991) Animal model for investigating the anxiogenic effects of self-administered cocaine. *Psychopharmacology* **103,** 455–461.
24. Xi, Z. X., Fuller, S. A., and Stein, E. A. (1998) Dopamine release in the nucleus accumbens during heroin self-administration is modulated by κ opioid receptors: an *in vivo* fast-cyclic voltammetry study. *J. Pharmacol. Exp. Ther.* **284,** 151–161.

20

Acute, Chronic, and Cancer Pain

Clinical Management

Allen W. Burton

1. Introduction

The International Association for the Study of Pain (IASP) defines pain as "an unpleasant sensory or emotional experience associated with actual or potential tissue damage, or described in terms of such damage" *(1)*. To successfully manage pain syndromes, the clinical situation, exact diagnosis, and the complex interplay of physiological and psychological factors must first be identified.

Pain, with the exception of neuropathic pain, generally follows a pattern of being initiated at the peripheral nociceptor level. Mechanical, thermal, or chemical stimuli are transduced into electrical signals, which are then transmitted to the spinal cord on myelinated a-delta (A-δ) and unmyelinated c-fibers. The myelinated A-δ transmission causes an immediate sensation of pain at the time of injury. The unmyelinated c-fiber transmission moves the electrical signals on into the next wave of pain, so-called "slow pain," which is modulated at the dorsal horn of the spinal cord and transmitted to the brain along the spinothalamic tract. Opportunities to modulate a pain signal occur peripherally at the nociceptor level, centrally at the dorsal horn level, and in the substantia gelatinosa *(2)*.

2. Materials

1. Morphine.
2. Hydromorphone.
3. Fentanyl.
4. Meperidine.
5. Oxycodone.

6. Hydrocodone.
7. Codeine.
8. Methadone.

3. Methods

3.1. Assessment of Pain

Many taxonomies exist for the physician to describe pain, including differentiating by neurophysiologic mechanism: nociceptive pain (both visceral and somatic) vs neuropathic pain; evaluating temporal factors: acute vs chronic; and pinpointing the etiology of pain: cancer-related pain, sickle cell-related pain, nonspecific low back pain, and so on. However, the actual assessment of pain often proves to be challenging, subjective in nature, and not clearly defined by one set of rules (*see* **Note 1**).

Pain reactions also differ from person to person, often evoking strong emotional responses, including depression, anxiety, and fear *(3)*. Physiological responses to pain include hypertension, tachycardia, tachypnea, and other indicators of sympathetic discharge, which are considered to be indirect indicators of acute pain. Typically, a diagnosis cannot be made on physiological responses alone, as they are often unreliable in assessing the intensity of pain and sometimes occur much later than the initial pain response. Therefore, the most reliable measure of pain is the patient's self-report, which gives a physician immediate feedback on how to proceed with treating or managing the pain.

MD Anderson Cancer Center's Brief Pain Inventory, the McGill Pain Questionnaire and others have been developed and validated to consistently quantify pain by utilizing a common language of rating the intensity of pain numerically on a scale of 0–10, with 0–3 representing mild pain, 4–7 moderate pain, and >7 representing severe pain (*see* Fig. 1 in **ref. *4***). By utilizing pain assessment tools, such as those listed above, physicians can successfully record the emotional and physiological responses of patients. Researchers can then go back to patient charts to learn more about the impact of various treatments for pain based on patient reporting *(5)*. Additionally, other aspects such as location, quality, extent (radiation), associated symptoms, and modulating factors, along with the responses to treatment, diagnostic studies, and the physical exam must be noted to determine a more accurate diagnosis (*see* **Note 2**).

It is important to keep in mind the limitations of technology. Once a diagnosis has been made, imaging studies can only confirm a diagnosis based on physical findings (i.e., fracture or herniated disk). Despite the fact that no one test can verify all of the underlying factors that cause pain, in general, the pain that patients feel must be treated as real and not imagined. Technology has not, and probably will not for some time, reach the point of quantifying the amount of pain felt based on traditional imaging studies. Thus far, pain-specific

neuroimaging techniques, including positron emission testing (PET) and functional magnetic resonance imaging (fMRI), remain on the forefront of the research realm *(6,7)*.

3.2. Acute Pain

3.2.1. Definitions and Pathophysiology

Acute pain typically refers to any pain syndrome that is recent in onset and that occurs postoperatively, whereas chronic pain refers to pain that persists beyond the expected duration of healing, which is usually approx 3 mo. Historically, prior to anesthesia, surgery and the postoperative period was an excruciatingly painful experience. However, even after the advent of surgical anesthesia, pain control was needed to enhance post-injury or surgical recovery because postoperative pain was often considered inevitable *(8)*. Inadequate postoperative pain treatment has many adverse sequelae, including deep venous thrombosis, atelectasis, and pneumonia as a result of inactivity *(9)*.

Among the medical community, there is a growing awareness that some surgeries may lead to chronic postsurgical pain syndromes. The procedures that most often lead to chronic pain are listed here in descending order, along with the approximate rates of diagnosed chronic pain in parenthesis: spinal fusion (30–60%), thoracotomy (22–67%), amputations (30–80%), mastectomy (11–47%), and hernia repair (2–20%) *(10)*. In light of these findings, a growing body of data has developed that supports the theory that better analgesia in the acute postoperative period may lead to a lower incidence in developing chronic pain *(11)*.

3.2.2. Treatment

Acute pain is usually treated with nonsteroidal antiinflammatory drugs (NSAIDs) and/or short-acting, "weak" opioids. In the postoperative setting, many choices exist for controlling pain, including intravenous (iv) patient-controlled analgesia (IPCA) and epidural infusions of local anesthetics combined with opioids, which are commonly set up as "patient-controlled epidurals" or PCEAs. Both PCEAs and IPCAs have proved to be safe and efficacious *(12)*, and IPCAs have even proved to be safe and effective in elderly patients undergoing extensive surgery *(13)*.

An IPCA device is set up to deliver a dose of pain medication iv on the patient's demand, by pushing a button. The dosing parameters are programmed into the computer-controlled pump. Typical settings allow a patient to "demand" a modest dose of medication every 10–15 min, with or without a continuous basal infusion of opioid. A "rescue" dose is available periodically as needed and can be administered by the nursing staff. Common medications and settings are found in **Table 1**. After dosing schedules are titrated appropri-

Table 1
**Intravenous Patient-Controlled Analgesia (IPCA) Medications
and Typical Dose Ranges**

Medication	PCA "demand dose" available q 10–20 min*	Continuous infusion (optional)*	Rescue dose available q 1–2 h*
Morphine	0.5–1.5 mg	0.5–1.0 mg/h	1–2 mg
Hydromorphone (Dilaudid)	0.2–0.8 mg	0.2–0.5 mg/h	0.5–1.0 mg
Fentanyl	12.5–25 mcg	12.5–25 mcg/h	25–50 mcg
Meperidine** (Demerol)	12.5–25 mg	12.5–25 mg/h	25–50 mg

*Suggested starting doses in opioid naïve patients. In elderly or debilitated patients, use the lower end of the dose range and titrate upwards as needed to comfort.

**Some physicians have gone away from the use of meperidine in this setting due to the build up of normeperidine with associated CNS excitatory effects including delirium and possibly seizures.

ately, patients are generally started on oral medications and oral analgesics at the same time, while discontinuing the use of the IPCA. Although epidural analgesia probably provides superior analgesia and may lead to better clinical outcomes in thoracic surgery, IPCAs and epidurals have not shown differences in clinical outcome in abdominal surgery *(2,14)*.

Commonly seen opioid-related side effects include nausea, pruritis, constipation, and mental clouding. Often in the perioperative setting, these side effects are mild and may be treated with an antiemetic, antihistamine, or at times a dose reduction of the current medications used. However, another option to treating side effects is to change opioids. When changing opioids, an attempt must be made to make equianalgesic conversions by utilizing a conversion table (*see* **Table 2**). As with other pain syndromes, so-called adjuvant analgesics are often used, such as NSAIDs in the postoperative period and physical modalities such as ice packs, deep breathing, and self-relaxation strategies.

3.3. Chronic Pain

3.3.1. Definitions and Pathophysiology

Chronic pain is defined as pain that lasts beyond the expected healing phase, which is defined by an arbitrary cutoff time of 3 mo. Bonica has estimated that 30% of the Western world's population suffers from chronic pain *(15)*. A recent study in the VA hospital found a 50% incidence of chronic pain in a survey of 300 randomized inpatients *(16)*.

Chronic pain syndromes come in many varieties; however, the most common is back pain *(17)*. Common etiologies include headache, postsurgical pain syn-

Table 2
Opioid Conversion Table*

Opioid	IV/SC opioid to IV/SC morphine	IV/SC morphine to IV/SC opioid	Oral opioid to oral morphine	Oral morphine to oral opioid	Oral morphine to IV/SC morphine: *Divide by 3*
Hydromorphone	5	0.2	5	0.2	IV/SC morphine to
Meperidine	0.13	8	0.1	10	oral morphine:
Oxycodone	–	–	1.5	0.7	*Multiply by 3*
Hydrocodone	–	–	0.5	2	

* Conversion ratios are approximate, and clinical conversations should be done carefully.

Guidelines: 1) Determine total amount of current opioid taken over a 24-h period that effectively controls pain. 2) Multiply by conversion factor(s) in the table above. (Convert to a morphine equivalent, then convert to a new opioid). Give 30–50% lower dose of the new opioid to account for partial cross-tolerance between opioids. 3) Divide the calculated 24-h dosage by number of doses to be given per day. 4) Add adequate PRN doses of new opioid for breakthrough pain (each prn dose ≈ 10–15% of total daily dose of new opioid prescribed). *Note:* Methadone, fnetanyl transdermal patches (Duragesic), and oral transmucosal fentanyl citrate (Actiq) do not follow standard conversions and need to be carefully titrated to desired effect.

dromes, and complex regional pain syndrome. Chronic pain begins at the nociceptor level, but with the passage of time other non-nociceptive factors become significant. Depression and anxiety seem to be nearly ubiquitous in all patients that suffer from severe chronic pain, making pain often seem magnified *(18)*.

3.3.2. Treatment

The diagnosis and treatment of chronic severe pain is best handled in a multidisciplinary approach. The algologist or pain specialist often utilizes medications, neural blockades, neurostimulation, physical methods, or other modalities to favorably alter the nociceptive input *(19–22)* and the patient must often have formal physiotherapy in order to recondition a weakened area or overcome muscle dystonias or focal muscle spasms. Because of lost self-esteem, hopelessness, and/or situational adjustment disorders, psychotherapy is a must in nearly all cases of chronic pain. This triad (treatment of pain, physiotherapy, and psychotherapy) of therapeutic intervention must be individualized based on the patient's needs and diagnosis. Also, in many cases, psychosocial issues abound, as there may be a loss of productivity that leads to disability issues, particularly in the case of work-related injuries. In the Western world, the explosion of workman's compensation and disability claims as a

result of back pain has been called epidemic in proportion, especially the controversy over the etiology of back pain *(22)*.

Chronic pain may be classified as somatic, visceral, or neuropathic in nature. Many chronic pain syndromes are mixed, thus requiring a combination of treatment approaches and medications targeting a variety of nociceptor sites. Chronic opioid therapy for noncancer-related pain follows this line of thinking directly in that it is most effective when utilized as part of a complete treatment package including physiotherapy and psychotherapy.

Pharmacologic approaches to the treatment of chronic pain consist mainly of NSAIDs, antiepileptics (AEDs), antidepressants, and less commonly, opioids (*see* **Table 3**). However, there is a growing agreement among physicians to use opioids to treat chronic noncancer-related pain *(23)*. The American Pain Society (APS) and the American Academy of Pain Medicine (AAPM) have issued a joint consensus statement supporting the use of opioid analgesics in chronic pain conditions as a humane, rational approach to treatment *(24)*.

3.3.3. Neuropathic Pain

3.3.3.1. Definitions and Pathophysiology

Neuropathic pain is characterized by pain that is generated in either the peripheral or central nervous system, not in a nociceptor. The pathway for neuropathic pain differs from that of visceral or nociceptive pain, which is initiated at the nociceptor level whereby a signal is processed via the peripheral and central nervous system. Patients characterize neuropathic pain as an "unfamiliar" sensation, with a burning, shooting, electrical, or numb, tingling quality to it. Any pain that a patient has difficulty describing in words is more than likely neuropathic pain.

Neuropathic pain may arise from various etiologies including nerve trauma, vascular disease, toxic-metabolic deficiencies, and infectious etiologies. Commonly seen types of neuropathic pain include painful diabetic neuropathy, complex regional pain syndrome, carpal tunnel syndrome, postherpetic neuralgia, spinal radiculopathy, trigeminal neuralgia, postchemotherapy pain syndromes, as well as others. Current theories on neuropathic pain, supported by much animal research reveal two critical elements in neuropathic pain: peripheral ectopic discharges and central sensitization *(25)*.

Ongoing, spontaneous ectopic neural discharges explain some cases of chronic neuropathic pain. Additionally, with continual afferent nociceptive input, central sensitization or "wind-up" occurs in the dorsal horn. This magnification of afferent input accounts for some of the extremely bizarre manifestations of chronic pain, such as allodynia, where the touch of a cotton swab may feel excruciatingly painful. However, in many cases the exact pathophysiology

Table 3
Adjuvant Analgesic Medications

Medications (by class)	Mechanism of Action	Toxicities Contraindications
NSAIDs	Inhibits prostaglandin synthesis in periphery and centrally, thus giving relief of inflammation and analgesia.	GI mucosa at risk (less with newer COX-2 inhibitors), renal toxicity.
AEDcs	Sodium channel blockade, inhibition of excitatory amino acids centrally, effective in neuropathic pain.	Various, generally CNS depressant-sedation, confusion, lethargy, and so on.
Antidepressants	Blocks reuptake of norepinephrine and serotonin thus enhancing analgesia in neuropathic pain.	Anticholinergic effects: sedation GI upset, weight gain.
Local Anesthetics	Sodium channel blockade, inhibits pain conduction.	Can cause neurotoxicity and cardiotoxicity with intravascular injection.
Adrenergic Agents	Enhances analgesia at spinal level, especially in neuropathic pain.	Hypotension, sedation.

of mixed nociceptive and neuropathic chronic pain states remains poorly understood.

3.3.3.2. TREATMENT

The most effective treatments for neuropathic pain include tricyclic antidepressants (TCAs), AEDs, and for severe pain, an opioid or tramadol may be helpful, as well as topical capsaicin, dextromethorphan, mexilitine, and venlafaxine *(26–30)*. In cases resistant to treatment with these agents, more interventional treatment options are frequently used such as neurostimulation and intrathecal infusions *(31,32)*.

3.4. Cancer-Related Pain

3.4.1. Definitions and Pathophysiology

It is estimated that up to 50% of patients undergoing treatment for cancer and up to 90% of patients with advanced cancer have pain *(33)*. Most (70%) cancer pain is caused by tumor involvement of organic structures, notably bone, neural tissue, viscera, or others. Up to 25% of cancer pain is a result of therapy, including chemotherapy, radiotherapy, or surgery *(34)*. Around 5–10% of cancer pain is accounted for by common pain syndromes, including back pain and headaches, which might have been exacerbated by the ongoing growth or treatment of cancer. Nearly all cancer-related pain is associated with and magnified by psychological or spiritual distress.

Because there are many types and origins of cancer-related pain, each with different treatment options, a thorough assessment is necessary to effectively manage cancer pain. Frequent reassessment is mandatory because of the dynamic nature of cancer progression and to rule out conditions that are considered oncologic emergencies *(35)*. These conditions include infection, fracture or impending fracture of a weight-bearing bone, bowel obstruction or perforation, spinal cord compression, and new metastatic disease (involving brain, epidural, or leptomeningeal metastasis). In these situations, palliative surgery, radiotherapy, or chemotherapy may be necessary to achieve significant relief.

3.4.2. Treatment

The treatment of cancer pain highly depends on the etiology of the pain and the severity of the associated symptoms. The cornerstone of cancer pain therapy is the use of opioids. According to the tenets and the cancer pain treatment guidelines set forth by the National Comprehensive Cancer Network (NCCN), the so-called "weak" opioids are used to treat mild to moderate pain dosed on an "as needed" basis. In moderate to severe pain, physicians should utilize the "strong" opioids on a long-acting dose schedule with a short-acting opioid available for breakthrough pain (*see* **Table 4**).

Table 4
Opioids: Generic and Trade Names

"Weak" Opiods	Parenteral Available?	Generic Available?	Elixir Available?
Codeine with acetaminophen (Tylenol # 3 and #4)*	N	Y	Y
Propoxyphene (Darvon, Darvocet)**	N	Y	N
Hydrocodone with acetaminophen (Vicoden, Lortab, Norco, Stagesic)***	N	Y	Y
"Strong" opiods			
Codeine*	N	Y	Y
Oxycodone (Roxicodone)	N	Y	Y
Oxycodone-CR (Oxycontin)****	N	N	N
Morphine (MSIR, Roxanol)	Y	Y	Y
Morphine-CR (Oramorph, MS Contin, Kadian)	N	Y	N
Fentanyl oral transmucosal (Actiq)*****	Y	N	N/A
Fentanyl transdermal (Duragesic)*****	Y	N	N/A
Hydromorphone (Dilaudid)	Y	Y	Y
Methadone (Dolophine)	Y	Y	Y

*Codeine is considered "weak" because of the small dose of codeine per tablet (30 mg in Tylenol #3 and 60 mg in Tylenol #4).

**Propoxyphene is available in combination with aspirin, acetaminophen or alone.

***Hydrocodone is available in different strengths with varying amounts of acetaminophen.

****CR = controlled release, this is a short-acting medication that is made "long-acting" by way of a controlled release oral vehicle or tablet.

*****Fentanyl citrate is available in an oral, short-acting (lozenge) or in a "long-acting" form as a time-release transdermal patch applied every 72 h.

Opioids produce analgesia through binding to specific opiate receptors in the brain and spinal cord *(36)*. The most useful analgesics in the treatment of cancer-related pain are the so-called "strong" opioids: morphine, oxycodone, fentanyl, hydromorphone, and methadone.

Morphine is the prototype opioid agonist. It is available in immediate-release and time-release tablets, liquid, and parenteral forms. All other opioids are compared to morphine to determine their relative analgesic potency (*see* **Table 2**). Like all opioids, morphine has no specific ceiling effect. However, at higher doses, side effects become more troublesome, especially sedation and confusion, because of the buildup of the metabolites, morphine-3, and morphine-6-glucuronide (M3G and M6G).

M6G is a more potent analgesic than M3G, whereas M3G has an excitatory effect, including myoclonus and hyperalgesia *(37)*. These metabolites, M3G and M6G, are eliminated in the kidney and thus morphine toxicity may especially be seen in patients with renal function impairment.

Oxycodone is a semisynthetic opioid that is available in short-acting tablets, immediate-release tablets, time-release tablets, and elixir. However, it is not available parenterally. Oxycodone is classified as a "strong" opioid with potency and dosing interval similar to morphine (long-acting drug every 8–12 h, with breakthrough dosing every 3 h as needed) *(38)*.

Fentanyl is a synthetic opioid which is 80-fold more potent than morphine. It is widely used in the parenteral form as an analgesic agent in the operating room and for postoperative epidural and iv patient-controlled analgesia. Additionally, two nonparenteral forms are available.

Transdermal fentanyl has become popular since the first studies in the late 1980s showed that it had efficacy and a similar side effect profile to other strong opioids *(39)*. Transdermal fentanyl is dosed in mcg/h with four different patch strengths available to correspond to parenteral fentanyl doses. After the initial patch application, systemic absorption is very low for the first 4 h while a reservoir of the drug is being established in the stratum corneum. Then, over the next 4 to 8 h, the plasma level of fentanyl rises steadily to become somewhat constant between 8–24 h. With a patch change every 72 h, the systemic levels of transdermal fentanyl remain very consistent *(40)*.

Oral transmucosal fentanyl citrate has recently been FDA approved for the use of breakthrough pain in opioid-tolerant cancer pain patients. This medication has shown promise since the early 1990s because of its potency and rapid onset. Its onset is comparable to iv administration as a significant analgesic effect occurs within 20 min *(41)*.

Hydromorphone is a semisynthetic opioid that is available both parenterally and orally, but not in a time-release preparation in the United States. It is known to be approx 5 times more potent than morphine, with a similar side effect profile.

Methadone, available in oral tablets, elixir, and parenteral forms, is a synthetic opioid that has shown promise as a second line drug for use in patients who experience inadequate analgesia or intolerable side effects from other opioids *(42)*. It is unique in many aspects: it is an intrinsically long-acting drug (not necessitating a time-release capsule or patch); it is relatively inexpensive; and it may have some clinically significant NMDA receptor blocking properties. Methadone's conversion is nonlinear to other opioids, perhaps being close to 1 to 1 mg/mg to morphine at low doses and at high doses perhaps close to 10 to 1 mg/mg. At high doses, methadone has shown to have a greater potency than morphine, thus necessitating a careful titration when rotating opioid medications *(43)*.

3.4.2.1. MANAGEMENT OF OPIOID-RELATED SIDE EFFECTS

Effective treatment or avoidance of opioid-related side effects is an important component in the treatment of cancer-related pain. Constipation is universal when taking opioids, but is treated through the use of daily stool softeners with a stimulant (senna, docusate). Opioid-related nausea might occur after an increase in dosage or initiation of opioid therapy. Often, metoclopramide is effective in treating opioid-related nausea (*see* **Table 5**) *(44)*.

The treatment of sedation and cognitive impairment is usually best accomplished either with dose reduction or opioid rotation (changing opioids in equianalgesic doses). If sedation is present without accompanying confusion, a psychostimulant such as methylphenidate might be given *(45)*. Cognitive impairment in a cancer patient may have an alternate etiology other than being opioid related. Some common causes are hypercalcemia, sepsis, renal failure, new CNS metastasis, or metabolic encephalopathy *(46)*.

3.4.2.2. ADJUVANT ANALGESICS

Adjuvant analgesics include NSAIDs, antidepressants, AEDs, local anesthetic agents, and muscle relaxants that are not given for their primary use, but for their analgesic properties *(47)*. Certain syndromes are especially responsive to treatment with these adjuvants. NSAIDs are often used in the treatment of painful bony metastasis, whereas antidepressants and/or anticonvulsants are often used in treating neuropathic pain syndromes.

3.4.2.3. ALTERNATE ROUTES OF ADMINISTRATION

Alternate routes of administration of analgesics must be considered in treating cancer pain when the oral route becomes ineffective or if the patient is unable to swallow medications. Intravenous, subcutaneous, rectal, epidural, and intrathecal routes all have a role in the treatment of cancer pain. Subcutaneous opioid infusions are very effective at treating difficult pain in patients

Table 5
Adjuvants Used to Treat Opioid-Related Side Effects

Medication	Mechanism	Side Effects
Nausea		
Metoclopramide	Central dopaminergic blocker (D1, D2), and promotes gastric emptying	Extrapyramidal side effects
Ondansetron	Blocks 5-HT3 receptors	Constipation
Prochlorperazine	Central D1 blockade	Anticholinergic effects
Droperidol	Central blockade of D1, NE, HT3, and GABA at CTZ	Sedation, akathesia
Pruritis		
Diphenhydramine	Histamine 1 receptor blocker	Somnolence, confusion
Constipation		
Senekot-S, Colace	Stool softener, osmotic effect to draw water into the bowel lumen	GI cramping
Sedation/Somnolence		
Methylphenidate	CNS Stimulant Sympathomimetic	Anxiety, insomnia
Modafanil	CNS Stimulant	Headache

that do not respond well to oral medications or cannot take oral medications *(48)*. Neuraxial analgesic delivery (epidural or intrathecal) is an effective route of pain control either in patients with difficulty to control pain or in patients suffering intolerable opioid-related side effects. Most often, combinations of opioids plus another agent are used in a neuraxial infusion, either via an external pump and catheter or an implanted pump and catheter *(49–51)*.

3.4.2.4. NERVE BLOCKS

Experts estimate that cancer pain is very difficult to treat in approx 10–15% of all patients. Selected nerve blocks may prove helpful to patients with resistant pain or in patients with severe opioid-related side effects. A good example is a neurolytic celiac plexus block, which has been demonstrated to help the majority of patients suffering from pain associated with pancreatic carcinoma. Physicians administering this type of block report a low complication rate *(51)*. It is important to utilize these blocks in the setting of comprehensive care of the patient. Although not necessarily a remedy, nerve blocks often make pain more manageable. For very resistant pain syndromes in the face of advanced cancer, sometimes neurosurgical destructive procedures are indicated including cordotomy and myelotomy. Another option is heavy sedation to make the pain tolerable, so-called "terminal sedation."

3.4.2.5. PALLIATIVE CARE

Palliative care has been defined as the active total care of patients whose disease is not responsive to curative treatments. Control of symptoms and psychological, social, and spiritual support are paramount to successful palliative care programs *(52)*. The goal of palliative care is to achieve the best possible quality of life for patients and their families *(53)*. This growing area of medicine is often practiced in inpatient units that utilizes a transitional approach of sending some patients home with home hospice care. This approach is a patient-centered, multidisciplinary, comfort-driven method of caring for the dying patient *(54)*.

4. Notes

1. The clinical awareness of pain syndromes has never been higher. As outlined in this chapter, many different taxonomies have been developed and are commonly used to categorize pain syndromes. However, at times, it still seems impossible to diagnose pain into an "either/or" category. Clinically, there is a great deal of overlap among pain syndromes. For example, a patient with chronic cancer-related pain may have an operation, thereby additionally experiencing acute pain postoperatively. Thus, the clinician must have a working knowledge of all pain states and their treatments.

2. As with other medical specialties, a good tenet of pain management includes doing a thorough history and physical examination on all patients experiencing pain. It is especially important to remember the complex interplay between nociception and psychological perturbations. It has been said that having to live with chronic pain brings out the worst in a person's psychological make-up. The clinician must set realistic goals of treatment for controlling pain, so that if having pain completely eliminated is not an option, then the patient's treatment plan must help the patient to manage and live satisfactory with a reduced amount of pain. The future is bright for pain sufferers, as much research and clinical effort is now being focussed on a more complete understanding of the pathophysiology of pain. As the neurochemistry is more clearly understood, more treatment options will become available. The critical analysis and application of these newer treatments will be challenging, but also very promising.

Acknowledgment

References

1. Merskey, H. and Bogduk, N. (1994) *Classification of Chronic Pain*. IASP, Seattle, WA.
2. Willis, W. D. (1988) Physiology of Pain Perception, in *Biowarning System in the Brain* (Takagi H., Oomura, Y., Ito, M., and Otsuka, M., eds.), University of Tokyo Press, Tokyo, Japan.
3. Thorn, B. E., Rich, M. A., and Boothby, J. L. (1999) Pain beliefs and coping attempts: Conceptual model building. *Pain Forum* **8,** 169–171.
4. Price, D. D., McGrath, P. A., Rafii, A., and Buckingham, B. (1983) The validation of visual analogue scales as ratio scale measures for chronic and experimental pain. *Pain* **17,** 45–56.
5. Farrar, J. T., Young, J. P., LaMoreaux, L., Werth, J. L., and Poole, R. M. (2001) Clinical importance of changes in chronic pain intensity measured on an 11-point numerical pain rating scale. *Pain* **94,** 149–158.
6. Rainville, P., Bushness, M. C., and Duncan, G. H. (2000) PET studies of the subjective experience of pain, in *Pain Imaging* (Casey, K. L. and Bushnell, M. C., eds.), IASP, Seattle, WA, pp. 123–156.
7. Davis, K. D. (2000) Studies of pain using functional magnetic resonance imaging, in *Pain Imaging* (Casey, K. L. and Bushnell, M.C., eds.), IASP, Seattle, WA, pp. 195-210.
8. Warfield, C. A. and Kahn, C. H. (1995) Acute pain management: programs in US hospitals and experiences and attitudes among US adults. *Anesthesiology* **83,** 1090–1094.
9. Kehlet, H. (1994) Postoperative pain relief-what is the issue? *Br. J. Anesth.* **72,** 375–378.
10. Perkins, L. and Kehlet, H. (2000) Incidence of chronic pain following surgery: a review. *Anesthesiology* **93,** 1123–1133.

11. Senturk, M., Ozcan, P. E., Talu, G. K., Kiyan, E., Camci, E., Ozyalcin, S., et al. (2002) The effects of three different analgesia techniques on long-term postthoracotomy pain. *Anesth. Analg.* **94,** 11–15.
12. Wigful, J. and Welchew, E. (2001) Survey of 1057 patients receiving post-operative patient-controlled epidural analgesia. *Anesthesia* **56,** 70–75.
13. Mann, C., Pouzeratte, Y., Boccara, G., Peccoux, C., Vergne, C., Brunat, G., et al. (2000) Comparison of intravenous or epidural patient-controlled analgesia in the elderly after major abdominal surgery. *Anesthesiology* **92,** 433–441.
14. Flisberg, P., Tornebrandt, K., Walther, B., and Lundberg, J. (2001) Pain relief after esophagectomy: Thoracic epidural analgesia is better than parenteral opioids. *J. Cardiothoracic Vasc. Anesth.* **15,** 282–287.
15. Bonica, J. J. (1987) Importance of the problem, in *Chronic Non-Cancer Pain*, (Andersson, S., Bond, M., Mehta, M., and Swerdlow, M., eds.), MTP, Lancaster, UK, p. 13.
16. Clark, J. D. (2002) Chronic pain prevalence and analgesic prescribing in a general medical population. *J. Pain Symptom Manag.* **23,** 131–137.
17. Fordyce, W. E. (1995) Chronic low back pain, in *Back Pain in the Workplace* (Fordyce, W. E., ed.), IASP, Seattle, WA, pp. 19–23.
18. Polatin, P. B., Kinney, R. K., Gatchel, R. J., Lillo, E., and Mayer, T. G. (1993) Psychiatric illness and chronic low back pain: The mind and the spine, which goes first? *Spine* **18,** 66–71.
19. Borodic, G. E. and Acquadro, M. A. (2002) The use of botulinum toxin for the treatment of chronic facial pain. *Clin. J. Pain* **3,** 21–27.
20. Staats, P. and North, R. B. (1996) Diagnostic nerve root blocks, facet blocks, and discography: a rational approach, in *Perspectives in Neurological Surgery* (Hadley, M. N., ed.), Quality Medical Publishing, St. Louis, MO.
21. Burchiel, K. J., Anderson, V. C., Brown, F. D., Fessler, R. G., Friedman, W. A., Pelofsky, S., et al. (1996) Prospective, multicenter study of spinal cord stimulation for relief of chronic back and extremity pain. *Spine* **21,** 2786–2794.
22. Winkelmuller, M. and Winkelmuller, W. (1996) Long-term effects of continuous intrathecal opioid treatment in chronic pain of nonmalignant etiology. *J. Neurosurg.* **85,** 458–467.
23. Schofferman J. (1999) Long-term opioid analgesic therapy for severe refractory lumbar spine pain. *Clin. J. Pain* **15,** 136–140.
24. American Academy of Pain Medicine homepage. http://www.painmed.org/ productpub/statements/opioidstmt.html, accessed on Mar. 4, 2002.
25. Gracely, R. H., Lynch, S. A., and Bennett, G. J. (1992) Painful neuropathy: altered central processing maintained dynamically by peripheral input. *Pain* **51,** 175–194.
26. Watson, C. P. and Babul, N. (1998) Efficacy of oxycodone in neuropathic pain: a randomized trial in postherpetic neuralgia. *Neurology* **50,** 1837–1841.
27. Boulton, A. J. (1999) Current and emerging treatments for the diabetic neuropathies. *Diabetes Rev.* **7,** 379–386.

28. Woolf, C. J. and Mannion, R. J. (1999) Neuropathic pain: etiology, symptoms, mechanisms, and management. *Lancet* **353,** 1959–1964.

29. Backonja, M., Beydoun, A., Edwards, K. R., et al. (1998) Gabapentin for the symptomatic treatment of painful neuropathy in patients with diabetes mellitus: a randomized controlled trial. *JAMA* **280,** 1831–1836.

30. Harati, Y., Gooch, C., Swenson, M., et al. (1998) Double-blind randomized trial of tramadol for the treatment of the pain of diabetic neuropathy. *Neurology* **50,** 1842–1846.

31. Kemler, M. A., Barendse, G. A. M., van Kleef, M., de Vet, H. C. W., Rijks, C. P. M., Furnee, C. A., et al. (2000) Spinal cord stimulation in patients with chronic reflex sympathetic dystrophy. *N. Engl. J. Med.* **343,** 618–624.

32. Staats, P. S., Luthardt, F., Shipley, J., et al. (2001) Long-term intrathecal ziconotide therapy: a case study and discussion. *Neuromodulation* **4,** 121–126.

33. Cleeland, C. S., Gonin, R., Hatfield, A. K., Edmonson, J. H., Blum, R. H., Stewart, J. A., et al. (1994) Pain and its treatment in outpatients with metastatic cancer. *NEJM* **330,** 592–596.

34. Higginson, I. J. (1997) Innovations in assessment: epidemiology and assessment of pain in advanced cancer, in *Proceedings of the 8th World Congress on Pain; Progress in Pain Research and Therapy* (Janson, T. S., Turner, J. A., and Wiesenfeld-Hallin Z., eds.), IASP, Seattle, WA, pp. 707–716.

35. Benedetti, C., Brock, C., Cleeland, C., et al. (2000) NCCN practice guidelines for pain. *Oncology* **11,** 135–150.

36. Yaksh, T. L. and Rudy, T. A. (1976) Analgesia mediated by a direct spinal action of narcotics. *Science* **192,** 1357–1358.

37. Portenoy, R. K., Khan, E., and Layman, M. (1991) Chronic morphine therapy for cancer pain: plasma and cerebrospinal fluid morphine and morphine-6-glucuronide concentrations. *Neurology* **41,** 1457–1461.

38. Poyhia, R., Vainio, A., and Kalso, E. (1993) A review of oxycodone's clinical pharmacokinetics and pharmacodynamics. *J. Pain Symptom Manage.* **8,** 63–67.

39. Miser, A. W., Narang, P. K., Dothage, J. A., Young, R. C., Sindelar, W., and Miser, J. S. (1989) Transdermal fentanyl for pain control in patients with cancer. *Pain* **37,** 15–21.

40. Varvel, J. R., Shafer, S. L., Hwang, S. S., Coen, P. A., and Stanski, D. R. (1990) Absorption characteristics of transdermally applied fentanyl. *Anesthesiology* **70,** 928–934.

41. Fine, P. G., Marcus, M., De Boer, A. J., and Van Der Oord, B. (1991) An open label study of oral transmucosal fentanyl citrate for the treatment of breakthrough cancer pain. *Pain* **45,** 149–153.

42. Davis, M. P. and Walsh, D. (2001) Methadone for relief of cancer pain: a review of pharmacokinetics, pharmacodynamics, drug interactions and protocols of administration. *Support Care Cancer* **9,** 73–83.

43. Bruera, E., Pereira, J., Watanabe, S., Belzile, M., Kuene, N., and Hanson, J. (1996)

Opioid rotation in patients with cancer pain. A retrospective comparison of dose ratios between methadone, hydromorphone, and morphine. *Cancer* **78,** 852–857.

44. Mannix, K. (1998) Palliation of nausea and vomiting, in *Oxford Textbook of Palliative Medicine* (Doyle, D., Hanks, G. W. C., and MacDonald, N., eds.), Oxford University Press, Oxford, England, pp. 489–499.

45. Bruera, E., Brenneis, C., Paterson, A. H., and MacDonald, R. N. (1989) Use of methylphenidate as an adjuvant to narcotic analgesics in patients with advanced cancer. *J. Pain Symptom Manag.* **4,** 3–6.

46. Bruera, E., MacMillan, K., Hanson, J., and MacDonald, R. N. (1989) The cognitive effects of the administration of narcotic analgesics in patients with cancer pain. *Pain* **39,** 13–16.

47. Driver, L. C., Strasser, F., and Burton, A. W. (2002) Adjuvant analgesics: a review. *Pain Practice*, (in press).

48. Bruera, E. D., Chadwick, S., Bacovsky, B., and MacDonald, R. N. (1985) Continuous subcutaneous infusion of narcotics using a portable disposable pump. *J. Palliative Care* **1,** 46–47.

49. Von Dongen, R. T. M., Crul, B. J. P., and De Bock, M. (1993) Long-term intrathecal infusion of morphine and morphine/bupivacaine mixtures in the treatment of cancer pain: a retrospective analysis of 51 cases. *Pain* **55,** 119–123.

50. Bennett G., Serafani M., Burchiel K., Hassenbusch S. J., et al. (2000) Evidence based review of the literature on intrathecal delivery of pain medication. *J. Pain Symptom Manag.* **20,**S12–36.

51. Eisenberg, E., Carr, D. B., and Chalmers, T. C. (1995) Neurolytic celiac plexus block for treatment of cancer pain: a meta-analysis. *Anesth. Analg.* **80,** 290–295.

52. Patrick, D. L., Engelberg, R. A., and Curtis, J. R. (2001) Evaluating the quality of dying and death. *J. Pain Symptom Manag.* **22,** 717–726.

53. Driver, L. C. and Bruera, E. (2000) Principles, in *The M. D. Anderson Palliative Care Handbook* (Driver L. C. and Bruera, E., eds.), The University of Texas Press, Houston, TX, pp. 3–5.

54. Von Gunten, C. F. (2002) Secondary and tertiary palliative care in US hospitals. *JAMA* **287,** 875–881.

21

Clinical Treatment of Opioid Addiction and Dependence

Walter Ling, Richard A. Rawson, and Margaret Compton

1. Introduction

Until the middle of the last century, achievement of abstinence was the only available treatment option for opioid dependence. Most often, addicts were simply expected to go "cold turkey," although abstinence was sometimes accomplished by way of inpatient hospitalization with adjunctive medications to help alleviate symptoms of craving and withdrawal. The general belief, however, was that abstinence was best achieved by correcting the addict's underlying psychopathology, which would result in the addiction simply going away. Rarely were addicts able to remain off drugs long enough to be truly rehabilitated, however, and for the most part, even after long hospitalizations, relapse was the predictable outcome.

With the introduction of methadone in the 1960s, this all changed. The discovery of methadone maintenance demonstrated for the first time that physical dependence on opiates could be addressed with a medication *(1)*. Addicts could be stabilized pharmacologically and efforts could then be directed toward psychological, social, and vocational rehabilitation. Once these were accomplished, a decision could be made whether or not to attempt abstinence by withdrawing the medication. But despite its repeated demonstrated success, methadone maintenance has been shrouded in controversy primarily because from a sociocultural perspective it is considered undesirable to provide an opiate to an opiate addict, and this belief has been the driving force in the search for alternative pharmacotherapies and methods of detoxification. Fear of methadone diversion, for example, was a major factor in developing Levo-alpha-acetylmethadol (LAAM), a longer-acting opioid agonist requiring less-

frequent dosing, and the development of antagonists such as naltrexone was predicated on their ability to block opiate effects. Buprenorphine, the most recently developed opiate medication, has both agonist and antagonist properties, and is therefore appealing from both pharmacological and sociocultural perspectives. Currently being used in much of Europe and Australia, it has just been approved by the US Food and Drug Administration in October, 2002.

Various detoxification strategies also continue to be advocated and are, from time to time, touted as medical breakthroughs. Detoxification, though, has been characterized by a low rate of completion and, even for completers, a high rate of relapse. Considering the serious risks associated with return to drug use, including hepatitis, HIV, and other forms of infectious disease, detoxification can only be legitimately considered as a transitional strategy to longer-term treatment *(2)* (*see* **Note 1**). Nonopioid medications like clonidine and lofexidine have been used as adjunctive medications for detoxification, and for anesthesia-assisted detoxification various anesthetics and the opioid antagonists naloxone and naltrexone are also used. This chapter will discuss the use of opioids for maintenance and detoxification of opiate dependence but it needs to be kept in mind that delivery of any pharmacotherapy needs to be accomplished within the context of a comprehensive treatment environment.

2. Materials

2.1. Methadone

A synthetic opioid agonist with properties similar to morphine, methadone was invented by the Germans during World War II in response to interruption of natural opiate supplies by the Allies. Methadone binds to the mu-, delta-, and kappa-opioid receptors, with its main effect on the mu (μ)-receptor, and its primary clinical manifestations are analgesia and respiratory depression. It is usually administered orally in a racemic mixture of its two enantiomers, R-methadone and S-methadone. It is well absorbed after oral administration with peak plasma concentration achieved in approx 2-1/2 h with the solution *(3)* and 3 h with the tablets (*see* **Fig. 1.** in **ref. 4**). Its duration of action after a single dose is somewhat shorter than the 12–48 h half-life seen after repeated dosing and the average half-life for patients on methadone maintenance is approx 24 h. Methadone has a high tissue distribution and is highly bound (over 85%) to plasma protein, mostly to α_1 acid protein. It undergoes hepatic metabolism and is excreted in the urine. Because of its basic and lipophylic properties, urinary pH has a significant effect on methadone elimination, with more excretion of unchanged methadone in acidic urine. Methadone is metabolized mainly by CYP3A4, an inducible enzyme, and continued methadone administration its own metabolism. Concomitant administration of other medications such as carbamazepine, phenytoin, refampin, zidovudine, barbiturates, spironolactone,

verapamil, diethylstilboestrol, and amitriptyline reduces or decreases methadone blood level, whereas other medications, such as fluoxetine and fluvoxamine, inhibit the enzyme CYP3A4 and increase methadone plasma concentration. It is thus important to consider concomitant medications for patients taking methadone *(5)*.

Pharmacological properties that make methadone a suitable treatment for opiate dependence are related to its ease of administration, high oral bioavailability, and relatively rapid onset of clinical effect after oral administration, and its relatively long half-life necessitating in most instances only once-daily oral dosing. Clinically, it suppresses the symptoms of opioid withdrawal and, in sufficient doses, it blocks the euphoric effects of subsequently administered heroin, thus discouraging continued illicit opiate use.

2.2. Levo-α-acetylmethadol (LAAM)

Also a product of the Germans during World War II, LAAM is a long-acting synthetic opioid agonist similar in action to morphine and methadone that affects the central nervous system (CNS) and smooth muscle. As with other opioid agonists, LAAM produces analgesia and sedation, and tolerance develops with repeated use. An abstinence syndrome occurs on cessation from chronic LAAM administration, but with slower onset, less intensity, and a more prolonged course than seen with other opiates *(6,7)*.

Following oral administration, LAAM is well absorbed and sequentially n-demethylated in the liver to nor-LAAM and dinor-LAAM. Nor-LAAM is 3–6 times more active than either LAAM or dinor-LAAM, both of which are about equal to methadone in activity. A detectable blood level generally appears within 30 min of oral administration, reaches peak levels within 4–8 h, and remains detectable for 90 h. Although peak and trough blood levels of LAAM vary considerably after single doses, steady-state plasma concentrations of its metabolites are much more stable after repeated dosing. The clinical effects of LAAM result from the combined pharmacological effects of the parent compound and its active metabolites. LAAM is excreted primarily in the feces with approx 20% excreted in the urine, largely as conjugates *(8)*.

Plasma concentrations of LAAM and its two active metabolites increase after multiple oral doses and the maximum concentration of each varies from three- to tenfold. The protein binding of LAAM and its metabolites in humans is weak, readily reversible, and does not appear to displace the binding of the drugs. Additionally, the amount of LAAM and its bound metabolites is sufficiently low so that their displacement by other drugs does not alter their pharmacological activity to a clinically significant degree *(9,10)*. The median terminal half-life of nor-LAAM and dinor-LAAM is 0.7 d and 3 d, respectively, but this varies considerably among individuals. The overall opiate

activity after oral LAAM administration, as measured by pupillary constriction, is best represented by the time course of nor-LAAM (11) (*see* **Note 2**).

2.3. Buprenorphine

A derivative of morphine, buprenorphine is a partial μ opioid agonist and a weak κ antagonist. Its clinical effects are primarily expressed at the μ receptor, and are similar to those of the full agonists, morphine, LAAM, and methadone, whose clinical effects are proportional to the dose administered *(12)*. Because buprenorphine is a partial agonist however, its agonist effects plateau at higher doses and begin to behave more like an antagonist. This "ceiling effect" gives rise to a high safety profile clinically, a low level of physical dependence, and only mild withdrawal upon cessation after prolonged administration, making buprenorphine especially advantageous for the treatment of opiate dependence *(13,14)* (*see* **Note 3**). Further, buprenorphine's slow dissociation from the receptors provides a long duration of action, allowing dosing schedules to vary from several times daily to several times a week. Taken orally, buprenorphine is not well absorbed and much of it is destroyed in the liver. However, buprenorphine is well absorbed through the lining of the oral cavity and when given sublingually, it reaches 60–70% of the plasma concentration achieved by the parenteral routes. After absorption, buprenorphine is widely distributed throughout the body with peak plasma concentration in approximately 90 minutes and a terminal half-life of 4–5 h. It is highly bound to plasma proteins and is inactivated by the enzymatic transformations, N-dealkylation, and conjugation *(15)*. Buprenorphine's metabolites are excreted mainly via the fecal route.

2.4. Naltrexone

A pure narcotic antagonist, naltrexone is produced by N-allyl substitution of naloxone with the cyclopropylmethyl radical of cyclazocine, combining the pure antagonist action of the former with the long duration of action and oral effectiveness of the latter *(16)* (*see* **Note 4**). Naltrexone is quickly absorbed after oral administration, reaching peak plasma concentration within 1 h, although it begins taking effect even sooner, and its effects are long lasting. A single oral dose of 50 mg naltrexone blocks the euphoric effects of 25 mg heroin for up to 24 h and at 150 mg, it blocks heroin effects for up to 3 d *(17)*. Naltrexone does not produce euphoria, it has only minimal side effects, including dysphoria in some patients *(18)*, and it is not addictive, which prevents street sale or abuse by addicts. Administration of naltrexone to patients with opioids in their system results in precipitated withdrawal and an opioid-free interval, generally 5–7 d for heroin and 10–14 d for methadone, is necessary prior to the initial dose *(19)*.

3. Methods

Clinical treatment of opiate dependence includes long-term maintenance that aims at stabilization of drug use, psychosocial rehabilitation, and short-term detoxification intended to achieve a state of abstinence. The most pragmatic and realistic approach, however, is to view opiate dependence as a chronic relapsing disease requiring extended therapy. Methadone, LAAM, and buprenorphine are all suitable medications for opiate maintenance treatment.

3.1. Maintenance

Management of maintenance therapy from a medical perspective is straightforward. The idea is to take advantage of the cross-tolerance between the opiate of abuse, most often heroin, but also other prescribed or nonprescribed opiates, and the maintenance medication. Patients should be titrated over a relatively short period of time, generally several days, to a dose that eliminates or greatly reduces drug craving and use without producing such undue side effects as sedation, and produces a degree of blockade to subsequently administered opiates, thus discouraging continued illicit drug use. Patients may, for example, be started on 30 mg methadone or LAAM, or 4–8 mg sublingual buprenorphine. The dose should be titrated upward until clinical stabilization is achieved with subsequent adjustments made as clinically indicated. Once the maintenance dose is reached, efforts can be made toward psychological, social, and vocational rehabilitation. Medication should be provided for as long as the disorder exists. Although some patients can successfully discontinue maintenance treatment, the number is small and the relapse rate is unacceptably high. It is important, therefore, that maintenance not be arbitrarily limited to a certain length of time and that physicians not prematurely encourage patients to discontinue treatment *(20)*.

Delivery strategies among the various maintenance medications differ somewhat. Because methadone has a relatively short half-life, approx 24 h, daily administration is required. LAAM, with its much longer duration of action, can be administered three times weekly, and buprenorphine's long duration of action allows for a wide range of dosing options. Methadone and LAAM, schedule II narcotics, are highly regulated by law and can only be administered by physicians in specially licensed narcotic treatment programs (NTPs). However, under a special provision of the Narcotic Treatment Act of 2000 *(21)*, buprenorphine, will be provided by qualified physicians in their general medical practice. This is expected to revolutionize treatment of heroin addicts in the U.S. and there are now some movements afoot to make methadone and LAAM administration less onerous as well. These changes are moving very slowly though and in the meantime it must be remembered that both are powerful

narcotics and should be given only to patients with a demonstrated degree of physical dependence.

Federal law requires that a thorough patient assessment be done prior to administration of any maintenance medication. This should include a complete history of addiction, as well as other medical history. Although patients who attend NTPs are almost always highly addicted or there would be little reason to seek such treatment, a certain degree of vigilance and caution are required especially when treatment is initiated. The major side effects from methadone and LAAM are sedation and respiratory depression in nondependent persons, but there have been a few reports of death involving patients early in treatment whose degree of physical dependence and perhaps individual sensitivity to the medications may be an issue. Because of its ceiling effect, buprenorphine is very safe and overdose is rare, but a small number of deaths have been reported as a result of illicit intravenous buprenorphine use at high doses and in combination with benzodiazepines, sedatives, hypnotics, and alcohol *(22)*.

The usual methadone maintenance dose varies from 50 or 60 mg to 100 mg or higher. The upper limit for LAAM maintenance is generally about 140 mg but varies significantly among individuals and there should not be a fixed idea of what the maximum dose ought to be. The tendency, however, in most treatment clinics, is for patients to receive an inadequate dose *(23)*. Most patients on methadone and LAAM can be maintained on a steady dose for extended periods without increases and tolerance to their therapeutic efficacy generally does not develop with long-term treatment. Overdose of methadone or LAAM can be treated with the narcotic antagonist naloxone but because of their long duration of action, especially with LAAM, repeated naloxone administration is required. Patients must be observed closely, especially for respiratory depression, until the effects of methadone or LAAM have run their course. For buprenorphine sublingual tablets, the recommended maintenance dose is 24–32 mg achieved over a period of several days to 1 or 2 wk. Buprenorphine's ceiling effect and its high receptor affinity allow for dosing schedules ranging from more than once a day to once every several days *(24)*. Unlike methadone and LAAM maintenance doses, which may need to be increased with time, the maintenance dose of buprenorphine tends to decrease with long-term treatment *(25)*.

Naltrexone, being an opiate antagonist, is unique in that patients must be completely opiate-free prior to the first dose. This can be ascertained by naloxone challenge, which involves giving a dose of naloxone intravenously, subcutaneously, or intramuscularly, and observing the patient for signs or symptoms of precipitated withdrawal. Even minor withdrawal symptoms preclude the administration of naltrexone because it is significantly more potent than naloxone and could cause severe and prolonged withdrawal effects. Because achiev-

ing a state of abstinence is often very difficult for addicts, it is perhaps in this instance that detoxification under heavy sedation may have a place.

3.2. Detoxification

Methadone and clonidine are the two most widely used medications currently available in the U.S. for opiate detoxification. LAAM has only limited use and buprenorphine, although already shown to be a suitable agent, has just been approved. Opiate-based detoxification is very straightforward clinically. The strategy is to substitute a prescribed opiate for the street heroin and once the addict is stabilized, to gradually reduce the dose to "0," usually with provision of ancillary medications such as clonidine to alleviate withdrawal effects. In settings where opiate-based medications are not available, clonidine and lofexidine, both non-narcotic medications, are used to help suppress such symptoms of withdrawal as gastrointestinal distress: nausea, vomiting, and diarrhea; and autonomic nervous system hyperactivity *(26,27)*. These medications, however, do not effectively relieve psychic symptoms such as anxiety and insomnia and benzodiazepines are often used for this purpose.

Because symptoms of opiate withdrawal are self-limiting and nonlife threatening, detoxification can generally be achieved in a matter of days. There has also been some recent interest in rapid and ultrarapid opiate detoxification (UROD), which is performed while the patient is under anesthesia or heavy sedation so that withdrawal discomfort is abbreviated, symptoms are more easily endured, and the patient awakens drug free. In most cases, the patient is prescribed long-term maintenance with naltrexone. Rapid detoxification strategies are not standardized, however, and the procedures are often considered by practitioners to be "trade secrets." Many patients continue to experience considerable withdrawal symptoms for days following rapid and ultrarapid detoxification and so it is uncertain whether these patients have actually achieved physiological detoxification or simply managed to get on naltrexone. Long-term follow-up has not, thus far, demonstrated advantages of these rapid and ultrarapid procedures and the risk involved, albeit small, remains an issue for clinicians *(25)* (*see* **Note 5**).

The problem with detoxification by whatever means and methods is the high rate of relapse. It is not particularly difficult to get off opiates but it is very difficult to stay off opiates. Virtually all of the follow-up data indicate that detoxification by itself results in low rates of completion and even for the completers, high rates of relapse. Thus, with the current HIV and hepatitis epidemic among drug users, detoxification seems especially difficult to justify as an end in itself and its use appears tenable only as a transition to some long-term treatment *(25)*.

4. Notes

1. Given our current understanding of the effects of chronic opiate administration on the nervous system and the tools we have on hand if treatment were strictly directed toward the medical goals of reduced mortality and improved patient health, opiate dependence treatment should be rather straightforward. But medical treatment is never delivered without a social context and this is certainly the case with opiate dependence. To be sure, the evolution of modern opiate pharmacotherapy has been strongly influenced by societal and political attitudes. In societal terms, for example, the discovery of methadone maintenance was a breakthrough because it meant a cure for heroin addiction or a return of the addict to the nonaddicted state. But this is not medically reasonable since, as we now know, the effects of chronic heroin addiction are very long lasting and perhaps even permanent. The more pragmatic view and the one proposed and advocated by Dole and Nyswander *(28)*, the original proponents of methadone treatment, is that the condition of a chronic heroin addict is similar to that of a diabetic whose pancreas has failed and so needs insulin for life. In other words, recognizing that the effect of heroin addiction on the brain is protracted and possibly permanent, treatment should aim at controlling manifestations of the addiction, improving health of the patient, reducing mortality and morbidity, and enabling a more normal lifestyle *(1,2)*.

2. Opiate dependence treatment thus far, however, has been greatly influenced by the public perception that addicts are basically "bad people" and that it is wrong to give them narcotics. Further, as noted earlier, LAAM was developed as much in response to fear of methadone street diversion as anything else even though this problem could have been dealt with quite adequately by supplying patients with take home doses of methadone. Certainly our nearly 40 yr of experience have shown that methadone street diversion has never been a public health problem and the small amount that is diverted is generally bought by addicts who should be treated with methadone in the first place. Moreover, the idea that LAAM's long duration of action would reduce the need for take-home doses actually became a disadvantage for patients because of the legal prohibition on take home LAAM.

3. In this context, buprenorphine seems a highly desirable medication because it has something for everyone. It has some agonist activity that addicts find acceptable and it has antagonist properties that make it less susceptible to abuse and more acceptable to society *(13,14,21)*. In fact, the exploration of buprenorphine for treatment of heroin dependence by Jasinski et al. *(29)* arose from the concept that it had properties reminiscent of both methadone and naltrexone. It seemed as though patients could be coaxed into taking a methadone-like drug to begin with and end up taking something like naltrexone *(13,14)*. Moreover, the addition of naloxone in a combination tablet has further reduced the abuse liability of buprenorphine. When the tablet is taken sublingually as prescribed, it is the buprenorphine effect that prevails since buprenorphine is well absorbed and

naloxone is not. If injected intravenously, however, the naloxone precipitates acute withdrawal in an opiate dependent person, discouraging iv abuse *(16,18)*.

4. The development of naltrexone was based on the idea that it completely blocks heroin effects and would thus not allow the addict to feel anything *(17,18)*. Realization did not come until much later that very few addicts wanted to "feel nothing" and that most would not take the medication.

5. The various detoxification strategies, including rapid and ultrarapid opiate detoxification, have also arisen more as a result of societal attitudes than medicine, although commercial interests have fostered these treatments as well. Despite data indicating that an overwhelming percentage of patients undergoing detoxification quickly relapse to heroin use and that those undergoing methadone detoxification generally do not even complete the process, efforts continue to develop a quicker and better detoxification strategy with the hope that it will change the basic outcome *(25)*. Results of a recently published six-month detoxification, which is about as long as it can be done, showed that most patients drop out of treatment as the sixth month is approached but even this has not discouraged detoxification proponents from pursuing the next strategy. Surely if there is any place for detoxification, it is as a transition to longer-term treatment, which at present is basically some form of maintenance pharmacotherapy *(20)*. For those few patients that may need short-term detoxification for whatever reason, the availability of buprenorphine should make the process relatively painless.

Acknowledgment

References

1. Dole, V. and Nyswander, M. (1965) A medical treatment for diacetylmorphine (heroin) addiction. *JAMA* **193,** 646–650.

2. Sees, K. L., Delucchi, K. L., Carmen, M., Rosen, A., Clark, H. W., Robillard, H., et al. (2000) Methadone maintenance vs 180-day psychosocially enriched detoxification for treatment of opioid dependence. *JAMA* **283(10),** 1303–1310.

3. Wolff, K., Hay, A. W. M., Raistrick, D., and Calvert, R. (1993) Steady-state pharmacokinetics of methadone in opioid addicts. *Eur. J. Clin. Pharmacol.* **44,** 189–194.

4. Nilsson, M. J., Widelov, E., Meresaar, U., and Anggard, E. (1982) Effect of urinary ph on the disposition of methadone in man. *Eur. J. Clin. Pharmacol.* **22,** 337–342.

5. Garrido, J. M. and Troconiz, I. F. (1999) Methadone: a review of its pharmacokinetic/pharmacodynamic properties. *J. Pharmacol. Toxicol.* **42,** 61–66.

6. Chen, K. K (1948) Pharmacology of methadone and related compounds. *Ann. NY Acad. Sci.* **51,** 83–87.

7. Fraser, H. F. and Isbell, H. (1952) Actions and addiction liabilities of alpha-acetylmethadols in man. *J. Pharmacol. Exper. Ther.* **105,** 458–465.

8. Misra, A. L. and Mule, S. J. (1975) L-a-Acetylmethadol (LAAM) pharmacokinetics and metabolism: current status. *Am. J. Drug Alcohol Abuse* **2,** 301–305.

9. Research Triangle Institute (1984, Sept.) Bioavailability and pharmacokinetics/pharmacodynamics of L-a-acetylmethadol and its metabolites: metabolism and pharmacokinetics of drugs. *Final Rep. Contr. #771-80-3705, Task #2.*

10. Toro-Goyco, E., Martin, B. R., and Harris, L. S. (1980) The binding of LAAM and its metabolites to blood constituents, in *Problems of Drug Dependence. 1979: Proc. 41st Ann. Sci. Mtg. Comm. Problems of Drug Dependence. NIDA Research Monograph #27* (Harris, L.S., ed.), Wash. DC, pp. 54–60.

11. Misra, A. L., Mule, S. J., Bloch, R., and Bates, T. R. (1978) Physiological disposition and biotransformation of l-a-[2-H] acetylmethadol (LAAM) in acutely and chronically treated monkeys. *J. Pharmacol. Exper. Ther.* **206(2),** 475–491.

12. Jasinski, D. R., Pevnick, J. S., and Griffith, J. D. (1978) Human pharmacology and abuse potential of the analgesic buprenorphine. *Arch. Gen. Psych.* **35,** 501–516.

13. Lewis, J. W. (1985) Buprenorphine. *Drug Alcohol Dep.* **14,** 363–372.

14. Walsh, S. L., Preston, K. L., Stitzer, M. L., Cone, E. J., and Bigelow, G.,E. (1994) Clinical pharmacology of buprenorphine: ceiling effects at high doses. *Clin. Pharmacol. Ther.* **55(5),** 569–580.

15. Walter, D. S. and Inturrisi, C. E. (1995) *Absorption, distribution, metabolism and excretion of buprenorphine in animals and humans in Buprenorphine: combining drug abuse with a unique opioid*, (Wiley-Liss, ed.), pp. 113–135.

16. Archer, S. (1980) Historical perspective on the chemistry and development of naltrexone, in *National Institute on Drug Abuse Monograph Series 28: Narcotic Antagonists: Naltrexone Pharmacochemistry and Sustained-Release Preparations* (Willette, R.,E. and Barnett, G. eds.), National Institute on Drug Abuse Monograph Series. Rockville, MD, pp. 3–10.

17. Martin, W. R., Jasinski, D. R. and Mansley, P. A. (1973) Naltrexone, an antagonist for the treatment of heroin dependence. *Arch. Gen. Psych.* **28,** 784–791.

18. Crowley, T. J., Wagner, J. E., Zerbe, G., and Mcdonald, M. (1985) Naltrexone-induced dysphoria in former opiate addicts. *Am. J. Psych.* **142,** 1081–1084.

19. Rawson, R. A. and Ling, W (1991) Opioid addiction treatment. *J. Psychoact. Drugs* **23(2),** 151–163.

20. Hall, S. M. (1983) Methadone treatment: a review of research findings, in *National Institute on Drug Abuse Series: Research on the Treatment of Narcotic Addiction: State of the Art* (Cooper, J. R., Altman, F., Brown, B. S., and Czechowicz, D. eds.), National Institute on Drug Abuse Treatment Monograph Series. Rockville, MD.

21. U.S. Congress. H.R.4365 "The Children's Health Act of 2000." (Signed Oct. 17, 2000) Section 3502 "Drug Addiction Treatment Act of 2000."

22. Kintz, P. (2001) Deaths involving buprenorphine: a compendium of French cases. *Forensic Sci. Int.* **121,** 65–69.

23. Ling, W. and Compton, P. (1997) Opiate maintenance therapy with LAAM, in *New Treatments for Opiate Dependence* (Stine, S. M. and Kosten, T. R., eds.), Guilford, New York, pp. 231–253.
24. Wesson, D. R. and Ling, W. (1991) Medications in the treatment of addictive disease. *J. Psychoact. Drugs* **23(4),** 365–370.
25. Ling, W., Huber, A., and Rawson, R. A. (2001) New trends in opiate pharmaco-therapy. *Drug Alcohol Rev.* **20,** 79–94.
26. Gold, M. S., Pottash, A. L., Sweeney, D. R., and Kleber, H. D. (1980) Efficacy of clonidine in opiate withdrawal: a study of thirty patients. *Drug Alcohol Abuse* **6,** 201–208.
27. Kleber, H. D., Topazian, M., Gaspari, J., Riordan, C. E., and Kosten, T. (1987) Clonidine and naltrexone in the outpatients treatment of heroin withdrawal. *Am. J. Drug Alcohol Abuse* **13,** 1–17.
28. Dole, V. P. and Nyswander, M. E (1983) Pharmacological treatment of narcotic addiction (the eighth Nathan B. Eddy memorial award lecture) in *NIDA Research Monograph #43*. National Institute on Drug Abuse Treatment Monograph Series. Rockville, MD, pp. 5–9.
29. Jasinski, D. R., Pevnick, J. S., and Griffith, J. D. (1978) Human pharmacology and abuse potential of the analgesic buprenorphine. *Arch. Gen. Psych.* **35,** 501–516.